INTESTINAL ORGANOIDS AS MODEL FOR CYSTIC FIBROSIS

Johanna Florentia Dekkers

Commissie: Prof. dr. H. Clevers
Prof. dr. E.E.S. Nieuwenhuis
Prof. dr. L.J. Braakman
Prof. dr. A.B.J. Prakken
Dr. H.R. de Jonge

Paranimfen: Annelotte M. Vonk
Sabine C. den Hartogh

Printing of this thesis was accomplished with financial support of the European Cystic Fibrosis Society, Galapagos and Vertex Pharmaceuticals

ISBN: 978-94-6295-361-1

Cover design: Proefschriftmaken.nl || Uitgeverij BOXPress
Printed & Lay Out by: Proefschriftmaken.nl || Uitgeverij BOXPress

INTESTINAL ORGANOIDS AS MODEL FOR CYSTIC FIBROSIS

Intestinale organoiden als model voor taaislijmziekte

(met een samenvatting in het Nederlands)

Proefschrift

ter verkrijging van de graad van doctor aan de Universiteit Utrecht
op gezag van de rector magnificus, prof.dr. G.J. van der Zwaan,
ingevolge het besluit van het college voor promoties in het openbaar te verdedigen
op dinsdag 3 november 2015 des middags te 2.30 uur

door

Johanna Florentia Dekkers

geboren op 29 november 1987, te Eindhoven

Promotor: Prof.dr. C.K. van der Ent

Copromotor: Dr. J.M. Beekman

CONTENTS

Chapter 1

General introduction

Partly adapted from: (1) Dekkers, Ent, Beekman, Novel opportunities for CFTR-targeting drug development using organoids, Rare Diseases 2013; and (2) Dekkers & Beekman, Primary cystic fibrosis intestinal organoids, Book chapter: in 'Mutation-specific therapies in cystic fibrosis – current status and prospects', Burkhard Tummler, UNI-MED, Bremen, 2014

GENERAL INTRODUCTION

Unique molecular profiles of the individual determine the manifestation of disease and response to therapy. Today's great challenge is to monitor and treat patients more precisely and effectively to meet their individual needs, i.e. personalized or precision medicine. In this context, establishing objective subject-specific measures of normal or pathogenic biological processes (biomarkers) is essential to develop therapeutic strategies and stratify patients for existing and novel treatments, preferentially before irreversible disease manifestations.

Among rare conditions, **cystic fibrosis (CF) is considered a model disease** as it has pioneered studies in genetics, molecular and cellular pathogenesis and drug discovery. While CF therapy has been symptomatic for decades, **novel breakthrough drugs** targeting the underlying molecular defect in CF provide exciting **opportunities for curative treatment**.

CYSTIC FIBROSIS PATHOPHYSIOLOGY

Cystic fibrosis (CF) is **the most common life-shortening autosomal recessive disease** that affects ~85,000 individuals worldwide, primarily in the Caucasian population. These numbers still rise due to extensive CF newborn screening programs, and increased diagnosis in second and third world countries[1]. CF is caused by mutations in the *cystic fibrosis transmembrane conductance regulator* (*CFTR*) gene that encodes an apical anion channel expressed by many cell types, but its function has mostly been studied in epithelial cells[2-5].

Decreased chloride and bicarbonate transport due to **loss of CFTR function leads to a number of abnormalities at mucosal surfaces in many organs**, including increased mucus viscosity of secretions in the pulmonary system. As a result, people with CF suffer from many pulmonary abnormalities, including chronic infections, aberrant neutrophilic inflammation and mucus plugging. Pancreatic insufficiency further contributes to malnutrition and poor growth. Loss-of-CFTR function also affects other organ systems, such as the sweat gland, the biliary duct of the liver, the male reproductive tract and the intestine[6-8]. Advanced lung disease and airway remodeling, characterized by progressive bronchiectasis, is the primary cause of morbidity and is responsible for ~80% of mortality. Pancreatic enzyme supplementation and intensive symptomatic treatment by multidisciplinary teams progressively improved the average life expectancy to ~37 years for CF newborns today, with *CFTR* genotype, infection status and quality of care as major determinants[6,7].

CFTR MUTATIONS

Almost 2,000 CFTR variants have been reported so far in the cystic fibrosis mutation database (www.genet.sickkids.on.ca), which can be grouped into six classes according to their predominant effect on CFTR processing and function; (I) no functional CFTR protein, (II) severely impaired folding and trafficking to the apical membrane, (III) defective channel opening or gating, (IV) altered channel conductance, (V) reduced apical expression of normally functioning CFTR, and (VI) increased apical membrane protein turnover[9] (**Fig. 1**).

The classification system provides **a useful framework for understanding the consequence of a genetic mutation at the molecular and cellular level**, which is important for the design of therapies aimed to repair specific CFTR defects. The classification of common *CFTR* mutations expressed by large groups of subjects has been well characterized, but remains poorly understood for the majority of rare mutations expressed by fewer subjects (www.CFTR2.org)[10]. **The classification system does not incorporate individual factors that may impact CFTR expression and function** independent of the *CFTR* genotype, and types mutations into two categorical groups in terms of residual function: class I, II, III and VI lack residual function, whereas class IV and V are associated with function[9].

Classification is furthermore difficult for CFTR variants that have multiple functional defects. This is exemplified by F508del, the most common *CFTR* mutation accounting for ~60% of all *CFTR* alleles worldwide and is typed as the prototypical class II mutation[11]. F508del primarily affects CFTR folding and apical trafficking, resulting in premature breakdown and low plasma membrane levels[12]. The small fraction of CFTR-F508del that reaches the apical cell surface has a partial gating defect and reduced plasma membrane stability[13]. Furthermore, the three-nucleotide deletion accounting for the F508del mutation alters the *CFTR* mRNA structure and reduces the translation efficiency[14]. So, **F508del is generally assigned to class II, but in-depth follow up studies also indicate that it belongs to at least two additional classes.**

Variation in disease severity and residual function

Although CF is a monogenic disorder, **genotype-phenotype relations are complex** and mechanisms involved are not well understood. *CFTR* mutations associate with a broad range of clinical phenotypes, including severe CF, mild CF, single-organ CFTR-related diseases or a course without clear symptoms (www.CFTR2.org)[10]. People who carry one mutated *CFTR* allele are at higher risk for multigenic disorders in the general population, such as pancreatitis, sinusitis, and male infertility[7]. On a population level, class I - III and VI mutations associate with severe disease, while class IV and V associate with milder CF. However, a **high degree of variability in disease**

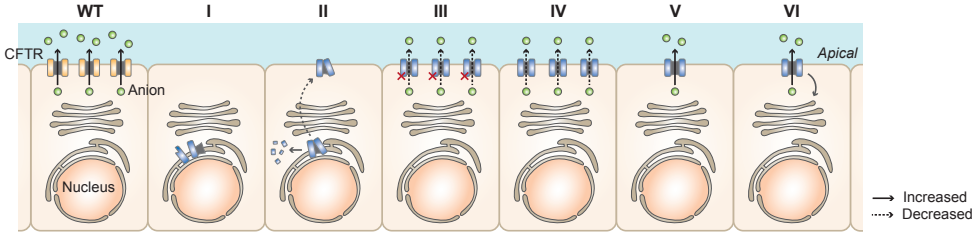

Defect	Non-functional protein syntesis	Impaired folding and trafficking	Defective regulation/ gating	Impaired conductivity	Reduced levels	Reduced stability
Mutation examples	G542X W1282X N1303K 711-1G>T	F508del A455E	G551D S1251N R1349D F508del	R117H R334W L927P	TG(13)T(5) A455E	c.120del23 F508del

Figure 1. The classification system for CFTR variants.

severity, complications and survival exists between subjects with mutations from a single class as well as with identical mutations[10,15,16].

Monozygous and dizygous twin studies and large population statistics indicate that the *CFTR* mutations, together with genetic modifiers, environmental factors and stochasticity, define the clinical course[7,17] (**Fig. 2**). **Some phenotypic features are closely determined by the *CFTR* genotype, whereas others are strongly influenced by genetic modifiers and/or environment**. For instance, pancreatic insufficiency closely associates with allelic variation in *CFTR* (e.g. all class I mutations and F508del)[18]. On the other hand, lung function, neonatal intestinal obstruction, diabetes, and body weight display strong genetic control independent of *CFTR*[19-22]. Of these, lung function is the most heterogeneous clinical outcome, with most considerable variation in F508del homozygotes. It has been difficult to detect relations between lung function and the *CFTR* genotype[18,23], with a few exceptions[24]. This illustrates it is difficult to predict the clinical course of the individual patient simply based on the *CFTR* genotype.

Individual CFTR function measurements have been used to diagnose CF already before the *CFTR* gene was cloned. Abnormal high sweat chloride concentrations have been found in the 50's and are nowadays still the standard for diagnosis in combination with *CFTR* genotyping[25,26]. Other individual CF markers, such as aberrant potential differences in the nasal mucosa or aberrant ion currents in *ex vivo* rectal biopsies[27,28], have been developed to improve diagnosis. These methods are suited for CF diagnosis and discriminate between severe (class I, II, III) and milder forms of disease (class IV and V) at the population level[29-34]**.** However, **technical and biological variability in these readouts prevent an accurate and robust individual residual CFTR function measurement**[35,36]. Many studies also suggest that variability of CFTR expression and function exists between subjects with identical mutations[37-42], but the correlation of this variability to disease severity remains poorly characterized. It indicates **a clear need for additional methodology that robustly and accurately quantitates CFTR residual function for the individual**. This is especially relevant for subjects with rare *CFTR* genotypes, who form a minority in Western populations (~10%), but are increasingly identified due to newborn screening and CF diagnosis in second and third world countries[10].

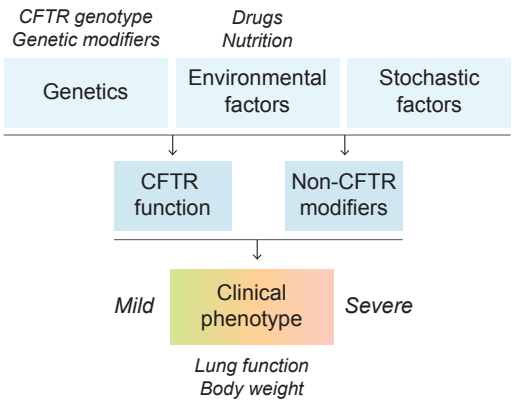

Figure 2. The complexity of genotype - phenotype relations in cystic fibrosis. The clinical course of CF subjects is determined by genetic, environmental and stochastic factors, and is highly variable between individuals. Whereas some phenotypic features are closely determined by the *CFTR* genotype (pancreatic insufficiency), others are strongly influenced by genetic modifiers (CF-related diabetes) or genetic modifiers and environment / stochastic factors (lung function, body weight).

CFTR FUNCTION AND REGULATION

CFTR is an adenosine triphosphate (ATP)-binding cassette (ABC) transporter family member[43]. It consists of two nucleotide-binding domains (NBD), one regulatory domain (R domain) that controls phosphorylation-dependent channel gating (opening and closing)[44], and two membrane-spanning domains (MSD) that form the anion-conducting pore (**Fig. 3a**). Phosphorylation of the R domain by cyclic adenosine monophosphate (cAMP)-dependent protein kinase (PKA) is the preferential route for activation *in vivo*, and is mimicked in the laboratory using forskolin that directly activates adenylyl cyclase (AC) to produce cAMP[45] (**Fig. 3b**). Other kinases have also been shown to phosphorylate CFTR, such as cAMP-dependent protein kinase C (PKC) and cyclic guanosine monophosphate (cGMP)-dependent protein kinase G (PKG) II[46]. Once phosphorylated, ATP binding to the NBDs triggers NBD dimerization and channel opening, while ATP hydrolysis triggers NBD separation and channel closing[47] (**Fig. 3a**).

CFTR activation depends on signaling pathways induced by ligands, including hormones (e.g. vasointestinal peptide, adrenaline)[48,49], inflammatory mediators (e.g. prostaglandin E_2)[50], bacterial toxins (e.g. cholera toxin)[51] and synthetic agonists of cAMP-activating receptors (e.g. salbutamol)[27]. Many of these ligands signal via G-protein coupled receptors (GPCRs), and collectively these systems control and rate-limit CFTR function in a tissue-specific fashion, e.g. CFTR activity in the intestine is relatively low and can be drastically increased by bacterial toxins that induce secretory diarrhea, whereas approximately 50% of maximal CFTR activity is observed in nasal mucosa without exogenous stimuli[29,30]. CFTR assembles into large and dynamic macromolecule complexes via adaptor proteins of the Na^+ / H^+ exchanger 3 regulatory factor (NHERF) family. These link the CFTR C-terminus to various signaling components, the actin cytoskeleton and receptors, such as

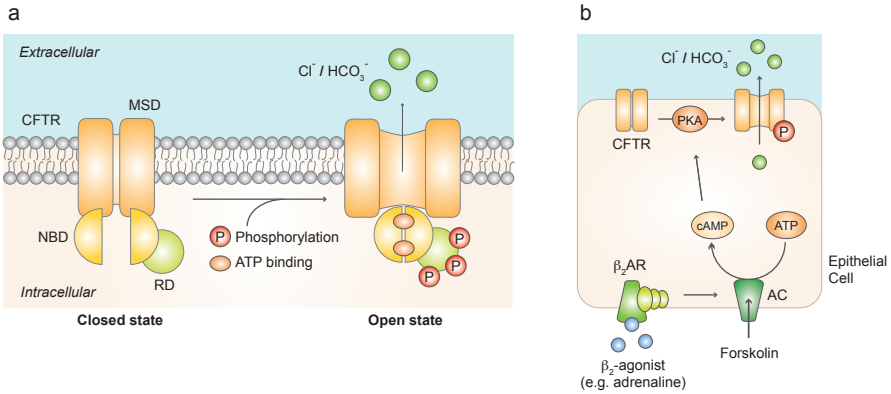

Figure 3. Regulation of CFTR function. (**a**) CFTR consists of two nucleotide-binding domains (NBD), one regulatory domain (R domain), and two membrane-spanning domains (MSD). Phosphorylation of the R domain triggers adenosine triphosphate (ATP)-dependent NBD dimerization and channel opening, resulting in transport of chloride (Cl^-) and bicarbonate (HCO_3^-) across the apical membrane. ATP hydrolysis into adenosine diphosphate (ADP) and inorganic phosphate (Pi) by the NBD2 triggers NBD separation and channel closing. (**b**) Binding of a β_2-agonist (such as adrenaline) to the β_2-adrenergic receptor (β_2AR) leads to cyclic adenosine monophosphate (cAMP) production by adenylyl cyclase (AC) and protein kinase A (PKA)-mediated CFTR activation. The chemical compound forskolin activates CFTR by direct stimulation of AC.

the β_2-adrenergic receptor, and modify CFTR activation and membrane dynamics, possibly in a tissue-specific manner[52,53].

CF THERAPIES

We have recently entered a phase in which **the therapeutic landscape is transforming** from 'one-size-fits-all' suppressive medicine to curative medicine tailored to the *CFTR* mutation (See **Table 1** for an overview). Conventional symptomatic CF treatments include antibiotics to suppress infections and exacerbations, pancreatic enzyme supplementation to improve digestion, anti-inflammatory agents and compounds that restore the airway surface liquid and mucus composition. At a late stage of severe lung disease, the final option is lung transplantation.

During the last decade, the increased understanding of CF at the molecular level has driven the **development of 'curative' CF therapies that target the underlying CFTR defect** at the DNA, RNA or protein level. Some approaches remain restricted to the lung, but aim to target all CF subjects (gene therapy). Other approaches act in a mutation-specific fashion, but can be administered systemically to reach multiple affected organs (CFTR pharmacotherapy). Except for treatments that aim to stably express wild-type CFTR in stem cells, current treatments would require life-long therapy. In addition to CFTR-restoring treatments, other *CFTR* mutation-independent strategies aim to compensate the lack of CFTR function through modulation of alternative chloride channels, such as calcium-activated chloride channels or reduce fluid absorption by inhibiting the epithelial Na^+ channel ENaC.

A curative systemic drug that is effective for all *CFTR* mutations has not yet been developed, but exciting successes have been achieved with systemic delivery of small molecule modulators that

CF pathofysiology	Therapy	Developmental stage	Primary defect	Route
CFTR gene defect	In vivo gene therapy Ex vivo gene editing (e.g. CRISPR/Cas9)	Phase II Pre-clinical	All mutations Most mutations*	Inhaled Inhaled
↓ *CFTR* mRNA defect	PTC read-through agents (e.g. PTC124/Ataluren) Oligo-mediated repair Spliceosome modulators	Phase III Pre-clinical Pre-clinical	Nonsense mutations Most mutations* Splice mutations	Oral Inhaled Inhaled
↓ CFTR protein defect	Correctors (e.g. VX-809/lumacaftor) Potentiators (e.g. VX-770/ivacaftor/KALYDECO) Activators (e.g. β_2-sympathicomimetica)	FDA-approved Available for patients Available for patients	Class II mutations Class III-V mutations Class III-V mutations	Oral Oral Inhaled / Oral
↓ Defective ion transport	Alternative channel modulators	Pre-clinical	All mutations	Inhaled / Oral
↓ Mucus plugging	ASL modulators (e.g. Hypertonic saline) Mucus modulators (e.g. Pulmozyme)	Available for patients Available for patients	All mutations All mutations	Inhaled Inhaled
↓ Infection ↑ Inflammation	Antibiotics (e.g. Tobramycin) Anti-inflammatory agents (e.g. Ibuprofen) Lung transplantation	Available for patients Available for patients Available for patients	All mutations All mutations All mutations	Inhaled / oral Inhaled / oral -

* Difficult for large or complex genetic rearrangements

Table 1. Overview of CF treatments currently available or under (pre-) clinical development. (ASL = airway surface liquid).

target CFTR trafficking or gating. The current status of the most important therapies that target the underlying defect in CF are discussed below.

DNA repair

In vivo gene therapy is an attractive approach to treat lung disease in all CF patients. Since cloning of the *CFTR* gene in 1989, many studies have aimed to introduce the wild-type *CFTR* gene in humans using viral or non-viral vectors. The method has proven to be extremely challenging, reflected by variable results of over 25 trials that have been performed to date. The **limited success of trials using viral vectors** related to difficulties in efficient delivery of DNA to target (stem) cells (e.g. because of mucus plugging) and safety, as anti-viral host immune responses can be provoked as well as oncogene activation when DNA-integrating vectors are used. Although synthetic vectors are associated with a clear loss of immunogenicity, the DNA plasmid used in early trials triggered an immune response because of its unmethylated CG dinucleotide (CpG) motifs[54]. Results of a recent multi-dose phase III trial of the UK CF gene therapy consortium using CpG-free synthetic vectors to deliver *CFTR* DNA will further define the potential of gene therapy in CF and may provide the essential proof-of-concept required in this field.

Another interesting approach would be autologous *CFTR* gene-corrected stem cell transplantation. The mutated ***CFTR* locus can be repaired by ex-vivo gene-editing techniques** using zinc-finger nucleases (ZFNs), transcription activator-like effector nucleases (TALENs) or clustered, regularly interfaced, short, palindromic repeats (CRISPR) / CRISPR-associated (Cas) 9. ZNFs and TALENs are engineered proteins that use their DNA binding domains to direct nuclease domains to specific DNA loci[55]. In contrast to ZNFs and TALENs, CRISPR/Cas9-mediated gene-editing is highly efficient due to the easy design of the DNA-targeting module. The system utilizes the type II prokaryotic CRISPR/Cas9 adaptive immune system and targets the Cas9 nuclease to any desired location via an engineered guide RNA based on complementary DNA-RNA hybridization. Cas9 induces site-specific double-strand breaks that are repaired either by non-homologous end-joining to yield indels or by homologous recombination if donor templates are available[56]. The field is currently starting to explore its potential for treatment of CF.

RNA repair

Other strategies have focused on editing *CFTR* mRNA transcripts. Partial repair of CFTR-F508del in human airway cells has been achieved by spliceosome-mediated RNA trans-splicing (SMaRT), in which *cis*-splicing of a specific pre-mRNA is suppressed, while *trans*-splicing between a pre-therapeutic RNA molecule and its pre-mRNA target is enhanced[57,58]. Others have reported insertion of the missing TTT bases in mRNA-F508del by RNA oligonucleotides complexes in cell lines[59]. These techniques may be applied for non-F508del mutations as well. In addition, altered splicing of *CFTR* mRNA (Class I or V; **Fig. 1**) may be repaired by increasing the expression of splicing factors, synthetic activators or U1 small nuclear RNAs that prevent exon skipping, or antisense oligonucleotides that block aberrant splice sites[60-62]. However, **clinical safety and efficacy of these mRNA-targeting therapies has not yet been proven** and delivery remains most likely restricted to the lung.

Repair of CFTR translation

Premature termination codon (PTC) read-through agents have been clinically assessed and can be orally administered for treatment of nonsense mutations leading to PTCs (Class I; **Fig. 1**) carried by ~10% of CF patients[63]. Ataluren (PTC124) was discovered as drug that selectively induces some ribosomal read-through of premature, but not conventional termination codons, allowing production of a full-length protein from nonsense-mutated mRNA[64]. Aminoglycoside antibiotics also have established read-trough capacity, but associate with severe cellular toxicity[65]. Although the first (pre)clinical Ataluren studies were promising[64,66], **phase III clinical studies reported limited efficacy in subjects with CF**[67-70] **or nonsense-mutated Duchenne muscular dystrophy**[71]. For CF, retrospective data analysis of the phase III study suggested that aminoglycoside co-treatment prevented PTC124 activity[70]. An additional study with CF patients who do not receive inhaled antibiotics will further define the potential of Ataluren for CF.

Repair of CFTR trafficking

CFTR-F508del has been the dominant target for the development of small molecule corrector strategies. Interventions that target defects in folding and processing of CFTR-F508del and **increase the number of channels at the plasma membrane** include (i) low-temperature culturing, (ii) introduction of second site suppressor mutations and (iii) pharmacological correction by compounds that bind directly to CFTR or interfere with the protein quality control system[72]. To search for high-quality correctors, cell-based high-throughput screening (HTS) with halide-sensing fluorescent probes or membrane potential dyes started approximately a decade ago and produced several classes of small molecule CFTR-F508del correctors[73]. However, the compounds that have been identified so far showed limited efficacy.

The Vertex compound **VX-809 (lumacaftor), the most successful corrector to date**, restored the CFTR-F508del channel activity to 15% of wild-type CFTR in primary airway epithelium[74]. A phase II clinical trial with VX-809 monotherapy in F508del homozygotes indicated an acceptable safety profile, but limited clinical efficacy. Except for a modest but significant improvement of sweat chloride levels, other clinical endpoints and CFTR biomarkers did not significantly differ from placebo controls[75]. Other studies with compounds that corrected apical CFTR-F508del levels *in vitro* also failed to achieve robust clinical effects[76,77]. Interestingly, a recent study reported a significant improvement in sweat chloride levels of F508del homozygous patients upon treatment with cysteamine, a US Food and Drug Administration (FDA)-approved drug that restores disturbed CF-dependent autophagy, in combination with epigallocatechin gallate (EGCG), a flavonoid derived from green tea that modulates proteolytic degradation of CFTR-F508del[78]. The clinical potential of this combination needs to be defined in follow up trials.

The limited *in vivo* efficacy of single corrector treatment may be explained by the complexity of the folding defects in CFTR-F508del. In the proposed cooperative folding model of CFTR, co-translational folding results in loosely folded individual domains and premature membrane assembly, whereas the compact native structure with critical NBD-MSD interfaces is formed post-translationally. Domain-domain interactions are critical during the full conformational maturation process. Misfolding of NBD1-F508del co-translationally destabilizes the conformation

of other domains and compromises domain assembly and formation of the NBD-MSD interfaces, enhancing ER-associated degradation and plasma membrane turnover mediated by the protein quality control system[72,79-81]. Studies using second site suppressor mutations in CFTR-F508del indicated that stabilization of the energetic stability of NBD1 as well as the NBD1-MSD2 interface is required for wild-type-like trafficking and function[82]. **The presence of distinct structural defects in CFTR-F508del may explain the limited success of corrector mono-therapy and supports the need for corrector combination therapies**. Understanding the structure and processing of CFTR and mechanism of action of existing correctors underlies the basis for the development of rationally designed corrector combination strategies.

Repair of CFTR gating

CFTR potentiators **increase chloride and bicarbonate transport across the apical membrane by enhancing the open probability** of the CFTR channel. Targets for potentiator monotherapy are CFTR variants that properly traffic to the apical membrane but have defects in gating (class III), conductance (class IV) or biosynthesis (class V), or corrector-repaired trafficking mutants (II) (**Fig. 1**). Many naturally occurring components have well-established CFTR potentiator activity, including the natural food components genistein, an isoflavonoid found in high concentrations in soy[83-85], and curcumin, a major constituent of turmeric[86,87]. As for correctors, HTS was performed to identify high-affinity potentiators, which were further developed into compounds with favorable pharmacokinetic properties[73]. Of these, **VX-770 (ivacaftor / KALYDECO™) is the first CFTR-targeting small molecule therapy approved for CF**. Clinical studies with subjects harboring at least one G551D allele reported a gain in forced expiratory volume in one second (FEV_1) % predicted of 10 points within the first four weeks of treatment, which maintained over the study period of 48 weeks[88,89]. Besides lung function, the treatment improved the risk of exacerbation, quality of life, nasal potential difference, sweat chloride concentration, body weight, hospitalization rate, the gastrointestinal pH and mucociliary clearance[88-92].

In addition to G551D, VX-770 enhanced the channel open probability of 9 other gating mutations to 30%-118% of wild-type CFTR in recombinant FRT cells[93]. A recent study with VX-770 reported G551D-like clinical effects for CF subjects with 8 out of the 9 gating mutations, including the most common Dutch gating mutation S1251N, but not for 3 subjects with G970R[94]. The FRT model furthermore identified various CFTR missense mutants with defects in channel processing (class II) and/or conductance (class IV) as candidates for future *in vivo* studies[95]. Of these, R117H was clinically assessed and the FDA approved VX-770 for CF subjects with this mutation (vrtx.investors.org).

While VX-770 or VX-809 single treatment showed limited clinical efficacy, **a phase III combination trial in F508del homozygotes reached its primary endpoint**, resulting from an increase in FEV_1 % predicted of 3.3 points in the treatment group versus placebo. While the increase in lung function was modest, the 30 to 39 % decrease in rate of pulmonary exacerbation of the treatment groups compared to placebo was more impressive[96]. Vertex is also assessing clinical effectiveness of other correctors in combination with VX-770, of which VX-661 soon enters phase III (vrtx.

investors.org). Various other companies have also discovered small molecule CFTR correctors and potentiators, which are currently under (pre)clinical development.

Enhancing CFTR activation

When endogenous CFTR-activating stimuli are rate limiting *in vivo*, maximizing CFTR activity could be an additional approach to enhance CFTR function, which may further enhance the impact of CFTR-restoring drugs. CFTR can be activated by compounds that directly interact with CFTR, stabilize the CFTR phosphorylated state (e.g. phosphatase inhibitors) or elevate intracellular cAMP (e.g. phosphodiesterase inhibitors or AC activators such as β_2-agonists; Fig. 3b)[97]. However, the impact of these approaches has never been studied in the context of mutations associated with residual function or in combination with direct CFTR-restoring drugs[98].

In summary, we have learned from clinical studies that aimed to repair the underlying defect in CF that: (i) approaches that target DNA, RNA or protein translation are under development, but clinical safety and efficacy has not yet been proven, (ii) CFTR-protein targeting therapy by systemic delivery of small molecules is feasible and impacts many aspects of CF, (iii) the first CFTR-repairing potentiator (VX-770 / ivacaftor / KALYDECO™) is approved for only ~5% of CF subjects, (iv) currently available CFTR modulators do not normalize CFTR-dependent biomarkers, and (v) the response to therapy between individuals is highly heterogeneous, also between subjects with identical CF-causing mutations (**Fig. 2**). So**, there is still a long road ahead towards effective treatment for all CF subjects.**

DEFINING EFFICACY OF CFTR-TARGETING TREATMENTS

Clinical endpoints are important measures to reflect how a patient 'feels, functions and survives' (e.g. hospitalization, quality of life and survival). To measure the efficacy of CF therapies in trials, clinical endpoints are usually complemented with surrogate clinical endpoints and other biomarkers to shorten the required trial period[99,100]. The FEV_1 is considered the most important surrogate endpoint because of its established link with survival[101], and has been widely used in clinical studies. However, FEV_1 sensitivity is a problem for children and subjects with mild lung disease, and large variability exists between individuals in FEV_1. Furthermore, with the arrival of CFTR-repairing treatments and the shift towards preventive medicine, **development and validation of biomarkers and surrogate endpoints other than** FEV_1 **is needed to predict long-term efficacy of CFTR modulators already before the onset of lung disease**.

In this context, assays that directly measure the individual's CFTR function *in vivo* or *in vitro* are gaining more value[35,36]. Classical biossays that measure CFTR-dependent ion transport in humans include the (i) sweat chloride test (*in vivo*)[25,26], (ii) nasal potential difference measurements (*in vivo*)[29,102] and (iii) intestinal current measurements (*ex vivo*)[30,103,104]. As discussed above, these measurements are generally used for CF diagnosis, but their role as predictive biomarkers for the efficacy of CFTR-repairing drugs is currently being explored[35,36]. **Primary *in vitro* models that incorporate the individual's genetic background are attractive models for measurement of the individual CFTR drug efficacy.**

INTESTINAL ORGANOIDS

Recent **advances in adult stem cell culture technology have enabled long-term *in vitro* expansion of intestinal organoids** or 'mini-guts' from material of murine or human origin[105-108]. These pure epithelial 3-D cultures recapitulate the *in vivo* tissue architecture in terms of cell polarity, self-renewal kinetics and cell-type composition and organization. Organoids contain a central lumen that is lined by the apical membrane, and multiple crypt domains that harbor the stem cells (**Fig. 4**). Organoids are passaged weekly by mechanical disruption into single crypts that easily reseal and form new organoids[109].

AIM AND THESIS OUTLINE

In this thesis, we aimed to develop a new methodology to quantitate CFTR function *in vitro*. We hypothesized that the analysis of patient-derived intestinal organoids would facilitate discrimination of CF individuals based on the residual and drug-induced CFTR function, and that these measurements are predictive for the individual disease expression and response to therapy. We expect impact on three major research themes that are currently highly relevant in CF: (i) the definition of (individual) relations between the *CFTR* genotype, residual function and disease expression, (ii) the definition of (individual) relations between the *CFTR* genotype, residual function and response to CFTR-directed therapies, and (iii) the development of better CFTR-targeting treatments.

In **Chapter 2**[111]**,** we used the organoid technology to develop a novel functional CFTR assay that depends on forskolin-induced swelling (**Fig. 5**). This assay was used throughout this thesis to discover novel approaches for optimal repair of mutant CFTR and to guide the development of

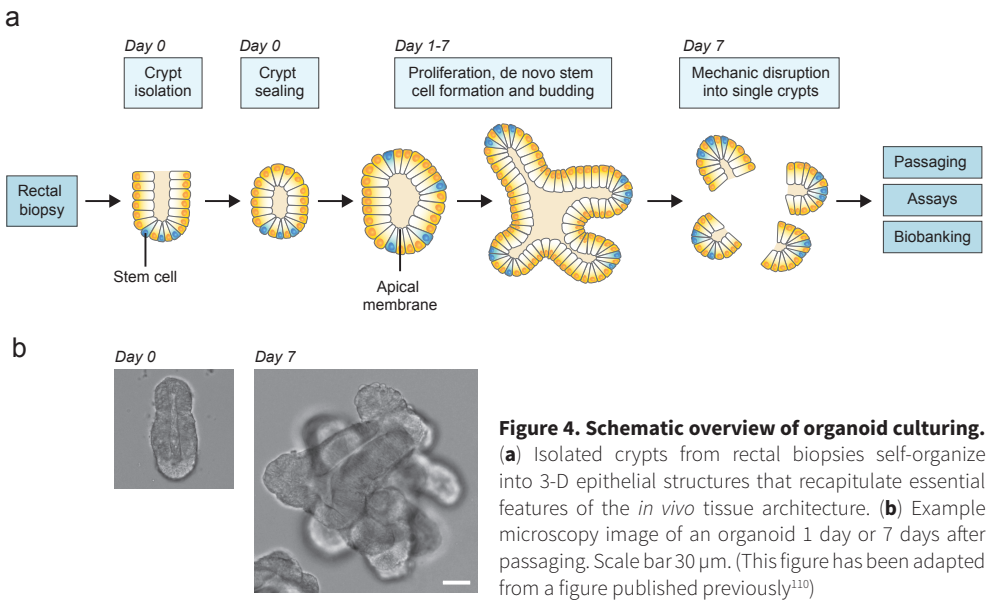

Figure 4. Schematic overview of organoid culturing. (**a**) Isolated crypts from rectal biopsies self-organize into 3-D epithelial structures that recapitulate essential features of the *in vivo* tissue architecture. (**b**) Example microscopy image of an organoid 1 day or 7 days after passaging. Scale bar 30 µm. (This figure has been adapted from a figure published previously[110])

personalized medicine for CF patients. A major challenge is to correct the many defects in folding of CFTR-F508del. With our collaborators at the McGill University of Montreal, we studied repair of CFTR-F508del by compounds that target distinct conformational defects (**Chapter 3**[112]). How do other CFTR folding mutants respond to correctors? In **Chapter 4,** we focused on corrector-mediated repair of CFTR-N1303K and CFTR-A455E, the second most common mutant in the Netherlands. We move from correctors to potentiators in **Chapter 5**. Because VX-770 treatment in subjects with a gating mutation does not normalize CFTR-dependent biomarkers, more effective gating strategies are needed. We collaborated with Dr. H.R. de Jonge (Erasmus University Medical Centre, Rotterdam) to answer the question: can we potentiate a potentiator? In **Chapter 6**, we hypothesized that endogenous CFTR-activating stimuli are rate limiting *in vivo*, and studied CFTR activation by β_2-agonists *in vitro* and *in vivo*. In **Chapter 7**, we characterized the residual and drug-corrected CFTR function in large panel of organoids, and identified two subjects with an extremely rare *CFTR* mutation as potential VX-770 responders. How did these patients respond to the drug *in vivo*? From pharmacological repair of the CFTR protein (**Chapter 2 - 7**), we switch to a DNA-based therapeutic approach in **Chapter 8**[113]**.** In collaboration with Prof. H. Clevers of the Hubrecht

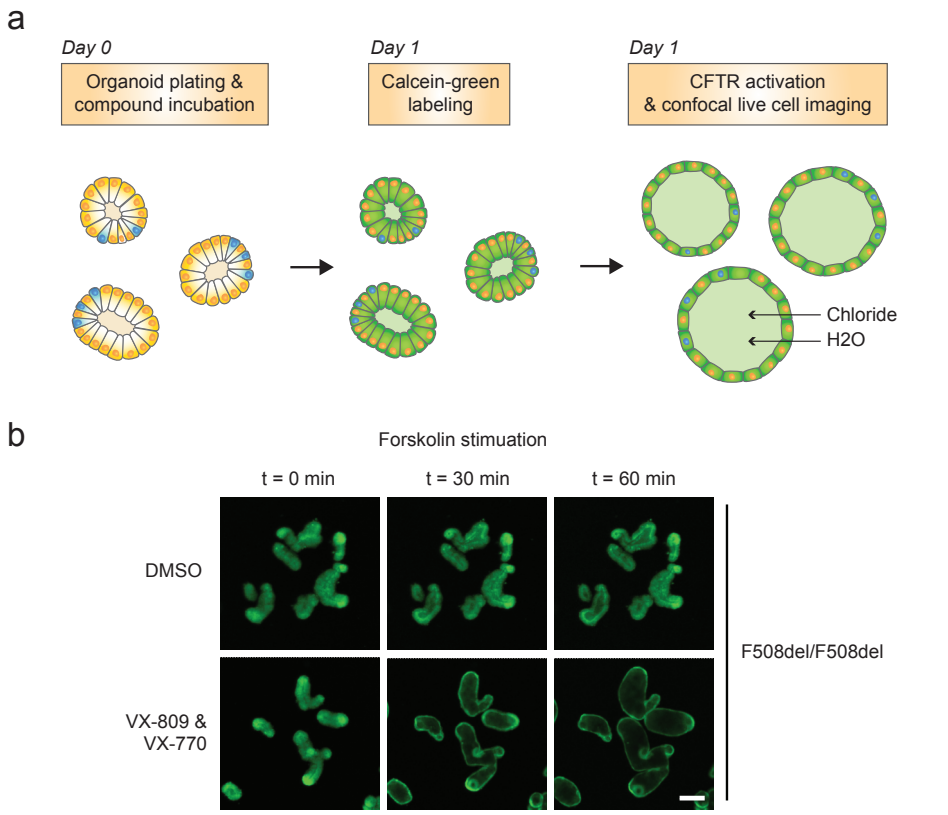

Figure 5. A novel assay to measure CFTR function in organoids. (**a**) Schematic representation of the 2-day assay to measure forskolin-induced organoid swelling. (**b**) Confocal images of calcein-green labeled F508del homozygous organoids with or without treatment of VX-770 + VX-809 at the indicated time points of forskolin stimulation. Scale bar 100 µm. (This figure has been adapted from a figure published previously[110])

Institute (Utrecht), we aimed to correct the mutant *CFTR-F508del* allele in intestinal adult stem cells using CRISPR/Cas9-mediated homologous recombination. In **Chapter 9**, we discuss the promises and challenges of organoid-based functional CFTR measurements in the currently changing landscape of CF medicine.

REFERENCES

1. Bell, S. C., De Boeck, K. & Amaral, M. D. New pharmacological approaches for cystic fibrosis: Promises, progress, pitfalls. *Pharmacol. Ther.* **S0163-7258**: 00122–3 (2014).
2. Rommens, J. M. *et al.* Identification of the cystic fibrosis gene: chromosome walking and jumping. *Science* **245,** 1059–1065 (1989).
3. Riordan, J. R. *et al.* Identification of the cystic fibrosis gene: cloning and characterization of complementary DNA. *Science* **245,** 1066–1073 (1989).
4. Kerem, B. *et al.* Identification of the cystic fibrosis gene: genetic analysis. *Science* **245,** 1073–1080 (1989).
5. Kartner, N. *et al.* Expression of the cystic fibrosis gene in non-epithelial invertebrate cells produces a regulated anion conductance. *Cell* **64,** 681–691 (1991).
6. Stoltz, D. A., Meyerholz, D. K. & Welsh, M. J. Origins of cystic fibrosis lung disease. *N. Engl. J. Med.* **372,** 351–362 (2015).
7. Cutting, G. R. Cystic fibrosis genetics: from molecular understanding to clinical application. *Nat. Rev. Genet.* **16,** 45–56 (2015).
8. De Lisle, R. C. & Borowitz, D. The cystic fibrosis intestine. *Cold Spring Harb Perspect Med* **3,** a009753 (2013).
9. Amaral, M. D. Novel personalized therapies for cystic fibrosis: treating the basic defect in all patients. *J. Intern. Med.* **277,** 155–166 (2015).
10. Sosnay, P. R. *et al.* Defining the disease liability of variants in the cystic fibrosis transmembrane conductance regulator gene. *Nat. Genet.* **45,** 1160–1167 (2013).
11. Bobadilla, J. L., Macek, M., Fine, J. P. & Farrell, P. M. Cystic fibrosis: a worldwide analysis of CFTR mutations--correlation with incidence data and application to screening. *Hum. Mutat.* **19,** 575–606 (2002).
12. Cheng, S. H. *et al.* Defective intracellular transport and processing of CFTR is the molecular basis of most cystic fibrosis. *Cell* **63,** 827–834 (1990).
13. Denning, G. M. *et al.* Processing of mutant cystic fibrosis transmembrane conductance regulator is temperature-sensitive. *Nature* **358,** 761–764 (1992).
14. Lazrak, A. *et al.* The silent codon change I507-ATC->ATT contributes to the severity of the ΔF508 CFTR channel dysfunction. *FASEB J.* **27,** 4630–4645 (2013).
15. McKone, E. F., Emerson, S. S., Edwards, K. L. & Aitken, M. L. Effect of genotype on phenotype and mortality in cystic fibrosis: a retrospective cohort study. *Lancet* **361,** 1671–1676 (2003).
16. Kerem, E. *et al.* The relation between genotype and phenotype in cystic fibrosis--analysis of the most common mutation (delta F508). *N. Engl. J. Med.* **323,** 1517–1522 (1990).
17. Gallati, S. Disease-modifying genes and monogenic disorders: experience in cystic fibrosis. *Appl Clin Genet* **7,** 133–146 (2014).
18. Correlation between genotype and phenotype in patients with cystic fibrosis. The Cystic Fibrosis Genotype-Phenotype Consortium. *N. Engl. J. Med.* **329,** 1308–1313 (1993).
19. Blackman, S. M. *et al.* Genetic modifiers play a substantial role in diabetes complicating cystic fibrosis. *J. Clin. Endocrinol. Metab.* **94,** 1302–1309 (2009).
20. Collaco, J. M., Blackman, S. M., McGready, J., Naughton, K. M. & Cutting, G. R. Quantification of the relative contribution of environmental and genetic factors to variation in cystic fibrosis lung function. *J. Pediatr.* **157,** 802–7.e1–3 (2010).
21. Bradley, G. M., Blackman, S. M., Watson, C. P., Doshi, V. K. & Cutting, G. R. Genetic modifiers of nutritional status in cystic fibrosis. *Am. J. Clin. Nutr.* **96,** 1299–1308 (2012).
22. Blackman, S. M. *et al.* Relative contribution of genetic and nongenetic modifiers to intestinal

obstruction in cystic fibrosis. *Gastroenterology* **131,** 1030–1039 (2006).

23. McKone, E. F., Goss, C. H. & Aitken, M. L. CFTR genotype as a predictor of prognosis in cystic fibrosis. *Chest* **130,** 1441–1447 (2006).

24. Gan, K. H. *et al.* A cystic fibrosis mutation associated with mild lung disease. *N. Engl. J. Med.* **333,** 95–99 (1995).

25. GIBSON, L. E. & COOKE, R. E. A test for concentration of electrolytes in sweat in cystic fibrosis of the pancreas utilizing pilocarpine by iontophoresis. *Pediatrics* **23,** 545–549 (1959).

26. Quinton, P. M. Chloride impermeability in cystic fibrosis. *Nature* **301,** 421–422 (1983).

27. Veeze, H. J. *et al.* Determinants of mild clinical symptoms in cystic fibrosis patients. Residual chloride secretion measured in rectal biopsies in relation to the genotype. *J. Clin. Invest.* **93,** 461–466 (1994).

28. Knowles, M. R. *et al.* Abnormal ion permeation through cystic fibrosis respiratory epithelium. *Science* **221,** 1067–1070 (1983).

29. Knowles, M. R., Paradiso, A. M. & Boucher, R. C. In vivo nasal potential difference: techniques and protocols for assessing efficacy of gene transfer in cystic fibrosis. *Hum. Gene Ther.* **6,** 445–455 (1995).

30. de Jonge, H. R. *et al.* Ex vivo CF diagnosis by intestinal current measurements (ICM) in small aperture, circulating Ussing chambers. *J. Cyst. Fibros.* **3 Suppl 2,** 159–163 (2004).

31. Wilschanski, M. *et al.* Mutations in the cystic fibrosis transmembrane regulator gene and in vivo transepithelial potentials. *Am. J. Respir. Crit. Care Med.* **174,** 787–794 (2006).

32. Bronsveld, I. *et al.* Residual chloride secretion in intestinal tissue of deltaF508 homozygous twins and siblings with cystic fibrosis. The European CF Twin and Sibling Study Consortium. *Gastroenterology* **119,** 32–40 (2000).

33. Sousa, M. *et al.* Measurements of CFTR-mediated Cl- secretion in human rectal biopsies constitute a robust biomarker for Cystic Fibrosis diagnosis and prognosis. *PLoS ONE* **7,** e47708 (2012).

34. Derichs, N. *et al.* Intestinal current measurement for diagnostic classification of patients with questionable cystic fibrosis: validation and reference data. *Thorax* **65,** 594–599 (2010).

35. Beekman, J. M. *et al.* CFTR functional measurements in human models for diagnosis, prognosis and personalized therapy: Report on the pre-conference meeting to the 11th ECFS Basic Science Conference, Malta, 26-29 March 2014. *J. Cyst. Fibros.* **13,** 363–372 (2014).

36. De Boeck, K. *et al.* CFTR biomarkers: time for promotion to surrogate end-point. *Eur. Respir. J.* **41,** 203–216 (2013).

37. van Meegen, M. A., Terheggen-Lagro, S. W. J., Koymans, K. J., van der Ent, C. K. & Beekman, J. M. Apical CFTR expression in human nasal epithelium correlates with lung disease in cystic fibrosis. *PLoS ONE* **8,** e57617 (2013).

38. Thomas, S. R., Jaffe, A., Geddes, D. M., Hodson, M. E. & Alton, E. W. Pulmonary disease severity in men with deltaF508 cystic fibrosis and residual chloride secretion. *Lancet* **353,** 984–985 (1999).

39. Borthwick, L. A. *et al.* Is CFTR-delF508 really absent from the apical membrane of the airway epithelium? *PLoS ONE* **6,** e23226 (2011).

40. Carvalho-Oliveira, I. *et al.* CFTR localization in native airway cells and cell lines expressing wild-type or F508del-CFTR by a panel of different antibodies. *J. Histochem. Cytochem.* **52,** 193–203 (2004).

41. Penque, D. *et al.* Cystic fibrosis F508del patients have apically localized CFTR in a reduced number of airway cells. *Lab. Invest.* **80,** 857–868 (2000).

42. Ho, L. P. *et al.* Correlation between nasal potential difference measurements, genotype and clinical condition in patients with cystic fibrosis. *Eur. Respir. J.* **10,** 2018–2022 (1997).

43. Hyde, S. C. *et al.* Structural model of ATP-binding proteins associated with cystic fibrosis, multidrug resistance and bacterial transport. *Nature* **346,** 362–365 (1990).

44. Gadsby, D. C. & Nairn, A. C. Regulation of CFTR Cl- ion channels by phosphorylation and dephosphorylation. *Adv. Second Messenger Phosphoprotein Res.* **33,** 79–106 (1999).

45. Cunningham, S. A., Worrell, R. T., Benos, D. J. & Frizzell, R. A. cAMP-stimulated ion currents in Xenopus oocytes expressing CFTR cRNA. *Am. J. Physiol.* **262,** C783–8 (1992). unmethylated unmethylated unmethylated

46. French, P. J. *et al.* Isotype-specific activation of cystic fibrosis transmembrane conductance regulator-chloride channels by cGMP-dependent protein kinase II. *J. Biol. Chem.* **270,** 26626–26631 (1995).

47. Vergani, P., Lockless, S. W., Nairn, A. C. & Gadsby, D. C. CFTR channel opening by ATP-driven tight dimerization of its nucleotide-binding domains. *Nature* **433,** 876–880 (2005).

48. Waldman, D. B., Gardner, J. D., Zfass, A. M. & Makhlouf, G. M. Effects of vasoactive intestinal peptide, secretin, and related peptides on rat colonic transport and adenylate cyclase activity. *Gastroenterology* **73,** 518–523 (1977).

49. Chan, H. C., Fong, S. K., So, S. C., Chung, Y. W. & Wong, P. Y. Stimulation of anion secretion by beta-adrenoceptors in the mouse endometrial epithelium. *J. Physiol. (Lond.)* **501 (Pt 3),** 517–525 (1997).

50. Fong, S. K. & Chan, H. C. Regulation of anion secretion by prostaglandin E2 in the mouse endometrial epithelium. *Biol. Reprod.* **58,** 1020–1025 (1998).

51. Thiagarajah, J. R. & Verkman, A. S. CFTR inhibitors for treating diarrheal disease. *Clin. Pharmacol. Ther.* **92,** 287–290 (2012).

52. Naren, A. P. *et al.* A macromolecular complex of beta 2 adrenergic receptor, CFTR, and ezrin/radixin/moesin-binding phosphoprotein 50 is regulated by PKA. *Proc. Natl. Acad. Sci. U.S.A.* **100,** 342–346 (2003).

53. Guggino, W. B. & Stanton, B. A. New insights into cystic fibrosis: molecular switches that regulate CFTR. *Nat. Rev. Mol. Cell Biol.* **7,** 426–436 (2006).

54. Armstrong, D. K., Cunningham, S., Davies, J. C. & Alton, E. W. F. W. Gene therapy in cystic fibrosis. *Arch. Dis. Child.* **99,** 465–468 (2014).

55. Wood, A. J. *et al.* Targeted genome editing across species using ZFNs and TALENs. *Science* **333,** 307 (2011).

56. Doudna, J. A. & Charpentier, E. Genome editing. The new frontier of genome engineering with CRISPR-Cas9. *Science* **346,** 1258096 (2014).

57. Liu, X. *et al.* Spliceosome-mediated RNA trans-splicing with recombinant adeno-associated virus partially restores cystic fibrosis transmembrane conductance regulator function to polarized human cystic fibrosis airway epithelial cells. *Hum. Gene Ther.* **16,** 1116–1123 (2005).

58. Mansfield, S. G. *et al.* 5' exon replacement and repair by spliceosome-mediated RNA trans-splicing. *RNA* **9,** 1290–1297 (2003).

59. Zamecnik, P. C., Raychowdhury, M. K., Tabatadze, D. R. & Cantiello, H. F. Reversal of cystic fibrosis phenotype in a cultured Delta508 cystic fibrosis transmembrane conductance regulator cell line by oligonucleotide insertion. *Proc. Natl. Acad. Sci. U.S.A.* **101,** 8150–8155 (2004).

60. Fernandez Alanis, E. *et al.* An exon-specific U1 small nuclear RNA (snRNA) strategy to correct splicing defects. *Hum. Mol. Genet.* **21,** 2389–2398 (2012).

61. Nissim-Rafinia, M. *et al.* Restoration of the cystic fibrosis transmembrane conductance regulator function by splicing modulation. *EMBO Rep.* **5,** 1071–1077 (2004).

62. Nissim-Rafinia, M. & Kerem, B. Splicing modulation as a modifier of the CFTR function. *Prog. Mol. Subcell. Biol.* **44,** 233–254 (2006).

63. Population variation of common cystic fibrosis mutations. The Cystic Fibrosis Genetic Analysis Consortium. *Hum. Mutat.* **4,** 167–177 (1994).

64. Welch, E. M. *et al.* PTC124 targets genetic disorders caused by nonsense mutations. *Nature* **447,** 87–91 (2007).

65. Howard, M., Frizzell, R. A. & Bedwell, D. M. Aminoglycoside antibiotics restore CFTR function by overcoming premature stop mutations. *Nat Med* **2,** 467–469 (1996).

66. Du, M. *et al.* PTC124 is an orally bioavailable compound that promotes suppression of the human CFTR-G542X nonsense allele in a CF mouse model. *Proc. Natl. Acad. Sci. U.S.A.* **105,** 2064–2069 (2008).

67. Kerem, E. *et al.* Effectiveness of PTC124 treatment of cystic fibrosis caused by nonsense mutations: a prospective phase II trial. *Lancet* **372,** 719–727 (2008).

68. Sermet-Gaudelus, I. *et al.* Ataluren (PTC124) induces cystic fibrosis transmembrane conductance regulator protein expression and activity in children with nonsense mutation cystic fibrosis. *Am. J. Respir. Crit. Care Med.* **182,** 1262–1272 (2010).

69. Wilschanski, M. *et al.* Chronic ataluren (PTC124) treatment of nonsense mutation cystic fibrosis. *Eur. Respir. J.* **38,** 59–69 (2011).

70. Kerem, E. *et al.* Ataluren for the treatment of nonsense-mutation cystic fibrosis: a randomised, double-blind, placebo-controlled phase 3 trial. *Lancet Respir Med* **2,** 539–547 (2014).

71. Finkel, R. S. *et al.* Phase 2a study of ataluren-mediated dystrophin production in patients with nonsense mutation Duchenne muscular dystrophy. *PLoS ONE* **8,** e81302 (2013).

72. Lukacs, G. L. & Verkman, A. S. CFTR: folding, misfolding and correcting the ΔF508 conformational defect. *Trends Mol Med* **18,** 81–91 (2012).

73. Rowe, S. M. & Verkman, A. S. Cystic fibrosis transmembrane regulator correctors and potentiators. *Cold Spring Harb Perspect Med* **3,** (2013).

74. Van Goor, F. *et al.* Correction of the F508del-CFTR protein processing defect in vitro by the investigational drug VX-809. *Proc. Natl. Acad. Sci. U.S.A.* **108,** 18843–18848 (2011).

75. Clancy, J. P. *et al.* Results of a phase IIa study of VX-809, an investigational CFTR corrector compound, in subjects with cystic fibrosis homozygous for the F508del-CFTR mutation. *Thorax* **67**, 12-8 (2011).

76. Leonard, A., Lebecque, P., Dingemanse, J. & Leal, T. A randomized placebo-controlled trial of miglustat in cystic fibrosis based on nasal potential difference. *J. Cyst. Fibros.* **11,** 231–236 (2012).

77. Zeitlin, P. L. *et al.* Evidence of CFTR function in cystic fibrosis after systemic administration of 4-phenylbutyrate. *Mol. Ther.* **6,** 119–126 (2002).

78. De Stefano, D. *et al.* Restoration of CFTR function in patients with cystic fibrosis carrying the F508del-CFTR mutation. *Autophagy* **10,** 2053–2074 (2014).

79. Du, K. & Lukacs, G. L. Cooperative assembly and misfolding of CFTR domains in vivo. *Mol. Biol. Cell* **20,** 1903–1915 (2009).

80. Hoelen, H. *et al.* The primary folding defect and rescue of ΔF508 CFTR emerge during translation of the mutant domain. *PLoS ONE* **5,** e15458 (2010).

81. Protasevich, I. *et al.* Thermal unfolding studies show the disease causing F508del mutation in CFTR thermodynamically destabilizes nucleotide-binding domain 1. *Protein Sci.* **19,** 1917–1931 (2010).

82. Rabeh, W. M. *et al.* Correction of both NBD1 energetics and domain interface is required to restore ΔF508 CFTR folding and function. *Cell* **148,** 150–163 (2012).

83. French, P. J. *et al.* Genistein activates CFTR Cl- channels via a tyrosine kinase- and protein phosphatase-independent mechanism. *Am. J. Physiol.* **273,** C747–53 (1997).

84. Sears, C. L. *et al.* Genistein and tyrphostin 47 stimulate CFTR-mediated Cl- secretion in T84 cell monolayers. *Am. J. Physiol.* **269,** G874–82 (1995).

85. Melin, P. *et al.* The cystic fibrosis mutation G1349D within the signature motif LSHGH of NBD2 abolishes the activation of CFTR chloride channels by genistein. *Biochem. Pharmacol.* **67,** 2187–2196 (2004).

86. Wang, W., Bernard, K., Li, G. & Kirk, K. L. Curcumin opens cystic fibrosis transmembrane conductance regulator channels by a novel mechanism that requires neither ATP binding nor dimerization of the nucleotide-binding domains. *J. Biol. Chem.* **282,** 4533–4544 (2007).

87. Bernard, K., Wang, W., Narlawar, R., Schmidt, B. & Kirk, K. L. Curcumin cross-links cystic fibrosis transmembrane conductance regulator (CFTR) polypeptides and potentiates CFTR channel activity by distinct mechanisms. *J. Biol. Chem.* **284,** 30754–30765 (2009).

88. Ramsey, B. W. *et al.* A CFTR potentiator in patients with cystic fibrosis and the G551D mutation. *N. Engl. J. Med.* **365,** 1663–1672 (2011).

89. Davies, J. C. *et al.* Efficacy and safety of ivacaftor in patients aged 6 to 11 years with cystic fibrosis with a G551D mutation. *Am. J. Respir. Crit. Care Med.* **187,** 1219–1225 (2013).

90. Accurso, F. J. *et al.* Effect of VX-770 in persons with cystic fibrosis and the G551D-CFTR mutation. *N. Engl. J. Med.* **363,** 1991–2003 (2010).

91. Rowe, S. M. *et al.* Clinical mechanism of the cystic fibrosis transmembrane conductance regulator potentiator ivacaftor in G551D-mediated cystic fibrosis. *Am. J. Respir. Crit. Care Med.* **190,** 175–184 (2014).

92. McKone, E. F. *et al.* Long-term safety and efficacy of ivacaftor in patients with cystic fibrosis who have the Gly551Asp-CFTR mutation: a phase 3, open-label extension study (PERSIST). *Lancet Respir Med* **2,** 902–910 (2014).

93. Yu, H. *et al.* Ivacaftor potentiation of multiple CFTR channels with gating mutations. *J. Cyst. Fibros.* **11,** 237–245 (2012).

94. De Boeck, K. *et al.* Efficacy and safety of ivacaftor in patients with cystic fibrosis and a non-G551D gating mutation. *J. Cyst. Fibros.* **13**: 674–80 (2014).

95. Van Goor, F., Yu, H., Burton, B. & Hoffman, B. J. Effect of ivacaftor on CFTR forms with missense mutations associated with defects in protein processing or function. *J. Cyst. Fibros.* **13,** 29–36 (2014).

96. Wainwright, C. E. *et al.* Lumacaftor-Ivacaftor in Patients with Cystic Fibrosis Homozygous

for Phe508del CFTR. *N. Engl. J. Med.* (2015). doi:10.1056/NEJMoa1409547

97. Verkman, A. S. & Galietta, L. J. V. Chloride channels as drug targets. *Nat Rev Drug Discov* **8,** 153–171 (2009).

98. Halfhide, C., Evans, H. J. & Couriel, J. Inhaled bronchodilators for cystic fibrosis. *Cochrane Database Syst Rev* **19**:(4):CD003428 (2005).

99. De Gruttola, V. G. *et al.* Considerations in the evaluation of surrogate endpoints in clinical trials. summary of a National Institutes of Health workshop. *Control Clin Trials* **22,** 485–502 (2001).

100. Biomarkers Definitions Working Group. Biomarkers and surrogate endpoints: preferred definitions and conceptual framework. *Clin. Pharmacol. Ther.* **69,** 89–95 (2001).

101. Corey, M., Edwards, L., Levison, H. & Knowles, M. Longitudinal analysis of pulmonary function decline in patients with cystic fibrosis. *J. Pediatr.* **131,** 809–814 (1997).

102. Middleton, P. G., Geddes, D. M. & Alton, E. W. Protocols for in vivo measurement of the ion transport defects in cystic fibrosis nasal epithelium. *Eur. Respir. J.* **7,** 2050–2056 (1994).

103. Mall, M., Hirtz, S., Gonska, T. & Kunzelmann, K. Assessment of CFTR function in rectal biopsies for the diagnosis of cystic fibrosis. *J. Cyst. Fibros.* **3 Suppl 2,** 165–169 (2004).

104. Li, H., Sheppard, D. N. & Hug, M. J. Transepithelial electrical measurements with the Ussing chamber. *J. Cyst. Fibros.* **3 Suppl 2,** 123–126 (2004).

105. Sato, T. *et al.* Single Lgr5 stem cells build crypt-villus structures in vitro without a mesenchymal niche. *Nature* **459,** 262–265 (2009).

106. Sato, T. *et al.* Long-term Expansion of Epithelial Organoids From Human Colon, Adenoma, Adenocarcinoma, and Barrett's Epithelium. *Gastroenterology* **141**: 1762–72 (2011).

107. Sato, T. *et al.* Paneth cells constitute the niche for Lgr5 stem cells in intestinal crypts. *Nature* **469,** 415–418 (2011).

108. Jung, P. *et al.* Isolation and in vitro expansion of human colonic stem cells. *Nat Med* **17**: 1225–7 (2011).

109. Sato, T. & Clevers, H. Growing self-organizing mini-guts from a single intestinal stem cell: mechanism and applications. *Science* **340,** 1190–1194 (2013).

110. Dekkers, J. F., van der Ent, C. K. & Beekman, J. M. Novel opportunities for CFTR-targeting drug development using organoids. *Rare Dis* **1,** e27112 (2013).

111. Dekkers, J. F. *et al.* A functional CFTR assay using primary cystic fibrosis intestinal organoids. *Nat Med* **19**: 939–45 (2013).

112. Okiyoneda, T. *et al.* Mechanism-based corrector combination restores ΔF508-CFTR folding and function. *Nat. Chem. Biol.* **9,** 444–454 (2013).

113. Schwank, G. *et al.* Functional repair of CFTR by CRISPR/Cas9 in intestinal stem cell organoids of cystic fibrosis patients. *Cell Stem Cell* **13,** 653–658 (2013).

Chapter 2

A functional CFTR assay using primary cystic fibrosis intestinal organoids

Johanna F Dekkers[1–3], Caroline L Wiegerinck[2,4], Hugo R de Jonge[5], Inez Bronsveld[6], Hettie M Janssens[7], Karin M de Winter-de Groot[1], Arianne M Brandsma[1,3], Nienke W M de Jong[1,3], Marcel J C Bijvelds[5], Bob J Scholte[8], Edward E S Nieuwenhuis[4], Stieneke van den Brink[9,10], Hans Clevers[9,10], Cornelis K van der Ent[1], Sabine Middendorp[2,4] & Jeffrey M Beekman[1–3]

[1]Department of Pediatric Pulmonology, [2]Center for Molecular and Cellular Intervention, [3]Department of Immunology, [4]Department of Pediatric Gastroenterology, Wilhelmina Children's Hospital, University Medical Centre Utrecht, The Netherlands, [5]Department of Gastroenterology & Hepatology, Erasmus University Medical Centre, Rotterdam, The Netherlands, [6]Department of Pulmonology, University Medical Centre Utrecht, The Netherlands, [7]Department of Pediatric Pulmonology, Erasmus University Medical Centre / Sophia Children's Hospital, Rotterdam, the Netherlands, [8]Department of Cell Biology, Erasmus University Medical Centre, Rotterdam, The Netherlands, [9]Hubrecht Institute for Developmental Biology and Stem Cell Research, and University Medical Center Utrecht, The Netherlands

Nature Medicine 2013;19:939-45

ABSTRACT

We have recently established conditions allowing long-term expansion of epithelial organoids from intestine, recapitulating essential features of the *in vivo* tissue architecture. Here, we apply this technology to study primary intestinal organoids of people suffering from cystic fibrosis, a disease caused by cystic fibrosis transmembrane conductance regulator (*CFTR)* gene mutations. Forskolin induces rapid swelling of organoids derived from healthy controls or wild-type mice, but this effect is strongly reduced in organoids of cystic fibrosis subjects or F508del-Cftr mice and absent in *Cftr*-deficient organoids. This is phenocopied by CFTR-specific inhibitors. Forskolin-induced swelling of *in vitro* expanded human control and cystic fibrosis organoids corresponds quantitatively with forskolin-induced anion currents in *ex vivo* freshly excised rectal biopsies. Function of F508del-CFTR is restored upon incubation at low temperature, as well as by CFTR-restoring compounds. This relatively simple and robust assay will facilitate diagnosis, functional studies, drug development and personalized medicine approaches in cystic fibrosis.

INTRODUCTION

The cystic fibrosis transmembrane conductance regulator (CFTR) protein functions as an anion channel, and is essential for fluid and electrolyte homeostasis at epithelial surfaces of many organs, including lung and intestine. Cystic fibrosis is caused by mutations in the *CFTR* gene[1-3], and disease expression is highly variable between individuals (www.cftr2.org). People with cystic fibrosis have a median life expectancy of approximately 40 years, and accumulate viscous mucus in the pulmonary and gastrointestinal tract that is associated with bacterial infections, aberrant inflammation and malnutrition[4]. Over *CFTR* 1900 mutations have been identified, but the most dominant mutation (~67% of total mutant alleles world wide) is a deletion of phenylalanine at position 508 (F508del-CFTR) (www.genet.sickkids.on.ca). This causes misfolding, ER-retention and early degradation of the CFTR protein that prevents its function at the plasma membrane[5]. Other *CFTR* mutations also impair protein folding or production, gating, conductance, splicing or interactions with other proteins[6].

Current therapies for cystic fibrosis are mainly symptomatic and focus to reduce bacterial pressure, inflammation, and normalize nutrient uptake and physical growth. Recently, multiple compounds have been identified that target mutation-specific defects of the CFTR protein itself[6,7]. Current clinical trials that target the basic defect aim to (i) induce premature stopcodon read-through, (ii) correct plasma membrane trafficking of CFTR (correctors), and (iii) enhance CFTR gating (potentiators). A phase III clinical trial has been completed successfully using the potentiator VX-770 (Ivacaftor, Kalydeco) in subjects with G551D-CFTR, demonstrating that mutation-specific drug targeting is feasible[8]. Combination therapy of a corrector (VX-809) and potentiator (VX-770) is currently assessed in a phase II clinical trial for subjects harboring F508del-CFTR.

Although CFTR-specific drug targeting is very promising, the level of functional CFTR restoration is still limited[9-11]. In addition, subjects show variable responses to these therapies due to yet undefined mechanisms[8,12-14], suggesting that the ability to predict individual drug responses would facilitate clinical efficacy and drug registration. Together, this indicates that development of new compounds and screening of drug efficacy at the level of individuals are urgently needed. Thus far, limited primary cell models are available to screen for compounds that restore mutant CFTR function. When such an *in vitro* model can be further expanded to analyse drug responses of individual subjects, it may improve drug efficacy by selecting drug-responsive subgroups.

Here, we demonstrate a rapid and quantitative assay for CFTR function in a mouse and human primary intestinal culture method that was recently developed[15-17]. The culture enables intestinal stem cells to expand into closed organoids containing crypt-like structures and an internal lumen lined by differentiated cells, recapitulating the *in vivo* tissue architecture. Intestinal CFTR is predominantly expressed at the apical membrane of the crypt cells where its activation drives secretion of electrolytes and fluids[18-20]. We found that forskolin[21] induces rapid swelling of both human healthy control and mouse wild-type organoids that completely depends on CFTR, as demonstrated by analysis of intestinal organoids from *Cftr*^{tm1Cam} knockout mice (*Cftr*$^{-/-}$) mice or individuals with cystic fibrosis, or upon chemical inhibition of CFTR. Forskolin-induced swelling by *in vitro*-expanded rectal organoids is comparable with forskolin-induced anion currents measured in *ex vivo* human rectal biopsies. Restoration of the function of F508del-CFTR mutant protein by low temperature and chemicals was easily detected by organoid-based fluid transport

measurements, and responses to CFTR-restoring drugs were variable between organoids derived from different F508del homozygous subjects. This robust assay is the first functional readout developed in human organoids, and will facilitate diagnosis, functional studies, drug development, and personalized medicine for cystic fibrosis.

RESULTS

Quantification of forskolin-induced organoid swelling

We first assessed whether forskolin, which raises intracellular cAMP and thereby activates CFTR, could mediate fluid secretion into the lumen of small intestinal organoids derived from wild-type mice. Using live cell microscopy, we observed a rapid expansion of the lumen and total organoid surface area when forskolin was added, while DMSO-treated organoids were unaffected (Fig. 1a; Supplementary video 1). Removal of forskolin reversed the swelling of organoids (Supplementary Fig. 1a).

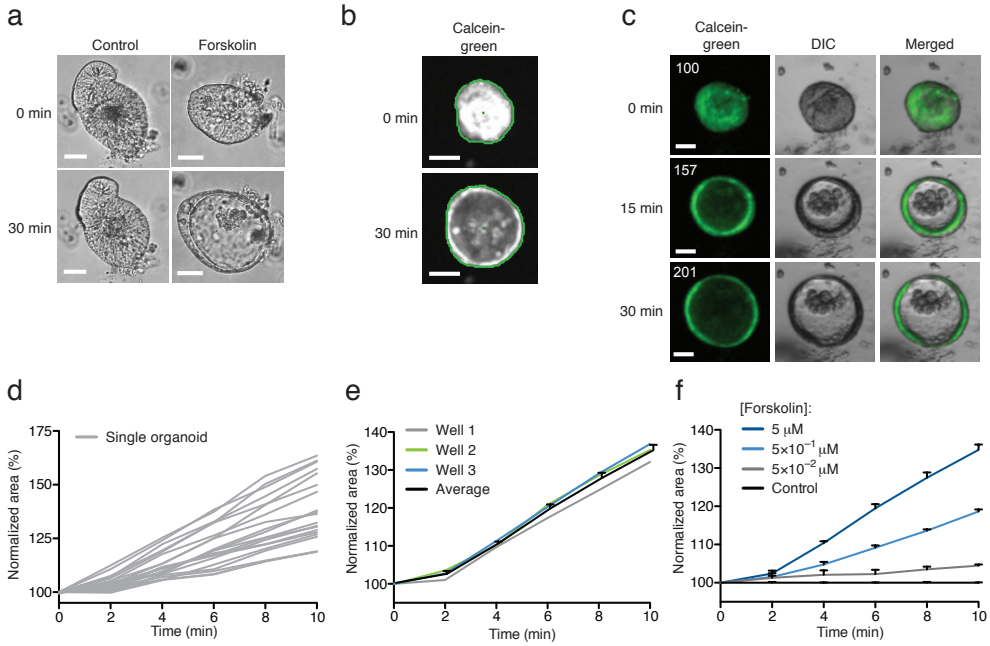

Figure 1. **Quantification of forskolin-induced mouse organoid swelling.** (**a**) Light microscopy analysis of organoids stimulated with forskolin or DMSO. Representative examples for the indicated time points after start of stimulation are shown. (**b**) Fluorescence confocal image of a calcein-green-labeled organoid with object recognition (green line) by image analysis software. (**c**) Representative example of a forskolin-stimulated calcein-green-labeled organoid. Differential interference contrast (DIC) and fluorescence was imaged using live cell confocal microscopy. Surface area relative to t = 0 is indicated in the top-left corner. (**d**) The surface area relative to t = 0 (normalized area) of all responding individual organoids from a single well. (**e**) The total organoid surface area normalized to t = 0 from three independent wells. The average response of the individual wells is indicated in black (mean ± s.e.m). (**f**) Dose-dependent increase of surface area by forskolin. Each line represents the average response from three individual wells as illustrated in (**e**) (mean ± s.e.m). Scale bars (**a–c**) 30 μm. All results are representative for at least three independent experiments.

Next, we quantified these responses by automated image analysis. We found excellent cell labelling (>100× over background) using calcein-green, a cell-permeable dye that gains fluorescence and is retained within living cells upon metabolic conversion. We quantified forskolin-induced swelling (FIS) of organoids using live cell confocal microscopy and imaging software that calculated the relative increase in the total area of all fluorescent objects for each time point upon forskolin addition per well (Fig. 1b,c; Supplementary Fig. 1b). The majority of organoids responded to forskolin stimulation (Fig. 1d). Approximately 5–10% of structures that were either very small or irregularly shaped and nonviable organoids did not respond to forskolin (Supplementary Fig. 1c,d), but their inclusion did not affect FIS measurement (Supplementary Fig. 1e). Time-dependent surface area increase of three independent wells showed limited variation (Fig. 1e), and a dose-dependent relation with forskolin (Fig. 1f). FIS of mouse organoids during the first 10 min is presented, as some wild-type mouse organoids burst and collapsed during longer stimulations (Supplementary Fig. 2a,b). Together, these results show that forskolin-induced organoid swelling can be quantified by automated fluorescent image analysis.

Forskolin-induced swelling of mouse organoids

High levels of *Cftr* mRNA in the organoids supported a role for Cftr in FIS (Supplementary Fig. 2d). To demonstrate that FIS is Cftr dependent, we used chemical inhibitors of CFTR[22,23], and *Cftr*$^{-/-}$[24] or *Cftr*^{tm1eur} (F508del-Cftr) mice[25,26]. Pre-incubation (2 h) with the CFTR inhibitors $CFTR_{inh}$-172[22] or GlyH-101[23] reduced FIS by respectively ~90% and ~75%, and their combination fully prevented FIS (Fig. 2a). In addition, FIS was absent in organoids of *Cftr*$^{-/-}$ mice (Fig. 2b,c; Supplementary video 1). Calcein-green labelling was comparable between wild-type and mutant organoids, indicating that *Cftr*$^{-/-}$ organoids were viable. Organoids of F508del-Cftr mice displayed low but detectable FIS (Fig. 2d,e; Supplementary video 1) that was sensitive to $CFTR_{inh}$-172 (Fig. 2f) suggesting residual Cftr activity as observed previously[25,26]. Together, these data demonstrate that FIS in mouse organoids is completely Cftr dependent.

To show that FIS can detect Cftr correction, we performed temperature-rescue experiments, a widely accepted method to increase F508del-CFTR function[27]. F508del-CFTR misfolding is reduced at 27 °C leading to enhanced levels of functional CFTR at the plasma membrane. Indeed, we observed increased FIS after overnight incubation of F508del-Cftr organoids at 27 °C (Fig. 2f). We next used the chemical correctors VRT-325[28] and Corr-4a[29] to restore F508del-Cftr function (references for CFTR-restoring compounds are provided in the online methods). Pre-incubation (24 h) with VRT-325 enhanced FIS whereas Corr-4a only slightly improved FIS, and was additive to correction by VRT-325 (Fig. 2g). CFTR inhibitors prevented FIS upon Cftr correction (Fig. 2f,g). Collectively, these results demonstrated that FIS of mouse organoids can reveal functional restoration of F508del-Cftr by correction approaches.

Forskolin-induced swelling of human organoids

We next assayed human intestinal organoid cultures. Mature CFTR (C-band, 170 kDa) and immature CFTR (B-band, 130 kDa) was detected by Western blot analysis in human healthy control organoids, but only B-band was detected in F508del-CFTR organoids (Fig. 3a). No CFTR B- or C-band was observed in organoids carrying E60X[30] and a non-reported allele that induces a frame shift in NBD2 at residue 1295 (4015delATTT). CFTR B- and C-band specificity was further

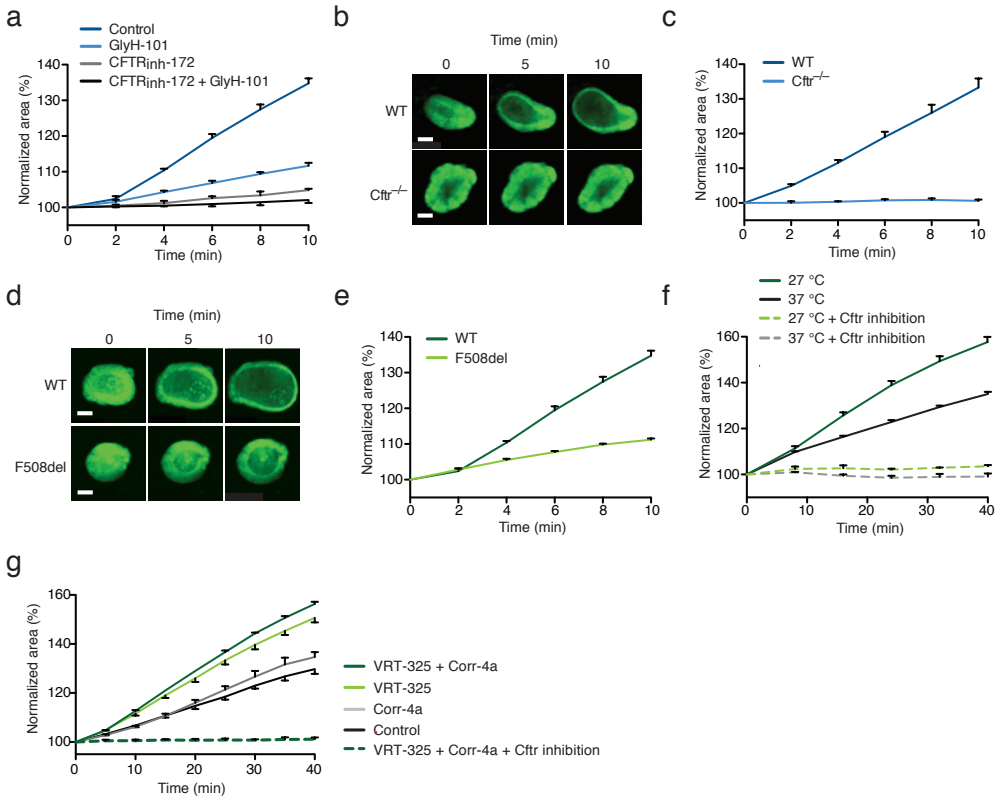

Figure 2. **Forskolin-induced swelling of mouse organoids is Cftr dependent.** (**a**) Normalized swelling curves of forskolin-stimulated calcein-green-labeled organoids pre-incubated with DMSO, CFTR-$_{inh}$172, GlyH-101 or both CFTR-$_{inh}$172 and GlyH-101 (mean ± s.e.m.). (**b**,**c**) Representative confocal microscopy images (**b**) and quantification of swelling (**c**) of calcein green–labeled *Cftr*$^{-/-}$ organoids and corresponding wild-type organoids in response to forskolin. Scale bars, 50 µm. (mean ± s.e.m.) (**d,e**) Similar to **b** and **d** but for F508del Cftr organoids. Scale bars, 50 µm. (mean ± s.e.m.) (**f**) Forskolin-induced swelling of calcein-green labeled F508del-Cftr organoids cultured for 24 h at 37 °C or 27 °C with or without CFTR inhibition (mean ± s.e.m.). Note that the timescale in **f** and **g** is larger. (**g**) Normalized forskolin-induced swelling of F508del-Cftr organoids pre-treated for 24 h with DMSO, VRT-325, Corr-4a or both correctors with or without CFTR inhibition (mean ± s.e.m.). All results are representative for at least three independent experiments.

indicated by Endo H and PNGase F treatment[5], respectively. CFTR colocalized with apical actin in healthy control organoids, but not in F508del-CFTR organoids (Fig. 3b). As for mouse organoids, rapid FIS of healthy control organoids was sensitive to chemical CFTR inhibition (Fig. 3c). Human organoids showed somewhat slower kinetics compared to mouse and rarely collapsed, and required longer pre-incubation time with CFTR inhibitors (3 h) (Fig. 3c; Supplementary Fig. 2c; Supplementary video 2).

We analysed FIS in a large number of intestinal organoids primarily derived from rectum but also from duodenum, ileum, and colon. We observed strong FIS in organoids derived from healthy control subjects (rectal organoids are shown in Fig. 3d, all organoids are presented in Supplementary Fig. 3a). Rectal organoids derived from individuals that are compound heterozygous for F508del and A455E[31], a genotype that is associated with mild cystic fibrosis[32], clearly displayed

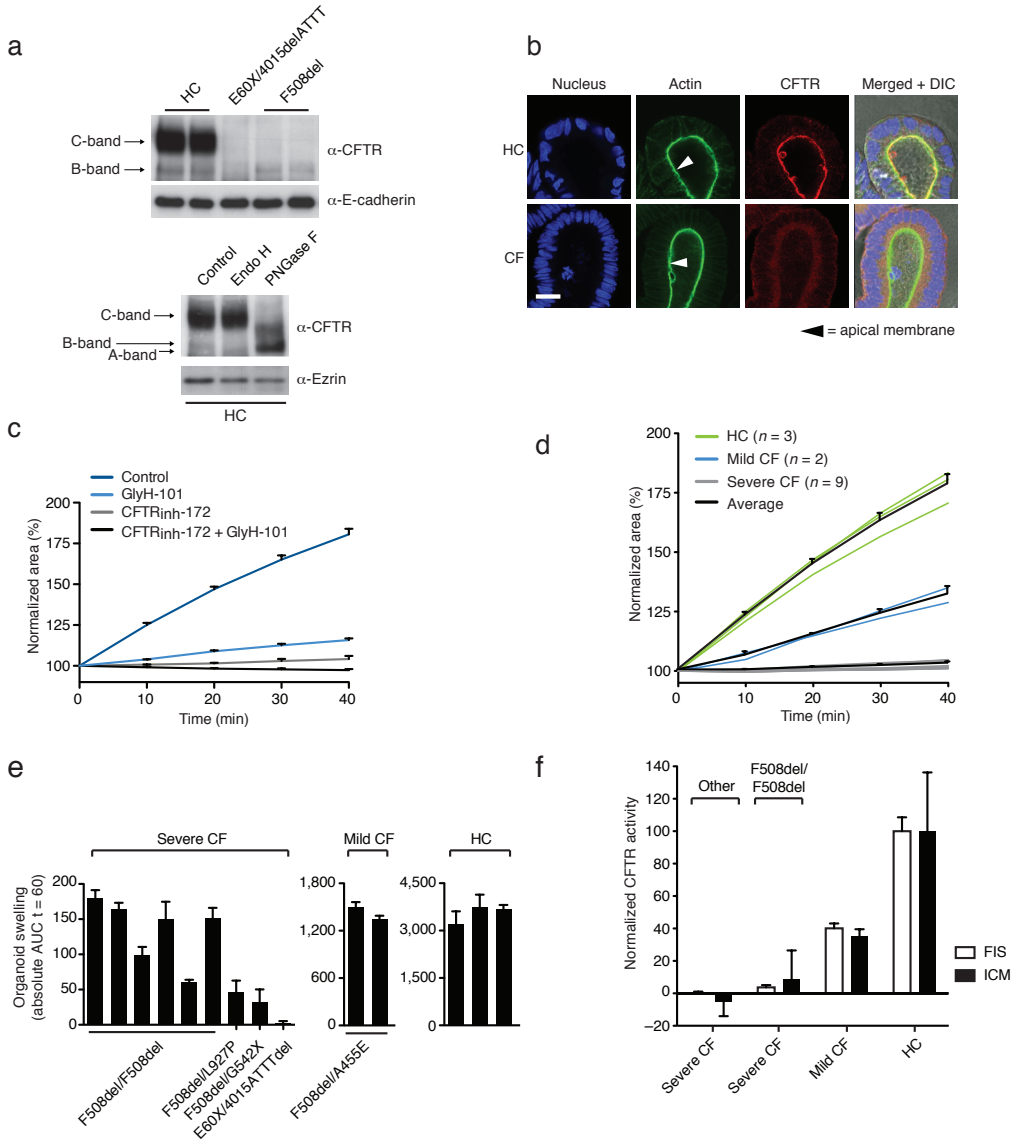

Figure 3. **Forskolin-induced swelling in human organoids is CFTR dependent.** (**a**) Western blot analysis of CFTR and E-cadherin (loading control) expression in human rectal healthy control (HC; *n* = 2), E60X/4015delATTT (*n* = 1), or homozygous F508del-CFTR organoids (*n* = 2; upper panel) and CFTR and ezrin (loading control) expression in whole cell lysates of human rectal organoids that were either not treated (control) or treated with the deglycosylation enzymes Endo H or PNGase F (lower panel). (**b**) CFTR detection by M3A7 in a healthy control or F508del-CFTR organoid, costained with phalloidin-FITC (actin) and DAPI (nucleus). Differential interference contrast (DIC) and fluorescence was imaged using confocal microscopy. Scale bars: 20 µm. (**c**) Quantification of forskolin-induced healthy control organoid swelling pre-incubated with DMSO, $CFTR_{inh}$-172, GlyH-101 or both $CFTR_{inh}$-172 and GlyH-101 (mean ± s.e.m.). (**d**) Forskolin-induced swelling of rectal organoids derived from three individual healthy controls, two individuals with a mild cystic fibrosis (CF) genotype (F508del/A455E) and nine individuals with a severe cystic fibrosis genotype (1 × E60X/4015ATTTdel; 1 × F508del/G542X; 1 × F508del/L927P; 6 × F508del/F508del). Average swelling of the different groups is indicated in black (mean ± s.e.m.). (**e**) FIS responses of organoids from healthy controls or cystic fibrosis subjects expressed as absolute area under the curve (AUC) calculated from

time lapses as illustrated in (**d**) (baseline = 100%, t = 60 min). Each bar represents AUC values averaged from at least three independent experiments per individual (mean ± s.e.m.). (**f**) Comparison of CFTR activity measured by FIS of organoids from healthy controls or cystic fibrosis subjects or by intestinal current measurements (ICM) of the corresponding rectal biopsies. ICM bars of the different indicated groups represent forskolin-induced CFTR-dependent cumulative chloride secretion (μA cm^{-2}) relative to the average healthy control response (set at 100%). FIS bars represent FIS expressed as area under the curve (AUC) averaged from at least three independent experiments per individual as illustrated in (**f**) relative to the average healthy control response (100%). (healthy control $n = 3$; mild cystic fibrosis $n = 2$; severe cystic fibrosis (F508del/F508del) $n = 5$; severe cystic fibrosis (Other; E60X/4015ATTTdel and F508del/G542X) $n = 2$; mean ± s.d.). All results are representative for at least three independent experiments. ICMs were performed on four rectal biopsies.

reduced FIS levels compared to healthy control organoids (Supplementary video 2). Subjects with severe cystic fibrosis genotypes (homozygous for F508del or compound heterozygous for F508del and L927P[33], or G542X[31]) displayed much lower FIS that was variable between individual subjects (Fig. 3e + Supplementary video 2). We observed no FIS in E60X/4015delATTT organoids (Supplementary video 2). Chemical inhibition of CFTR abolished all FIS responses of organoids from subjects with cystic fibrosis (Supplementary Fig. 3b).

FIS measurements of *in vitro* expanded organoids derived from healthy controls or individuals with cystic fibrosis, subdivided into severe and mild genotypes, correlated tightly with forskolin-induced intestinal current measurements (ICM) performed on rectal suction biopsies[34,35] from which these organoids originated (Fig. 3f). Most ICM tracings of biopsies from individual with cystic fibrosis showed residual forskolin-induced anion currents that corresponded with a quantitatively similar CFTR-dependent forskolin response in the FIS assay (a representative ICM tracing, a paired analysis of FIS and ICM for individual subjects and Spearman's rank correlation analysis ($R = 0.84$, $P = 0.001$) is provided in Supplementary Fig. 4a–c, respectively). Together, these data indicated that FIS in human organoids can accurately measure CFTR function, and show that residual CFTR function in rectal organoids may differ between individuals homozygous for the F508del-CFTR mutation.

CFTR restoration in organoids of cystic fibrosis subjects

We next assessed functional restoration of F508del-CFTR in human organoids by low temperature, or the chemical correctors VRT-325, Corr-4a, C8 (http://cftrfolding.org), VX-809[36] and the potentiator VX-770[9]. Incubation of F508del-CFTR homozygous organoids at low temperature (27 °C) increased FIS as expected (Fig. 4a). We next established dose-response curves for single treatment of VX-809 (upon 24 h pre-incubation) or VX-770 (added simultaneously with forskolin) in organoids from six homozygous F508del subjects (Fig. 4b), and measured EC50 values of 135 ± 40 nM, and 161 ± 39 nM, respectively. These dose-responses are within ranges reported in human bronchial epithelial cells[9,36]. VX-809 combined with VX-770 induced increased levels of FIS, which was abolished by chemical CFTR inhibition (Fig. 4c). Next, multiple correctors were assayed to improve FIS upon 24 h pre-incubation in F508del homozygous organoids. All correctors increased FIS albeit with a different efficacy (Fig 4d–f + Supplementary video 3; see Supplementary Fig. 5a for non-rectal organoids). We observed that VRT-325 and Corr-4a or C8 and Corr-4a synergistically increased FIS, which was in contrast with the additive effect of VRT-325 and Corr-4a in mouse organoids (Fig. 2g). F508del-CFTR correction approaches by temperature and chemicals were all sensitive

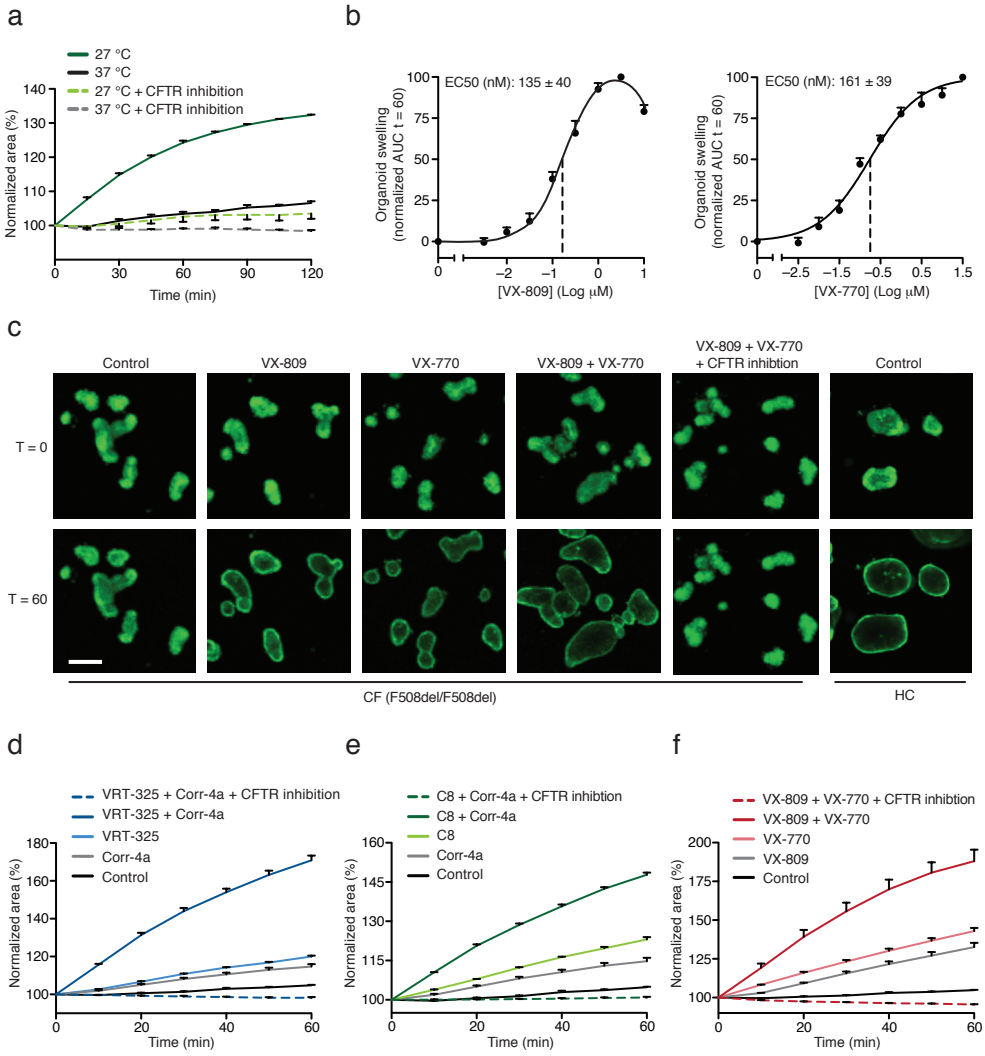

Figure 4. Chemical CFTR correction in human rectal organoids from cystic fibrosis subjects. (**a**) Normalized swelling of forskolin-induced calcein-green labeled F508del-CFTR organoids cultured for 24 h at 37 °C or 27 °C with or without CFTR inhibition (mean ± s.e.m.). (**b**) EC50 of F508del organoids for VX-809 or VX-770. The lines represent FIS expressed as area under the curve (AUC; baseline 100%, t = 60 min) calculated from time lapses as presented in (**d–f**) relative to DMSO (0%) treated and VX-809 log(0.5) μM or VX-770 log(1.5) μM (100%) treated organoids. (*n* = 6 F508del homozygous organoids; mean ± s.e.m.) (**c**) Representative confocal microscopy images of calcein-green labeled healthy control or F508del-CFTR organoids in response to forskolin upon pharmacological restoration of CFTR. Scale bars 100 μm. (**d–f**) Time lapses of normalized forskolin-induced swelling of F508del-CFTR organoids pre-treated for 24 h with DMSO, VRT-325 (10 μM), Corr-4a (10 μM), or both correctors with or without CFTR inhibition (**d**), with DMSO, C8 (10 μM), Corr-4a (10 μM), or both correctors with or without CFTR inhibition (**f**) or stimulated with the corrector VX-809 (24 h pre-treatment, 3 μM), the potentiator VX-770 (simultaneous with forskolin, 3 μM) or combined compound treatment with or without CFTR inhibition (**f**) (mean ± s.e.m.).

to CFTR inhibitors (Fig. 4a,c–f). These data indicate that FIS can reliably measure correction or potentiation of F508del-CFTR.

We studied FIS responses to a panel of CFTR-restoring drugs in rectal organoids derived from nine individuals harbouring various severe *CFTR* mutations, including six F508del homozygous organoids. We observed different drug-induced FIS between F508del homozygous organoids (Fig. 5a–c; see Supplementary Fig. 5b for F508del/A455E organoids). FIS was variable between organoids upon incubation with single drugs, and the distribution of high and low responders was unique for a restoration approach (Fig. 5a–c; subject order is similar to Fig. 3e in the 'Severe CF' panel). CF5 appears to be a low responder to any corrector or VX-770, but showed an exceptionally small response to VRT-325. CF3 and CF5 organoids displayed similar responses to VX-809, but differed in their response to C8. The measured FIS over expected FIS

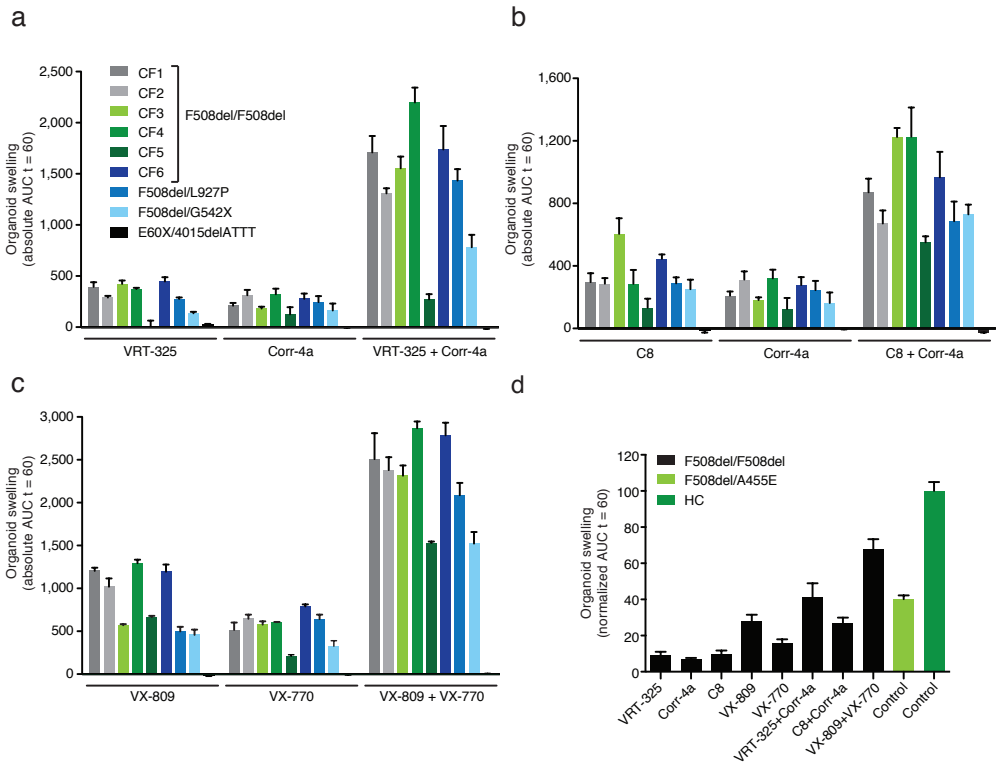

Figure 5. Differential FIS between organoids of subjects with cystic fibrosis upon chemical CFTR restoration. (**a–c**) Quantification of FIS in organoids derived from nine individuals with cystic fibrosis pre-treated for 24 h with VRT-325 (10 μM), Corr-4a (10 μM), or both correctors (**a**), with C8 (10 μM), Corr-4a (10 μM), or both correctors (**b**) or stimulated with VX-809 (24 h pre-treatment, 3 μM), VX-770 (simultaneous with forskolin, 3 μM) or both compounds (**c**). The bars correspond to the bars depicted in **Fig. 3e** of the 'Severe CF' panel. Each bar represents FIS expressed as absolute area under the curve (AUC) calculated from time lapses as presented in **Fig. 4d–f** (baseline = 100%, t = 60 min) corrected for FIS of DMSO-treated organoids and averaged from at least three independent experiments performed with weekly intervals (mean ± s.e.m.). (**d**) Average FIS responses of compound-treated F508del/F508del organoids (*n* = 6 from **a–c**) and DMSO-treated F508del/A455E organoids (*n* = 2) relative to average FIS of DMSO-treated healthy control organoids (*n* = 3) expressed in AUC calculated from time lapses as illustrated in **Fig. 4d–f** (baseline = 100%; t = 60 min; mean ± s.e.m.).

(additive values of single treatment; illustrated in Supplementary Fig. S6) indicated stronger synergy between VRT-325 and Corr-4a than C8 and Corr-4a, and was rather constant between most organoids. All F508del compound heterozygous organoids also responded to correction, but no correction or potentiation was observed in E60X/4015delATTT organoids (Fig. 5a–c). Next, we compared efficacy of F508del-CFTR restoring approaches by comparing FIS levels with mock-treated F508del/A455E or healthy control organoids (Fig. 5d). This comparison indicated that VX-809 is the most potent corrector, and that combined treatment with VX-809 and VX-770 induces FIS beyond levels observed in F508del/A455E organoids, reaching ~60% of healthy control levels. Together, these results demonstrate that the potency of CFTR-targeting compounds to restore CFTR function varies widely between organoids of individuals with cystic fibrosis, including F508del-CFTR homozygous organoids.

DISCUSSION

Collectively, our results indicate that FIS of mouse and human intestinal organoids is CFTR dependent. The rapid FIS likely results from the near-physiological characteristics of intestinal organoids. Previous data indicate that forskolin can increase luminal expansion in organoid-like structures grown from renal MDCK, colonic LIM1863 cell lines or mouse intestinal spheroids[20,37,38], but the larger amplitude and rate of the FIS likely results from higher CFTR expression levels in the primary tissue culture model used here.

Fluid transport measured by FIS in rectal organoids correlated to the ICM performed on the corresponding rectal suction biopsies. The FIS assay can therefore be a valuable supplement to the electrical measurements of CFTR function currently carried out in cystic fibrosis treatment and research centres and may serve to complement ICM data. Using ICM and FIS, we found that most F508del-CFTR subjects showed some residual CFTR function, suggesting that F508del-CFTR is expressed at the apical surface at low levels[39,40]. This is also supported by the induction of FIS by the potentiator VX-770 in the absence of correctors, as previously was reported for human bronchial epithelial cells[9]. Clinical data also support low apical F508del-CFTR expression in F508del homozygous subjects[41].

The paired FIS and ICM allows comparison of fluid secretion rates and ion fluxes as measured by ICM. Based on the geometry of the organoids during FIS, and the assumptions that the average organoid lumen is a sphere, average swelling is similar in all three dimensions and linear during an experiment, we calculated an initial fluid secretion rate of 26 ± 23 (mean ± s.d.) ml h^{-1} cm^{-2} in healthy control organoids (corresponding with an estimated current of 1.0×10^2 μA cm^{-2} on the basis of isotonic chloride secretion). When we assume isotonic chloride secretion during ICM, we estimated that the measured currents would correspond with an approximate fluid secretion rate of 12 μl h^{-1} cm^{-2}. This rate largely exceeds values reported previously for cysts from MDCK cells[42], and for airway epithelium[43].

We demonstrate that FIS can measure functional restoration of CFTR by drugs. Notably, we observed that drug responses between organoids derived from subjects with cystic fibrosis are variable, even between F508del-CFTR homozygous organoids. This raises the possibility that this *in vitro* assay may predict *in vivo* drug-responsiveness of individual subjects. An ideal therapeutic model for cystic fibrosis would be to screen effectiveness of available CFTR-restoring

drugs directly after diagnosis to optimize treatment at the personal level before disease onset. Personalized medicine approaches may also facilitate the development and approval of drugs to which only subgroups of subjects respond, and limit the economic risks associated with drug research. Furthermore, FIS of organoids can be used for approval of drugs in subjects that are genotypically mismatched with drugs that have been validated for a specific *CFTR*-genotype. Interim phase II results of a current trial published on websites of the North American Cystic Fibrosis Foundation (www.cff.org) and Vertex (www.vrtx.com) indicate that drug-responses to VX-809 and VX-770, or VX-770 monotreatment[14], are highly variable between CFTR F508del subjects. However, the predictive potential of organoid-based CFTR function measurements for *in vivo* drug responsiveness remains to be established.

Currently, individual drug responses may be predicted using *ex vivo* rectal biopsies[44] or primary airway tissue culture models[45]. Compared with these techniques, organoid cultures appear superior to generate large data sets from individual subjects. CFTR function analysis in organoid cultures is relatively easy, fast and robust. The organoids auto-differentiate into tissue-recapitulating structures in 96-well plates that allows measurement of up to 80 organoids per well and up to 96 conditions per experiment. In this format, dose-response curves measured in triplicate for multiple drugs per individual can be easily generated at multiple culture time points as demonstrated here.

Using our image analysis approach, higher throughput approaches to identify novel compounds that restore CFTR function may be developed. When we compare the drug responses in organoids with the limited clinical data that has been published in F508del-CFTR homozygous subjects[13,14] (www.cff.org), only the combination of VX-809 and VX-770 has been reported to improve lung function in approximately 50% of F508del homozygous subjects. This combination induces approximately 1.5-fold higher FIS levels in F508del-CFTR homozygous organoids as compared to untreated F508del/A455E organoids, and up to 60% of healthy control FIS. It is not uncommon that treatment effects in *in vitro* models are superior to effects measured *in vivo*, but the fold correction in the FIS assay also exceeds the correction in cultured human bronchial epithelium by approximately 2-fold[9,36]. This may indicate that tissue-specific factors may control corrector efficacy. It is also likely that FIS rates are underestimated in healthy control organoids when CFTR expression is no longer rate limiting for FIS beyond a particular threshold by e.g. basolateral ion transport. These data may suggest that novel CFTR-restoring drugs may have clinical impact when FIS reaches levels up to ~60% of wild-type FIS.

Two important aspects of organoid cultures render this technology highly suitable for follow-up studies. Firstly, organoids can be greatly expanded while maintaining intact stem cell compartments during long-term culture (over 40 passages)[16]. Generation of large cell numbers will aid cell biological and biochemical studies of CFTR-dependent cellular alterations, and is a prerequisite for high throughput screens. Secondly, primary cell banks from individuals with cystic fibrosis can be generated by storage of organoids in liquid nitrogen. These can be used to identify and study cellular factors associated with clinical phenotypes, and would allow for analysis of newly developed drugs at the individual level using materials that have been previously acquired.

In addition, this assay may be suitable for development of drugs to treat secretory diarrhoea, a life threatening condition that results from CFTR hyper-activation by pathogenic toxins such as cholera toxin[46] (Supplementary Fig. 7), and for electrolyte homeostasis studies in general.

In summary, we described a quick and robust assay for quantification of CFTR function using a primary intestinal culture model that recapitulates essential features of the *in vivo* tissue architecture. This relatively simple assay will facilitate diagnosis, functional studies, drug development as well as personalized medicine approaches in cystic fibrosis.

METHODS

Mice

Cftr^{tm1Cam} knockout mice (*Cftr*$^{-/-}$)[24] were back-crossed with FVB mice and *Cftr*^{tm1eur} (F508del-Cftr)[25,26] were back-crossed with C57Bl/6 (F12) mice. Congenic FVB *Cftr*$^{-/-}$ mice or C57Bl/6 F508del-Cftr mice were used with their wild-type littermates. The mice were maintained in an environmentally controlled facility at the Erasmus Medical Center Rotterdam and approved by the local Ethical Committee.

Human material

Approval for this study was obtained by the Ethics Committee of the University Medical Centre Utrecht and the Erasmus Medical Centre Rotterdam. Informed consent was obtained from all subjects participating in the study. Rectal organoids from healthy controls and subjects with cystic fibrosis were generated from four rectal suction biopsies after intestinal current measurements (ICM) obtained (i) during standard cystic fibrosis care (E60X/4015ATTTdel; F508del/G542X; F508del/L927P; 5 × F508del/F508del), (ii) for diagnostic purposes (1 × healthy control) or (iii) during voluntary participation in studies approved by the local Ethics Committee (2 × healthy control, 1 × F508del/F508del). Material from an F508del-CFTR homozygous individual and a healthy control was derived from proximal ileum rest-sections upon surgery due to meconium ileus. Four duodenal biopsies were obtained from two subjects with cystic fibrosis by flexible gastroduodenoscopy to generate F508del/F508del and F508del/Exon17del organoids. The same procedure was used to obtain four biopsies from two subjects with suspected celiac disease. The biopsies were macroscopically and pathologically normal and used to generate healthy control organoids.

Crypt isolation and organoid culture from mouse intestine

Mouse organoids were generated from isolated small intestinal (SI) crypts and maintained in culture as described previously[15]. Rspo1-conditioned medium (stably transfected Rspo-1 HEK293T cells were kindly provided by Dr. C. J. Kuo, Department of Medicine, Stanford, CA) was used instead of recombinant Rspo-1 and added to the culture medium at a 1:10 dilution. *Cftr*$^{-/-}$ and F508del-Cftr organoids were obtained from proximal and distal SI segments, respectively. Organoids from passage 1–10 were used for confocal imaging.

Crypt isolation and organoid culture from human biopsies

Crypt isolation and culture of human intestinal cells have been described previously[16]. In short, biopsies were washed with cold complete chelation solution and incubated with 10 mM EDTA for 30 (small intestine) or 60 (rectum) min at 4 °C. Supernatant was harvested and EDTA was

washed away. Crypts were isolated by centrifugation and embedded in matrigel (growth factor reduced, phenol-free, BD bioscience) and seeded (50–200 crypts per 50 µl matrigel per well) in 24-well plates. The matrigel was polymerized for 10 min at 37 °C and immersed in complete culture medium: advanced DMEM/F12 supplemented with penicillin/streptomycin, 10 mM HEPES, Glutamax, N2, B27 (all from Invitrogen), 1 µM *N*-acetylcysteine (Sigma) and growth factors: 50 ng ml^{-1} mEGF, 50% Wnt3a-conditioned medium (WCM) and 10% Noggin-conditioned medium (NCM), 20% Rspo1-conditioned medium, 10 µM Nicotinamide (Sigma), 10 nM Gastrin (Sigma), 500 nM A83-01 (Tocris) and 10 µM SB202190 (Sigma). The medium was refreshed every 2–3 days and organoids were passaged 1:4 every 7–10 days. Organoids from passage 1–10 were used for confocal live cell imaging. For production of WCM and NCM, Wnt3a-producing L-Cells (ATCC, nr: CRL-264) were selected for high expressing sub-clones and human full-length noggin was stably transfected into HEK293T cells, respectively. Amounts and activity of the expressed factors in each batch were assessed using dot blots and luciferase reporter plasmids (TOPflash and FOPflash; Millipore) as described previously[47,48].

Stimulation assays

Human or mouse organoids from a 7-day old culture were seeded in a flat-bottom 96-well culture plate (Nunc) in 5 µl matrigel commonly containing 20–80 organoids and 100 µl culture medium. One day after seeding, organoids were incubated for 60 min with 100 µl standard culture medium containing 10 µM calcein-green (Invitrogen). For optimal CFTR inhibition, organoids were pre-incubated for 2 h (mouse) or 3 h (human) with 50 µM $CFTR_{inh}$-172, 50 µM GlyH-101 or their combined treatment (both from Cystic Fibrosis Foundation Therapeutics, Inc). After calcein-green treatment (with or without CFTR inhibition), 5 µM forskolin was added and organoids were directly analyzed by confocal live cell microscopy (LSM710, Zeiss, 5× objective). Three wells were used to study one condition and up to 60 wells were analyzed per experiment. For CFTR correction, organoids were pre-incubated for 24 h with 10 µM VRT-325, 10 µM Corr-4a, 10 µM C8 (all from Cystic Fibrosis Foundation Therapeutics, Inc), 3 µM VX-809 (Selleck Chemicals LLC, Houston, USA) or combinations as indicated. For CFTR potentiation, 3 µM VX-770 (Selleck Chemicals LLC) was added simultaneously with forskolin. Dilutions of VX-809 and VX-770 were used as indicated in Fig. 4b.

Quantification of organoid surface area

Forskolin-stimulated organoid swelling was automatically quantified using Volocity imaging software (Improvision). The total organoid area (XY plane) increase relative to t = 0 of forskolin treatment was calculated and averaged from three individual wells per condition. The area under the curve (AUC) was calculated using Graphpad Prism.

Statistical analysis

A Kolmogorov-Smirnov test was used to test whether the ICM and FIS data were normally distributed. A paired student's T-test was used to compare FIS with or without pre-selection of responding organoids (Supplementary Fig. 1e). A Spearman's rank correlation test was used to correlate ICM measurements with organoid swelling (Supplementary Fig. 4c). $P < 0.05$ was

considered as statistically significant. All data were analyzed in SPSS statistics version 20.0 for Windows.

RNA isolation and qPCR

From human duodenal organoids that were cultured for >12 weeks, RNA was isolated with the RNeasy minikit (Qiagen) and quantified by optical density. cDNA was synthesized from 1 µg of RNA by performing a reverse-transcription PCR (Invitrogen). From mouse small intestinal organoids that were cultured for >6 weeks, RNA was isolated using Trizol (Invitrogen) and quantified by optical density. cDNA was generated from 500 ng by the iScript™ cDNA synthesis kit (Bio Rad). Messenger RNA (mRNA) levels of human *CFTR* and mouse *Cftr* were determined by quantitative real-time RT-PCR with the SYBR Green method (Bio-Rad). Glyceraldehyde-3-phosphate dehydrogenase (*GADPH*) or β*2m* mRNA abundance was used to measure cDNA input.

Western blot analysis

For CFTR protein detection, organoids from healthy controls or subjects with cystic fibrosis were lysed in Laemmli buffer supplemented with complete protease inhibitor tablets (Roche). Lysates were analyzed by SDS-PAGE and electrophoretically transferred to a polyvinylidene difluoride membrane (Millipore). The membrane was blocked with 5% milk protein in TBST (0.3% Tween, 10 mM Tris pH8 and 150 mM NaCl in H_2O) and probed overnight at 4 °C with a combination of the mouse monoclonal CFTR-specific antibodies 450, 570 and 596 (1:5000, Cystic Fibrosis Folding consortium), followed by incubation with HRP-conjugated secondary antibodies and ECL development. For CFTR deglycosylation, healthy control organoids were lysed in RIPA buffer (50 mM Tris pH 8.0, 150 mM NaCl, 0.1% SDS, 0.5% sodium deoxycholate and 1% triton) supplemented with complete protease inhibitor tablets (Roche) and incubated with PNGase F and Endo H for 3 h at 33 °C (both from New England BioLabs).

Immunocytochemistry

Complete organoids from a 5-day old culture were incubated with methanol (sigma) for 10 min at –20 °C. Organoids were probed with the mouse monoclonal CFTR-specific antibody M3A7 (1:25; AB4067 from Abcam) for 16 h at 4 °C, followed by simultaneous incubation of alexa fluor 649-conjugated secondary antibodies (1:500; from Sigma) and phalloidin-FITC for 1 h at 4 °C (1:200; from Sigma). Organoids were embedded in Mowiol containing DAPI (1:10000) and analyzed by confocal microscopy as described previously[49].

Intestinal current measurement (ICM)

Transepithelial chloride secretion in human rectal suction biopsies (four per subject) was measured as described previously[34] using a recent amendement (repetitive prewashing)[35] which better accentuates forskolin-induced anion current responses by reducing basal cAMP levels. In short, the biopsies were collected in phosphate-buffered saline on ice and directly mounted in adapted micro-Ussing chambers (aperture 1.13 or 1.77 mm^2). After equilibration, the following compounds were added in a standardized order to the mucosal (M) or serosal (S) side of the tissue: amiloride (0.01 mM, M), to inhibit amiloride sensitive electrogenic Na^+ absorption; carbachol (0.1 mM, S), to initiate the cholinergic Ca^{2+}- and protein kinase C-linked Cl^- secretion;

DIDS (0.2 mM, M), to inhibit DIDS-sensitive, non-CFTR Cl^- channels like the Ca^{2+}-dependent Cl^- channels (CaCCs); histamine (0.5 mM, S), to reactivate the Ca^{2+}-dependent secretory pathway and to measure the DIDS-insensitive component of Ca^{2+}-dependent Cl^- secretion; forskolin (0.01 mM, S), to fully activate CFTR-mediated anion secretion. Crude short circuit currents (Isc) values (μA) were converted to μA cm^{-2} based on the surface area of the aperture.

ACKNOWLEDGEMENTS

We thank K. Schneeberger (Department of Pediatric Gastroenterology, Wilhelmina Children's Hospital, University Medical Centre Utrecht, The Netherlands) for technical assistance, the Department of Pediatric Gastroenterology of the Wilhelmina Children's Hospital (Utrecht, The Netherlands) for performing gastroduodenoscopy to obtain intestinal biopsies, K. Tenbrock (Department of Pediatrics, the RWTH Aachen University, Germany) and J.C. Escher (Department of Pediatric Gastroenterology, Erasmus MC-Sophia Children's Hospital, Rotterdam, the Netherlands) for providing intestinal rest-material, C.J. Kuo (Department of Medicine, Stanford, CA) for providing the Rspondin1-producing cell line, R.J. Bridges (Dept of Physiology and Biophysics, Rosalind Franklin University of Medicine and Science, North Chicago, USA) and Cystic Fibrosis Foundation Therapeutics (CFFT) for providing the C1-C18 compounds, and J. Riordan (Dept of Biochemistry and Biophysics, University of North Carolina, Chapel Hill, USA) and CFFT for providing the CFTR monoclonal antibodies, P.W. van Leeuwen for assistance with statistical analyses and C.B.M. ten Brink for assistance with Volocity software. This work was supported by grants of the Dutch Cystic Fibrosis Foundation (NCFS) and the Wilhelmina Children's Hospital (WKZ; OZF-2010) Foundation.

Competing Financial Interest

J.M.B., C.K.E., J.F.D. are inventors on a patent application related to these findings. H.C. is an inventor on several patents related to these findings.

REFERENCES

1. Riordan, J. R. *et al.* Identification of the cystic fibrosis gene: cloning and characterization of complementary DNA. *Science* **245**, 1066–1073 (1989).
2. Rommens, J. M. *et al.* Identification of the cystic fibrosis gene: chromosome walking and jumping. *Science* **245**, 1059–1065 (1989).
3. Kerem, B. *et al.* Identification of the cystic fibrosis gene: genetic analysis. *Science* **245**, 1073–1080 (1989).
4. Ratjen, F. & Döring, G. Cystic fibrosis. *Lancet* **361**, 681–689 (2003).
5. Cheng, S. H. *et al.* Defective intracellular transport and processing of CFTR is the molecular basis of most cystic fibrosis. *Cell* **63**, 827–834 (1990).
6. Riordan, J. R. CFTR function and prospects for therapy. *Annu. Rev. Biochem.* **77**, 701–726 (2008).
7. Clancy, J. P. & Jain, M. Personalized medicine in cystic fibrosis: dawning of a new era. *Am. J. Respir. Crit. Care Med.* **186**, 593–597 (2012).
8. Ramsey, B. W. *et al.* A CFTR potentiator in patients with cystic fibrosis and the G551D mutation. *N. Engl. J. Med.* **365**, 1663–1672 (2011).
9. Van Goor, F. *et al.* Rescue of CF airway epithelial cell function in vitro by a CFTR potentiator, VX-770. *Proc. Natl. Acad. Sci. U.S.A.* **106**, 18825–18830 (2009).
10. Rabeh, W. M. *et al.* Correction of both NBD1 energetics and domain interface is required to

restore ΔF508 CFTR folding and function. *Cell* **148**, 150–163 (2012).

11. Welch, E. M. *et al.* PTC124 targets genetic disorders caused by nonsense mutations. *Nature* **447**, 87–91 (2007).

12. Sermet-Gaudelus, I. *et al.* Ataluren (PTC124) induces cystic fibrosis transmembrane conductance regulator protein expression and activity in children with nonsense mutation cystic fibrosis. *Am. J. Respir. Crit. Care Med.* **182**, 1262–1272 (2010).

13. Clancy, J. P. *et al.* Results of a phase IIa study of VX-809, an investigational CFTR corrector compound, in subjects with cystic fibrosis homozygous for the F508del-CFTR mutation. *Thorax* **67**, 12-18 (2011)

14. Flume, P. A. *et al.* Ivacaftor in subjects with cystic fibrosis who are homozygous for the F508del-CFTR mutation. *Chest* **142**, 718–724 (2012).

15. Sato, T. *et al.* Single Lgr5 stem cells build crypt-villus structures in vitro without a mesenchymal niche. *Nature* **459**, 262–265 (2009).

16. Sato, T. *et al.* Long-term expansion of epithelial organoids from human colon, adenoma, adenocarcinoma, and Barrett's epithelium. *Gastroenterology* **141**, 1762-1772 (2011)

17. Sato, T. *et al.* Paneth cells constitute the niche for Lgr5 stem cells in intestinal crypts. *Nature* **469**, 415–418 (2011).

18. Field, M. Intestinal ion transport and the pathophysiology of diarrhea. *J. Clin. Invest.* **111**, 931–943 (2003).

19. Venkatasubramanian, J., Ao, M. & Rao, M. C. Ion transport in the small intestine. *Curr. Opin. Gastroenterol.* **26**, 123–128 (2010).

20. Currid, A., Ortega, B. & Valverde, M. A. Chloride secretion in a morphologically differentiated human colonic cell line that expresses the epithelial Na+ channel. *J. Physiol. (Lond.)* **555**, 241–250 (2004).

21. Cunningham, S. A., Worrell, R. T., Benos, D. J. & Frizzell, R. A. cAMP-stimulated ion currents in Xenopus oocytes expressing CFTR cRNA. *Am. J. Physiol.* **262**, C783–788 (1992).

22. Thiagarajah, J. R., Song, Y., Haggie, P. M. & Verkman, A. S. A small molecule CFTR inhibitor produces cystic fibrosis-like submucosal gland fluid secretions in normal airways. *FASEB J.* **18**, 875–877 (2004).

23. Muanprasat, C. *et al.* Discovery of glycine hydrazide pore-occluding CFTR inhibitors: mechanism, structure-activity analysis, and in vivo efficacy. *J. Gen. Physiol.* **124**, 125–137 (2004).

24. Ratcliff, R. *et al.* Production of a severe cystic fibrosis mutation in mice by gene targeting. *Nat. Genet.* **4**, 35–41 (1993).

25. French, P. J. *et al.* A delta F508 mutation in mouse cystic fibrosis transmembrane conductance regulator results in a temperature-sensitive processing defect in vivo. *J. Clin. Invest.* **98**, 1304–1312 (1996).

26. Wilke, M. *et al.* Mouse models of cystic fibrosis: phenotypic analysis and research applications. *J. Cyst. Fibros.* **10 Suppl 2**, S152–71 (2011).

27. Denning, G. M. *et al.* Processing of mutant cystic fibrosis transmembrane conductance regulator is temperature-sensitive. *Nature* **358**, 761–764 (1992).

28. Loo, T. W., Bartlett, M. C. & Clarke, D. M. Rescue of DeltaF508 and other misprocessed CFTR mutants by a novel quinazoline compound. *Mol. Pharm.* **2**, 407–413 (2005).

29. Pedemonte, N. *et al.* Small-molecule correctors of defective DeltaF508-CFTR cellular processing identified by high-throughput screening. *J. Clin. Invest.* **115**, 2564–2571 (2005).

30. Strandvik, B. *et al.* Spectrum of mutations in the CFTR gene of patients with classical and atypical forms of cystic fibrosis from southwestern Sweden: identification of 12 novel mutations. *Genet. Test.* **5**, 235–242 (2001).

31. Kerem, B. S. *et al.* Identification of mutations in regions corresponding to the two putative nucleotide (ATP)-binding folds of the cystic fibrosis gene. *Proc. Natl. Acad. Sci. U.S.A.* **87**, 8447–8451 (1990).

32. Zielenski, J. Genotype and phenotype in cystic fibrosis. *Respiration* **67**, 117–133 (2000).

33. Hermans, C. J., Veeze, H. J., Drexhage, V. R., Halley, D. J. & van den Ouweland, A. M. Identification of the L927P and delta L1260 mutations in the CFTR gene. *Hum. Mol. Genet.* **3**, 1199–1200 (1994).

34. de Jonge, H. R. *et al.* Ex vivo CF diagnosis by intestinal current measurements (ICM) in small aperture, circulating Ussing chambers. *J. Cyst. Fibros.* **3 Suppl 2**, 159–163 (2004).

35. De Boeck, K. *et al.* New clinical diagnostic procedures for cystic fibrosis in Europe. *J. Cyst. Fibros.* **10 Suppl 2**, S53–66 (2011).

36. Van Goor, F. *et al.* Correction of the F508del-CFTR protein processing defect in vitro by the investigational drug VX-809. *Proc. Natl. Acad. Sci. U.S.A.* **108**, 18843–18848 (2011).

37. Liu, J., Walker, N. M., Cook, M. T., Ootani, A. & Clarke, L. L. Functional Cftr in crypt epithelium of organotypic enteroid cultures from murine small Intestine. *Am. J. Physiol., Cell Physiol.* 302, C1492-1503 (2012)

38. Li, H., Yang, W., Mendes, F., Amaral, M. D. & Sheppard, D. N. Impact of the cystic fibrosis mutation F508del-CFTR on renal cyst formation and growth. *Am. J. Physiol. Renal Physiol.* **303**, F1176–1186 (2012).

39. Gee, H. Y., Noh, S. H., Tang, B. L., Kim, K. H. & Lee, M. G. Rescue of ΔF508-CFTR trafficking via a GRASP-dependent unconventional secretion pathway. *Cell* **146**, 746–760 (2011).

40. Luo, Y., McDonald, K. & Hanrahan, J. W. Trafficking of immature DeltaF508-CFTR to the plasma membrane and its detection by biotinylation. *Biochem. J.* **419**, 211–9– 2 p following 219 (2009).

41. Geborek, A. & Hjelte, L. Association between genotype and pulmonary phenotype in cystic fibrosis patients with severe mutations. *J. Cyst. Fibros.* **10**, 187–192 (2011).

42. Sullivan, L. P., Wallace, D. P. & Grantham, J. J. Coupling of cell volume and membrane potential changes to fluid secretion in a model of renal cysts. *Kidney Int.* **45**, 1369–1380 (1994).

43. Smith, J. J. & Welsh, M. J. Fluid and electrolyte transport by cultured human airway epithelia. *J. Clin. Invest.* **91**, 1590–1597 (1993).

44. Roth, E. K. *et al.* The K+ channel opener 1-EBIO potentiates residual function of mutant CFTR in rectal biopsies from cystic fibrosis patients. *PLoS ONE* **6**, e24445 (2011).

45. Wong, A. P. *et al.* Directed differentiation of human pluripotent stem cells into mature airway epithelia expressing functional CFTR protein. *Nat. Biotechnol.* **30**, 876–882 (2012).

46. Thiagarajah, J. R. & Verkman, A. S. CFTR inhibitors for treating diarrheal disease. *Clin. Pharmacol. Ther.* **92**, 287–290 (2012).

47. de Lau, W. *et al.* Lgr5 homologues associate with Wnt receptors and mediate R-spondin signalling. *Nature* **476**, 293–297 (2011).

48. Korinek, V. *et al.* Constitutive transcriptional activation by a beta-catenin-Tcf complex in APC-/- colon carcinoma. *Science* **275**, 1784–1787 (1997).

49. Beekman, J. M. *et al.* Syntenin-mediated regulation of Sox4 proteasomal degradation modulates transcriptional output. *Oncogene* **31**, 2668-2679 (2012)

SUPPLEMENTARY FIGURES

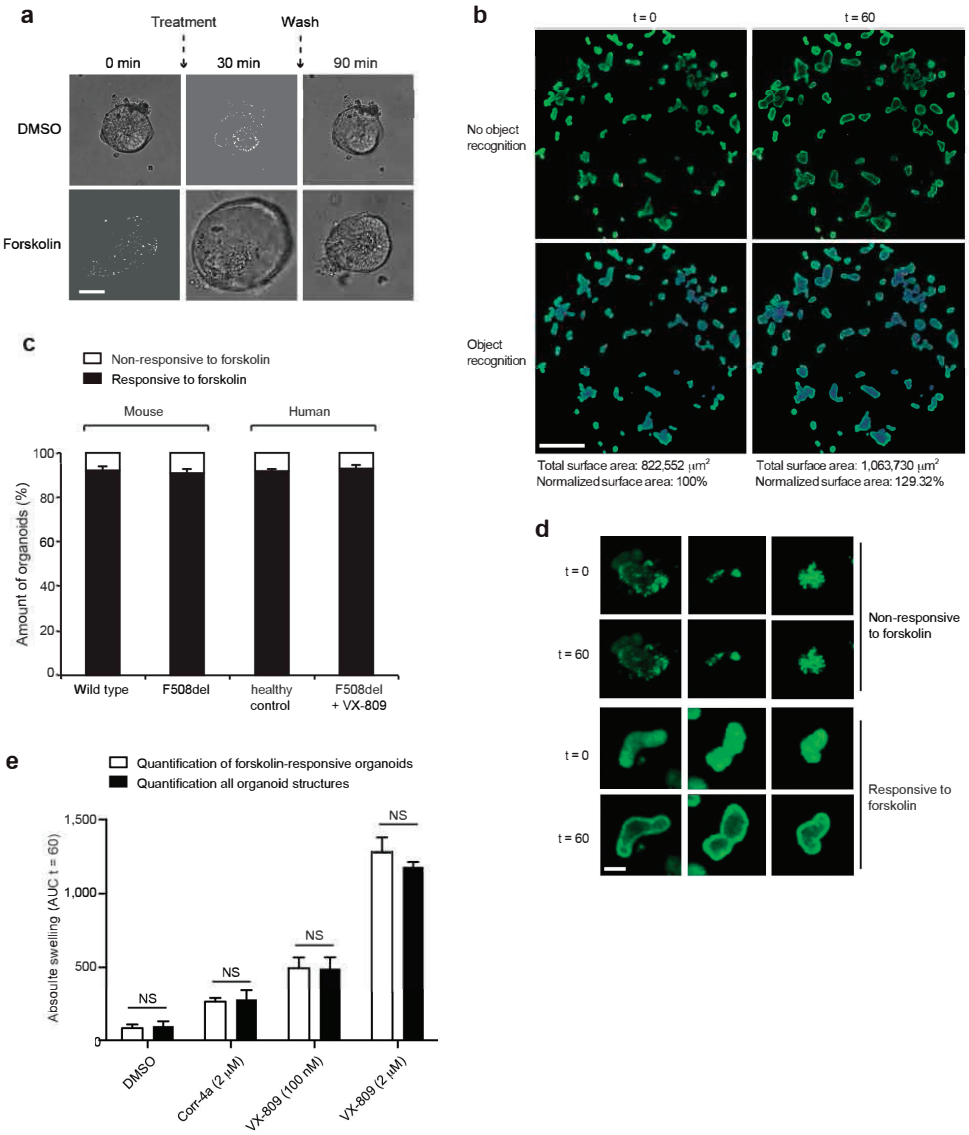

Supplementary Figure 1. Organoid swelling in reponse to forskolin. (a) Light microscopy analysis of wild-type mouse organoids stimulated with forskolin or DMSO. Representative examples for the indicated time points after start of stimulation are shown. The forskolin-induced swelling (FIS) of organoids was reversed upon removal of forskolin by washing. Scale bar 30 µm. (b) Examples of quantification of total organoid surface area using Volocity imaging software. A representative confocal image is shown of calcein-green-labeled rectal F508del-CFTR organoids pre-treated for 24 h with VX-809 in a well of a 96-well plate at the indicated time points of forskolin treatment. Scale bar 520 µm. (c) Percentages of forskolin responding and non-responding objects from different origin with or without drug treatment calculated from three independent experiments. (d) Representative confocal images of irregularly shaped (non-responding) or normally shaped (responding) organoids at the indicated time points of forskolin simulation. Scale bar 60 µm (e) Quantification of FIS expressed in absolute area under the curve (AUC) calculated from time lapses as illustrated in Fig. 4d-f (baseline = 100%, t = 60 min) with or without pre-selection of responding structures. NS = not significant.

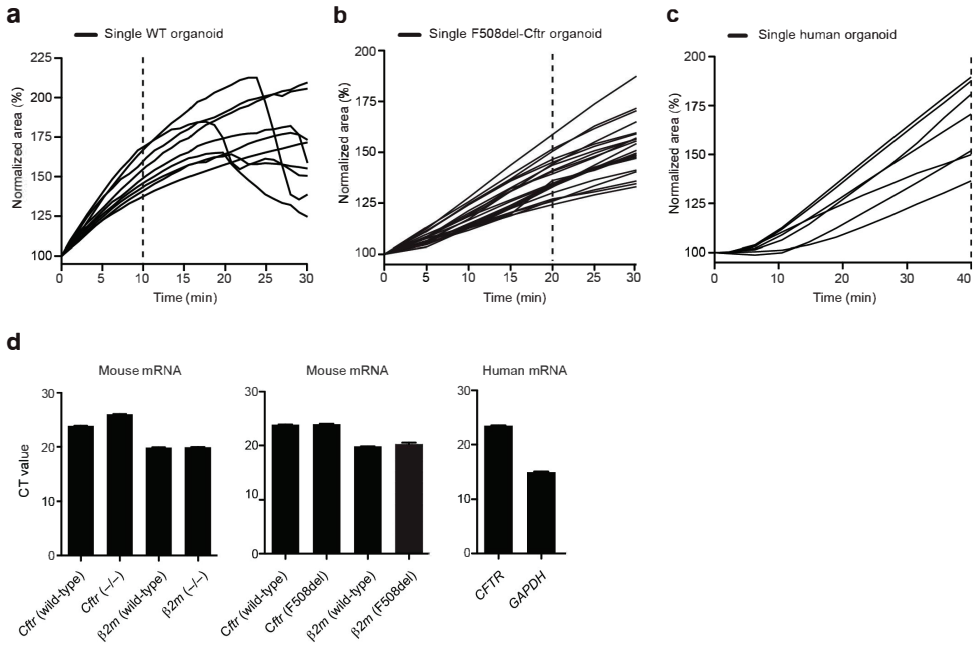

Supplementary Figure 2. Time lapses of forskolin-induced swelling in mouse and human organoids, and CFTR mRNA expression in mouse and human organoids. Normalized surface area increase of individual forskolin-stimulated (a) wild-type (WT), (b) F508del-Cftr (temperature-rescued) and (c) small intestinal organoids from healthy controls. The averaged FIS of different organoid types was analyzed for different time points to prevent measurement of collapsing organoids (dashed lines). (d) The bars show real-time PCR cycle threshold (CT) values representing mRNA levels of CFTR, [32m or GAPDH isolated from small intestinal F508del-Cftr (left graph) or Cftr, (middle graph) organoids and their corresponding wild-types, or healthy control small intestinal organoids.

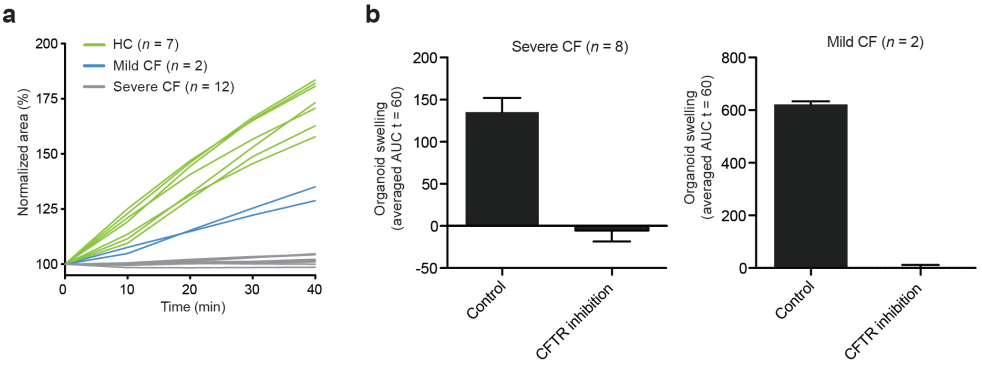

Supplementary Figure 3. Forskolin-induced swelling in organoids from healthy controls and cystic fibrosis subjects (a) Forskolin-stimulated swelling of intestinal organoids derived from seven individual healthy controls (HC; 2 x duodenum, 1 x ileum, 1 x colon, 3 x rectum), two subjects with a mild cystic fibrosis (CF) genotype (F508del/A455E; rectum) and 12 subjects with a severe cystic fibrosis genotype (duodenum: F508del/F508del and F508del/Exon17del; leum: F508del/F508del; rectum: 1 x E60X/4015delATTT; 1 x F508del/G542X; 1 x F508del/L927P; 6 x F508del/F508del). (b) Forskolin-induced swelling expressed in AUC calculated from time lapses of organoids area increase (baseline = 100%, t = 60) of rectal organoids with a mild or severe cystic fibrosis (CF) genotype with or without CFTR inhibition by CFTRinh-172 and GlyH-101 (severe genotype: F508del/G542X, F508del/L927P and F508del/F508del (6 x); mild genotype: F508del/A455E n = 2); mean± s.e.m.).

a

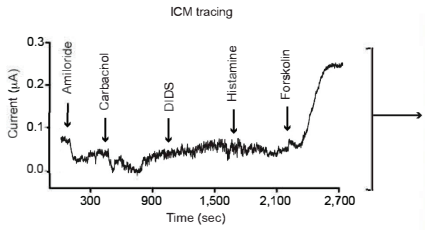

b

	Forskolin-induced swelling (AUC t = 60)	SD	Forskolin-induced Cl^- secretion (µ Amp cm^{-2})	SD
E60X/4015delATTT	2.63	4.56	–5.1	3.9
F508del/G542X	32.49	30.65	0.5	0.8
F508del/F508del	60.52	4.75	7	3.1
F508del/F508del	149.93	49.52	5.3	1.7
F508del/F508del	98.21	21.45	7.9	3.2
F508del/F508del	164.14	20.54	9.1	4.4
F508del/F508del	179.33	23.90	–10.1	–3.7
F508del/A455E	1494.00	118.03	14.2	4.4
F508del/A455E	1343.33	81.29	17	4.7
Healthy control	3191.33	724.50	26.3	12.8
Healthy control	3755.00	762.86	57	18.2
Healthy control	3666.75	287.97	50.1	14.5

c

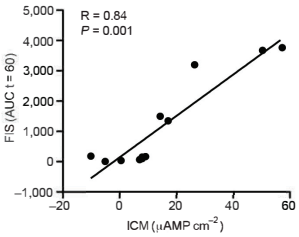

Supplementary Figure 4. Paired measurement of CFTR function by FIS or ICM. (a) Representative intestinal current measurement (ICM) tracing of F508del-CFTR rectal biopsies. (b) Overview of paired FIS and ICM responses of different individuals. FIS is expressed as absolute area under the curve (AUC) calculated from time lapses as illustrated in Fig. 4d-f (baseline = 100%, t = 60 min) and is averaged from at least three independent experiments performed with weekly interval. The ICM values represent average forskolin-induced current responses from four rectal biopsies of the same individual. (c) Correlation plot of FIS and ICM values from (b). R (= correlation coefficient) and P-value were calculated by SPSS using a Spearman's rank correlation test.

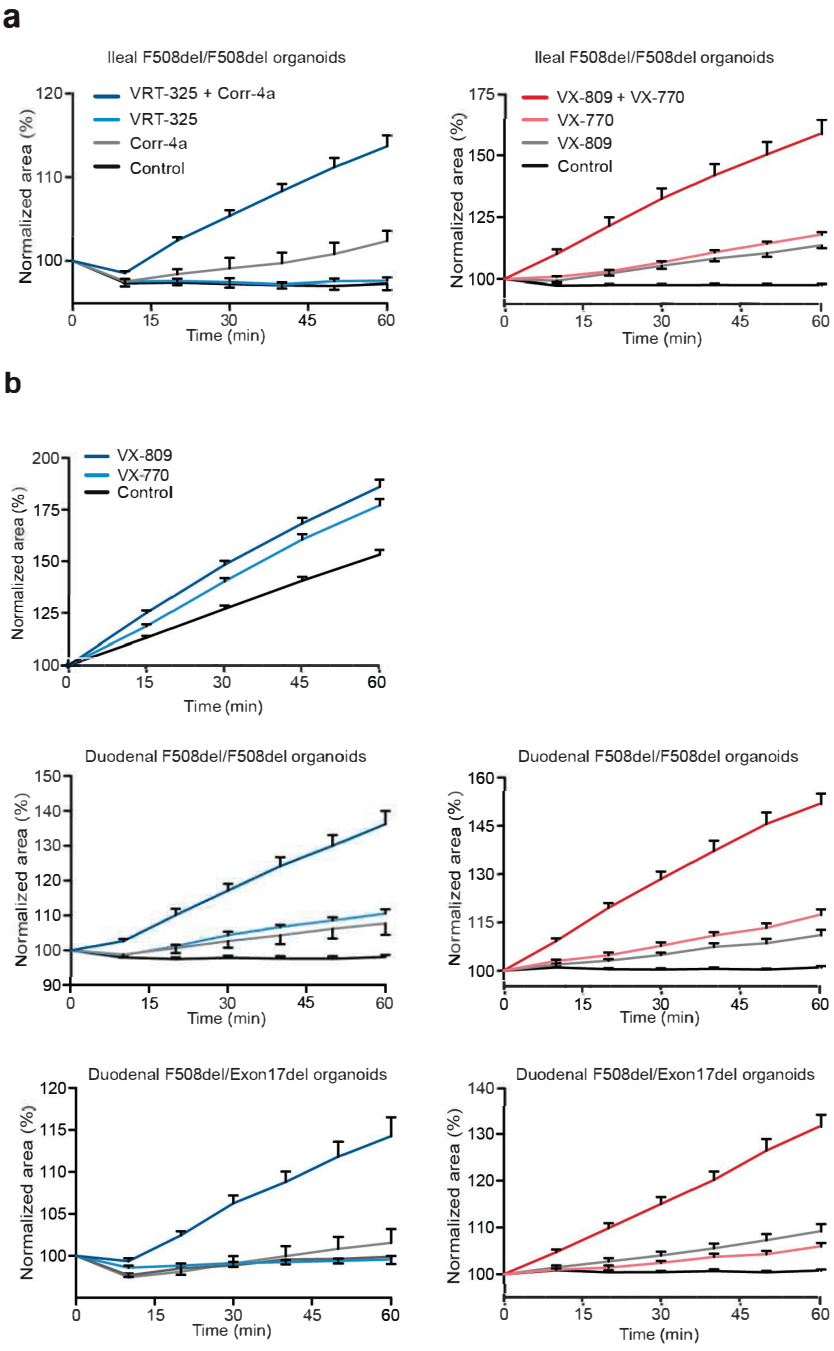

Supplementary Figure 5. Chemical CFTR correction of non-rectal intestinal or rectal F508del/A455E organoids. (a) Time lapses of normalized forskolin-induced swelling of small intestinal organoids pre-treated for 24 h with DMSO, VRT-325, Corr-4a, or both correctors or stimulated with VX-809 (24 h pre-treatment), VX-770 (simultaneous with forskolin) or their combined treatment (mean± s.e.m.). (b) Chemical correction of rectal F508del / A455E organoids. Normalized forskolin-induced swelling of rectal F508del/A455E organoids stimulated with VX-809 (24 h pre-treatment) or VX-770 (simultaneous with forskolin) (mean± s.e.m.).

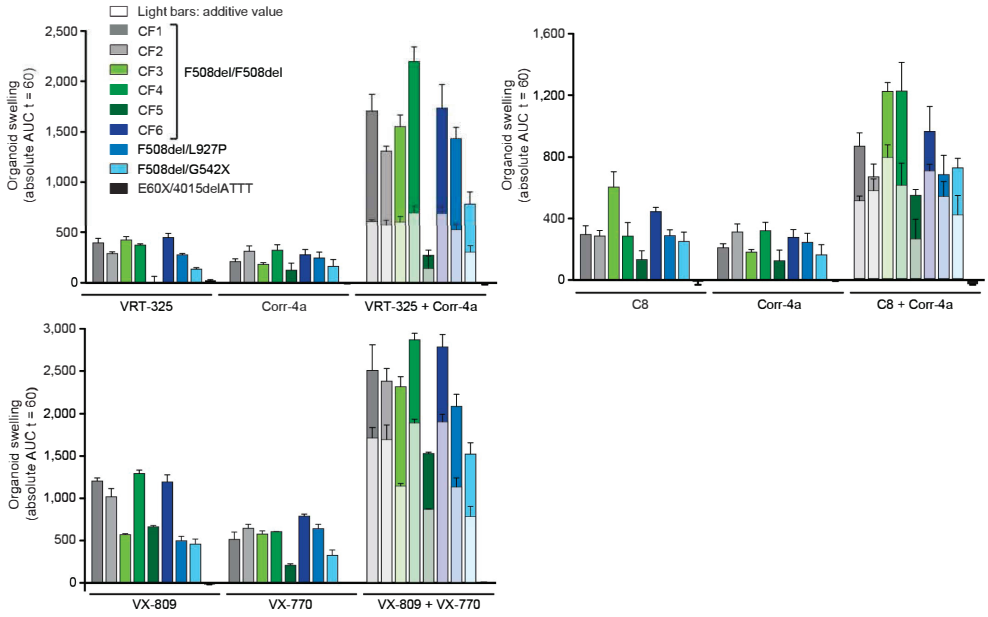

Supplementary Figure 6. Synergy between CFTR correctors. Comparison of measured responses (total bars) and additive (internal bars) responses in rectal organoids upon single or combined drug treatment as indicated in Fig. 5.

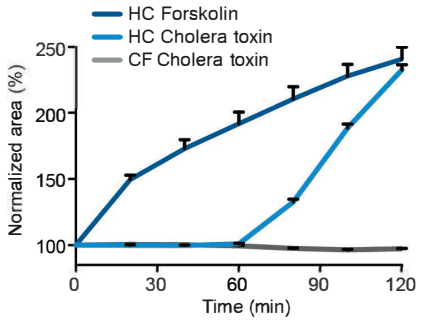

Supplementary Figure 7. Cholera toxin-induced organoid swelling in human rectal organoids is CFTR dependent. Forskolin and cholera toxin induce swelling of healthy control (HC)-derived or F508del/F508del organoids (CF). The cholera toxin response is delayed compared to forskolin (mean± s.e.m.) and absent in F508del/F508del organoids. Results are representative for three different experiments.

Chapter 3

Mechanism-based corrector combination synergistically restores ΔF508-CFTR folding and function in cystic fibrosis

Tsukasa Okiyoneda[1], Guido Veit[1], Johanna F. Dekkers[2,3,4], Miklos Bagdany[1], Naoto Soya[1], Haijin Xu[1], Ariel Roldan[1], Alan S. Verkman[5], Mark Kurth[6], Agnes Simon[7], Tamas Hegedus[8], Jeffrey M. Beekman[2,3,4], Gergely L. Lukacs[1,9,10]

[1]Department of Physiology and [9]Biochemistry and [10]GRASP, McGill University, Montréal, Quebec H3G 1Y6, Canada, [2]Department of Pediatric Pulmonology, [3]Department of Immunology, [4]Centre for Molecular and Cellular Intervention, University Medical Centre, Utrecht, The Netherlands, [5]Departments of Medicine and Physiology, University of California San Francisco, San Francisco, [6]Department of Chemistry, University of California Davis, Davis, California, [7]Department of Molecular Pharmacology, Research Center for Natural Sciences, Hungarian Academy of Sciences, Budapest, Hungary, [8]MTA-SE Molecular Biophysics Research Group and Department of Biophysics and Radiation Biology, Semmelweis University, Budapest, Hungary

Nature Chemical Biology 2013;9:444-54

ABSTRACT

The most common cystic fibrosis mutation, ΔF508 in the nucleotide binding domain-1 (NBD1), impairs cystic fibrosis transmembrane conductance regulator (CFTR)-coupled domain folding, plasma membrane expression, function and stability. VX-809, a promising investigational corrector of ΔF508-CFTR misprocessing, has limited clinical benefit and an incompletely understood mechanism, hampering drug development. Given the effect on second-site suppressor mutations, robust ΔF508-CFTR correction most likely requires stabilization of NBD1 energetics and the interface between membrane-spanning domains (MSDs) and NBD1, which are both established primary conformational defects. Here we elucidate the molecular targets of available correctors: class-I stabilizes the NBD1-MSD1 and NBD1-MSD2 interfaces, and class II targets NBD2. Only chemical chaperones, surrogates of class III correctors, stabilize human ΔF508-NBD1. Although VX-809 can correct missense mutations primarily destabilizing the NBD1-MSD1/2 interface, functional plasma membrane expression of ΔF508-CFTR also requires compounds that counteract the NBD1 and 2 stability defects in cystic fibrosis bronchial epithelial cells and intestinal organoids. Thus, the combination of structure-guided correctors represents an effective approach for cystic fibrosis therapy.

INTRODUCTION

Cystic fibrosis transmembrane conductance regulator (CFTR) is an ATP-binding cassette transporter and functions as a cAMP-dependent Cl^- channel at the apical plasma membrane (PM) of epithelial cells[1]. CFTR comprises two membrane spanning domains (MSD1, MSD2) with four cytosolic loops (CL1-4), and three cytosolic domains: a regulatory (R) and two nucleotide-binding domains (NBD1, NBD2). The predicted domain swapped architecture forms multiple domain-domain interfaces that appear to be critical in the structural and functional integrity of CFTR[2,3] (Fig.1a). Newly synthesized CFTR is N-glycosylated and undergoes co-translational domain folding and post-translational, coupled-domain assembly in the ER[2,4-7], aided by a network of molecular chaperones[8,9] (Fig.S1a). Upon traversing the Golgi complex, CFTR core-glycans are converted into complex-glycans, a convenient indicator that the conformationally native CFTR bypassed the ER quality control checkpoints[1,9].

CF, one of the most common inherited disease in the Caucasian population, is caused by loss-of-function mutations of CFTR that lead to the imbalance of airway surface fluid homeostasis, mucus dehydration, bacterial colonization, and consequently recurrent lung infection, the primary cause of morbidity and mortality in CF[1,10]. Deletion of F508 (ΔF508) in the NBD1, the most prevalent CFTR mutation present in ~90% of CF patients, causes global misfolding of CFTR and ER associated degradation (ERAD) via the ubiquitin proteasome system, resulting in marginal or no PM expression of the partially functional channel[1,9,11]. The residual PM channel activity of ΔF508-CFTR could be enhanced by modulating biosynthetic processing, peripheral stability, and channel gating by reducing temperature, chemical chaperones or small molecules[12-15].

While symptomatic therapies have increased the life expectancy of CF patients, considerable efforts have been devoted to identify compounds that can increase either the mutant biosynthetic processing efficiency and cell surface density ("correctors") or the activity of resident mutant CFTR at the PM ("potentiators")[16]. VX-770 (ivacaftor), the only approved potentiator drug, substantially enhances the channel function of several mutants[17], as opposed to available "correctors" that remain modestly effective with incompletely understood mechanism[11,14,18]. In principle, correctors may facilitate ΔF508-CFTR folding via direct binding as pharmacological chaperones (PC)[19], or indirectly, as chemical chaperones (CC, e.g. glycerol, TMAO and myo-inositol)[13,20]. Correctors may also enhance functional expression of the mutant as proteostasis regulators (PR)[9] by modulating the cellular machineries responsible for folding, degradation, and vesicular trafficking of ΔF508-CFTR (e.g. 4-phenylbutyrate, HDAC inhibitor, HSF1-inducers and kinase inhibitors, see for review[16]). VX-809, the most promising investigational corrector, restores the mutant PM expression and function to <15% of WT-CFTR in immortalized and primary human bronchial epithelia[11]. Although circumstantial evidence suggests that VX-809, similarly to some of the previously identified correctors (e.g. C3 [VRT-325] and C4 [corr-4a]) and potentiators (e.g. P1 [VRT-532] and VX-770), directly targets ΔF508-CFTR during ER biogenesis, the molecular basis of correction remains elusive[11,21]. While VX-809-induced ΔF508-CFTR PM activity is potentiated by two fold with VX-770 in preclinical settings[11], additional improvement seems to be required in corrector efficacy to achieve substantial clinical benefit in CF[18].

Recent studies revealed that the ΔF508-NBD1 is thermodynamically and kinetically destabilized at physiological temperature and suggested that NBD1 stabilization would

effectively counteract ΔF508-CFTR misprocessing[22,23]. Substantial stabilization of the ΔF508-NBD1 by suppressor mutations, however, resulted in a modest increase in folding and PM expression of the ΔF508-CFTR[24,25]. Remarkably, synergistic rescue (65-80%) of ΔF508-CFTR folding was achieved by simultaneous stabilization of the ΔF508-NBD1 and the NBD1-MSD2 interface with suppressor mutations[24,25], suggesting that correction of both primary structural defects is necessary and sufficient to restore ΔF508-CFTR function to WT-like level in most CF patients. These findings may imply that correction of only one of the primary (NBD1 or the NBD1-MSD2 interface) or a secondary structural defect (e.g. NBD2 misfolding[4]) accounts for the ΔF508-CFTR limited rescue efficiency by correctors identified to date[9,11,14,18,19,26]. As a corollary, corrector combinations that counteract distinct conformational defects may synergistically restore ΔF508-CFTR folding and function in analogy to combination of suppressor mutations acting on the primary folding defects[24,25] (Fig. S1b).

Based on *in vitro* assays of isolated ΔF508-NBD1 in combination with *in vivo* CFTR processing, functional assays, and *in silico* docking analysis, as well as published data[19], here we propose that correctors can be mechanistically classified into three groups. Using combination of VX-809 acting on the NBD1-MSD1/2 interface with two other classes of chemicals synergistically restores ΔF508-CFTR folding, PM expression, stability, and function in cell culture models and intestinal organoids from CF patients. Thus, chemical targeting of multiple conformational defects is able to counteract ΔF508-CFTR misfolding, demonstrating that structure-guided corrector combination may provide a novel and efficient therapeutic strategy in CF.

RESULTS

Class-I correctors in concert with NBD1 genetic stabilization robustly restore ΔF508-CFTR folding, PM expression and function

We postulated that small molecule combinations targeting both primary folding defects would achieve WT-like folding and processing of ΔF508-CFTR as documented in case of second site suppressor mutations[24,25]. To categorize the available corrector molecules (Table S1) according to their preferential targets, the rescue efficiency of ΔF508-CFTR containing either the genetically stabilized NBD1 by R1S mutation (G550E, R553Q, R555K, F494N, second site mutations are defined in Table S2) or the NBD1-MSD2 interface by the R1070W mutation in the cytoplasmic loop 4 (CL4, Fig.1a) was determined. Previous studies have shown that either R1S or R1070W second-site mutation partially rescued the ΔF508-CFTR folding and PM expression to ~10% of the WT[24,25]. We confirmed that R1070W or R1S suppressor mutation increased the ΔF508-CFTR PM density from <2 % to 7 or 16% of the WT level, respectively, determined by cell surface ELISA in BHK cells[24] (Fig.1b and Fig.S2a). The PM density of ΔF508-CFTR-R1S and ΔF508-CFTR-R1070W was enhanced to 93-100% and 30-34% of the WT, respectively, by VX-809, C18 (a VX-809 analogue) or C3, the most effective correctors in our screen. This suggests that VX-809, C18 and C3 preferentially target the NBD1/MSD2 interface over the NBD1 energetic defect and they were designated as class-I correctors (Fig.1b and Fig.S2a, *red symbols*). The preferential rescue of the NBD1-MSD2 interface and NBD1 stability defects was estimated by the augmented PM density of ΔF508-CFTR-R1S (Res_{R1S}) and ΔF508-CFTR-R1070W (Res_{R1070W}), respectively, a measure that indicates the capacity of correctors to synergize with the respective suppressor mutation (Fig.S2a). The ratio of Res_{R1S}

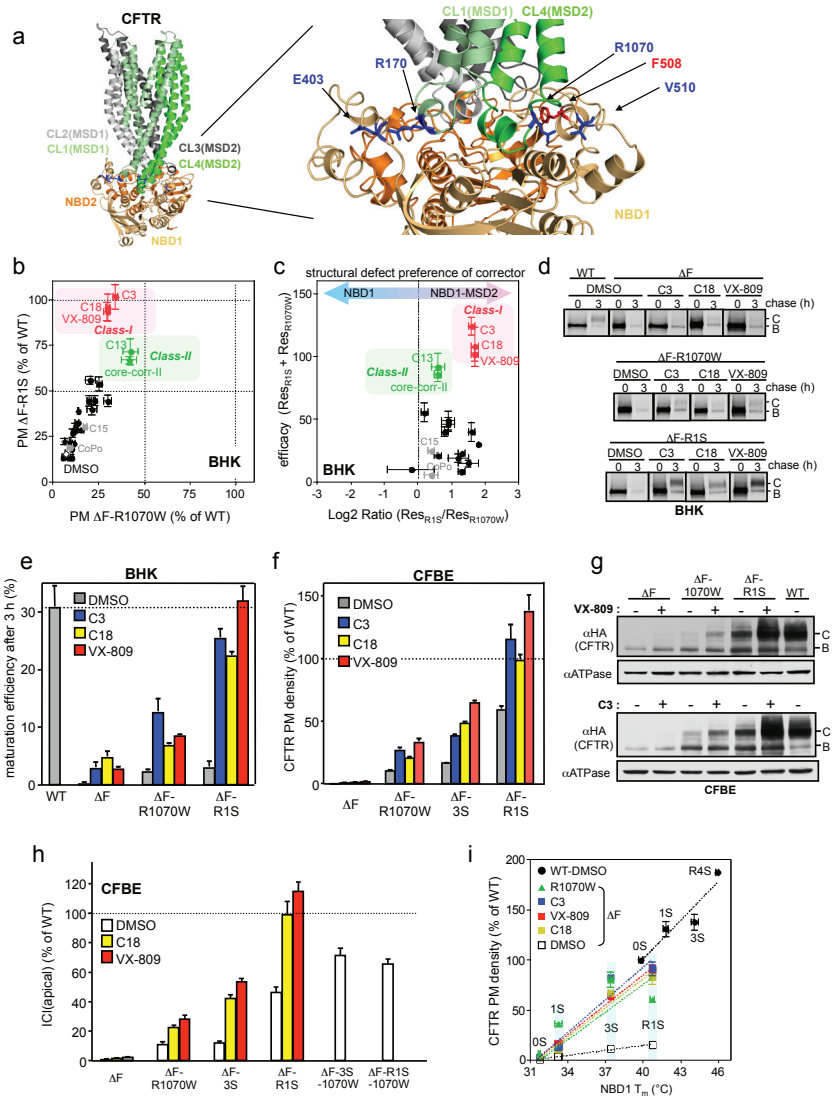

Figure 1. Combination of corrector and suppressor mutation synergistically restores ΔF508-CFTR folding, PM expression and function. (a) NBDs-MSDs interfaces in the CFTR open structural model[33]. Some critical interface residues are indicated. (b) Relative PM density of ΔF508-CFTR containing R1S (Y-axis) or R1070W (X-axis) upon corrector treatment was measured by ELISA in BHK cells (n=6-12). Correctors indicated by black symbols are listed in Fig.S2a. (c) Structural preference of correctors to NBD1-MSD2 interface over NBD1 stability defect was visualized by plotting sum of correction (Res_{R1S} + Res_{R1070W}, Y-axis) as a function of log_2 ratio of the augmented PM density of ΔF508-CFTR with R1S and R1070W (Res_{R1S}/Res_{R1070W}, X-axis). (d-e) Maturation efficiency of ΔF508-CFTR was measured by metabolic pulse-chase experiments (d) and quantified by densitometry (e, n=3-4). B, immature core-glycosylated; C, mature complex-glycosylated form. (f-h) PM density (f, n=8-20), cellular expression (g) and function (h, n=3-4) of ΔF508-CFTR with or without suppressor mutation was measured by ELISA, immunoblotting and apical Cl^- current (ICl(apical)), respectively, in CFBE41o- Tet-on cells. Na^+/K^+-ATPase (ATPase) was used as a loading control. (i) Correlation between T_m of NBD1 variants of 0S, 1S, 3S, R1S and R4S (listed in Table S2) and PM density of the respective CFTR variants in BHK cells (n=8-12) in the presence or absence of correctors. The data were fitted by linear regression analysis and slopes were listed in the result as %/°C unit. Correctors (C3 at 10 μM; C18 or VX-809 at 3 μM) were treated for 24 h at 37°C. Data are means ± SEM.

over Res_{R1070W} suggests that VX-809, C18 or C3 has ~3.5 fold more stronger stabilizing effect on the NBD1-MSD2 interface than on the NBD1 (Fig.1c). This inference was confirmed by using ΔF508-CFTR variants containing functionally analogous suppressor mutations; 3S [F494N, Q637R, and F429S] and R [G550E, R553Q, R555K] or V510D that stabilize the NBD1 or the NBD1-MSD2 interface, respectively[6,24,27,28]. VX-809, C18 or C3 increased PM density of ΔF508-CFTR-3S and ΔF508-CFTR-R from 7-25% to 60-120% of WT and their complex-glycosylation, but was less effective in case of ΔF508-CFTR-V510D similar to ΔF508-CFTR-R1070W (Fig.S2b-c). Comparable difference was obtained by analyzing the magnitude of fold-correction relative to that induced by the respective second-site mutation(s) alone. The reduced rescue efficiency of the ΔF508-CFTR-3S relative to ΔF508-CFTR-R1S by class-I correctors may be attributed to the more efficient stabilization of the NBD1-NBD2 interface with R1S suppressor mutation.

Metabolic pulse-chase experiments confirmed that only combination of VX-809, C18 or C3 with NBD1 (R1S) but not with interface stabilization (R1070W or V510D) enhanced ΔF508-CFTR folding efficiency near to the WT level (22-32%), indicating a 4-8-fold synergism between class-I correctors and R1S mutation effect (Fig.1d-e). Dual acting compounds such as C15 (corr-2b[29]) and CoPo-22 (CoPo[30]) combining both corrector and potentiator effect slightly enhanced the PM density of ΔF508-CFTR variants (Fig.1b and Fig.S2a, *gray symbols*).

Consistent with the results obtained in BHK cells, the WT-like ΔF508-CFTR complex-glycosylation and PM density was reproduced by genetic stabilization of NBD1 and NBD1-MSD2 interface in polarized human immortalized CF bronchial respiratory epithelial (CFBE41o-) cells, as well as by the combination of class-I corrector and NBD1 suppressor mutations (Fig.S3a-d). Class-I correctors increased the PM density, complex-glycosylation and apical Cl^- current (ICl(apical)) of ΔF508-CFTR to ~100-130 % and ~30 % of the WT level in the presence of R1S and R1070W, respectively, in CFBE41o- cells expressing the mutant channel under the control of tetracycline responsive promoter (Fig.1f-h and Fig.S3e), confirming the preferential effect of class-I correctors on the NBD1-MSD2 interface in CFBE41o- cells (Fig.S3f).

To evaluate the efficiency of class-I corrector as a function of the ΔF508-NBD1 conformational stability, the relationship between NBD1 stability (reflected by the T_m values of 0S, 1S [F494N], 3S or R4S suppressor mutant of ΔF508-NBD1 or WT-NBD1, listed in Table S2) and PM density of the respective CFTR variants was established. The WT-CFTR PM expression was dependent on the NBD1 stability at an 8-fold steeper slope (12.9±3.1 %/°C) compared to that of ΔF508-CFTR (1.7±0.2 %/°C), confirming the critical role of the F508 side chain in CFTR coupled domain folding[5] (Fig.1i). Similar to the R1070W mutation[24] (12.4±2.0 %/°C), VX-809 (9.8±0.7 %/°C), C18 (9.6±1.3 %/°C) or C3 (10.8±2.1 %/°C) restored the WT-like coupling between NBD1 stability (T_m) and ΔF508-CFTR PM expression, supporting the possibility that class-I correctors stabilize the NBD1-MSD2 interface (Fig.1i). Interestingly, the improvement of WT-CFTR PM expression by NBD1 stabilization reinforces the notion that the inherent conformational fluctuation of the NBD1 partly accounts for limited processing efficiency of the WT channel[24] (Fig.1e and i).

Mechanisms of action of CFTR correction

To assess whether VX-809 or C18 binds directly to ΔF508-CFTR as a PC, the functional stability of the temperature-rescued mutant channel was determined in artificial planar phospholipid bilayer[24,31]. These experiments used the ΔF508-CFTR-2RK, incorporating R29K and R555K mutations to

improve the channel reconstitution success by modestly enhancing the PM expression after the 26°C rescue while preserving the ΔF508-CFTR channel gating and functional stability defects as reported before[31] (Fig.S4a-c). The open probability (P_o) of the phosphorylated ΔF508-CFTR-2RK channel was progressively decreased from 0.21 to 0.09 upon raising the temperature from 24°C to 36°C (Fig.2a-b). In contrast, the P_o of the WT[31,32] was increased from 0.35 to 0.47 (Fig.2a-b). VX-

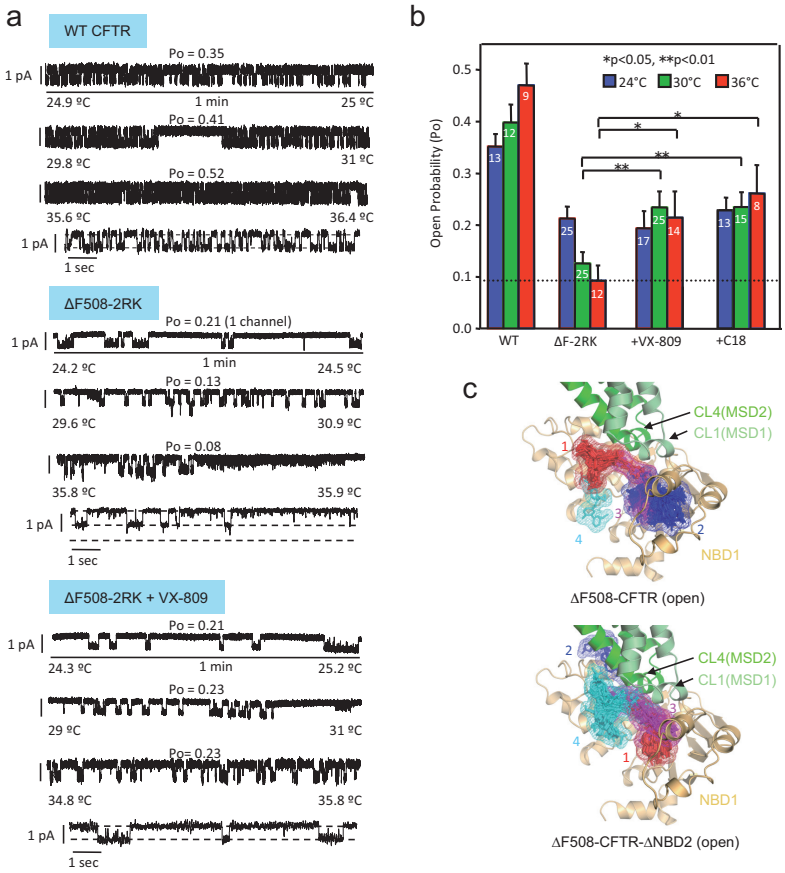

Figure 2. VX-809 functions as a pharmacological chaperone of CFTR. (a-b) Effect of VX-809 and C18 correctors on the thermal inactivation of reconstituted ΔF508-2RK-CFTR Cl^- channel into artificial phospholipid bilayer. (a) Representative records show the activity of WT or ΔF508-2RK CFTR at around 24°C, 30°C or 36°C during temperature ramp in the absence or presence of 3 μM VX-809. The processing defect of the ΔF508-CFTR variants was rescued at 26°C prior to microsome isolation. Channel activity is also shown for each condition at higher time resolution at 36°C. The closed (c) and open (o) states of the channels are indicated by dashed lines. Traces for ΔF508-2RK CFTR in the absence (at 24°C) or presence of VX-809 (at 36°C) were derived from separate records to be representative of the mean Po. (b) The open probability (P_o) of PKA-activated CFTR channels was analyzed at the indicated temperature as described in panel a. Total duration of single channel records for WT and ΔF508-2RK was at least 15 min. Number of independent recordings was indicated in the bars (n=8-25). Data represent means ± SEM and significance was tested by paired t-test. *<0.05, **p<0.01. (c) VX-809 *in silico* docking to open ΔF508-CFTR (top panel) or ΔF508-CFTR-ΔNBD2 model (bottom panel) obtained by AutoDock. Four VX-809 clusters are ranked based on their lowest binding energy pose in ascending order, and the first four clusters are illustrated on the model using PyMOL. For clarity, NBD2 and R-domain are hidden from the full-length model. Red, blue, magenta, cyan: clusters of VX-809 with increasing binding free energy.

809 and C18 prevented the mutant thermal inactivation and maintained the P_o = 0.21 and 0.26, respectively, at 36°C during the course of the measurement (Fig.2a-b and Fig.S4d), providing evidence that these compounds directly interact with the channel.

To delineate potential VX-809 target sites, *in silico* docking was performed on the NBD1 crystal structure (PDB:2BBT) and two CFTR homology models[3,33] following the deletion of the F508 using AutoDock. VX-809 was docked to NBD1-CL1(MSD1), NBD1-CL4(MSD2), and NBD1-NBD2 interfaces (Fig.2c, Fig.S5 and Table S3). Some of these sites have been reported as putative corrector binding sites[34,35]. To test the *in silico* predictions, the NBD1-CL4 and NBD1-CL1 interfaces were disrupted by R1070W or F508G[4,5,24,36] and the CF-causing R170G mutation (http://www.genet.sickkids.on.ca/app), respectively, in WT CFTR. The R170G substitution probably disrupts the electrostatic interaction between R170 (CL1) and E403 (NBD1) (Fig.1a), while the F508G interferes with the F508 hydrophobic patch formation at the NBD1-CL4 interface without directly compromising NBD1 energetics[3,24]. These events lead to primary destabilization of the NBD1-CL1 or NBD1-CL4 interfaces with subsequent misfolding of multiple CFTR domains[5]. Remarkably, the severe processing and PM expression defects of the mutants were almost completely corrected

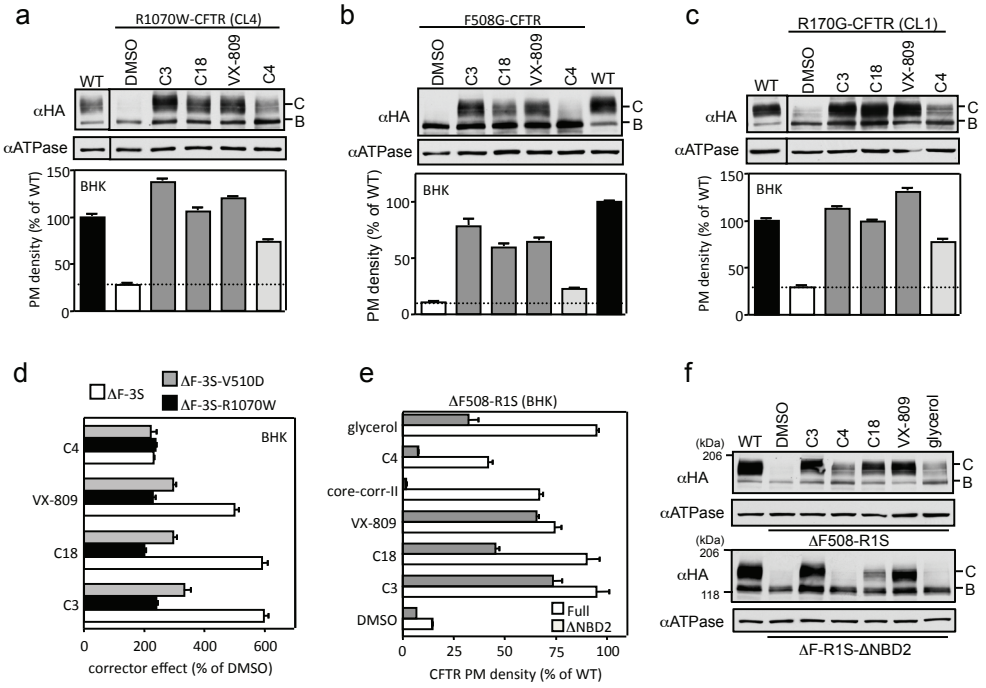

Figure 3. Probing corrector mechanism by using a panel of CFTR variants. (a-c) Effect of correctors (C3 or C4 at 10 μM, C18 or VX-809 at 3 μM for 24 h at 37°C) on cellular expression (upper) and PM density (lower) of R1070W (a), F508G (b), and R170G (c) CFTR variants in BHK cells, measured by Western blotting and cell surface ELISA (n=8), respectively. (d) Effect of V510D or R1070W mutation on the PM density of corrector treated ΔF508-CFTR-3S measured by cell surface ELISA in BHK cells and expressed as % of the respective DMSO control (n=8). Same data are also shown in Fig.S6a as % of the WT. (e-f) Effect of NBD2 deletion (ΔNBD2) on the corrector effect on the PM density (e, n=6-9) and cellular expression (f) of ΔF508-CFTR-R1S. Correctors (5 μg/ml core-corr-II, 10% glycerol, others are same as panel a-c) were treated for 24 h at 37°C. Data represent means ± SEM.

by VX-809, C18 or C3 (Fig.3a-c). Conversely, stabilizing the NBD1-CL4 interface by V510D or R1070W mutation in the absence of F508 attenuated the relative efficiency of class-I correctors but not of C4 on ΔF508-3S-CFTR (Fig.3d and Fig.S6a). Moreover, V510D mutation which improves the WT CFTR expression conceivably by stabilizing the NBD1-CL4 interface and marginally the NBD1 itself[24], also attenuated the effect of class-I correctors on WT CFTR (Fig.S6b). Surprisingly, V510D but not the R1S mutation, substantially corrected the R170G defect (Fig.S6c), suggesting that the NBD1-CL1 interface defect is either directly or indirectly coupled to the NBD1-CL4 interface destabilization. The rescue of R170G-CFTR expression by class-I correctors, however, was partially diminished by the V510D mutation (Fig.S6d). Besides *in silico* docking prediction (Fig.S5a, c and e), the stronger effect of VX-809 on the CL1 mutants compared to transmembrane (TM) helix 1 mutants such as G85E and G91R (Fig.S7a) also supports the model that VX-809 targets the interdomain interface composed of NBD1 and CL1-CL4, containing the respective coupling helices[1].

To further dissect the VX-809 target, we assessed its effect on the steady-state expression of WT CFTR domain combinations, representing stalled biosynthetic folding intermediates[5,37]. This approach is favored by the observation that the conformation of early folding intermediates is similar between WT and ΔF508-CFTR[38]. VX-809 increased the level of WT and ΔF508 MSD1-NBD1 (M1N1) equally (Fig.S7b), as well as the WT MSD1 and MSD1-NBD1-R (Fig.S7c) but not the domain combinations that lacked MSD1 (Fig.S7d-e), suggesting that VX-809 can target MSD1 and may stabilize the domain interface composed of CL1/CL4.

To determine the possible role of VX-809 at the NBD1-NBD2 interface, NBD2 deletion mutants (CFTR-ΔNBD2) were used considering the similar folding characteristics of WT and CFTR-ΔNBD2[5-7]. Class-I correctors and the R1S mutation synergistically rescued the ΔF508-CFTR-ΔNBD2 PM expression to 50-75 % of its WT counterpart as in the case of the full-length molecule (Fig.3e-f), ruling out a significant role of NBD1-NBD2 or NBD2-MSDs interfaces in the CFTR correction (Fig. S5c-f). This result was in agreement with the prediction of preserved VX-809 binding sites on the CFTR-ΔNBD2 model (Fig.2c). In contrast, NBD2 deletion virtually eliminated the ΔF508-CFTR-R1S correction by C4 (a C13 analogue)[14] or core-corr-II[39] (Fig.3e-f). Therefore, we designated C4 and core-corr-II as members of class-II correctors, the second most efficient group of correctors (Fig.1b-c and Fig.S2a, *green symbols*). Preventing class-II corrector effect by the NBD2 deletion is consistent with *in silico* docking predictions, supporting the putative binding of C4 and core-corr-II to the NBD1-NBD2 and/or NBD2-MSD1/2 interfaces (Fig.S8-9), and with the weaker rescue efficiency of class-II correctors on the NBD1-MSD1/2 interface mutants (R1070W, F508G or R170G) compared to that of class-I correctors (Fig.3a-c). These results are also in line with the observation that the C4 rescue effect is exerted only after the completion of MSD2 translation[37]. Although *in silico* docking predicted the regulatory insertion (RI)[40] as a possible binding site of class-II correctors in NBD1 (Fig.S8-9), this scenario was ruled out because C4 remained effective for the ΔF508-CFTR-ΔRI containing energetically stabilized NBD1[22,23] (Fig.S9f).

Chemical chaperones but none of the available correctors stabilize ΔF508-NBD1

Although none of the correctors tested appears to preferentially stabilize the NBD1 according to the structural complementation analysis (Fig.1b-c), it remains possible that correctors can exert limited conformational stabilization effect on the human ΔF508-NBD1 similar to that of RDR1 on the mouse ΔF508-NBD1[19]. To assess this possibility, first the thermal unfolding propensity of the domain was monitored by differential scanning fluorimetry (DSF)[24]. Initial studies were carried

out on the human ΔF508-NBD1 containing a single solubilizing mutation F494N (ΔF508-NBD1-1S), followed by validation on the native ΔF508-NBD1 with significantly reduced protein yield and increased thermal sensitivity. Most of the available correctors including RDR1, a PC stabilizer of the mouse ΔF508-NBD1[19], failed to counteract the conformational instability of the human ΔF508-NBD1-1S and ΔF508-NBD1, reflected by their 8~9°C lower melting temperature (T_m) relative to their WT counterparts (Fig.4a-c and Fig.S10a). C6, C11 (dynasore) or C12 weakly increased the T_m of ΔF508-NBD1-1S but this effect was minimal on the ΔF508-NBD1 (Fig.4a-c and Fig.S10a). Accordingly, C11 neither attenuated the *in vitro* ubiquitination of the unfolded NBD1 by the chaperone-dependent E3 ubiquitin ligase CHIP[24] (Fig.S10b) nor enhanced the PM expression of the CD4T-ΔF508-NBD1-1S chimera (see below). In contrast, ATP and chemical chaperones (CCs; glycerol, TMAO, myo-inositol and D-sorbitol) substantially enhanced the T_m of ΔF508-NBD1-1S and ΔF508-NBD1 (Fig.4a-c and Fig.S10a). The DSF results were substantiated by monitoring the NBD1 *in vivo* folding in the context of the CD4T-ΔF508-NBD1-1S chimera. PM density measurement of the chimeras, as a validated surrogate readout of the biosynthetic processing efficiency[5,24], showed that only CCs (e.g. glycerol and myo-inositol) and solubilizing mutations (R4S) but none of the correctors stabilized the cytosolic ΔF508-NBD1-1S anchored to the truncated CD4 reporter molecule (Fig.4d).

Considering the enhanced conformational dynamics of amino acid residues 507-511 in the isolated ΔF508-NBD1-3S shown by hydrogen deuterium exchange and mass spectrometry (HDX-MS)[41], we tested whether VX-809 can limit the conformational dynamics of this region. We confirmed the accelerated deuteration of the 505-509 amino acid peptide in ΔF508-NBD1-1S relative to its WT counterpart[41], but not the remaining >60 peptides, representing 98% sequence coverage of NBD1-1S (Fig.4e-h and Fig.S10c). VX-809, however, was unable to suppress the HDX kinetics of the 505-509 segment, as well as the remaining peptides, suggesting that VX-809 is unable to elicit localized conformational stabilization on the ΔF508-NBD1-1S (Fig.4e-h).

Combinations of correctors and/or chemical chaperone targeting complementary structural defects restore folding, processing, PM expression and stability of ΔF508-CFTR in BHK cells

Based on this study and other published data[19,35,37], correctors could be categorized in three classes (Fig.5a). Class-I (C3, C18 and VX-809) primarily stabilizes the NBD1-CL1/4 interface, class-II (core-corr-II and C4 analogues [C4, C13]) targets NBD2 and/or its interface, and class-III stabilizes the ΔF508-NBD1 (e.g. RDR1 on mouse NBD1[19]). Since RDR1 did not influence the human NBD1 stability (Fig.4), we used CCs, such as glycerol as surrogate class-III correctors in our proof-of-principle studies. Combination of chemicals with complementary structural targets is predicted to synergistically restore ΔF508-CFTR coupled domain folding in analogy to pairs of suppressor mutations[24,25] (Fig.S1b). While class-I corrector (VX-809, C18 or C3) with class-II corrector (C4 or core-corr-II) only modestly rescued ΔF508-CFTR PM level (<10% of WT CFTR), combination of class-I corrector and glycerol enhanced the ΔF508-CFTR PM expression to 30-50% of the WT, supporting that correction of both primary defects is required for the robust ΔF508-CFTR rescue (Fig.5b). This synergistic rescue with class-I corrector and glycerol that individually only achieved <8% rescue was further improved by class-II correctors and enhanced the ΔF508-CFTR PM expression to ~60-110% of WT (Fig.5b). Similar phenotypes were confirmed by monitoring the accumulation of complex-glycosylated ΔF508-CFTR with immunoblotting (Fig.5b). Metabolic pulse-chase

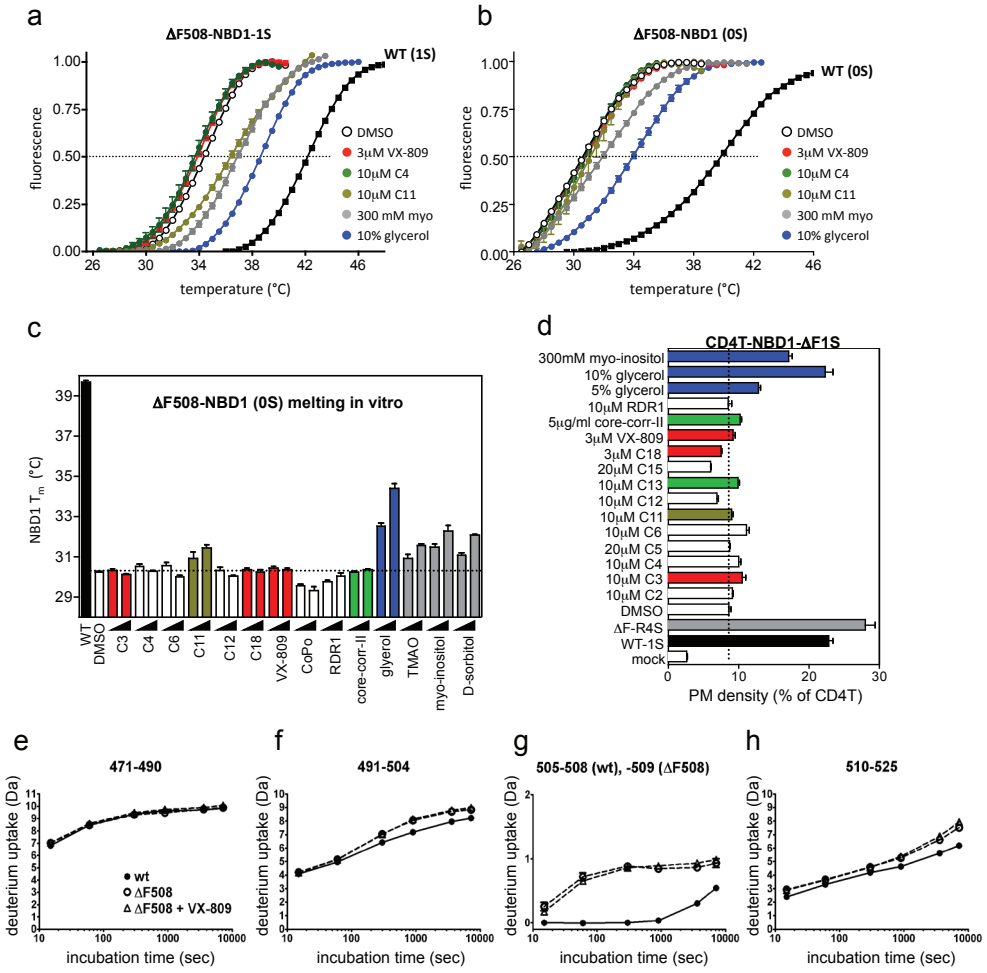

Figure 4. Effect of correctors on the isolated NBD1 stability *in vitro* and *in vivo*. (a-c) Melting temperature (T_m) of isolated human ΔF508-NBD1-1S (a) or ΔF508-NBD1 (b, c) was measured *in vitro* by differential scanning fluorimetry (DSF)[5,24]. WT-NBD1-1S or WT-NBD1 was used as a positive control. The indicated correctors or chemical chaperones (CC) (see Table S1) were included during thermal unfolding at the following concentration: C1, C2, C3, C4, C5, C6, C7, C9, C11, C12, C13, C14, C17, CoPo (3 μM and 10 μ M), C8, C15, C16 (10 μM and 20 μM), C18, VX-809 (1 μM and 3 μM), RDR1 (5 μM and 15 μM), core-corr-II (2.5 μg/ml and 5 μg/ml), glycerol (5% and 10%), TMAO, taurine, myo-inositol and D-sorbitol (150 mM and 300 mM). Thermal unfolding scans of ΔF508-NBD1-1S (a) and ΔF508-NBD1 (b) in the presence of selected correctors are shown. (c) T_m of ΔF508-NBD1 in the presence of corrector or chemical chaperone was determined by DSF as in panel b. Data represent means ± SEM (n=3). Statistically significant change in T_m was considered larger than mean ± 3SD (30.2 ± 0.4°C) of DMSO treated ΔF508-NBD1 T_m. (d) PM density of the CD4T-ΔF508-NBD1-1S in COS7 cells was measured by cell surface ELISA using anti-CD4 Ab. Cells were treated with the indicated corrector for 24 h at 37°C. CD4T-WT-NBD1-1S (WT-1S) and CD4T-ΔF508-NBD1-R4S (ΔF-R4S) were used as positive control. Red and green bars indicate correctors that belong to class-I and class-II, respectively. Data represents mean ± SEM (n=8-12). (e-h). Conformational dynamics of wt and ΔF508-NBD1-1S determined by HDX-MS following continuous D_2O labelling fro 5 min in the presence or absence of 10 μM VX-809 as described in Methods. Data are means ± SEM (n=3). Representative peptides are selected from a total of more than sixty peptides obtained by pepsin digestion.

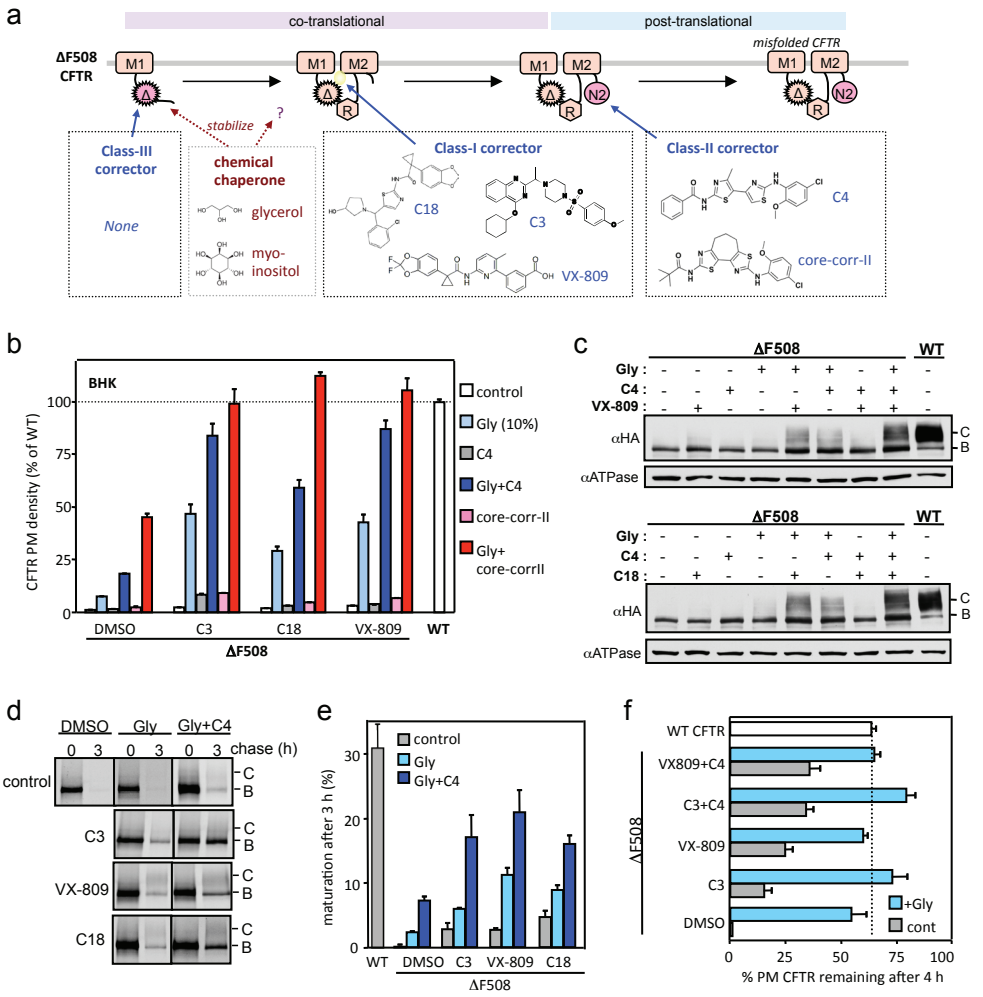

Figure 5. Combination of correctors targeting distinct structural defects completely restores ΔF508-CFTR folding, PM expression and stability in BHK cells. (a) Schematic model shows the proposed targets of the available correctors based on *in vitro*, *in vivo* and *in silico* analysis. Chemical chaperones (CC, e.g. glycerol and myo-inositol) preferentially, but presumably not exclusively stabilize the ΔF508-NBD1. VX-809, C18 and C3 target the NBD1-MSD1/2 interface, while C4 and core-corr-II target the NBD2. (b-f) ΔF508-CFTR PM density (b, n=6-12), cellular expression (c), ER folding efficiency (d-e, n=3-4) and PM stability after 4 h (f, n=5-12) were determined upon treatment with the correctors (10 μM C3 or C4; 3 μM C18 or VX-809, 5 μg/ml core-corr-II ; 10% glycerol) or their combinations in BHK cells by cell surface ELISA, Western blotting, metabolic pulse-chase technique and cell surface ELISA, respectively. All data represent means ± SEM.

experiments and ELISA revealed that the combined treatment increased the ΔF508-CFTR folding efficiency to ~70% of the WT level (Fig.5d-e) and largely rescued the mutant PM stability defect (Fig.5f). Thus, the largely normalized ER folding efficiency and PM stability of ΔF508-CFTR in the presence of two classes of correctors with glycerol account for the WT-like PM expression.

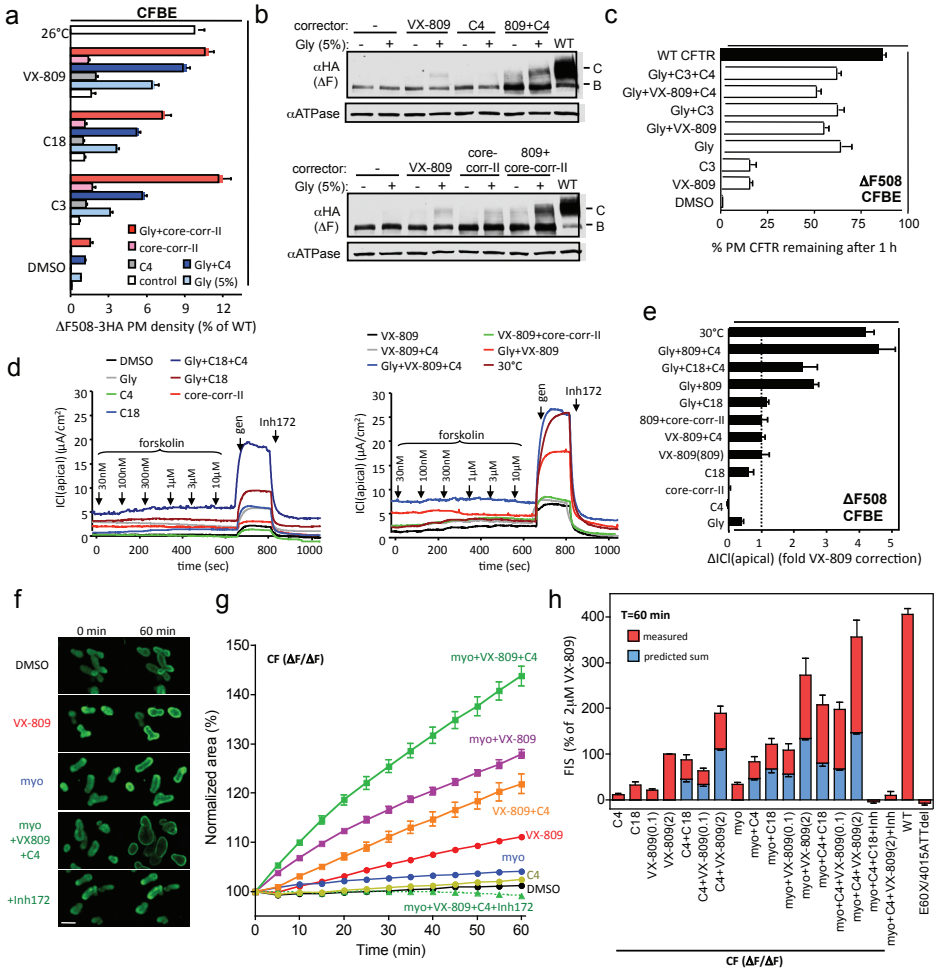

Figure 6. Corrector combination synergistically restores ΔF508-CFTR functional expression in polarized epithelial cells and rectal organoids from ΔF508 homozygous CF patients. (a-e) ΔF508-CFTR PM density (a, n=7-22), cellular expression (b), PM stability (c, n=16) and function (d, n=3) in CFBE41o- Tet-on cells. Correctors were applied as indicated (C3 or C4 at 10 μM, C18 or VX-809 at 3 μM, core-corr-II at 2.5 μg/ml, glycerol [Gly] at 5%) for 24 h at 37°C. For comparison, DF508-CFTR was rescued by low temperature at 26°C or 30°C for 36-48 h. (d) Representative records of enhanced ΔF508-CFTR ICl(apical) by corrector are shown. The current was stimulated by consecutive addition of forskolin and 100 μM genistein (gen) followed by CFTR inhibition with 20 μM CFTR inhibitor-172 (Inh_{172}). (e) Summary of the peak, Inh_{172}-sensitive ICl(apical) of ΔF508-CFTR in CFBE41o- cells after treatment of correctors (n=3-4). (f) Fluorescence laser confocal images of calcein-green loaded CF rectal organoids before and after forskolin-induced swelling (FIS) for 60 min in the presence of the indicated corrector (2 μM, VX-809, C4 or 125 mM myo-inositol (myo)), and inhibitor (Inh; 50 μM CFTR inhibitor-172 and GlyH-101). For ΔF508-CFTR correction, organoids were pre-incubated for 20-24 hours with correctors. Bar, 140 μm. (g) Time course of FIS of CF organoids from a representative experiment. Organoids were treated overnight with the indicated correctors as described in Methods. Cell volume was expressed as percentage of initial cell cross-sectional area before forskolin stimulation. (h) Statistical analysis of FIS. Relative cell areas are expressed as percentage of the area of 2 μM VX-809 treated cells after 60 min of FIS. Besides the measured FIS (red bar), the predicted sum of the individual corrector (2 μM C3, C4, C18; 0.1 or 2 μM VX-809; 125 mM myo-inositol) effect is indicated, assuming additive effect (blue bar). The mean FIS from three healthy controls (WT) is included. No FIS was observed after treatment of myo-inositol, C4 and VX-809 in organoids carrying E60X/4015ATTdel CFTR mutant[42]. Data represent means ± SEM from six independent experiments performed on three ΔF508 homozygous patients.

ΔF508-CFTR rescue is synergistically augmented by VX-809 in combination with class-II corrector and chemical chaperone in polarized respiratory epithelial cells

The rationally selected chemical combination also conferred synergistic rescue of ΔF508-CFTR in polarized respiratory epithelial cells. The ΔF508-CFTR PM density in CFBE41o- cells treated with a class-I corrector was enhanced by ~3-fold in the presence of 5% glycerol that was further augmented by class-II corrector (C4 or core-corr-II), representing ~5 fold increase of the VX-809 effect (Fig.6a). Combined treatment of two classes of correctors with glycerol enhanced the PM density of ΔF508-CFTR to ~10% of the WT CFTR level, a comparable efficacy to that achieved by low temperature (26°C) rescue (Fig.6a). Consistently, combination of VX-809, C4, and glycerol synergistically restored the ΔF508-CFTR complex-glycosylation (Fig.6b), PM stability (Fig.6c), and function at the apical PM in CFBE41o- epithelia (Fig.6d-e). Similar enhancement was observed in other polarized epithelial cell models. The combined treatment enhanced the PM density of ΔF508-CFTR to ~40% and ~15% of the WT level in Madin-Darby Canine Kidney (MDCKII) and human lung papillary adenocarcinoma epithelial cells (NCI-H441), respectively (Fig.S11).

Chemical combination largely restores ΔF508-CFTR function in rectal organoids from CF patients

Finally, the efficacy of the mechanism-based corrector combination was evaluated on human rectal organoids derived from CF patients homozygous for the ΔF508 mutation[42]. CFTR channel activity was measured by monitoring the forskolin-induced swelling (FIS) of organoids, since the cross-sectional area of organoids was proportional with CFTR-mediated chloride and coupled water transport[42]. While class-I corrector (C18 or VX-809) modestly improved the FIS of $^{\Delta F508/\Delta F508}$CFTR organoids, combining with myo-inositol[43], a CC selected based on its minimal toxicity, synergistically enhanced the ΔF508-CFTR-dependent FIS to 30-60% of that observed in organoids from healthy individuals (WT) (Fig.6f-h). The rescued ΔF508-CFTR mediated FIS was completely prevented with CFTR blockers (Inh_{172} and GlyH101) (Fig.6f-h). Likewise, organoids expressing non-functional, truncated CFTR variants (E60X/4015ATTdel) also failed to display any FIS (Fig.6h). Remarkably, VX-809, C4 and myo-inositol jointly restored the ΔF508-CFTR-dependent FIS by >80% of the WT. Comparison of individual and combination of correctors on FIS of $^{\Delta F508/\Delta F508}$*CFTR* organoids indicates a 2-2.5-fold synergism for dual and triple compound combinations (Fig.6h, compare *blue* and *red bars*). Together, these results demonstrate that mechanism-based corrector combinations are potentially capable to robustly rescue ΔF508-CFTR folding and function in cell culture models and primary human CF organoids.

DISCUSSION

Here we show that combination of correctors targeting complementary conformational defects can overcome their individually modest impact and synergistically restore the ΔF508-CFTR processing and PM channel function. Using *in vivo*, *in vitro,* and *in silico* analyses, we identified subsets of correctors that preferentially target the primary conformational defect at the NBD1-MSD1(CL1)/MSD2(CL4) interface (class-I) or the consequential NBD2 misassembly (class-II). None of the available correctors belong to class-III that targets the human ΔF508-NBD1 energetic defect. Only CCs, such as glycerol and myo-inositol, can substitute for a class-III corrector by stabilizing

the human ΔF508-NBD1 both *in vitro* and *in vivo*. While we cannot rule out that glycerol has multiple targets in ΔF508-CFTR, NBD2 deletion diminished the glycerol effect on PM expression and complex-glycosylation of ΔF508-R1S-CFTR, but left the ΔF508-CFTR-R1070W expression largely unaffected (Fig.3e-f and Fig.S7f-g). These observations imply that glycerol may primarily stabilize the NBD1. The proposed corrector classification also provides a plausible explanation for the additive effect of C3 (class-I) and C4 (class-II)[44,45] or VX-809 (class-I) and C4 (class-II), the attenuated efficiency of C3 and VX-809[11] and the synergism of class I and CCs (as surrogate of class-III) (Fig.5-6). The limited synergy between class-I and class-II correctors in the absence of CC indicates that suppression of ΔF508-CFTR primary defects is a prerequisite for correction of the secondary NBD2 defect.

Interestingly, class-I, class-II corrector or glycerol also augmented the PM expression of WT CFTR that has intrinsic low folding efficiency (~30%)[1] (Fig.S12a). The WT CFTR rescue efficiency by VX-809 or C18 but not C4 was suppressed in the presence of V510D mutation and, to a lesser extent by 3S or R4S mutation (Fig.S12b), consistent with the limited conformational instability of the NBD1-MSD2 interface and NBD1 in WT CFTR[24]. These observations with the overlapping VX-809 *in silico* docking data on ΔF508 and WT CFTR (Fig.S12c), as well as MSD1 stabilization are consistent with the possibility that VX-809, similarly to the V510D mutation, targets the conformationally unstable WT NBD1-MSD1/2 interface.

By selectively increasing the ER folding efficiency and the PM stability in multiple cellular models, VX-809 was predicted to overcome a kinetic folding trap and/or stabilize the native-like conformer by direct interaction with ΔF508-CFTR[11]. Here we provide compelling evidence that inhibition of ΔF508-CFTR-2RK thermal inactivation is a consequence of VX-809 or C18 direct interaction at the single molecule level. Although VX-809 prevented the functional inactivation upon raising the temperature from 24°C to 36°C, extended exposure to 36°C attenuated the VX-809-induced functional rescue probably due to stabilization only one of the primary folding defects (NBD1-MSD1/2 interface). This interpretation is in line with the modest effect of NBD1-MSD1/2 interface genetic stabilization[46], compared to that of the NBD1[32], and likely explains the negligible effect of VX-809 on the ΔF508-CFTR-I539 thermal inactivation reported recently[35]. Notably, direct interaction of C3 as well as potentiators P1 and VX-770 with purified CFTR was also inferred based on their modulation of the channel ATPase and transport activity[21,47,48].

Definitive identification of VX-809 binding site(s) in the absence of a functionally inert, cross-linkable adduct remains a challenge and is further exacerbated by the coupled folding and misfolding mechanism of CFTR domains[5,7] that may allow allosteric corrections of folding defects from different binding sites. However, our comprehensive analysis by *in silico* predictions, in concert with *in vitro* assays (DSF and HDX-MS) using isolated human NBD1s and *in vivo* studies using full-length CFTRs with deletion and point mutations, strongly suggest that the NBD1-CL1/4 represents a primary target of VX-809, a conclusion that partly overlaps with the recent proposition of the Riordan lab[35].

Importantly, mutations confined to the TM helix-1 (G85E, G91R) and CL2 (M266R, W277R) of MSD1 could also be partially rescued, presumably via targeting the coupled interface defect at the NBD1-CL1/4. These results, jointly with those obtained using CFTR fragments and CL1 mutations, provide a plausible model of VX-809 action that binds to MSD1 and stabilizes the CL1-CL4 coupling helix, a critical step to form the proper interactions between NBD1-MSD1/2 and facilitate the cooperative CFTR domain assembly upon completion of NBD2 translation[24,25,35].

Counteracting the processing defect of the CF causing R170G and other missense mutation localized to the TM helix-1 and CL1/4 described here and previously[35] by class-I correctors also suggests that VX-809 may be successfully utilized alone in a variety of rare CF mutations.

While the additive effect of corrector pairing has been previously observed[11,44,45], the rationale for corrector combination remained elusive. Mechanism-based classification of correctors permitted a rationally designed corrector combination approach that achieved a remarkable improvement in ΔF508-CFTR rescue efficiency. Chemical correction of NBD1, NBD1-MSD1/2 interface, and NBD2 instabilities almost completely restores the ΔF508-CFTR folding, PM expression, stability, and function in BHK cells. The ΔF508-CFTR rescue by corrector combinations was weaker in kidney and respiratory epithelial cells (10-30% of the WT) than in BHK cells. This could be attributed to modest NBD1 stabilization by reduced glycerol concentration (5%) that was required to maintain epithelial polarity.

Combined correction of the three structural defects largely restored the ΔF508-CFTR transport function in human $^{\Delta F508/\Delta F508}$*CFTR* organoids. While this effect may be an overestimate due to the rate limiting transport capacity of the basolateral PM in the WT intestinal organoid, the VX-809-induced ΔF508-CFTR chloride transport was augmented ~4-fold by class-II compound and CC based on the FIS measurements. Considering that VX-809 improves ΔF508-CFTR PM function to ~15% of WT CFTR in primary human bronchial epithelia[11] with marginally translatable clinical benefit[18], it is reasonable to assume that structural defect-targeted rational corrector combination will eventually confer sufficiently enhanced CFTR transport capacity in respiratory epithelial cells to achieve significant clinical improvements in most $^{\Delta F508/\Delta F508}$*CFTR* patients.

None of the available correctors but CCs can counteract the human ΔF508-NBD1 conformational defect according to *in vitro* and *in vivo* folding studies. This represents a bottleneck of CF pharmacological therapy, since systemic administration of CCs is not feasible. To achieve improved pharmacological corrections in combination with class-I correctors (e.g. VX-809), identification of NBD1 stabilizer is required. Initial isolation of PCs stabilizing the NBD1 could be envisioned by high-throughput screening (HTS) of diverse compounds or fragment libraries *in vitro*, *in vivo* or *in silico* using ΔF508-NBD1 or ΔF508-CFTR cell-based functional or biochemical assays[14,19]. Exploiting NBD1-MSD1/2 interface stabilization by second site suppressor mutation or class-I correctors (e.g.VX-809) may bias HTS efforts towards the isolation of NBD1 stabilizing small molecules. We believe that the successful identification of NBD1 stabilizer would make the mechanism-based corrector combination therapy feasible for most CF patients.

METHODS

Cell lines

Full-length and truncated human CFTR variants with the 3HA-tag in the 4th extracellular loop[49] were constructed by PCR mutagenesis (Table S2). Detailed information on PCR mutagenesis is available from the authors on request. BHK cells stably expressing CFTR variants were generated and grown as previously[24]. MDCK type II cells stably expressing CFTR-3HA variants were generated by lentivirus infection under puromycin selection (1-5 μg/ml) and grown in Dulbecco's modified Eagle's medium (DMEM) (Invitrogen, Carlsbad, CA) supplemented with 10% fetal bovine serum (FBS). CFBE41o- Tet-on and NCI-H441 Tet-on cells stably expressing CFTR-3HA variants under

tetracycline responsive promoter were generated by lentivirus transduction using the Lenti-X TetON Advanced Inducible Expression System (Clontech, Mountain View, CA) under puromycin (3 µg/ml) and G418 selection (0.2 mg/ml) and grown in minimal essential medium (MEM, Invitrogen) supplemented with 10% FBS, 2 mM L-glutamine and 10 mM HEPES, and RPMI-1640 Medium (ATCC) supplemented with 10% FBS. For propagation, the CFBE41o- cells were cultured in plastic flasks coated with an extracellular matrix (ECM mix) consisting of 10 µg/ml human fibronectin (EMD), 30 µg/ml PureCol collagen preparation (Advanced Biomatrix) and 100 µg/ml bovine serum albumin (Sigma-Aldrich) diluted in LHC basal medium (Invitrogen). The CFTR-3HA expression was induced by 0.5 or 1 µg/ml doxycycline treatment for 4 days.

Human material

Rectal suction biopsies were obtained for intestinal current measurements (ICM) during standard CF care by a procedure described previously[42] that has been approved by the Ethics Committee of the University Medical Centre Utrecht and the Erasmus Medical Centre of Rotterdam.

Differential scanning fluorimetry (DSF)

Melting temperature of recombinant human NBD1 was measured as previously[24]. DSF scans of NBD1 (7-12 µM) were obtained in 150 mM NaCl, 20 mM $MgCl_2$, and 10 mM HEPES, pH 7.5 and were performed using a Stratagene Mx3005p (Agilent Technologies, La Jolla, CA) qPCR instrument in the presence of 2X Sypro Orange. The medium ATP concentration was kept at 2.5 mM unless otherwise indicated.

Measurement of CFTR cell surface density and stability

Cell surface CFTR-3HA density and stability was measured by ELISA using anti-HA Ab as previously[49]. The PM density of CD4-NBD1 chimeras was measured by cell surface ELISA using anti-CD4 (OKT4) Ab in transiently transfected COS-7 cells as described[5,24]. Cell surface density of CFTR and CD4-NBD1 chimeras was normalized by protein concentration based on BCA assay. Data were presented as mean values ± SEM from at least 2 independent experiments that consist of multiple (3-8) measurements.

Western blotting and pulse-chase experiments

Western blotting and pulse-chase experiments were performed as previously[49]. Cells were treated with correctors for 24 h at 37°C and during the pulse-labeling and chase period.

Apical Cl^- current (ICl(apical)) measurement

Apical Cl^- current measurements was essentially performed as described[50]. CFBE41o- cells were plated on ECM-mix coated 12 mm Snapwell filters (Corning, Corning, NY) at a density of 1×10^5 cells/cm^2. Polarized epithelia (≥ 5 days post confluence) were mounted in Ussing chambers, bathed in Krebs-bicarbonate Ringer and continuously bubbled with 95% O_2 and 5% CO_2. To impose a chloride gradient, Cl^- was replaced by gluconate in the apical compartment. To functionally isolate the apical PM, the basolateral PM was permeabilized with 100 µM amphotericin B and the epithelial sodium channel was inhibited with 100 µM amiloride. CFTR activity was stimulated by

apical forskolin (0.03-10 μM) and genistein (100 μM) followed by the addition of CFTR inhibitor 172 (Inh_{172}, 20 μM) to determine CFTR-mediated apical Cl^- current (ICl(apical)). Measurements were performed at 37°C. The transepithelial resistance (TER) of CFBE was predominantly between 200-1700 Ω/cm^2. Although combination of three chemicals, including glycerol, reduced the TER of permeabilized CFBE cells to <180 Ω/cm^2, the CFTR-mediated ICl(apical) was measured by monitoring only the CFTR-Inh_{172}-sensitive component of the forskolin and genistein stimulated ICl(apical).

Temperature-dependent CFTR channel activity in phospholipid bilayer

WT or ΔF508 CFTR reconstitution and channel activity were essentially measured as described previously[24]. Detailed description of method is included in the Supplementary Methods.

In silico docking

In silico docking of VX-809, C4 and core-corr-II was performed using *AutoDock* 4.2. A detailed description of the preparation of CFTR and ligand files, as well as running and analyzing the docking simulation is included in the online Supplementary Materials.

Hydrogen deuterium exchange and mass spectrometry (HDX-MS)

Localized conformational dynamics of isolated NBD1s was measured by HDX-MS essentially as described[41] and is detailed in the Supplementary Methods.

CFTR transport activity of human rectal organoids

Human rectal organoids were isolated as described in Supplementary Methods. Organoids were seeded from a 7 day-old culture in 4 μl matrigel placed into a flat-bottom 96-well culture plate (Nunc) and commonly contained 40-80 organoids and 100 μl culture medium. To visualize volume changes, one day after seeding, organoids were loaded with 10 μM calcein-green for 60 min (Invitrogen). After calcein-green treatment (with or without CFTR inhibition), 5 μM forskolin was added and the organoids morphology was monitored by time-lapse fluorescence laser confocal microscopy (LSM710, Zeiss, 5x objective). To inhibit CFTR, organoids were pre-incubated with 50 μM CFTRInh-172 and 50 μM GlyH-101 (Cystic Fibrosis Foundation Therapeutics, Inc) for 3 h. Images were collected in every 10 min for 90 min in a top stage incubator (5% CO_2 at 37°C). Each condition was monitored in triplicate wells. For ΔF508-CFTR correction, organoids were pre-incubated for 20-24 hours with 2 μM C4, 2 μM C18, 100 nM or 2 μM VX-809 or 125 mM myo-inositol (Sigma-Aldrich) as single treatment or in combinations. DMSO concentration was identical under all conditions and did not exceed 0.2 % (w/v). The organoid surface area was quantified using Volocity (Improvision) imaging software. The normalized total organoid surface area was calculated and averaged from three individual wells per condition. The area under the curve (AUC) was calculated using Prism (GraphPad Software).

Acknowledgements

We thank L. Konerman (Univ. Western Ontario, London, Canada), T. Wales and J. Engen (Notheastern Univ., Boston, USA), M.J. Chalmers and P.R. Griffin (The Scripps Research Institute-

Scripps Florida, USA) for valuable advices to set up the HDX-MS technique, D. Gruenert (UCSF, San Francisco, USA) for the parental CFBE41o- cell line, R.J. Bridges (Rosalind Franklin University of Medicine and Science, North Chicago, USA), the CFFT Inc. for CFTR modulator panels and D. Thomas (McGill University, Canada) for kindly providing RDR compounds. We are grateful for the financial support of the Dutch Cystic Fibrosis foundation and the Wilhelmina Children's Hospital Research fund to J.B., the Hungarian National Science Foundation (MB08C-80039 and ERA-Chemistry OTKA grant 102166) to A.S., the EU (FP7-IRG 239270) to T.H., The Tara K. Telford Fund for Cystic Fibrosis Research at the University of California/Davis and The National Institutes of Health (Grants DK072517 and GM089153) to M.K., NIH-NIDDK, CFFT Inc., Cystic Fibrosis Canada, CFI, and CIHR to G.L.L. T.H. is a Bolyai Fellow of the Hungarian Academy of Sciences. G.V. was partly supported by an EMBO and FRSQ Fellowship. G.L.L. is a Canada Research Chair.

REFERENCES

1. Riordan, J.R. CFTR function and prospects for therapy. *Annu Rev Biochem* **77**, 701-26 (2008).
2. He, L. et al. Multiple membrane-cytoplasmic domain contacts in the cystic fibrosis transmembrane conductance regulator (CFTR) mediate regulation of channel gating. *J Biol Chem* **283**, 26383-90 (2008).
3. Serohijos, A.W. et al. Phenylalanine-508 mediates a cytoplasmic-membrane domain contact in the CFTR 3D structure crucial to assembly and channel function. *Proc Natl Acad Sci U S A* **105**, 3256-61 (2008).
4. Du, K., Sharma, M. & Lukacs, G.L. The DeltaF508 cystic fibrosis mutation impairs domain-domain interactions and arrests post-translational folding of CFTR. *Nat Struct Mol Biol* **12**, 17-25 (2005).
5. Du, K. & Lukacs, G.L. Cooperative assembly and misfolding of CFTR domains in vivo. *Mol Biol Cell* **20**, 1903-15 (2009).
6. He, L. et al. Restoration of domain folding and interdomain assembly by second-site suppressors of the DeltaF508 mutation in CFTR. *FASEB J* **24**, 3103-12 (2010).
7. Cui, L. et al. Domain interdependence in the biosynthetic assembly of CFTR. *J Mol Biol* **365**, 981-94 (2007).
8. Rosser, M.F., Grove, D.E., Chen, L. & Cyr, D.M. Assembly and misassembly of cystic fibrosis transmembrane conductance regulator: folding defects caused by deletion of F508 occur before and after the calnexin-dependent association of membrane spanning domain (MSD) 1 and MSD2. *Mol Biol Cell* **19**, 4570-9 (2008).
9. Balch, W.E., Roth, D.M. & Hutt, D.M. Emergent properties of proteostasis in managing cystic fibrosis. *Cold Spring Harb Perspect Biol* **3** (2011).
10. Boucher, R.C. New concepts of the pathogenesis of cystic fibrosis lung disease. *Eur Respir J* **23**, 146-58 (2004).
11. Van Goor, F. et al. Correction of the F508del-CFTR protein processing defect in vitro by the investigational drug VX-809. *Proc Natl Acad Sci U S A* **108**, 18843-8 (2011).
12. Denning, G.M. et al. Processing of mutant cystic fibrosis transmembrane conductance regulator is temperature-sensitive. *Nature* **358**, 761-4 (1992).
13. Sato, S., Ward, C.L., Krouse, M.E., Wine, J.J. & Kopito, R.R. Glycerol reverses the misfolding phenotype of the most common cystic fibrosis mutation. *J Biol Chem* **271**, 635-8 (1996).
14. Pedemonte, N. et al. Small-molecule correctors of defective DeltaF508-CFTR cellular processing identified by high-throughput screening. *J Clin Invest* **115**, 2564-71 (2005).
15. Varga, K. et al. Enhanced cell-surface stability of rescued DeltaF508 cystic fibrosis transmembrane conductance regulator (CFTR) by pharmacological chaperones. *Biochem J* **410**, 555-64 (2008).
16. Hanrahan, J.W., Sampson, H.M. & Thomas, D.Y. Novel pharmacological strategies to treat cystic fibrosis. *Trends Pharmacol Sci* **34**, 119-25 (2013).
17. Van Goor, F. et al. Rescue of CF airway epithelial cell function in vitro by a CFTR potentiator, VX-770. *Proc Natl Acad Sci U S A* **106**, 18825-30 (2009).

18. Clancy, J.P. et al. Results of a phase IIa study of VX-809, an investigational CFTR corrector compound, in subjects with cystic fibrosis homozygous for the F508del-CFTR mutation. *Thorax* **67**, 12-8 (2012).

19. Sampson, H.M. et al. Identification of a NBD1-binding pharmacological chaperone that corrects the trafficking defect of F508del-CFTR. *Chem Biol* **18**, 231-42 (2011).

20. Howard, M. et al. Mammalian osmolytes and S-nitrosoglutathione promote Delta F508 cystic fibrosis transmembrane conductance regulator (CFTR) protein maturation and function. *J Biol Chem* **278**, 35159-67 (2003).

21. Kim Chiaw, P., Wellhauser, L., Huan, L.J., Ramjeesingh, M. & Bear, C.E. A chemical corrector modifies the channel function of F508del-CFTR. *Mol Pharmacol* **78**, 411-8 (2010).

22. Protasevich, I. et al. Thermal unfolding studies show the disease causing F508del mutation in CFTR thermodynamically destabilizes nucleotide-binding domain 1. *Protein Sci* **19**, 1917-31 (2010).

23. Wang, C. et al. Integrated biophysical studies implicate partial unfolding of NBD1 of CFTR in the molecular pathogenesis of F508del cystic fibrosis. *Protein Sci* **19**, 1932-47 (2010).

24. Rabeh, W.M. et al. Correction of both NBD1 energetics and domain interface is required to restore DeltaF508 CFTR folding and function. *Cell* **148**, 150-63 (2012).

25. Mendoza, J.L. et al. Requirements for efficient correction of DeltaF508 CFTR revealed by analyses of evolved sequences. *Cell* **148**, 164-74 (2012).

26. Robert, R. et al. Correction of the Delta phe508 cystic fibrosis transmembrane conductance regulator trafficking defect by the bioavailable compound glafenine. *Mol Pharmacol* **77**, 922-30 (2010).

27. Loo, T.W., Bartlett, M.C. & Clarke, D.M. The V510D suppressor mutation stabilizes DeltaF508-CFTR at the cell surface. *Biochemistry* **49**, 6352-7 (2010).

28. Teem, J.L. et al. Identification of revertants for the cystic fibrosis delta F508 mutation using STE6-CFTR chimeras in yeast. *Cell* **73**, 335-46 (1993).

29. Pedemonte, N. et al. Dual activity of aminoarylthiazoles on the trafficking and gating defects of the cystic fibrosis transmembrane conductance regulator chloride channel caused by cystic fibrosis mutations. *J Biol Chem* **286**, 15215-26 (2011).

30. Phuan, P.W. et al. Cyanoquinolines with independent corrector and potentiator activities restore DeltaPhe508-cystic fibrosis transmembrane conductance regulator chloride channel function in cystic fibrosis. *Mol Pharmacol* **80**, 683-93 (2011).

31. Hegedus, T. et al. F508del CFTR with two altered RXR motifs escapes from ER quality control but its channel activity is thermally sensitive. *Biochim Biophys Acta* **1758**, 565-72 (2006).

32. Aleksandrov, A.A. et al. Allosteric modulation balances thermodynamic stability and restores function of DeltaF508 CFTR. *J Mol Biol* **419**, 41-60 (2012).

33. Dalton, J., Kalid, O., Schushan, M., Ben-Tal, N. & Villa-Freixa, J. New Model of Cystic Fibrosis Transmembrane Conductance Regulator Proposes Active Channel-like Conformation. *J Chem Inf Model* (2012).

34. Kalid, O. et al. Small molecule correctors of F508del-CFTR discovered by structure-based virtual screening. *J Comput Aided Mol Des* **24**, 971-91 (2010).

35. He, L. et al. Correctors of {Delta}F508 CFTR restore global conformational maturation without thermally stabilizing the mutant protein. *FASEB J* **27**, 536-45 (2013).

36. Thibodeau, P.H. et al. The cystic fibrosis-causing mutation deltaF508 affects multiple steps in cystic fibrosis transmembrane conductance regulator biogenesis. *J Biol Chem* **285**, 35825-35 (2010).

37. Grove, D.E., Rosser, M.F., Ren, H.Y., Naren, A.P. & Cyr, D.M. Mechanisms for rescue of correctable folding defects in CFTRDelta F508. *Mol Biol Cell* **20**, 4059-69 (2009).

38. Zhang, F., Kartner, N. & Lukacs, G.L. Limited proteolysis as a probe for arrested conformational maturation of delta F508 CFTR. *Nat Struct Bio* **5**, 180-3 (1998).

39. Yu, G.J. et al. Potent s-cis-locked bithiazole correctors of DeltaF508 cystic fibrosis transmembrane conductance regulator cellular processing for cystic fibrosis therapy. *J Med Chem* **51**, 6044-54 (2008).

40. Aleksandrov, A.A. et al. Regulatory insertion removal restores maturation, stability and function of DeltaF508 CFTR. *J Mol Biol* **401**, 194-210 (2010).

41. Lewis, H.A. et al. Structure and dynamics of NBD1 from CFTR characterized using crystallography

and hydrogen/deuterium exchange mass spectrometry. *J Mol Biol* **396**, 406-30 (2010).

42. Dekkers, J. et al. A functional CFTR assay using primary cystic fibrosis intestinal organoids. *Nat Med* **in press**.

43. Zhang, X.M. et al. Organic solutes rescue the functional defect in delta F508 cystic fibrosis transmembrane conductance regulator. *J Biol Chem* **278**, 51232-42 (2003).

44. Wang, Y., Loo, T.W., Bartlett, M.C. & Clarke, D.M. Additive effect of multiple pharmacological chaperones on maturation of CFTR processing mutants. *Biochem J* **406**, 257-63 (2007).

45. Pedemonte, N., Tomati, V., Sondo, E. & Galietta, L.J. Influence of cell background on pharmacological rescue of mutant CFTR. *Am J Physiol Cell Physiol* **298**, C866-74 (2010).

46. Liu, X., O'Donnell, N., Landstrom, A., Skach, W.R. & Dawson, D.C. Thermal instability of DeltaF508 cystic fibrosis transmembrane conductance regulator (CFTR) channel function: protection by single suppressor mutations and inhibiting channel activity. *Biochemistry* **51**, 5113-24 (2012).

47. Wellhauser, L. et al. A small-molecule modulator interacts directly with deltaPhe508-CFTR to modify its ATPase activity and conformational stability. *Mol Pharmacol* **75**, 1430-8 (2009).

48. Eckford, P.D., Li, C., Ramjeesingh, M. & Bear, C.E. Cystic Fibrosis Transmembrane Conductance Regulator (CFTR) Potentiator VX-770 (Ivacaftor) Opens the Defective Channel Gate of Mutant CFTR in a Phosphorylation-dependent but ATP-independent Manner. *J Biol Chem* **287**, 36639-49 (2012).

49. Okiyoneda, T. et al. Peripheral protein quality control removes unfolded CFTR from the plasma membrane. *Science* **329**, 805-10 (2010).

50. Veit, G. et al. Proinflammatory cytokine secretion is suppressed by TMEM16A or CFTR channel activity in human cystic fibrosis bronchial epithelia. *Mol Biol Cell* **23**, 4188-202 (2012).

SUPPLEMENTARY RESULTS

Considering that multiple indirect evidences indicate that the active site of CFTR correctors is located at the cytoplasmic loops–NBD1 interface, we performed *in silico* docking to study VX-809 binding at the atomic level. We used both the closed[3] and open[33] CFTR models, since the interface configuration of the NBDs-MSDs was different in these homology models. *In silico* docking was also performed to the X-ray structure of NBD1 (PDBID:2BBT) to mimic corrector binding during or immediately after NBD1 translation, preceding complete domain-domain assembly. Solubilizing mutations in the 2BBT structure were reverted to WT (see details in the Supplementary Methods below).

In the simulation using the NBD1 crystal structure, VX-809 bound to the isolated NBD1 at the CL1/4 or the hypothetical NBD2 interface (Fig.S5a). AutoDock in both the closed and open CFTR full structures indicated that VX-809 primarily binds to the site I at the CL1/4-NBD1/2 interface (Fig.2c, Fig.S5c and e). In the open CFTR model, VX-809 also docked the site II at the β-subdomain located in the NBD1-NBD2 interface (Fig.S5e). We further performed *in silico* docking of VX-809 to the ΔF508-CFTR-ΔNBD2 model considering that NBD2 is dispensable for the CFTR folding[5] and that VX-809 effect was almost completely retained upon ΔNBD2 (Fig.3e-f and Fig. S9f-g). In the CFTR-ΔNBD2 model, the CL1/4-NBD1 interface near the ΔF508 cavity[34] was predicted as the binding site in addition to the site I and site II (Fig.S5d and f).

According to *in silico* docking, C4 and core-corr-II are bound to NBD1 at the CL1/4 or the NBD2 interface similar to VX-809 (Fig.S8a and Fig.S9a). However, the binding free energies of C4 and core-corr-II were higher than that of VX-809 (-8.4 and -7.8 compared to -9.9 kcal/mol,

respectively; see Table S3), consistent with the observation that the C4 and core-corr-II rescue efficiency was lower than VX-809. In the two CFTR models, C4 was predicted to bind to site I at the MSD1/2-NBD1/2 interface, site II and site III at the NBD1-NBD2 interface and the site near regulatory insertion (site RI) (Fig.S8b and d). C4 binding, however, was diminished at both site I and site RI in the closed CFTR-ΔNBD2 model, and at both site II and site III in the open CFTR-ΔNBD2 model while the binding at the site I in the open CFTR-ΔNBD2 model remained (Fig.S8c and e). Considering that the NBD2 was indispensable for the C4 rescue effect (Fig.3e-f and Fig. S7f-g), site II and site III likely represent the functionally relevant binding sites for C4. The RI region could be ruled out as a critical C4 binding site for rescue effect, since deletion of the RI region largely preserved the C4-induced rescue of ΔF508-CFTR-ΔRI (Fig.S9h). Similar prediction was obtained by *in silico* docking of core-corr-II to the two CFTR models and suggests that core-corr-II may preferentially bind to the NBD1-NBD2 interface at the site II (Fig.S9).

In summary, the results of *in silico* docking are in good agreement with experiments suggesting the CL1/4-NBD1 regions as the site of VX-809 interaction. The docking algorithm is sensitive enough on the homology models to yield preferential binding to the CL1/4 and not to the symmetrical CL2/3 interface region and explain, at least in part, the differences in the molecular mechanism of CFTR variants rescue by VX-809, C4, and core-corr-II.

SUPPLEMENTARY METHODS

Antibodies and Reagents

Antibodies (Abs) were obtained from the following sources. Monoclonal anti-CFTR Ab L12B4 (recognizing NBD1) and M3A7 (recognizing NBD2) were purchased from Millipore Bioscience Research Reagents (Temecula, CA). Mouse monoclonal anti-HA Ab was from Covance Innovative Antibodies (Berkeley, CA). Chemicals were obtained from Sigma-Aldrich (St. Louis, MO) at the highest grade available. Most of the CFTR correctors were obtained from Cystic Fibrosis Foundation Therapeutics (CFFT), VX-809 from Selleck (Houston, TX), class II compounds were synthesized as described[39]. All of the correctors used in this study are listed in Table S1.

NBD1 protein purification

Recombinant human NBD1 proteins were purified from *E. coli* as previously described[24]. The NBD1 protein was concentrated to 3–5 mg/ml in buffer containing 150 mM NaCl, 1 mM ATP, 2 mM $MgCl_2$, 1 mM TCEP, 10% Glycerol and 10 mM HEPES, pH 7.8.

Microsome Preparation

Microsomes were isolated by differential centrifugation from BHK cells stably expressing 3HA-tagged WT or ΔF508-2RK CFTR as described[24]. To enrich for the complex-glycosylated ΔF508-2RK CFTR, cells were incubated at 26°C for ~36 hours followed by treatment with 150 μg/ml cycloheximide (CHX, 26°C for 12 h) before microsome isolation[49]. WT CFTR expressing cells were treated with 150 μg/ml CHX for 3 hours to eliminate the ER-localized core-glycosylated form.

Planar lipid bilayer studies

A planar phospholipid bilayer was made of a 2:1 (wt/wt) mixture of 1-palmitoyl-2-oleoyl-sn-glycero-3-phosphoethanolamine (POPE) and 1-palmitoyl-2-oleoyl-sn-glycero-3-phospho-L-serine (POPS, Avanti Polar Lipids, Alabaster, AL) in n-decane solution at a final lipid concentration of 25 mg/ml and formed over a 200 or 250 µm hole in a polystyrene chamber by monitoring the increase in its capacitance to 150–200 pF. The bilayer was bathed in symmetrical 300 mM Tris-HCl, 10 mM HEPES (pH 7.2), 5 mM $MgC1_2$, and 1 mM EGTA. Microsomes (10-20 µg proteins) isolated from CFTR expressing BHK cells were prephosphorylated in the presence of 100U/ml protein kinase A (PKA) catalytic subunit (Promega) and 2 mM for MgATP at room temperature for 10 min, added to the cis compartment and fused to planar lipid bilayer. CFTR channel activity was recorded in the presence of 100 U/ml PKA catalytic subunit and 2 mM MgATP. Currents were measured with a BC-535 amplifier (Warner Instrument, Hamden, CT). Voltage was clamped at V_m = −60 mV. In temperature ramp experiments the chamber was heated from room temperature to 36°C at a rate of ~1-2°C/min. Single channel activities were acquired using pClamp 8.1 (Axon Instruments) at 10 kHz, filtered at 200 Hz with low pass 8 pole Bessel filter and stored digitally. Records were filtered at 50 Hz and analyzed using Clampfit 10.3 (Axon Instruments). We applied 50% cut off between open and closed levels and events shorter than 10 ms were excluded from the analysis. Single channel open probability (P_o) was determined as NP_o divided by the number of channels, where NP_o was obtained from event detection features of Clampfit 10.3 and N represents the number of channels.

HDX-MS

HDX was initiated by mixing 1-2 µL of NBD1 stock solution to 15 volumes of D_2O-based buffer (pD 7.5, based on $pD = pH_{read} + 0.40$)[51] containing 150 mM NaCl, 1 mM ATP, 2 mM $MgCl_2$, 1 mM TCEP and glycerol, resulting in a final D_2O concentration of more than 90 % (v/v). The final concentration of glycerol was adjusted to 1%. The mixtures were incubated for 15 sec, 1min, 5 min, 15 min, 1 h and 2 h at room temperature and then quenched by adding the 2-2.5 µL aliquot of the mixture to 300 mM phosphate buffer including 8 M urea, pH 2.5 (quenching buffer). Quenched solutions were flash frozen in MeOH containing dry ice and samples were stored at -80°C.

Prior to high performance liquid chromatography (HPLC)-MS analysis, the labeled protein solutions were thawed, and immediately loaded onto the injection valve. Deuterated NBD1 was digested in an on-line immobilized pepsin column prepared in-house. On-line pepsin digestion was carried out at flow rate of 50 µL/min for ~1.5 min, and resulting peptides were trapped on C18 trapping column (Optimized Technologies, Oregon city, OR). Following desalting for 1.5 min (at 150 µl/min flow rate), peptides were loaded onto a C18 column (1 mm i.d. × 50 mm, Thermo Fisher Scientific, Waltham, MA) through a six-port valve. Peptides were separated using a 13-90% linear gradient of acetonitrile containing 0.1% formic acid for 6 min at 50 µl/min. Chromatographic separation was performed using an Agilent 1100 HPLC system. To minimized back-exchange, the column, solvent delivery lines, injector and other accessories were immersed in an ice bath. The C18 column was directly connected to the electrospray ionization source of LTQ Orbitrap XL (Thermo Fisher Scientific). Mass spectra of peptides were acquired in positive-ion mode for m/z 200-2000. Identification of peptides was carried out in separate experiments by tandem MS (MS/MS) analysis in data-dependent acquisition mode and using collision-induced

dissociation. All MS/MS spectra were analyzed using SEQUEST program (Thermo Fisher Scientific). Searching results from SEQUEST were further manually inspected and only those verifiable were considered in HDX analysis. Triplicate measurements were carried out for each time points. HDExaminer (Sierra Analytics, Modesto, CA) were used to determine the deuteration level as a function of labeling time. The deuterium level of peptides were not corrected for back-exchange, and therefore presented values reflect the relative exchange levels across the protein samples[52].

IN SILICO DOCKING

Preparation of the proteins.

Proteins were prepared initially in PDB format. The structure of the ΔF508-NBD1 was obtained from the PDB database (PDBID:2BBT)[41]. The F504N and Q646R solubilizing mutations were reverted back to F504 and Q646 followed by energy minimization in *SYBYL* (Tripos Inc.) using the AMBER force-field[53] with AMBERF99 charges[54]. Two full-length models, one representing the closed state (http://dokhlab.unc.edu/research/CFTR/home.html)[3], the other representing the open state[33] were selected for docking. For comparability, both models were trimmed to contain amino acids 81-365, 391-648, 855-1154, and 1208-1429. The F508 was deleted followed by the adjustment of the neighboring residues using the *Modloop server*[55] and by energy minimization using the AMBER force-field with AMBERF99 charges[54]. All the amino acid numbers mentioned in the paper correspond to the amino acid numbering in the WT CFTR.

Preparation of ligands.

Ligands were prepared in mol2 format. VX-809 was downloaded from the *PubChem Compound Database* in 3D sdf format and converted to mol2 format by *SYBYL*. Molecules C4 and core-corr-II were drawn in 2D using *ChemBioDraw Ultra 12.0* (CambridgeSoft) and saved in mol2 format. Their coordinates were copied to the *PRODRG server*[56] to obtain an initial 3D structure. The resulting mol2 files of C4 and core-corr-II were corrected to contain appropriate atom types and were subjected to energy minimization in *SYBYL*. Tripos force-field with Gasteiger-Hückel charges were used until the RMS gradient of the energy derivative reached 0.01 kcal/mol/Å.

Running the docking simulations.

The docking was performed using *AutoDock*[57]. Input files were prepared using *AutoDock 4.2* with *AutoDockTools* (MGLTools 1.5.4). Ligands were loaded with Gasteiger charges and were saved in pdbqt format. Polar hydrogen atoms and Kollmann charges were added to the proteins. The grid box was centered on coordinates 95 Å, 70 Å, 170 Å and its size was set to 70Å x 70Å x 70Å with 0.5 Å spacing to include the two NBDs and the coupling helices (Fig.S5b). To achieve this box size, AutoDock was compiled with a value of MAX_GRID_POINTS higher than the default 126 that allowed us to set 140 grid points in each direction. Lamarckian Genetic Algorithm was used for docking with default settings, except for the parameters ga_pop_size (300) and ga_num_evals (30,000,000) to perform exhaustive sampling. Three docking simulations with different random seeds for each drug and structure were run on the Hungarian HPC infrastructure (NIIF Institute, Hungary). 250 hits from each run were collected.

Analysis of the docking simulations.

All the 750 poses for each docking were used for analysis. These conformations were analyzed using *SciPy* (http://www.scipy.org) and in house written python scripts. A python package for *SciPy* called *hcluster* was used to perform hierarchic clustering based on root means square deviation (RMSD) using the centroid distance measure. The threshold for forming flat clusters was set to include conformations with RMSD values smaller than 3 Å into each cluster. Binding poses were clustered by RMSD and ordered by the binding pose with the lowest binding free energy in each cluster. The four clusters, in which the pose with the lowest binding free energy exhibits one of the lowest binding free energies, are shown in figures, which were prepared in PyMOL (DeLano Scientific LLC). The CFTR amino acid binding sites of correctors were determined using PyMOL by selecting residues in less than 4 Å distance from every molecule in each cluster.

Crypt isolation and organoid culture from human rectal biopsies

Crypt isolation and culture of human intestinal organoids have been described previously[58]. In short, rectal biopsies were washed with cold complete chelation solution and incubated with 10 mM EDTA for 60-120 minutes at 4°C. Supernatant was harvested and EDTA was washed away. Crypts were isolated by centrifugation and embedded in matrigel (growth factor reduced, phenol-free, BD bioscience) and seeded (50-100 crypts per 50 µl matrigel per well) in 24-well plates. The matrigel was polymerized for 10 minutes at 37°C and immersed in complete culture medium: advanced DMEM/F12 supplemented with penicillin/streptomycin, 10 mM HEPES, Glutamax, N2, B27 (all from Invitrogen), 1 mM *N*-acetylcysteine (Sigma) and growth factors: 50 ng/ml mEGF, 50% Wnt3a-conditioned medium and 10% Noggin-conditioned medium, 20% Rspo1-conditioned medium, 10 µM Nicotinamide (Sigma), 10 nM Gastrin (Sigma), 500 nM A83-01 (Tocris) and 10 µM SB202190 (Sigma). The medium was refreshed every 2-3 days and organoids were passaged 1:4 every 7-10 days. Organoids from passage 1-10 were used for confocal live cell imaging.

In vitro ubiquitination of NBD1

In vitro ubiquitination of purified ΔF508-1S-NBD1 was performed as previously[24]. NBD1-1S (1 µM) was incubated for 5 min at 34°C with 0.1% DMSO (as control) or C11 in reaction buffer (20 mM HEPES, pH 7.5, 50 mM NaCl, 5 mM $MgCl_2$, 2 mM DTT, 20 µM MG-132, 5 µg/ml leupeptine, 5 µg/ml pepstatin A) in the presence of 2 µM Hsc70. After the heat denaturation, the CHIP-mediated NBD1 ubiquitination was initiated by incubation at 26°C for 2 hours with 0.1 µM E1, 4 µM UbcH5c, 3 µM CHIP and 10 µM ubiquitin (Sigma). NBD1was analyzed with immunoblotting with anti-NBD1 (L12B4) antibody.

SUPPLEMENTARY REFERENCES

51. Glasoe, P.K. & Long, F.A. Use of glass electrodes to measure acidities in deuterium oxide. *J Phys Chem* **64**, 188-9 (1960).
52. Wales, T.E. & Engen, J.R. Hydrogen exchange mass spectrometry for the analysis of protein dynamics. *Mass spectrometry reviews* **25**, 158-70 (2006).
53. Cornell, W.D., Cieplak, P., Bayly, C.I., Gould, I.R., Merz Jr., K.M., Ferguson, D.M., Spellmeyer, D.C., Xov, T., Caldwell, J.W., Kollman, P.A. A second generation force field for the simulation of proteins, Nucleic Acids, and Organic Molecules. . *J Am Chem Soc* **117**, 5159 (1995).

54. Wang, J., Cieplak, P., Kollmann P.A. How well does a restrained electrostatic potential (RESP) model perform in calculating conformational energies of organic and biological molecules? *J Comput Chem* **21**, 1049-1074 (2000).

55. Fiser, A. & Sali, A. ModLoop: automated modeling of loops in protein structures. *Bioinformatics* **19**, 2500-1 (2003).

56. Schuttelkopf, A.W. & van Aalten, D.M. PRODRG: a tool for high-throughput crystallography of protein-ligand complexes. *Acta Crystallogr D Biol Crystallogr* **60**, 1355-63 (2004).

57. Morris, G.M. et al. AutoDock4 and AutoDockTools4: Automated docking with selective receptor flexibility. *J Comput Chem* **30**, 2785-91 (2009).

58. Sato, T. et al. Long-term expansion of epithelial organoids from human colon, adenoma, adenocarcinoma, and Barrett's epithelium. *Gastroenterology* **141**, 1762-72 (2011).

59. Kleizen, B., van Vlijmen, T., de Jonge, H.R. & Braakman, I. Folding of CFTR is predominantly cotranslational. *Molecular cell* **20**, 277-87 (2005).

60. Lukacs, G.L. & Verkman, A.S. CFTR: folding, misfolding and correcting the DeltaF508 conformational defect. *Trends Mol Med* **18**, 81-91 (2012).

a

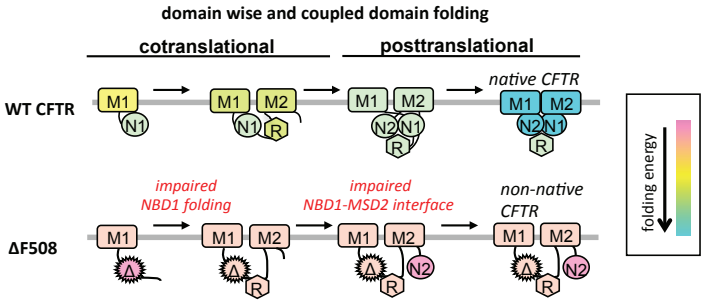

b

maneuver	Primary folding defect		rescue effect
	NBD1	NBD1-MSD2 interface	
second site suppressor mutation (genetic rescue)	3S, R1S	-	<20%
	-	R1070W, V510D	5-10%
	3S, R1S	R1070W, V510D	~80%
corrector (pharmacological rescue)	*corrector A*	-	<5%
	-	*corrector B*	<10%
	corrector A	*corrector B*	*~80% ?*
structure-based corrector screening	*corrector A*	R1070W	*50-80% ?*
	3S, R1S	*corrector B*	*50-80% ?*

Figure S1. Schematic models of CFTR folding and ΔF508-induced misfolding. (a) In the WT CFTR, MSD1 (M1), NBD1 (N1), MSD2 (M2) and NBD2 (N2) folds co-translationally to metastable states[5,24,59,60]. Coupled domain folding and assembly facilitate proper domain-domain interaction and *vice versa*, and energetically favors the native tertiary structure formation of CFTR. Progressive enthalpic stabilization of individual domains during co- and post-translational folding is indicated by pseudocolors. In case of the ΔF508 mutation, both NBD1 energetics and domain-domain interactions (primarily the NBD1-MSD2 interface) are impaired due to the conformational and topological defects, rendering all four major domains structurally unstable[5]. (b) Strategies to rescue the ΔF508-CFTR folding defect. While either stabilization of ΔF508-NBD1 or the NBD1-MSD2 interface by second site suppressor mutations such as 3S and R1S or R1070W and V510D, respectively, achieves marginal improvement in the ΔF508-CFTR folding (<20%), simultaneous stabilization of these primary structural defects can lead to the robust and synergistic rescue (~80%)[24]. In analogy, available correctors may only restore one of the primary structural defect that likely account for the limited rescue efficiency of ΔF508-CFTR. Corrector pairs acting on different primary structural defects, however, may restore ΔF508-CFTR folding synergistically. Suppressor mutations can be instrumental for a structural based corrector screening to identify correctors that either stabilize the NBD1 and/or the NBD1-MSD2 interface based on the possible synergism.

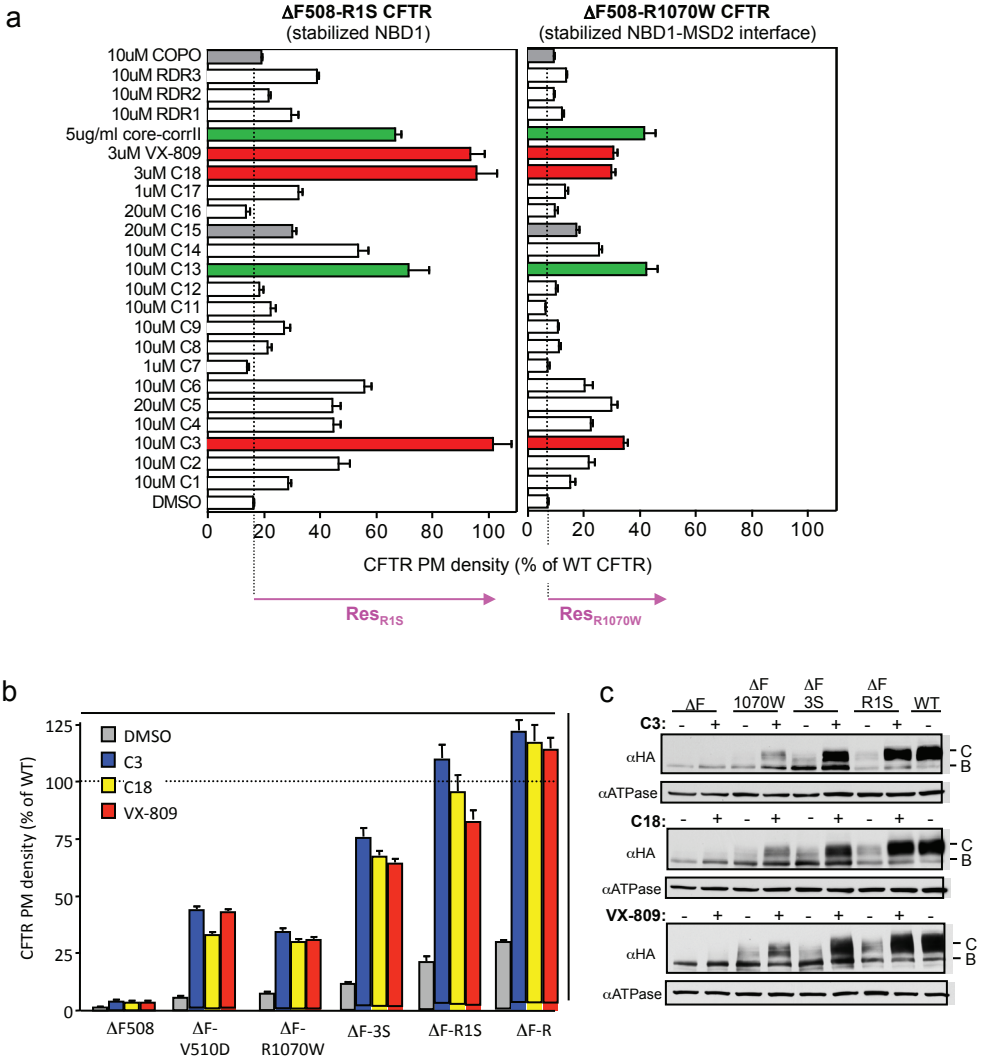

Figure S2. Differential augmentation of correction ΔF508-CFTR containing stabilized NBD1 or NBD1-MSD2 interface in BHK cells. (a) PM density of ΔF508-CFTR containing R1S (left) or R1070W (right) mutations was measured by cell surface ELISA using anti-HA Ab and expressed as % of WT CFTR. BHK cells, stably expressing the indicated construct, were treated with correctors for 24 h at 37°C. All the data were also plotted in Fig.1b-c. Red and green bars indicate correctors that belong to class-I and class-II, respectively. Grey bars represent dual acting corrector-potentiator compounds. Data are means ± SEM (n=6-12). The augmented PM density of ΔF508-CFTR after corrector treatment in the presence of either R1S (Res_{R1S}) or R1070W (Res_{R1070W}) mutation is illustrated. (b-c) Second site suppressor mutations differentially enhance the ΔF508-CFTR rescue by class-I correctors. The PM density (b) and steady-state expression (c) of ΔF508-CFTR variants were determined by ELISA (means ± SEM, n=8) and Western blotting with anti-HA Ab, respectively. The PM density data were also plotted in Fig.1i (Y-axis). Na^+/K^+-ATPase (ATPase) was used as a loading control. Correctors (10 μM C3, 3 μM C18 or 3 μM VX809) were treated for 24 h at 37°C. B, immature core-glycosylated; C, mature complex-glycosylated form.

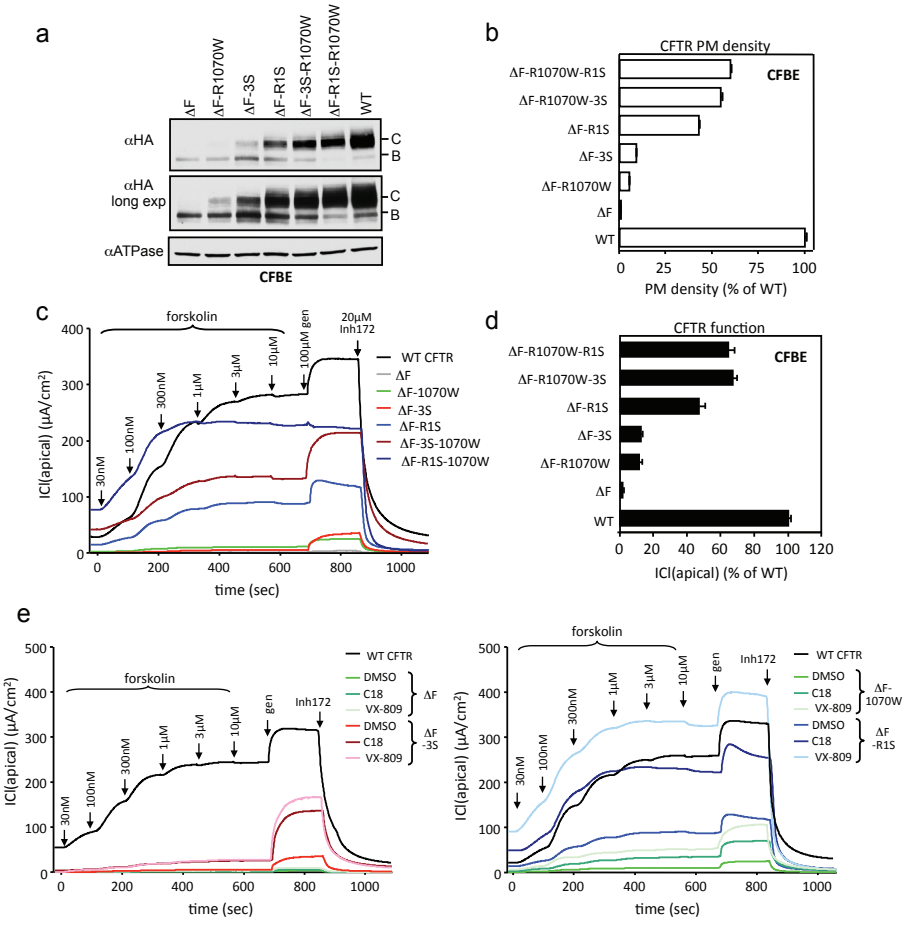

Figure S3. The suppressor mutations and correctors synergistically rescue the PM expression and function of ΔF508-CFTR in polarized CFBE41o- epithelial cells. (a-c) The consequence of suppressor mutations-induced NBD1 and/or NBD1-MSD2 interface stabilization on the PM density, complex-glycosylation and function of ΔF508-CFTR in CFBE41o- Tet-on cells. The steady-state expression (a), PM density (b, n=12-24) and apical Cl^- current (c-d, n=3-4) of ΔF508-CFTR-3HA were measured by Western blotting, ELISA and short circuit current, respectively. Data represent means ± SEM. CFTR expression was induced for 3-4 days with doxycycline as described in Method. (e) The effect of class-I corrector combination with suppressor mutations on the apical chloride current. Representative apical Cl^- currents obtained in polarized CFBE41o- Tet-on cells expressing the indicated CFTR variants after 24 h pre-treatment with or without correctors (3μM C18 or VX-809) at 37°C. The measurements were performed in presence of a basolateral to apical chloride gradient and the current was stimulated by consecutive addition of 30 nM, 100 nM, 300 nM, 1 μM, 3 μM, 10 μM forskolin and 100 μM genistein followed by CFTR inhibition with 20 μM inhibitor 172 (Inh172). The peak current values are plotted in Fig.S5d and Fig.1h. (f) Augmented PM density of ΔF508-R1S (Res_{R1S}) and ΔF508-R1070W CFTR (Res_{R1070W}) by class-I corrector in CFBE41o- Tet-on cells was calculated as in Fig.S2a (left). The log_2 ratio of Res_{R1S} over Res_{R1070W} indicates the preferential effect of class-I correctors on the NBD1-MSD2 interface (right).

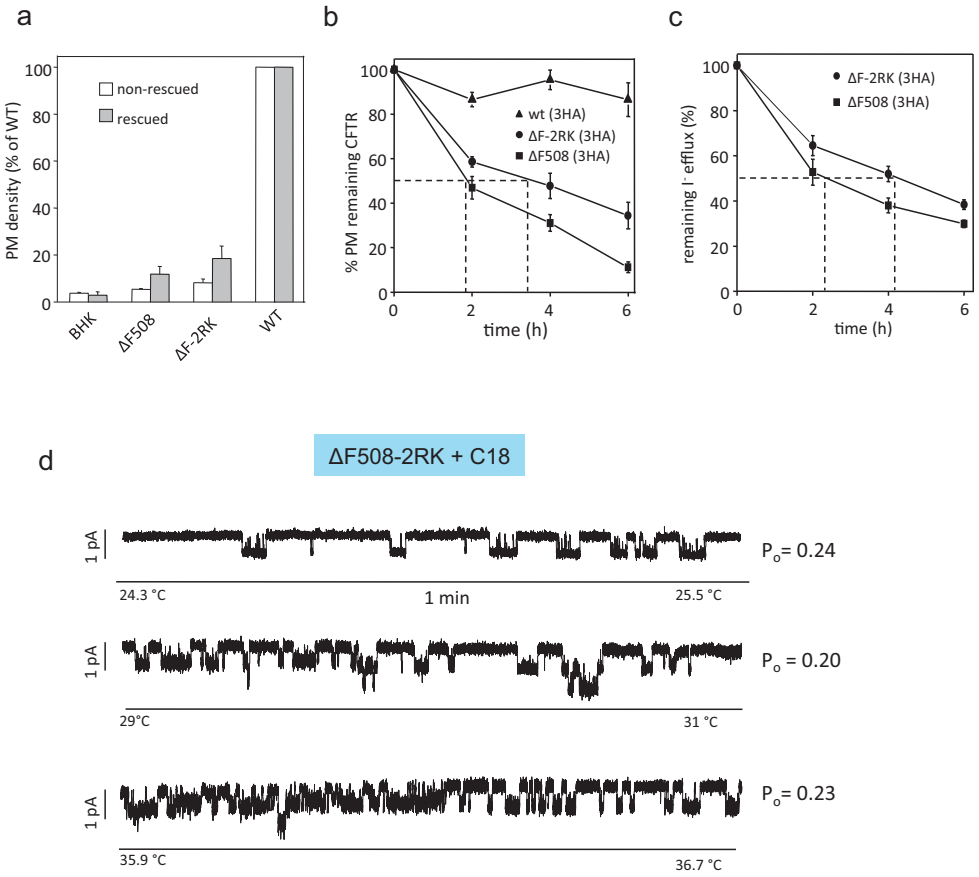

Figure S4. C18 prevents thermal inactivation of the ΔF508-2RK CFTR channel *in vitro*. (a-c) The effect of the 2RK mutation on the ΔF508-CFTR biochemical and functional phenotype. (a) The PM density of the CFTR constructs was measured by cell surface ELISA in BHK cells. The 2RK mutation modestly improved the ΔF508-CFTR low temperature rescue. (b) 2RK mutation modestly increased the PM stability of the mutant relative to the WT, measured by PM ELISA. (c) The 2RK mutation increased the functional PM stability of the rescued ΔF508 CFTR, measured by iodide efflux assay. (d) Representative records (~1 min) of the reconstituted ΔF508-CFTR-2RK channel in artificial phospholipid bilayer in the presence of 3 μM C18 during the temperature ramp at ~24°C, ~30°C and ~36°C. Open probability (P_o) of the CFTR channel activity was analyzed at the indicated temperature as described in Supplementary Method and summarized in Fig.2b. Traces shown at 30°C and 36°C belong to the same record, while originates from a different on at 24°C._

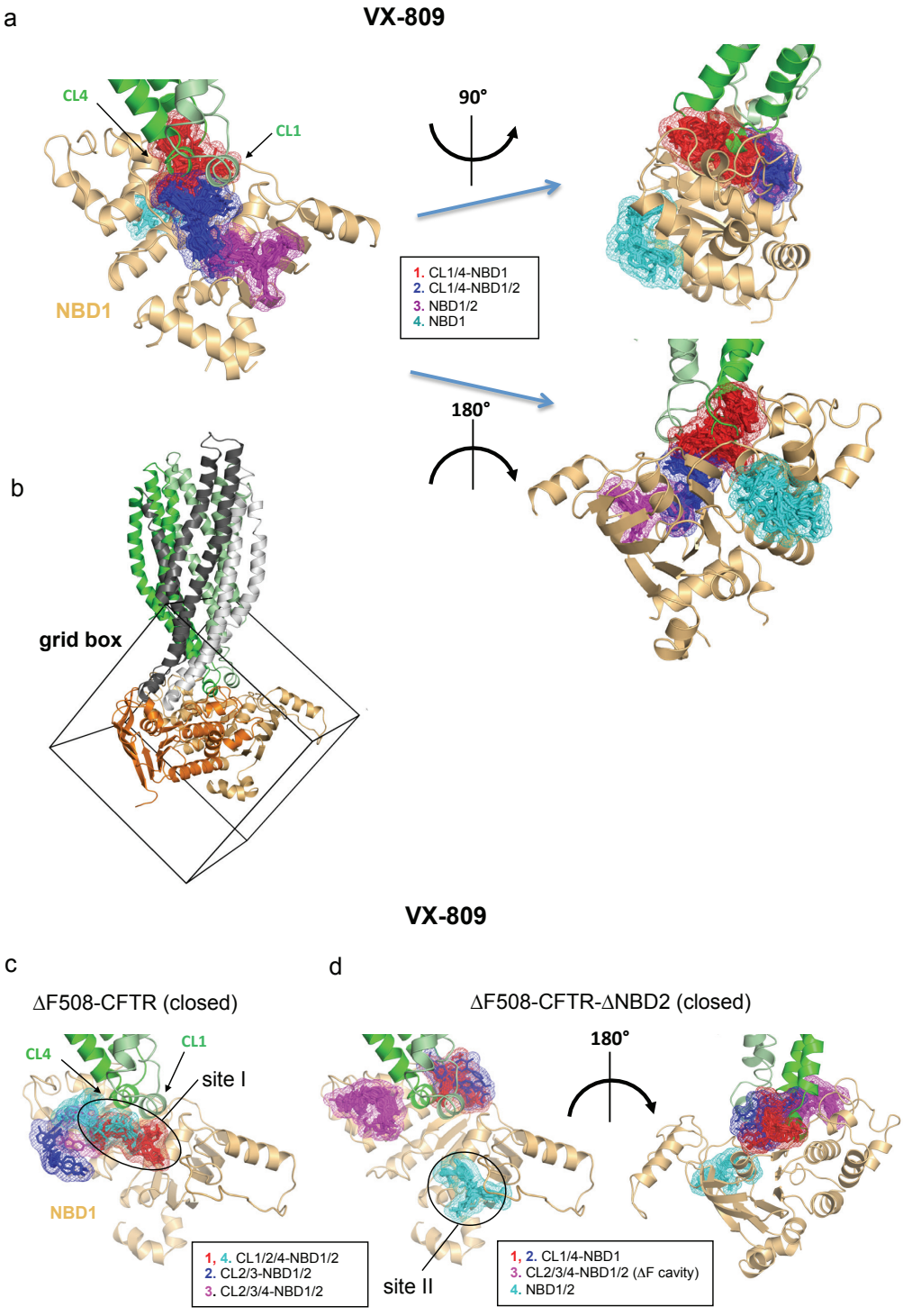
a
VX-809
CL4
CL1
NBD1
90°
1. CL1/4-NBD1
2. CL1/4-NBD1/2
3. NBD1/2
4. NBD1
180°
b
grid box
VX-809
c
ΔF508-CFTR (closed)
CL4
CL1
site I
NBD1
1, 4. CL1/2/4-NBD1/2
2. CL2/3-NBD1/2
3. CL2/3/4-NBD1/2
d
ΔF508-CFTR-ΔNBD2 (closed)
180°
site II
1, 2. CL1/4-NBD1
3. CL2/3/4-NBD1/2 (ΔF cavity)
4. NBD1/2

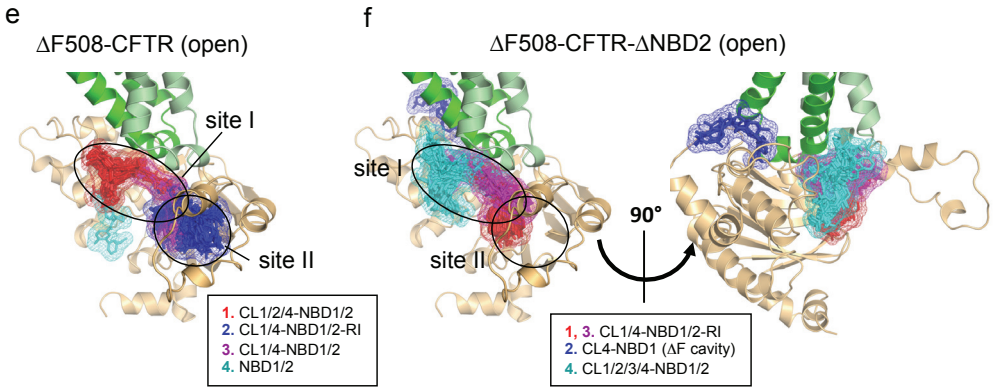

Figure S5. Docking of VX-809 to the ΔF508-NBD1 crystal structure, as well as to the closed and open ΔF508-CFTR models. (a) VX-809 was docked to the X-ray structure of NBD1 lacking the F508 (PDBID:2BBT). Views from three different orientations are presented. The cytosolic loops (CL1 and CL4) are shown for comparison to the full-length CFTR models. Clusters are depicted in mesh representation to indicate their volume. Red, blue, magenta, and cyan of VX-809 clusters represent increasing binding free energy with the corresponding color number specifying the domain binding. The size of individual clusters and their average binding energy can be found in Table S3. The CFTR binding sites were determined using PyMOL by selecting amino acids in less than 4 Å distance from every molecule in each cluster. (b) For *in silico* docking to ΔF508-CFTR the search space includes NBD1, NBD2 and major parts of CL1-4. The grid box is depicted on the closed CFTR model. Color-coding is the same as in (a) and Fig.1a. (c-f) VX-809 *in silico* docking to the closed and open ΔF508-CFTR. VX-809 primary binding is indicated as site I at the CL1/4-NBD1/2 interface in the full-length closed and open molecules. In closed CFTR-ΔNBD2 an additional binding site is predicted at the β-subdomain (site II) (c-d). In the open CFTR model VX-809 docked to site I and II in both the full-length, as well as in CFTR-ΔNBD2 (f). NBD2 is hidden in the full-length model to facilitate comparison. Color coding is the same as in Fig.S5b.

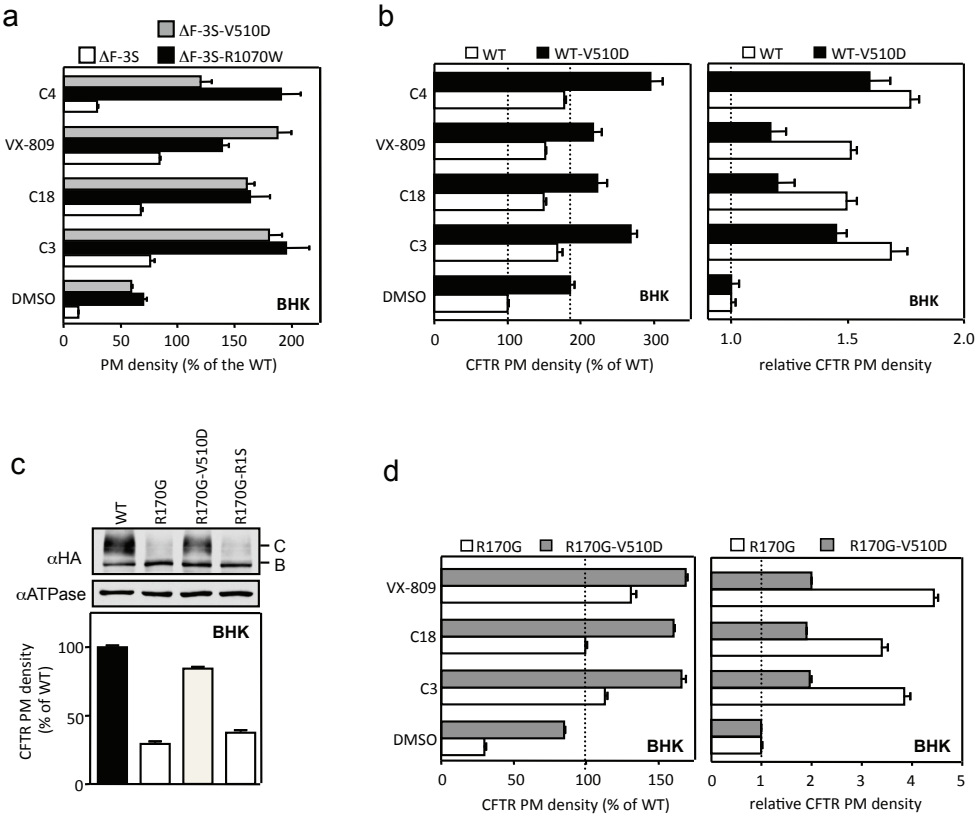

Figure S6. The effect of NBD1-CL4 stabilization on the corrector-induced rescue of CFTR variants in BHK cells. (a) PM density of ΔF508-CFTR-3S, ΔF508-R1070W-CFTR-3S and ΔF508-V510D-CFTR-3S was measured by cell surface ELISA in BHK cells treated with correctors for 24 h at 37°C. The same data are also plotted in Fig.3d as % of the respective DMSO controls. (b) The effect of correctors on the PM density of WT CFTR and V510D-CFTR (WT + V510D) was measured by cell surface ELISA as in panel (a). Correction efficiency was normalized for WT (left), and for the respective DMSO control (right). (c) Steady-state expression (upper) and PM density (lower) of R170G-CFTR with stabilized NBD1-MSD2 interface (V510D) or NBD1 (R1S) were examined by Western blotting and cell surface ELISA, respectively. (d) The effect of correctors on the PM density of R170G-CFTR and R170G-V510D-CFTR was measured by ELISA as in panel b. ELISA data represent means ± SEM (n=8). Cells were exposed to correctors (10 μM C3, 3 μM C18, 3 μM VX809 or 10 μM C4) for 24 h at 37°C.

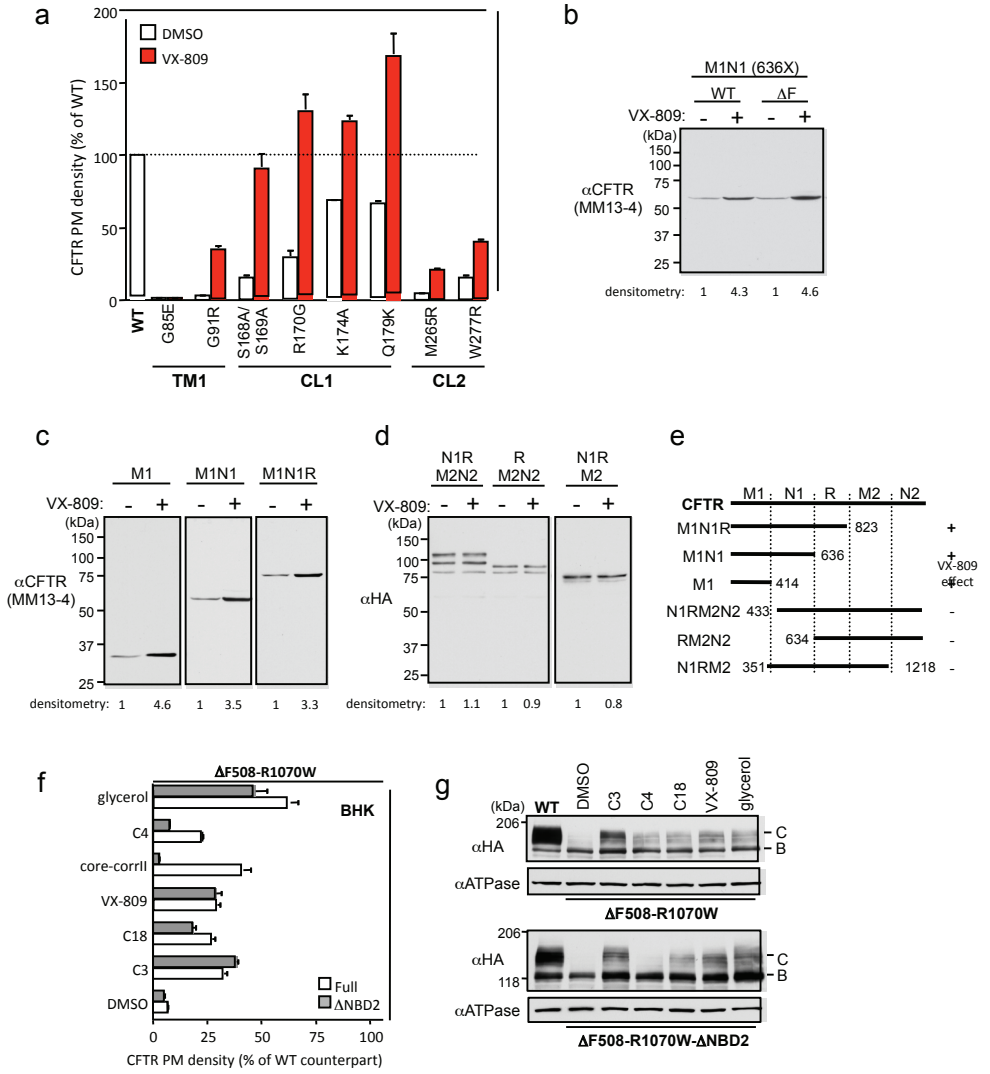

Figure S7. The effect of correctors on the expression of TM1, CL1 and CL2 CFTR mutants, CFTR domain combinations and CFTR-ΔNBD2. (a) PM density of MSD1 CFTR mutants in TM1 (G85E, G91R), CL1 (S168/S169A, R170G, K174A, Q179K) and CL2 (M265R, W277R) were measured by cell surface ELISA in BHK cells treated with 3 μM VX-809 for 24 h at 37°C. (b-e) Effect of VX-809 on the steady-state expression of CFTR domain combinations was examined by Western blotting with anti-CFTR-NT (MM13-4) or anti-HA Abs. VX-809 was treated as in panel a. (b) Both WT and ΔF508 MSD1-NBD1 fragments were accumulated by VX-809. (c-d) VX-809 increased the cellular expression of the WT CFTR domains containing MSD1, but not without MSD1. The relative level of the CFTR domains quantified by densitometry is indicated. (e) Summary of the VX-809 effect on the expression of WT CFTR domain combinations. CFTR domain boundaries are indicated as amino acid residues in the primary sequence. M1, MSD1; N1, NBD1; M2, MSD2; N2, NBD2. (f-g) Effect of NBD2 deletion (ΔNBD2) on the corrector effect on the PM density (f) and cellular expression (g) of ΔF508-R1070W-CFTR, measured by ELISA and Western blotting with anti-HA Ab, respectively. Cells were exposed to correctors (10 μM C3, 3 μM C18, 3 μM VX809, 10 μM C4, 5 μg/ml core-corr-II or 10% glycerol) for 24 h at 37°C (f-g). All ELISA data represent means ± SEM (n=6-9).

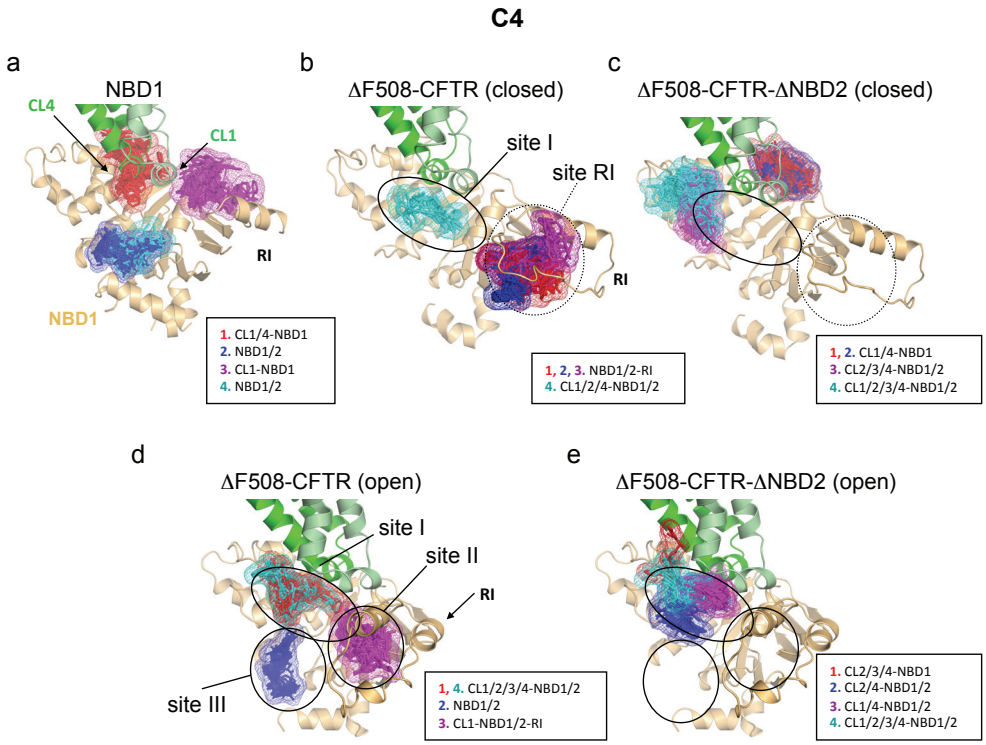

Figure S8. ***In silico*** **docking of C4 to the ΔF508-NBD1 crystal structure, the closed and the open ΔF508-CFTR models.** (a) C4 was docked to the X-ray structure of NBD1 lacking the F508 (PDBID:2BBT) with reverted solubilizing mutations. (b) In the closed CFTR model, C4 associates with site I and the RI (regulatory insertion). (c) C4 binding, however, was diminished both at site I and the RI in ΔF508-CFTR-ΔNBD2. (d-e) While C4 interacts with site II and III at the NBD1/NBD2 interface in the open CFTR model, these interactions are abolished in the CFTR-ΔNBD2 model. Color-coding is as in Fig.S5.

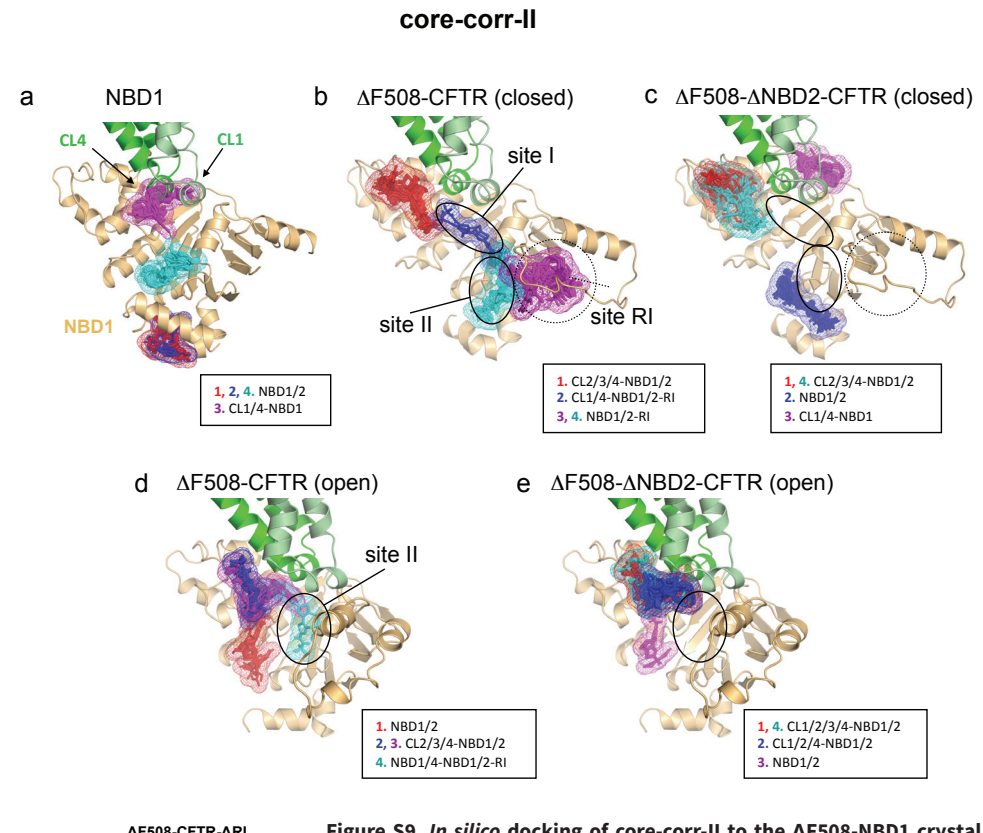

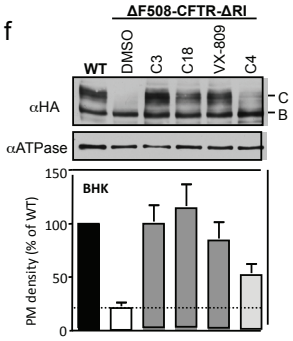

Figure S9. ***In silico*** **docking of core-corr-II to the ΔF508-NBD1 crystal structure, as well as to the closed and open ΔF508-CFTR models.** (a) Core-corr-II, similar to that of VX-809 and C4, is docked to the NBD1 binding cavity of the CL4. (b) In the closed CFTR model, core-corr-II binds to sites I, II and RI. (c) These interactions either weakened or disappeared in the absence of NBD2. (d-e) In the open CFTR model, core-corr-II binds to site II and partially to site I. (e) Core-corr-II association with site II is abolished in CFTR-ΔNBD2 model. Color-coding is as in Fig.S5. (f) Class-II correctors binding to the Regulatory Insertion (RI) cannot account for the rescue effect since deletion of the RI (ΔRI) does not diminish the corrector rescue efficiency. The steady state expression (upper) and PM density (lower) were examined by anti-HA immunoblotting and ELISA (n=6-9, ± SEM), respectively. Cells were exposed to correctors (10 μM C3, 3 μM C18, 3 μM VX809, 10 μM C4, 5 μg/ml core-corr-II or 10% glycerol) for 24 h at 37°C.

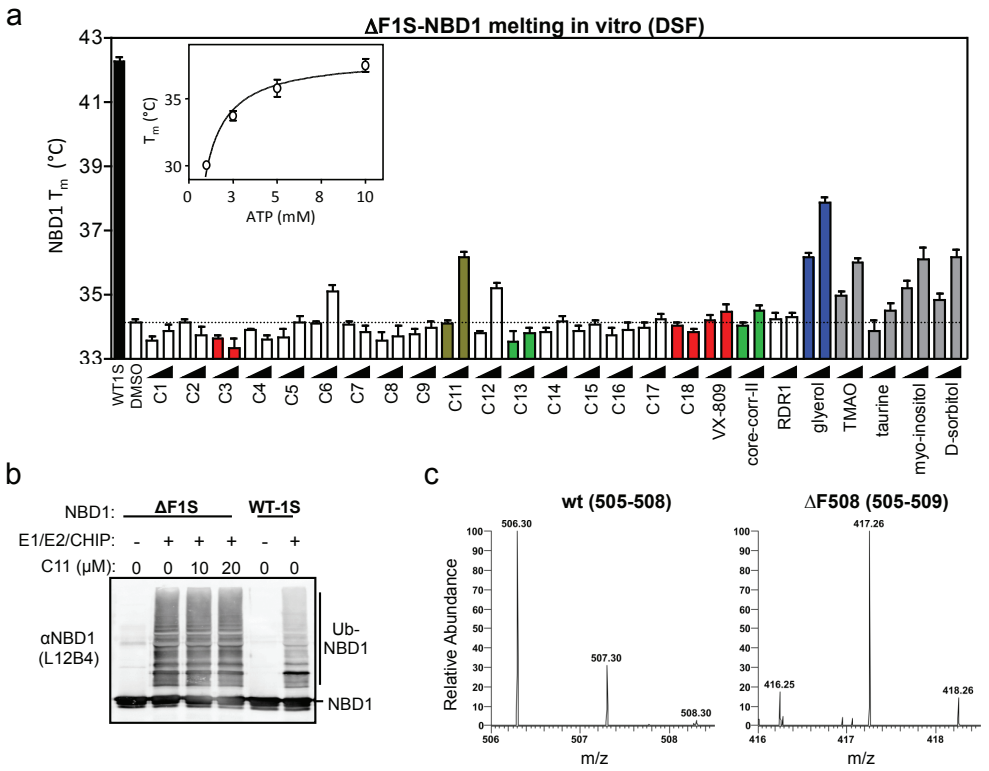

Figure S10. Effect of correctors on the isolated NBD1 stability *in vitro*. (a) Melting temperature (T_m) of isolated human ΔF508-NBD1-1S was measured *in vitro* by differential scanning fluorimetry (DSF)[24]. WT-NBD1-1S was used as a positive control. The indicated correctors or chemical chaperones (CC) (see Table S1) were included during thermal unfolding at the following concentration: C1, C2, C3, C4, C5, C6, C7, C9, C11, C12, C13, C14, C17, CoPo (3 μM and 10 μM), C8, C15, C16, (10 μM and 20 μM), C18, VX-809 (1 μM and 3 μM), RDR1 (5 μM and 15 μM), core-corr-II (2.5 μg/ml and 5 μg/ml), glycerol (5% and 10%), TMAO, taurine, myo-inositol and D-sorbitol (150 mM and 300 mM). Thermal unfolding scans of ΔF508-NBD1-1S in the presence of selected correctors are shown in Fig.4a. Data represent means ± SEM (n=3). Statistically significant change in T_m was considered larger than mean ± 3SD of DMSO treated ΔF508-NBD1-1S (34.1 ± 1.5°C). (b) Effect of C11 on the *in vitro* ubiquitination of WT or ΔF508-NBD1-1S by CHIP was analyzed by Western blotting with anti-NBD1 (L12B4) antibody as previously[24]. (c) Representative mass spectra of singly charged peptides after 5 min labelling with D_2O; ^{505}NIIF^{508} (NIIF + H^+ = 506.30) of wt NBD1-1S (left panel) and ^{505}NIIG^{509} (NIIG + H^+ = 416.25) of ΔF508-NBD1-1S (right panel) at 22 °C. Theoretical monoisotopic masses of singly charged peptides are shown.

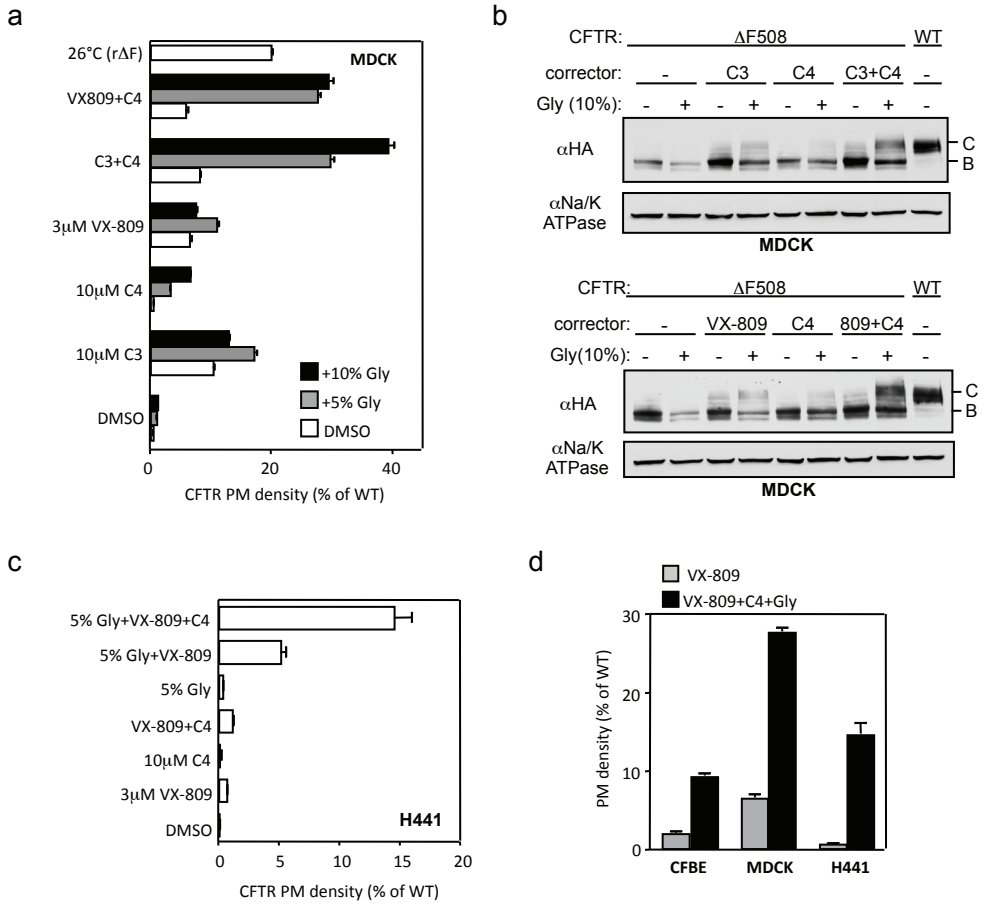

Figure S11. ΔF508-CFTR rescue by corrector combination in MDCKII and NCI-H441 polarized epithelia. (a, b) PM density (a) and steady-state expression (b) of ΔF508-CFTR in MDCKII cells were measured by ELISA (n=8) and Western blotting, respectively. Correctors were treated with or without 5% or 10% glycerol (Gly) at 37°C for 24 h. Same concentration of the correctors were used in both panel a and b. Low temperature (26°C) rescued ΔF508-CFTR (rΔF) was used as a positive control. (c) PM density of ΔF508-CFTR in NCI-H441 Tet-on cells (n=8). Data represent means ± SEM. (d) Corrector combination synergistically rescues the Δ F508-CFTR in MDCKII and NCI-H441 Tet-on epithelial cells. PM density of cells treated with VX-809 (3 μM) or corrector combination (3 μM VX-809, 10 μM C4 and 5% glycerol (Gly)) was determined by cell surface ELISA (n=6-16).

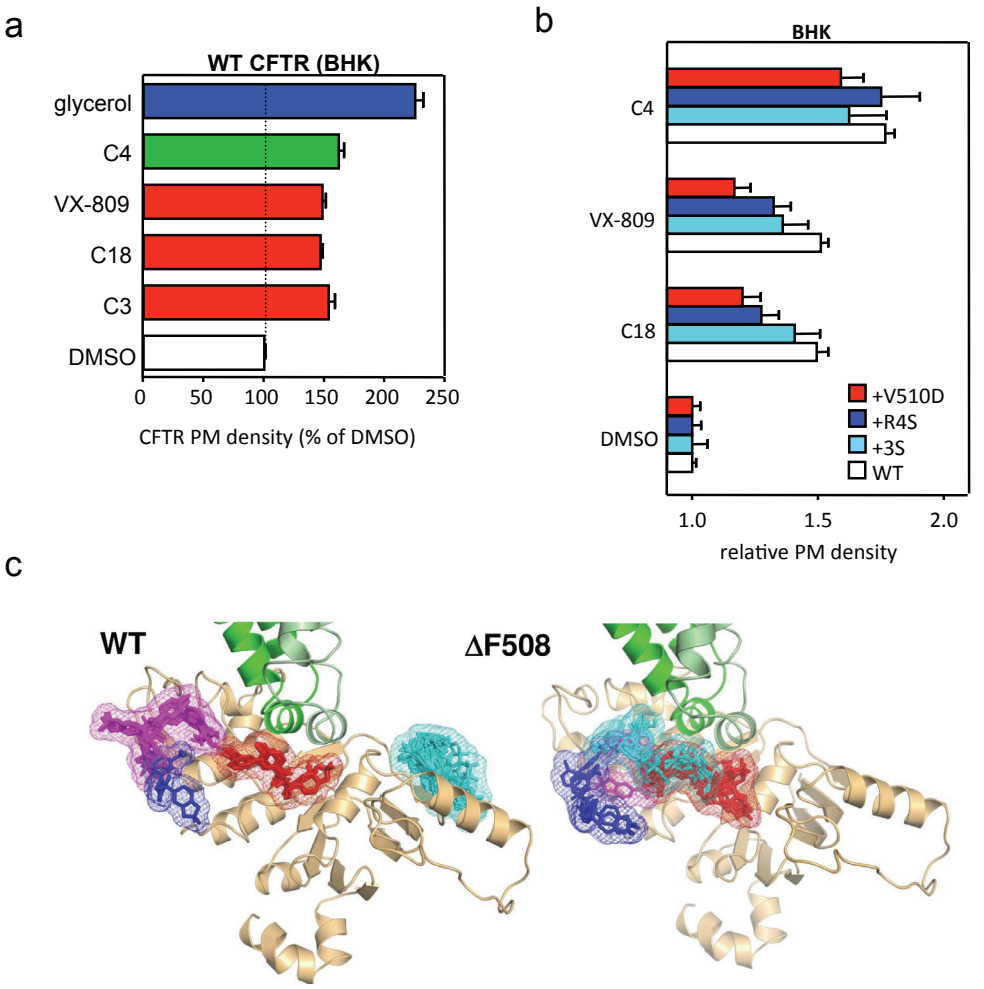

Figure S12. Effect of correctors on WT CFTR PM expression in BHK cells. (a) PM density of WT CFTR was measured by cell surface ELISA in BHK cells treated with correctors (10 μM C3, 10 μM C4, 3 μM C18, 3 μM VX-809 or 10% glycerol) at 37°C for 24 h. (b) Effect of second-site suppressor mutations on the corrector efficacy on WT CFTR expression was determined by cell surface ELISA. Correctors were treated as panel a. Data represent means ± SEM (n=8). (c) Comparison of VX-809 in silico docking to WT and ΔF508 CFTR closed conformation. Docking and analysis was performed as described in the Methods. The poses of VX-809 with the lowest energies (red) occupy the site I as in the case of the ΔF508 (right; see also Fig.S5c). A low energy cluster (magenta) in the WT partially overlaps with two low energy clusters (blue and turquoise) in the ΔF508 CFTR. At the back of RI and the β-subdomain an additional docking site appears (turquoise) in the WT. These results suggest that partially overlapping targets of VX-809 in the WT and mutant protein.

Chapter 4

Optimal repair of distinct CFTR folding mutants by correctors in rectal cystic fibrosis organoids

Johanna F. Dekkers[1,2], Adrian Gogorza[1,2], Evelien Kruisselbrink[1,2], Annelotte M. Vonk[1,2], Hettie M. Janssens[3], Karin M. de Winter-de Groot[1], Cornelis K. van der Ent[1], Jeffrey M. Beekman[1,2]

[1]Department of Pediatric Pulmonology, [2]Laboratory of Translational Immunology, Wilhelmina Children's Hospital, University Medical Centre, Utrecht, The Netherlands, [3]Department of Pediatric Pulmonology, Sophia Childrens Hospital/Erasmus MC-University Medical Center, Rotterdam, the Netherlands

Submitted

ABSTRACT

Small molecule therapies that restore defects in CFTR gating (potentiators) or trafficking (correctors) are being developed for cystic fibrosis (CF) in a mutation-specific fashion. Options for pharmacological correction of CFTR-F508del are being excessively studied, but correction of other trafficking mutants that may also benefit from corrector treatment remains largely unknown. We studied correction of the folding mutants CFTR-F508del, -A455E and -N1303K by VX-809 and 18 other correctors (C1 to C18) using a functional CFTR assay in human intestinal CF organoids. Function of both CFTR-F508del and -A455E was enhanced by a variety of correctors, but no residual or corrector-induced activity was associated with CFTR-N1303K. Importantly, VX-809-induced correction was most dominant for CFTR-F508del, while correction of CFTR-A455E was highest by a subgroup of compounds called bithiazoles (C4, C13, C14, C17) and C5. These data support the development of mutation-specific correctors for optimal treatment of different CFTR trafficking mutants, and identify C5 and bithiazoles as the most promising compounds for correction of CFTR-A455E.

INTRODUCTION

Loss-of-function mutations in the *cystic fibrosis transmembrane conductance regulator* (*CFTR*) gene cause the autosomal recessive disorder cystic fibrosis (CF). Novel therapeutic strategies target mutation-specific defects of the CFTR protein, such as repair of (i) CFTR apical trafficking by correctors (e.g. VX-809)[1] and (ii) CFTR gating by potentiators (e.g. VX-770)[2].

The last decade, correctors have been identified from screens using CFTR-F508del, the most common trafficking mutant expressed by 90% of all CF subjects[3]. Recently, the corrector VX-809 (lumacaftor) has been clinically approved for F508del homozygous subjects in combination with VX-770 (ivacaftor/KALYDECO™)[4,5], demonstrating for the first time that mutation-specific corrector therapy is feasible. Multiple correctors that have been identified in previous screens for F508del, but failed to reach clinical phase, are distributed by the Cystic Fibrosis Foundation Therapeutics for experimental purpose (termed C1 to C18[6-12]). While corrector-based treatment options are being excessively elaborated for CFTR-F508del, the efficacy of known correctors for other trafficking mutants remains largely unknown and has thus far not been studied in primary CF cells.

We have recently developed an assay in human primary intestinal organoids[13-15] to study residual and drug-corrected function of mutant CFTR[14,16]. Forskolin-induced swelling (FIS) of organoids quantitates CFTR function in a subject-specific manner, and was used to characterize correction of the trafficking mutants CFTR-F508del, -A455E or -N1303K by VX-809 and C1 to C18.

RESULTS

Defining optimal assay conditions for intestinal organoids expressing distinct *CFTR* mutations

To define optimal assay conditions for organoids expressing different *CFTR* mutations, swelling of organoids derived from subjects homozygous for F508del or compound heterozygous for F508del and A455E, N1303K or a class I (resulting in no functional CFTR protein) mutation was assessed at 5 different forskolin concentrations with or without VX-809 (Fig. 1). We first confirmed folding and trafficking defects in CFTR-F508del, -A455E and -N1303K by Western blot analysis that indicated highly reduced levels of complex-glycosylated CFTR (C-band) in mutated compared to wild-type CFTR organoids (Fig. 1a). No CFTR expression was detected in organoids expressing two class I mutations, confirming specificity for CFTR (Fig. 1a). As described previously[16], organoid swelling was presented as absolute area under the curve (AUC) calculated from 60 min time tracings of the surface area increase of calcein-green-labeled organoids relative to t = 0 (Fig. 1b,c). The basal and VX-809-induced swelling was forskolin dose-dependent and highest for F508del / A455E organoids (Fig. 1c). FIS of F508del / N1303K and F508del / class I organoids was similar, suggesting that only limited to no function was associated with N1303K. Based on Fig. 1c, we selected 0.5 μM forskolin for F508del / A455E and 5 μM forskolin for the other genotypes to study corrector effects of C1-C18. Of note, FIS of F508del / A455E organoids at 0.5 μM forskolin is mainly conferred by the *CFTR-A455E* allele, as the responses of F508del / class I organoids were near background level at this forskolin dose (Fig. 1c). FIS of organoids compound heterozygous for F508del and N1303K or a class I mutation was analyzed for 120 instead of 60 minutes to increase assay sensitivity (Fig. 1d,e).

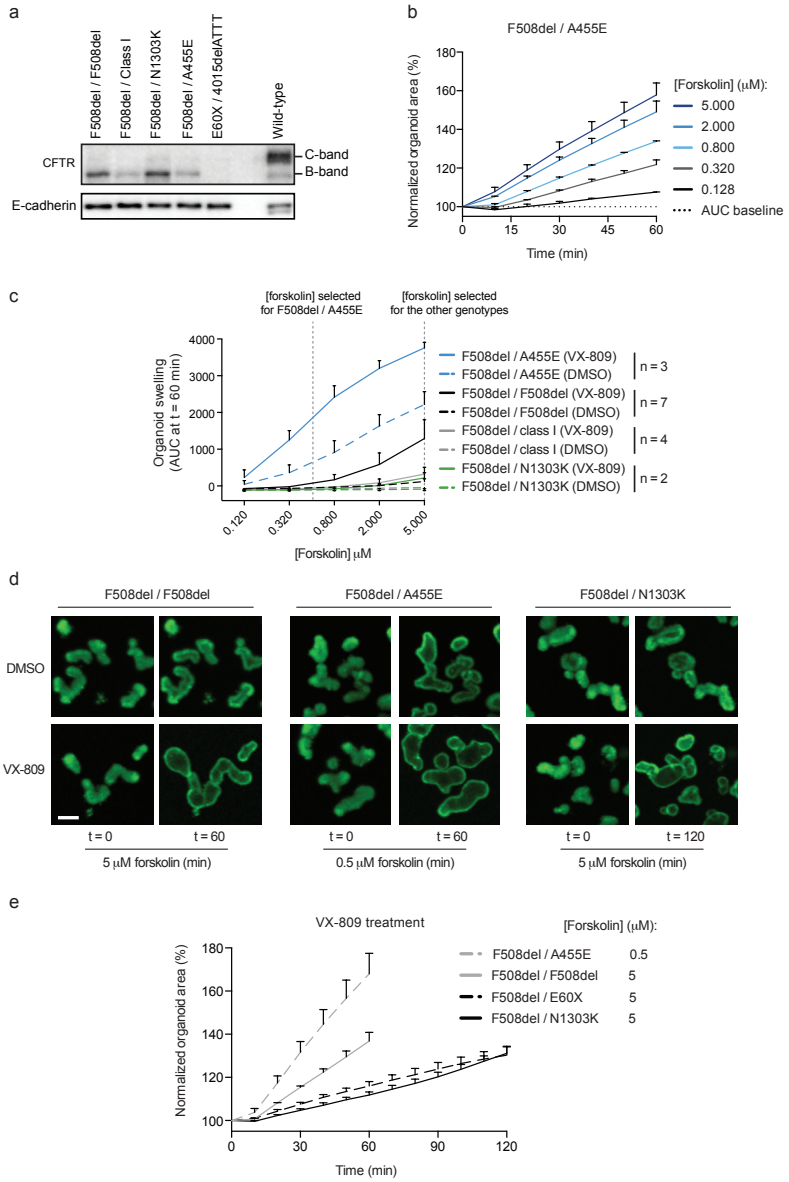

Figure 1. Definition of optimal assay conditions for intestinal organoids expressing distinct *CFTR* mutations. (a) Western blot detection of immature (B-band) and mature (C-band) CFTR in organoids with various *CFTR* genotypes. (b) Time tracing of the forskolin-induced surface area increase relative to t = 0 (normalized area) of F508del / A455E organoids at different forskolin concentrations averaged from two independent wells. Mean ± SD. (c) Forskolin-induced swelling (FIS) of organoids expressing various *CFTR* mutations with or without 24 h pre-treatment of VX-809 (3 μM), expressed as the absolute area under the curve (AUC) calculated from time tracings shown in b (baseline = 100%, t = 60 min). The class I mutations include E60X, G542X, R1162X and DELE2.3. n = number of CF subjects; each subject was measured at 2 to 5 independent culture time points in duplicate. Mean ± SD. (d) Representative confocal images of calcein-green-labeled CF organoids with or without 24 h pre-treatment of VX-809 at the indicated time points of forskolin stimulation. Scale = 100 μm. (e) Example time tracing of VX-809(3 μM)-corrected organoids stimulated with 0.5 or 5 μM forskolin and analyzed for 60 or 120 minutes, depending on the *CFTR* genotype. Data were averaged from two independent wells. Mean ± SD.

To conclude, the assay conditions defined here displayed optimal conditions to assess corrector-repaired FIS of organoids with distinct CFTR folding mutations.

Defining optimal corrector concentrations using CFTR-F508del homozygous organoids

We next measured FIS of F508del / F508del organoids that were treated with VX-809 or different concentrations of C1-C18 to identify optimal compound dosages (Fig. 2). The tested dosages for C1-C18 were based on compound potency data described in the CFFT compound order from or in literature. Compared to FIS of non-corrected organoids, we observed a dose-dependent increase in FIS for most compounds, but a similar or reduced FIS for C1, C7, C9, C10, C11 and C16, indicating lack of functional CFTR-F508del repair by these compounds (Fig. 2). Reduced FIS may point towards compound toxicity. One concentration per compound was selected for further analysis based on Fig. 2 for the functional correctors, or on literature for the non-functional correctors (Fig. 2). In conclusion, we identified functional and non-functional CFTR-F508del correctors and selected optimal C1-C18 concentrations for efficacy esting using organoids with distinct trafficking mutants.

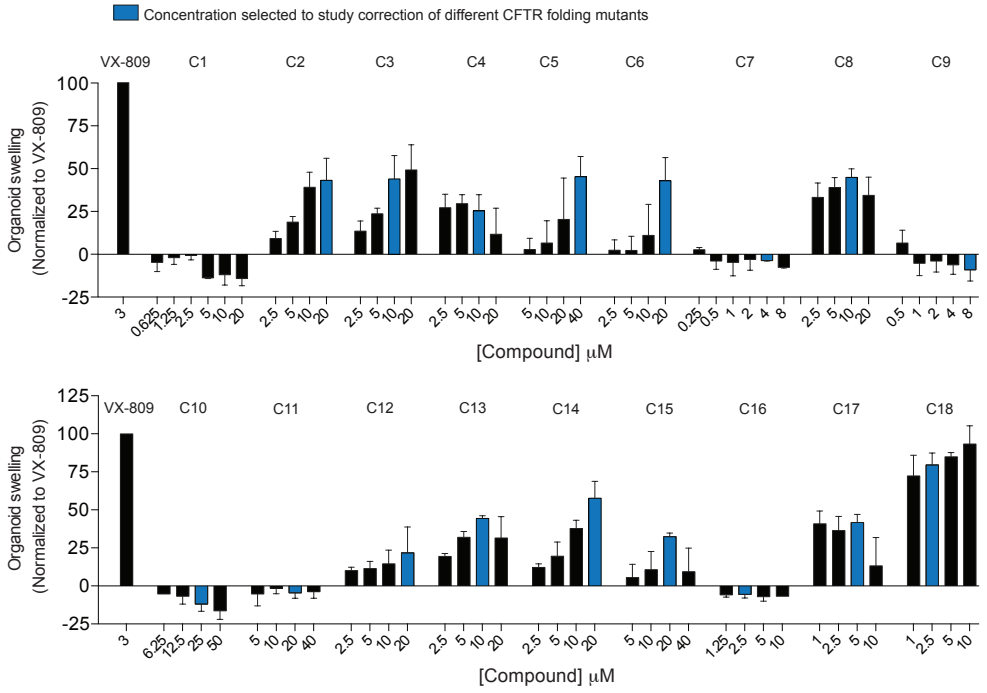

Figure 2. Definition of optimal corrector concentrations for CFTR-F508del. (a) Forskolin-induced swelling (FIS) of F508del homozygous organoids pre-treated for 24 h with VX-809 (3 μM) or titrations of C1-C18, expressed as the area under the curve (AUC) calculated from time tracings shown in Fig. 1b (baseline = 100%, t = 60 min). Responses were corrected for the FIS of DMSO-treated organoids and normalized to the VX-809 condition. Data were averaged from 3 independent experiments measured in duplicate. Mean ± SD

Correction of CFTR-F508del, -A455E and -N1303K by VX-809 and C1-C18

To study mutation-specific CFTR repair by correctors, FIS of organoids derived from donors homozygous for F508del or compound heterozygous for F508del and a nonsense mutation, A455E or N1303K was assessed using assay conditions defined from Fig. 1 and Fig. 2 (Fig. 3a). The data were normalized to VX-809 to correct for *CFTR* mutation-dependent assay differences (Fig. 3b). In this way, compounds that selectively act on a specific mutation can be identified. In line with Fig. 2, most compounds except for C1, C7, C9, C10, C11 and C16 corrected FIS of all cultures. The relative correction patterns of F508del / F508del, F508del / class I and F508del / N1303K organoids were comparable (Fig. 3b), as well as the absolute correction patterns of F508del / class I and F508del / N1303K organoids (Fig. 3c), indicating that none of the compounds functionally corrected CFTR-N1303K. Interestingly, FIS was greatly increased by C4, C5, C13, C14 and C17 specifically for F508del / A455E organoids, reaching 120% to 170% of the response to VX-809 (100%), while VX-809 was the most dominant corrector for the other genotypes (Fig. 3b). Of these A455E-specific compounds, C5 contains a phenylquinolin group and C4, C13, C14 and C17 share a bithiazole chemical structure (ChEMBL). Swelling was absent in organoids expressing two class I mutations, indicating corrector-induced FIS is fully CFTR-dependent (Fig. 3d). In line with the functional CFTR data (Fig. 3b), detection of maturated CFTR levels (C-band) by Western blot indicated that correction of CFTR-F508del or CFTR-A455E was dominated by VX-809 or C17, respectively (Fig. 3e). While VX-809 and C17 did not functionally repair CFTR-N1303K (Fig. 3b,c), they increased CFTR-N1303K protein levels (Fig. 3e), indicating that function and C-band expression are not directly related for this mutation. Together, these data indicate that optimal correction of distinct trafficking mutations requires different chemical correctors.

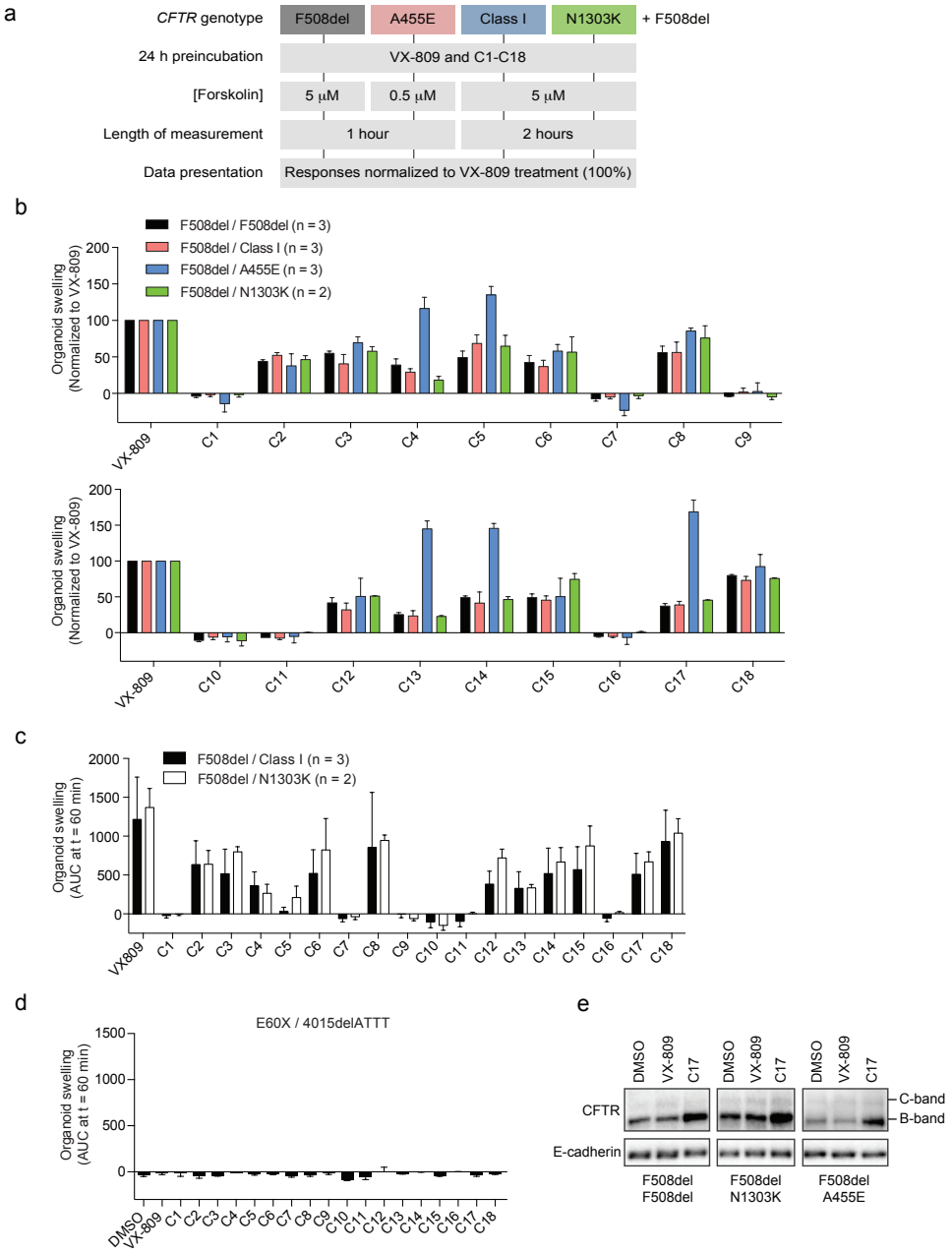

Figure 3. Correction of CFTR-F508del, -A455E or -N1303K by VX-809 and C1-C18. (a) Overview of *CFTR* genotype-specific assay conditions. (b,c) Forskolin-induced swelling (FIS) of organoids expressing various *CFTR* mutations pre-treated for 24 h with VX-809 (3 μM) or C1-C18 using concentrations defined in Fig. 2. Responses were corrected for the FIS of DMSO-treated organoids and expressed as the normalized (b) or absolute (c) area under the curve (AUC) calculated from time tracings shown in Fig. 1b (baseline = 100%, t = 60 or 120 min). (d) Forskolin-induced swelling of corrector-stimulated organoids expressing 2 class I mutations. (b-d: The nonsense mutations include E60X, G542X and R1162X. n = number of CF subjects; each subject was measured at 2 independent culture time points in triplicate. Mean ± SD). (e) Western blot detection of immature (B-band) and mature (C-band) CFTR in organoids expressing various *CFTR* mutations upon treatment with DMSO, VX-809 (3 μM) or C17 (5 μM).

DISCUSSION

We assessed for the first time correction of multiple CFTR trafficking mutants in primary cells by assessment of forskolin-induced swelling (FIS) assay in rectal organoids using 19 chemical correctors[16,17]. As residual function for the different trafficking mutants was different (Fig. 1c,e), assay conditions were adapted to enable optimal detection of correction of the various mutants (Fig. 3a). Organoids with A455E have considerable residual function and the forskolin dose was reduced to enable optimal detection of corrector efficacy. In contrast, for F508del / Class I and F508del / N1303K the FIS measurement was prolonged from 60 to 120 min to increase assay sensititvity. Normalization of the corrector-repaired datasets to VX-809 allowed comparison of the 4 different genotypes and to pinpoint functional correction specifically to CFTR-A455E or -N1303K (Fig. 3b).

This approach indicated that repair of CFTR-A455E was highest by a subgroup of 4 correctors sharing a bithiazole group and by C5 containing a phenylquinolin group (Fig. 3b). Recent data already indicated that corrector-mediated repair of CFTR-A455E function (Dekkers *et al*. manuscript submitted) and expression[18] is feasible, but the preference of certain correctors for CFTR-A455E compared to CFTR-F508del has never been shown. These findings support that CFTR-A455E and CFTR-F508del contain distinct folding defects. Recent observations indicated that the bithiazole C4 acts as a class II corrector targeting the NBD2-MSD1 interface, which repairs CFTR-F508del expression and function synergistically when combined with class I correctors (VX-809) that target the NBD1-MSD2 interface[19]. The specific folding defects and corrector target domains in CFTR-A455E need to be further defined.

The similarity between the relative (Fig. 3b) and absolute (Fig. 3c) correction profiles of F508del / N1303K, F508del / F508del and F508del / class I organoids indicate that FIS of F508del / N1303K cultures depends most likely on CFTR-F508del, and that function of CFTR-N1303K is not restored by any C1 to C18 corrector. These data support other findings demonstrating that CFTR-N1303K could not be functionally repaired by VX-809 or VX-770 in human intestinal organoids (Dekkers *et al*. manuscript submitted) and Fischer rat thyroid (FRT) cells[21]. In line with ectopic CFTR expression studies in cell lines[22], increased B-band and decreased C-band levels are detected for CFTR-N1303K compared to wild-types (Fig. 1a). Although the expression levels of this mutant can be partially restored by correctors[22] (Fig. 3e), development of novel treatment strategies is required to repair the specific defect in CFTR-N1303K that blocks its function.

In conclusion, we studied functional CFTR repair by VX-809 and C1 to C18 in primary intestinal CF organoids with different trafficking mutants and observed correction of CFTR-F508del and -A455E by 13 out of 19 compounds, while none of these compounds restored function of CFTR-N1303K. Most importantly, C5 and a subgroup of compounds that share a bithiazole chemical structure achieved highest repair of CFTR-A455E, while correction of CFTR-F508del was dominated by VX-809. These data indicate for the first time in primary human CF cells that the CFTR corrector efficacy selectively depends on the type of folding and trafficking defect and support the development of mutation-specific corrector strategies that are optimal for distinct CFTR mutants.

METHODS

Compounds

VX-809 (Selleck Chemicals LLC, Houston, USA) and C1-C18 (CFF therapeutics) were ordered as dry powder. DMSO stock solutions (10 mM for C2, and 20 mM for all other compounds) were prepared simultaneously for all compounds, stored at -80, and used within 6 months after storage. Stock solutions were refrozen (-20) for maximal 2 times or stored at -20 maximally 1 month.

Human material

Approval for this study was obtained by the Ethics Committee of the University Medical Centre Utrecht and the Erasmus Medical Centre Rotterdam. Informed consent was obtained from all subjects participating in the study. Organoids from healthy controls and cystic fibrosis subjects were generated from four rectal suction biopsies after intestinal current measurements (ICM) obtained (i) during standard cystic fibrosis care (ii) for diagnostic purposes or (iii) during voluntary participation in studies.

Crypt isolation and organoid culture from rectal suction biopsies

Methods were slightly adapted from protocols described previously[14,16]. In short, crypts were isolated, and seeded in 50% matrigel (growth factor reduced, phenol-free, BD bioscience) in 24-well plates (~10–30 crypts in three 10µl matrigel droplets per well). Growth medium[16] was further supplemented with Primocin (1:500; Invivogen). Vancomycin and gentamycin (both from Sigma) were added during the first week of culture. The medium was refreshed every 2–3 days and organoids were passaged ~1:5 every 7–10 days.

The forskolin-induced swelling assay

Methods to measure forskolin-induced organoid swelling described previously[16] were slightly adapted. In short, rectal CF organoids (passage 1–30) from a 7–10-day old culture were seeded in a flat-bottom 96-well culture plate (Nunc) in 5 µl 50% matrigel commonly containing 20–80 organoids immersed in 100 µM complete culture medium, with or without 3 µM VX-809 (Selleck Chemicals LLC, Houston, USA) or C1-C18 at concentrations as indicated in Fig. 2. One day after seeding, organoids were incubated for 30 min with 3 µM calcein-green (Invitrogen) in complete culture medium. After calcein-green staining, forskolin was added at concentrations as indicated in the figures and organoids were directly analyzed by confocal live cell microscopy (LSM710, Zeiss, 5× objective) for 60 (F508del / F508del and F508del / A455E) or 120 minutes (F508del / class I and F508del / N1303K). Two (Fig. 1+2) or three (Fig. 3) wells were used per condition. Per individual, each experiment was repeated at 3-5 different time points.

Quantification of forskolin-induced swelling

Forskolin-stimulated organoid swelling was automatically quantified using Volocity imaging software (Improvision). The total organoid area (xy plane) increase relative to t = 0 of forskolin treatment was calculated and averaged from two individual wells per condition. In some cases, cell debris and unviable structures were manually excluded based on criteria described in detail in

a standard operating procedure (SOP). The area under the curve (AUC; t = 60 or 120 min; baseline = 100%) was calculated using Graphpad Prism.

Western blot analysis

Organoids that were untreated or treated with VX-809 or C17 were lysed in Laemmli buffer supplemented with complete protease inhibitor tablets (Roche). Lysates were analyzed by SDS-PAGE and electrophoretically transferred to a polyvinylidene difluoride membrane (Millipore). The membrane was blocked with 5% milk protein in TBST (0.3% Tween, 10 mM Tris pH8 and 150 mM NaCl in H_2O) and probed 3 h at RT with mouse monoclonal E-cadherin-specific (1:10000; DB Biosciences) or CFTR-specific antibodies (450, 570 and 596; 1:3000; Cystic Fibrosis Folding Consortium), followed by incubation with HRP-conjugated secondary antibodies and ECL development.

Acknowledgements

We thank S. Heida-Michel, M. Geerdink, M.C.J. Olling-de Kok (Department of Pediatric Pulmonology, Wilhelmina Children's Hospital, University Medical Centre, Utrecht, The Netherlands), E.M. Nieuwhof-Stoppelenburg and E.C. van der Wiel (Department of Pediatric Pulmonology, Erasmus University Medical Centre / Sophia Children's Hospital, Rotterdam, the Netherlands) for providing intestinal biopsies, R.J. Bridges (Department of Physiology and Biophysics, Rosalind Franklin University of Medicine and Science, North Chicago, USA) and Cystic Fibrosis Foundation Therapeutics (CFFT) for providing the C1-C18 compounds, and J. Riordan (Department of Biochemistry and Biophysics, University of North Carolina, Chapel Hill, USA) and CFFT for providing the CFTR monoclonal antibodies. This work was supported by grants of the Dutch Cystic Fibrosis Foundation (NCFS) as part of the HIT-CF program, the Wilhelmina Children's Hospital (WKZ) Foundation, and the Dutch Health Organization ZonMw, the Netherlands

Competing Financial Interest

J.M.B., C.K.E., J.F.D. are inventors on a patent application related to these findings.

REFERENCES

1. Van Goor, F., Yu, H., Burton, B. & Hoffman, B. J. Effect of ivacaftor on CFTR forms with missense mutations associated with defects in protein processing or function. *J. Cyst. Fibros.* **13,** 29–36 (2014).
2. Yu, H. *et al.* Ivacaftor potentiation of multiple CFTR channels with gating mutations. *J. Cyst. Fibros.* **11,** 237–245 (2012).
3. Cheng, S. H. *et al.* Defective intracellular transport and processing of CFTR is the molecular basis of most cystic fibrosis. *Cell* **63,** 827–834 (1990).
4. Boyle, M. P. *et al.* A CFTR corrector (lumacaftor) and a CFTR potentiator (ivacaftor) for treatment of patients with cystic fibrosis who have a phe508del CFTR mutation: a phase 2 randomised controlled trial. *Lancet Respir Med*. **2**: 527–38 (2014).
5. Wainwright, C. E. *et al.* Lumacaftor-Ivacaftor in Patients with Cystic Fibrosis Homozygous for Phe508del CFTR. *N. Engl. J. Med.* (2015). doi:10.1056/NEJMoa1409547
6. Pedemonte, N. *et al.* Small-molecule correctors of defective DeltaF508-CFTR cellular processing identified by high-throughput screening. *J. Clin. Invest.* **115,** 2564–2571 (2005).
7. Van Goor, F. *et al.* Rescue of DeltaF508-CFTR trafficking and gating in human cystic fibrosis

airway primary cultures by small molecules. *Am. J. Physiol. Lung Cell Mol. Physiol.* **290,** L1117–30 (2006).

8. Loo, T. W., Bartlett, M. C., Wang, Y. & Clarke, D. M. The chemical chaperone CFcor-325 repairs folding defects in the transmembrane domains of CFTR-processing mutants. *Biochem. J.* **395,** 537–542 (2006).
9. Hirth, B. H. *et al.* Discovery of 1,2,3,4-tetrahydroisoquinoline-3-carboxylic acid diamides that increase CFTR mediated chloride transport. *Bioorg. Med. Chem. Lett.* **15,** 2087–2091 (2005).
10. Robert, R. *et al.* Structural analog of sildenafil identified as a novel corrector of the F508del-CFTR trafficking defect. *Mol. Pharmacol.* **73,** 478–489 (2008).
11. Macia, E. *et al.* Dynasore, a cell-permeable inhibitor of dynamin. *Dev. Cell* **10,** 839–850 (2006).
12. Yoo, C. L. *et al.* 4'-Methyl-4,5'-bithiazole-based correctors of defective delta F508-CFTR cellular processing. *Bioorg. Med. Chem. Lett.* **18,** 2610–2614 (2008).
13. Sato, T. *et al.* Paneth cells constitute the niche for Lgr5 stem cells in intestinal crypts. *Nature* **469,** 415–418 (2011).
14. Sato, T. *et al.* Long-term Expansion of Epithelial Organoids From Human Colon, Adenoma, Adenocarcinoma, and Barrett's Epithelium. *Gastroenterology.* **141**: 1762–72 (2011).
15. Jung, P. *et al.* Isolation and in vitro expansion of human colonic stem cells. *Nat Med.* **17**: 1225–7 (2011)
16. Dekkers, J. F. *et al.* A functional CFTR assay using primary cystic fibrosis intestinal organoids. *Nat Med.* **19**: 939–45 (2013).
17. Dekkers, J. F., van der Ent, C. K. & Beekman, J. M. Novel opportunities for CFTR-targeting drug development using organoids. *Rare Dis* **1,** e27112 (2013).
18. Cebotaru, L., Rapino, D., Cebotaru, V. & Guggino, W. B. Correcting the cystic fibrosis disease mutant, A455E CFTR. *PLoS ONE* **9,** e85183 (2014).
19. Okiyoneda, T. *et al.* Mechanism-based corrector combination restores ΔF508-CFTR folding and function. *Nat. Chem. Biol.* **9,** 444–454 (2013).
20. van Meegen, M. A. *et al.* CFTR-mutation specific applications of CFTR-directed monoclonal antibodies. *J. Cyst. Fibros.* **12,** 487–496 (2013).
21. Van Goor F, Yu H, Burton B, Hoffman BJ. Effect of ivacaftor on CFTR forms with missense mutations associated with defects in protein processing or function. *J Cyst Fibros*. **13**: 29–36 (2014).
22. Rapino, D. *et al.* Rescue of NBD2 mutants N1303K and S1235R of CFTR by small-molecule correctors and transcomplementation. *PLoS ONE* **10,** e0119796 (2015).

Chapter 5

Potentiator combinations in rectal cystic fibrosis organoids synergize in a CFTR mutation-specific manner

Johanna F. Dekkers[1,2], Peter Van Mourik[1,2], Annelotte M. Vonk[1,2], Evelien Kruisselbrink[1,2], Gitte Berkers[1], Karin M. de Winter - de Groot[1], Hettie M. Janssens[3], Inez Bronsveld[4], Cornelis K. van der Ent[1], Hugo R. de Jonge[5]* and Jeffrey M. Beekman[1,2]*

[1]Department of Pediatric Pulmonology, [2]Laboratory of Translational Immunology, Wilhelmina Children's Hospital, University Medical Centre, Utrecht, The Netherlands, [3]Department of Pediatric Pulmonology, Erasmus University Medical Centre / Sophia Children's Hospital, Rotterdam, the Netherlands. [4]Department of Pulmonology, University Medical Centre, Utrecht, The Netherlands, [5]Department of Gastroenterology & Hepatology, Erasmus University Medical Centre, Rotterdam, The Netherlands,

*These authors contributed equally

Submitted

ABSTRACT

The potentiator VX-770 (ivacaftor / KALYDECO™) targets defective gating of CFTR and has been approved for treatment of cystic fibrosis (CF) subjects carrying G551D, S1251N or one of 8 other mutations. Still, the current potentiator treatment does not normalize CFTR-dependent biomarkers, indicating the need for development of more effective potentiator strategies. We have recently pioneered a functional CFTR assay in primary rectal organoids and used this model to characterize interactions between VX-770, genistein and curcumin, the latter 2 being natural food components with established CFTR potentiation capacities. Results indicated that all possible combinations of VX-770, genistein and curcumin synergistically repaired function of CFTR-S1251N and -G551D, even under suboptimal CFTR activation and compounds concentrations, conditions that may predominate *in vivo*. Genistein and curcumin also synergistically enhanced CFTR function in F508del homozygous organoids that were treated with VX-770 and the prototypical CFTR corrector VX-809. These results indicate that potentiators can synergize in restoring CFTR function *in vivo* and support the use of multiple potentiators for treatment of CF.

.

INTRODUCTION

Cystic fibrosis (CF) is the most common autosomal recessive, life-shortening disorder in the Caucasian population caused by mutations in the *cystic fibrosis transmembrane conductance regulator* (*CFTR*) gene leading to defective CFTR-mediated epithelial ion transport[1,2]. The nearly 2000 *CFTR* mutations that have been identified (www.genet.sickkids.on.ca) so far are categorized into six classes according to their effect on CFTR expression and function[3,4]. The most common mutant CFTR-F508del, expressed by ~90% of all CF individuals, has defects in protein folding and trafficking (class II) and channel gating (class III), and has thermal instability at the apical cell surface (class VI)[5,6]. Classical class III mutations (e.g. G551D and S1251N) affect ~5% of CF subjects and lead to normal apical CFTR processing but severe functional impairment[3] (www.genet.sickkids.on.ca).

Novel therapeutic strategies that target mutation-specific defects of the CFTR protein include repair of CFTR mistrafficking by correctors and defective CFTR channel gating by potentiators[7-10]. The potentiator VX-770 (ivacaftor, KALYDECO™) dramatically improved pulmonary function in subjects with G551D, S1251N or 8 other mutations for which the drug has now been US Food and Drug Administration (FDA)- and European Medicines Agency (EMA)-approved[11-14]. More recently, VX-770 combined with the corrector VX-809 (lumacaftor) showed modest but significant effects on lung function of F508del homozygous subjects (approximately 45-50% of all subjects)[15,16]. These studies demonstrate that mutation-specific drug targeting is feasible, but also support the need for more effective treatments, as these treatment do not normalize CFTR-dependent biomarkers for most patients[11-17].

Aside VX-770, many other compounds are able to potentiate CFTR, including the natural food components genistein, an isoflavonoid found in high concentrations in soy[18-20], and curcumin, a major constituent of turmeric[21,22]. Studies have indicated that both VX-770 and curcumin activate CFTR channels in the absence of adenosinetriphosphate (ATP)[21-24], while genistein is known to promote ATP-dependent CFTR gating[20,25,26]. In line with their different mode of CFTR potentiation, recent patch clamp studies showed synergistic effects of curcumin and genistein on the gating of G551D-CFTR channels[26,27]. These findings suggest that potentiators with a different mode of action may likewise enhance clinical VX-770 effectiveness.

We recently developed a functional CFTR assay in human intestinal CF organoids[28,29] that was used to study *CFTR* gene-editing[30] and CFTR modulator mechanisms of action[31-33]. One of these studies reported the robust repair of CFTR-F508del trafficking by the combination of structure-guided correctors[32], but data on repair of CFTR gating by potentiator combinations in primary CF cells is lacking. Rapid swelling of organoids induced by forskolin is used to measure the residual and drug-corrected CFTR activity in a subject-specific manner. The robust organoid growth[34-37] and CFTR assay conditions[28,29] allow us to generate large and accurate datasets using drug combinations and forskolin-dose-response curves (Dekkers *et al*. manuscript submitted). We here tested the impact of potentiator combinations on mutant CFTR function in freshly excised rectal biopsies and in organoids generated from these tissues. Results indicated synergy between VX-770, genistein and curcumin in potentiating CFTR in a mutation-specific manner, and support the combination of potentiators as therapeutic strategy for CF.

Intestinal current measurements of F508del / S1251N rectal biopsies treated with VX-770 and genistein

Because different CFTR activation mechanisms for VX-770 (ATP-independent) and genistein (ATP-dependent) have been described[20,23-26], we first assessed treatment of VX-770, genistein and their combination by intestinal current measurements (ICM) on human rectal biopsies derived from 17 F508del homozygotes or 7 compound heterozygotes expressing F508del and the gating mutation S1251N (Fig. 1). We observed a chloride secretory response to forskolin, which was ~5 times greater in F508del / S1251N compared to F508del / F508del biopsies (Fig. 1a,b). In biopsies expressing S1251N, the response to forskolin (~34 % of healthy control; HC) was increased by VX-770 (~42 % of HC) and even further enhanced by genistein (~59 % of HC) (Fig. 1c), while potentiator activity was not detected in F508del homozygous biopsies (Fig. 1a-c). To conclude, these data

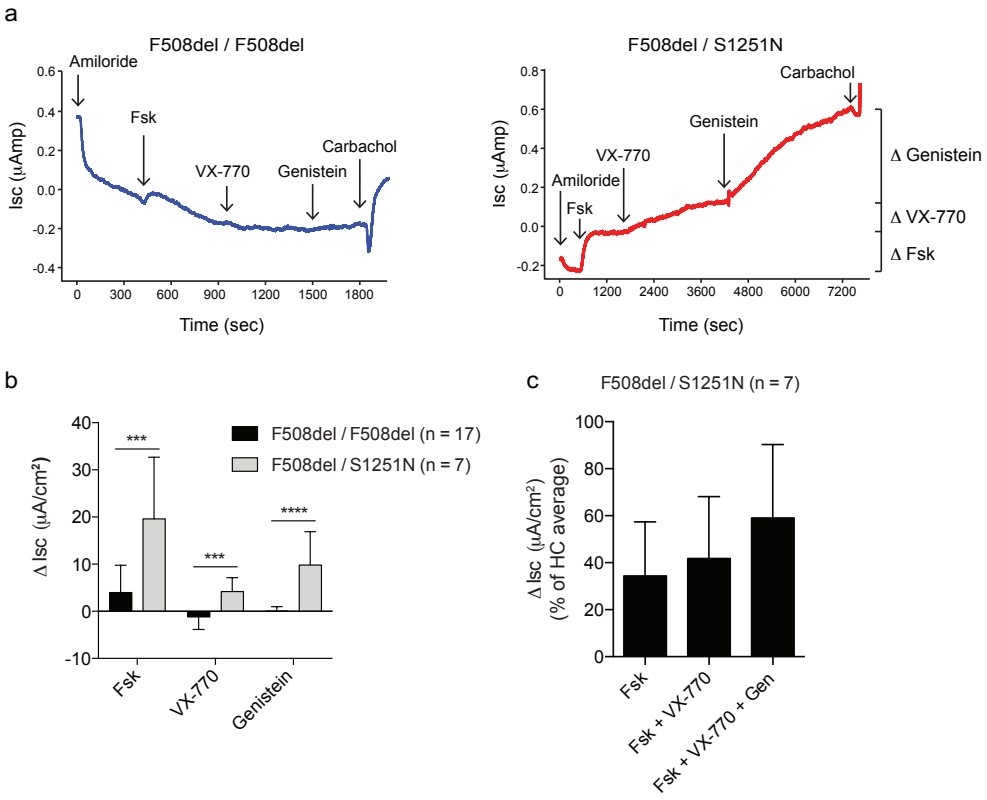

Figure 1. Intestinal current measurements of F508del / S1251N rectal biopsies treated with VX-770 and genistein. (a) Examples of intestinal current measurement (ICM) tracings of a F508del / F508del or F508del / S1251N rectal biopsy incubated with compounds as indicated (amiloride 100 µM; forskolin (fsk) 10/100 µM; VX-770 20 µM; genistein 50 µM; carbachol 100 µM). (b) Delta Isc ICM values of biopsies derived from 17 F508del / F508del (2–4 biopsies per subject) and 7 F508del / S1251N subjects (1–4 biopsies per subject). (c) Delta Isc ICM values of biopsies derived from 7 F508del / S1251N subjects (1–4 biopsies per subject), normalized to the average response to forskolin of healthy controls (Δ Isc of 57 µA/cm²; n = 43).

indicate that ICM can detect potentiator activity on CFTR-S1251N, but not on CFTR-F508del, and that treatment of VX-770 and genistein together is more effective than of VX-770 alone.

Incubation of VX-770, genistein and curcumin in rectal organoids derived from F508del / S1251N CF subjects

To investigate functional CFTR-repair by different potentiators at larger scale, we analyzed effects of VX-770, genistein, curcumin and their combinations on forskolin-induced swelling (FIS) of organoids derived from CF subjects compound heterozygous for F508del and the gating mutation S1251N. As described previously[28], organoid swelling was presented as absolute area under the curve (AUC) calculated from 60 min time tracings of the surface area increase of calcein-green-labeled organoids relative to t = 0 (Fig. 2a,b). We assessed titrations of VX-770, genistein and curcumin using suboptimal forskolin concentrations (0.128 and 0.5 μM) (Fig. 2c-e) to remain within the dynamic range of the swelling assay (Fig. 2f,g) and to facilitate an optimal detection of potentiator activity. All compounds dose-dependently increased FIS of organoids, with highest potency for VX-770 and lowest potency for curcumin (Fig. 2c-e).

Next, we studied VX-770 and genistein combination therapy using a forskolin dose-range (0.008 - 5 μM) (Fig 2f,g) and observed that near-saturating (3 or 50 μM; Fig. 2f) and suboptimal (0.1 or 10 μM; Fig. 2g) concentrations of VX-770 or genistein increased basal FIS in a forskolin dose-dependent manner. Interestingly, genistein greatly enhanced VX-770-repaired FIS and synergistic effects were observed at low forskolin concentrations (Fig 2f,g). In line with other data (Dekkers *et al*. manuscript submitted), the drug-induced FIS of S1251N-expressing organoids reached maximal rates (= AUC of ~3000) at high forskolin levels (Fig 2f,g). The genistein dose-dependent increase in FIS of VX-770-treated organoids also indicated synergy between VX-770 and genistein, even at genistein levels <10 μM (Supplementary Fig. S1a).

Subsequently, combinations of VX-770, genistein and curcumin were investigated at near-saturating (Fig. 2h; 3, 50 and 50 μM) and suboptimal (Fig. 2i; 0.1, 10 and 10 μM) potentiator dosages using fixed forskolin concentrations, which were defined from Fig. 2f,g. At near-saturating potentiator concentrations, the FIS responses upon combination treatments (duo or trio) greatly exceeded the calculated additive responses of the single treatments, indicating synergistic effects between all potentiator combinations (Fig. 2h). None of the potentiator treatments induced swelling in organoids expressing two class I mutations, indicating full CFTR dependency of the treatments (data not shown). Stimulations with suboptimal potentiator concentrations again indicated strong synergy between VX-770 and genistein, but a weaker synergy between curcumin and VX-770 or genistein (Fig. 2i). In line with Fig. 2h and 2i, synergy between curcumin and VX-770 or genistein was curcumin dose-dependent and appeared more prominent at higher curcumin concentrations (>12.5 μM; Supplementary Fig. S1b,c).

We also assessed CFTR-S1251N protein expression detected by Western blot upon chronic stimulation (48 h) of VX-770, genistein, curcumin or potentiator combinations (Fig. 2j,k). The effect of chronic treatment ranged from no effect to a small reduction of maturated CFTR C-band, with largest reduction induced by VX-770 + curcumin or VX-770 + genistein + curcumin (~70% of mock-treated; Fig. 2k).

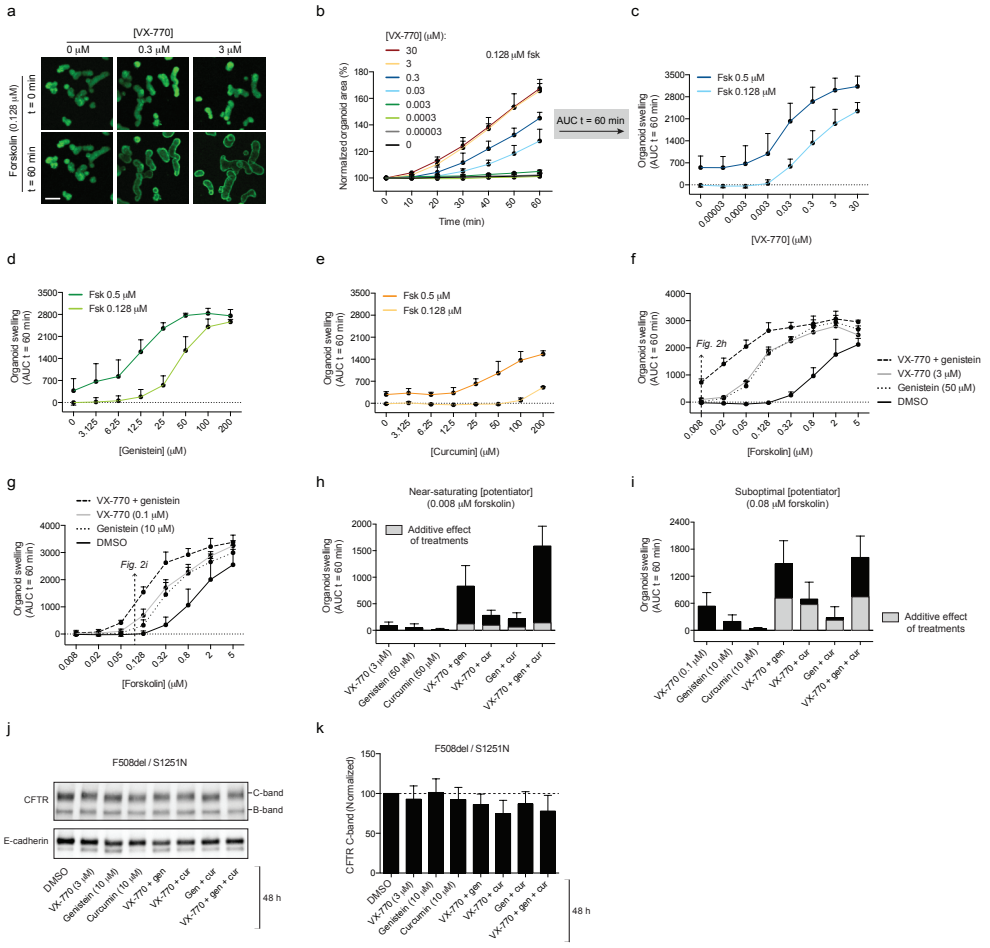

Figure 2. Incubation of VX-770, genistein and curcumin in rectal organoids derived from F508del / S1251N CF subjects. (a) Representative confocal images of calcein-green-labeled F508del / S1251N organoids at the indicated time points of forskolin (0.128 µM) stimulation. Scale bar = 130 µm. (b) A time tracing of the forskolin(0.128 µM)-induced surface area increase relative to t = 0 (normalized area) of F508del / S1251N organoids at different VX-770 concentrations averaged from two independent wells. Mean ± SD. (c-e) Forskolin(fsk)-induced swelling (FIS) expressed as the absolute area under the curve (AUC) calculated from time tracings shown in b (baseline = 100%, t = 60 min) of organoids stimulated with multiple dosages of VX-770 (c), genistein (d) or curcumin (e) at the indicated forskolin concentrations. (f,g) FIS of organoids stimulated with near-saturating (f) or suboptimal (g) concentrations of VX-770, genistein or both using a dose range of forskolin. (h,i) FIS of organoids stimulated with near-saturating (h) or suboptimal (i) concentrations of VX-770, genistein (gen), curcumin (cur) or their combinations at the indicated concentrations of forskolin, corrected for the FIS without addition of a potentiator. (c-i represent data averaged from 3 F508del / S1251N subjects. Each subject was measured at 2 to 5 independent culture time points in duplicate. Mean ± SD. The SD indicates the inter-subject variation). (j) Expression of CFTR and E-cadherin in whole cell lysates of F508del / S1251N organoids detected by Western blot upon treatments as indicated (48 h). Immature (B-band) and mature (C-band) CFTR is indicated. (h) Quantification of CFTR C-band by Image J from Western Blots as shown in j. Data of 3 different F508del / S1251N cultures was averaged, each culture was assessed in 1-3 independent experiments. Mean ± SD.

In conclusion, all potentiator combinations synergistically repaired function of CFTR-S1251N, supporting that VX-770, genistein and curcumin potentiate CFTR by different mechanisms. The synergy was detected at suboptimal activation of CFTR and suboptimal potentiator levels, conditions that may predominate *in vivo*.

Incubation of VX-770, genistein and curcumin in rectal organoids derived from a F508del / G551D CF subject

We next analyzed effects of VX-770, genistein, curcumin and their combinations on FIS of F508del / G551D organoids (Fig. 3) using an experimental setup comparable to Fig. 2. Because CFTR-S1251N has a higher residual activity than CFTR-G551D (Fig. 2f,g and 3e,f), different forskolin concentrations are required for optimal drug testing in F508del / S1251N and F508del / G551D organoids (Fig. 2 and Fig. 3). Titrations of VX-770, genistein and curcumin indicated a dose-dependent increase in FIS of F508del / G551D organoids, with highest potency for VX-770 and lowest potency for curcumin (Fig. 3a-c), similar as observed for F508del / S1251N organoids (Fig. 2c-e).

VX-770 and genistein at near-saturating (Fig. 3d,e) or suboptimal (Fig. 3f) concentrations synergistically repaired FIS of F508del / G551D organoids at suboptimal forskolin levels. Compared to S1251N-expressing organoids (Fig. 2f,g), optimal detection of synergy between VX-770 and genistein in F508del / G551D organoids required somewhat higher forskolin levels, probably because of the low residual function associated with CFTR-G551D (Fig. 3e,f). Furthermore, both VX-770 and genistein induced FIS to a similar extent in S1251N-expressing organoids (Fig. 2f,g), while the effect of genistein was much lower compared to VX-770 in G551D-expressing cultures (Fig. 3e,f). This indicates that channel gating by genistein, but not by VX-770, is critically dependent on the site of the class III mutation within the multi-domain structure of the CFTR channel.

We selected optimal forskolin concentrations based on Fig. 3e,f to study the effect of curcumin in addition to VX-770 and genistein using near-saturating (Fig. 3g) or suboptimal (Fig. 3h) potentiator concentrations and observed strong synergy between the 3 compounds (Fig. 3g,h). In contrast to F508del / S1251N organoids (Fig. 2i), curcumin, in combination with VX-770, was highly effective at suboptimal dose in organoids with G551D (Fig. 2h), indicating that CFTR-G551D is more sensitive to curcumin than CFTR-S1251N. Chronic incubation of potentiators revealed that CFTR C-band expression was minimally affected by single or combination treatment with VX-770 and genistein, and modestly reduced in conditions containing curcumin (~ 70% of vehicle Fig. 3i,j).

To conclude, CFTR-S1251N and -G551D respond different to identical potentiator levels and CFTR phosphorylation conditions, indicating that different molecular mechanisms underlie the gating defects of these mutants.

Incubation of VX-770, genistein and curcumin in rectal organoids derived from F508del / F508del CF subjects

Combinations of VX-770, genistein and curcumin were also assessed in organoids homozygous for the most common *CFTR* mutation F508del. The hierarchy of the compound potency (VX-770 > genistein > curcumin) was similar as observed for organoids with a gating mutation (Fig. 2c-e and 3a-c), but potentiator-induced FIS rates were much lower in F508del homozygous organoids, even when a saturating forskolin dose was used (5 μM) (Fig. 4a-c). Synergy between VX-770 and genistein was observed using near-saturating potentiator dosages (0.05 - 0.8 μM forskolin; Fig.

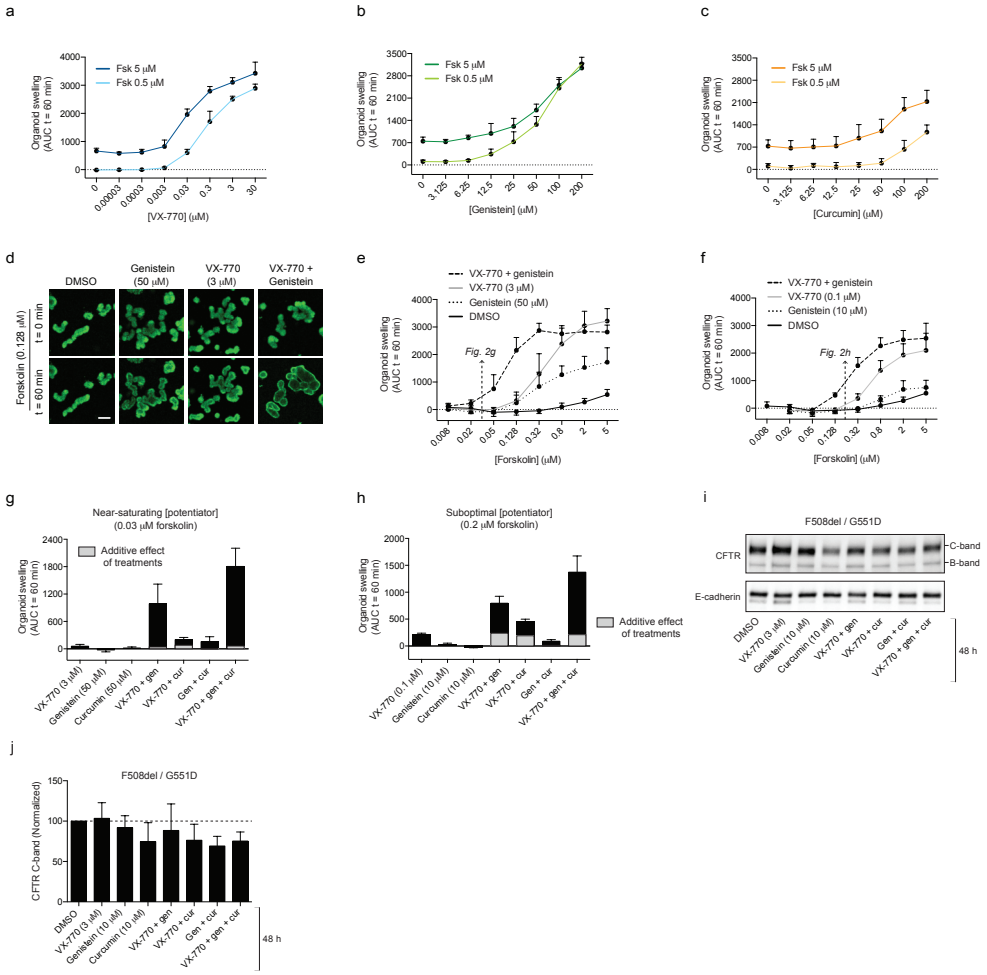

Figure 3. Incubation of VX-770, genistein and curcumin in rectal organoids derived from a F508del / G551D CF subject. (a-c) Forskolin(fsk)-induced swelling (FIS) expressed as the absolute area under the curve (AUC) calculated from time tracings shown in Fig. 2b (baseline = 100%, t = 60 min) of organoids stimulated with multiple dosages of VX-770 (a), genistein (b) or curcumin (c) at the indicated forskolin concentrations. (d) Representative confocal images of calcein-green-labeled organoids at the indicated time points of forskolin (0.128 µM) stimulation. Scale bar = 130 µm. (e,f) FIS of organoids stimulated with near-saturating (e) or suboptimal (f) concentrations of VX-770, genistein or both using a dose range of forskolin. (g,h) FIS of organoids stimulated with near-saturating (g) or suboptimal (h) concentrations of VX-770, genistein (gen), curcumin (cur) or their combinations at the indicated concentrations of forskolin, corrected for the FIS without addition of a potentiator. (a-c and e-h represent data from 1 F508del / G551D subject measured at 3 to 4 independent culture time points in duplicate. Mean ± SD. The SD indicates the inter-experiment variation). (i) Expression of CFTR and E-cadherin in whole cell lysates of F508del / G551D organoids detected by Western blot upon treatments as indicated (48 h). Immature (B-band) and mature (C-band) CFTR is indicated. (j) Quantification of CFTR C-band by Image J from Western Blots as shown in i. Data of 3 independent experiments was averaged. Mean ± SD.

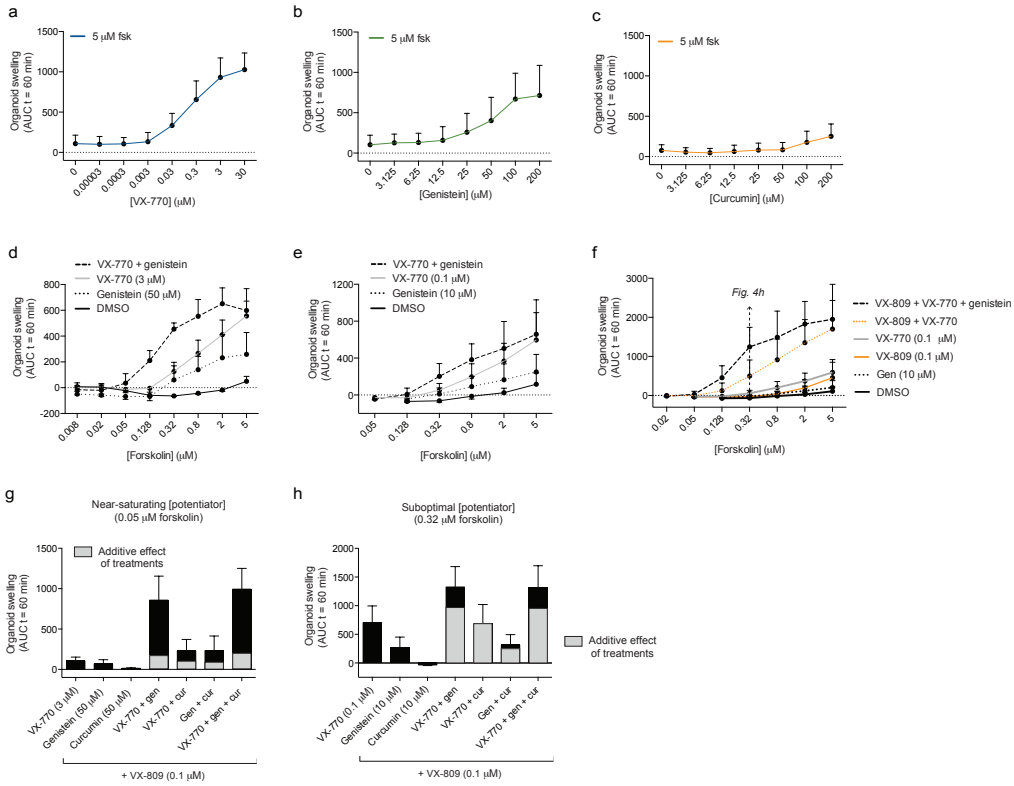

Figure 4. Incubation of VX-770, genistein and curcumin in rectal organoids derived from F508del / F508del CF subjects. (a-c) Forskolin(fsk)-induced swelling (FIS) expressed as the absolute area under the curve (AUC) calculated from time tracings shown in Fig. 2b (baseline = 100%, t = 60 min) of organoids stimulated with multiple dosages of VX-770 (a), genistein (b) or curcumin (c) at the indicated forskolin concentrations. (d,e) FIS of organoids stimulated with near-saturating (d) or suboptimal (e) concentrations of VX-770, genistein or both using a dose range of forskolin. (f) The effect of VX-809 preincubation (24 h) on FIS of organoids stimulated with VX-770 or genistein using a dose range of forskolin. (g,h) FIS of organoids pre-incubated with VX-809 for 24h, and stimulated with near-saturating (g) or suboptimal (h) concentrations of VX-770, genistein (gen), curcumin (cur) or their combinations at the indicated concentrations of forskolin, corrected for the VX-809-repaired FIS without addition of a potentiator. (All figures represent data averaged from 3 F508del / F508del subjects. Each subject was measured at 2 to 5 independent culture time points in duplicate. Mean ± SD. The SD indicates the inter-subject variation).

4d) and VX-770 and genistein additively increased FIS using suboptimal dosages (0.32 – 2 μM forskolin; Fig. 4e). Importantly, genistein greatly enhanced FIS of organoids that were treated with VX-770 or VX-770 and VX-809, even at genistein levels < 10 μM (Fig. 4f and Supplementary Fig. S2a,b). In VX-809-corrected organoids, synergy between VX-770 and genistein was clearly detected both at near saturating (3 and 50 μM; Fig. 4g) and suboptimal (0.1 and 10 μM; Fig. 4h) potentiator concentrations. Curcumin at high (50 μM; Fig. 4g) dose increased FIS in addition to VX-770, gensitein or VX-770+genistein to a modest extent, but curcumin at low (10 μM; Fig. 4h) dose did not increase FIS of VX-809-corrected organoids in addition to VX-770 or genistein (Fig. 4g,h).

In conclusion, these data indicate that FIS of VX-809-corrected or non-corrected CFTR-F508del homozygous organoids is synergistically repaired by VX-770 and genistein, but only to a modest extent by curcumin.

DISCUSSION

We characterized interactions between VX-770 (ivacaftor, KALYDECO™) and the natural food components genistein and curcumin for CFTR potentiation using rectal CF biopsies and primary intestinal CF organoids as *ex vivo* models. While CFTR repair by corrector / corrector or corrector / potentiator combinations has been abundantly examined[15,28,32,38-40], only a few studies have reported interactions between potentiators[27,38], and similar studies in primary cells including VX-770 are completely lacking. Here we provide proof-of-concept that potentiator combinations can exert synergistic effects in a *CFTR* mutation-specific fashion, supporting the development of potentiator combination therapy in clinical practice, especially for people expressing gating mutations.

In line with previous studies[41], we observed that potentiator activity is detected by ICM in rectal biopsies expressing a CFTR gating mutation (Fig. 1). However, while we did observe a chloride secretory response to forskolin in F508del homozygous biopsies of some CF patients, a further stimulation by CFTR potentiators appeared marginal or absent (Fig. 1a,b). In contrast, the organoid assay (FIS) allowed clear detection of both residual function and potentiator activity, indicating higher sensitivity to detect repair of CFTR-F508del gating, in comparison to ICM. Since ICM was able to detect limited residual function in F508del homozygous biopsies, it appears that especially potentiator delivery is difficult in the fresh rectal biopsies. Organoid measurements furthermore allow generation of large subject-specific datasets with forskolin and potentiator dose-ranges and inter-experimental variance, while ICM is in general restricted to maximal 4 biopsies. Compared to stable drug responses of organoids that can be generated for the individual (Dekkers *et al*. Manuscript submitted), we have experienced greater variability between different ICM measurements (Fig. 1c) as well as between different biopsies and the limited amount of biopsies severely hinders the inclusion of e.g. control stimulation (data not shown). On the other hand, ICM is one of the few techniques capable of measuring CFTR activity in native epithelium *ex vivo*, is completely free of potential cell culture artifacts, and can be used as an *ex vivo* biomarker to study drug effectiveness *in vivo*[42,43] Clearly, both methods are complementary and need to be validated further as diagnostic, prognostic, and therapeutic biomarkers.

Opening of the CFTR gate is regulated by phosphorylation of the regulatory(R)-domain and ATP-dependent dimerization of the nucleotide binding domain(NBD)1 and NBD2. Intriguingly, both VX-770 and curcumin activate CFTR channels in the absence of ATP, suggesting that they bind directly to the channel pore and bypass the conventional ATP-dependent gating mechanism[21-24]. In contrast, genistein is known to promote ATP-dependent gating of CFTR, probably by binding to the NBD2 and/or the NBD1-NBD2 interface and inhibiting ATP hydrolysis[20,25,26]. As expected from their different mode of potentiation and previous findings[26,27], combinations of genistein with VX-770 or with curcumin synergistically repaired FIS of organoids carrying the “pure” gating mutations S1251N and G551D (Fig. 2 and 3). Remarkably, however, we also observed synergy between curcumin and VX-770, indicating that the binding sites for these potentiators, or their mechanism of ATP-independent gating are not identical either. Data of rectal biopsies (Fig. 1) and organoids (Fig. 2h,i; 3g,h) indicate that at near-saturating concentrations of VX-770 S1251N- and G551D-CFTR activity can be further enhanced by other potentiators, in particular by genistein. This supports previous observations in other G551D-expressing cell models[8,24] showing that

the open probability (*Po*) of VX-770-treated G551D-CFTR remains far below the *Po* of wild-type CFTR channels. On the basis of these *in vitro* findings we have recently initiated clinical studies to investigate *in vivo* effects of genistein supplementation in Dutch CF subjects with the S1251N mutation that are treated with VX-770.

Previous studies report that the functional response of CFTR-wild-type and -F508del channels to genistein is bell-shaped, i.e. enhanced in a low concentration range and inhibited in a higher concentration range, suggesting the existence of a high affinity activatory binding site and a low affinity inhibitory binding site in CFTR[44,45]. The inhibitory effect of genistein was not observed for CFTR-G551D, most likely because the G551D mutation abolishes the low affinity inhibitory binding site[20,46], which argues for the therapeutic use of genistein in G551D-expressing subjects. Remarkably, our results indicated that genistein (up to 200 μM) dose-dependently and uniformly increased FIS of organoids for all three mutants investigated, i.e. G551D, S1251N and F508del, without signs of inhibition at the highest dose (Fig. 2d, 3b and 4b). Possibly, the inhibitory effect of genistein on CFTR-F508del depends on the cell model used, or the genistein concentration that reaches CFTR in organoids is lower than the concentration in the surrounding medium. Compounds need to penetrate the matrigel that serves as 3D support, enter via the basolateral epithelial membrane and diffuse to the apical site to reach CFTR, which may differentially impact the efficacy of CFTR modulators. This may also explain why curcumin mono treatment of CFTR-G551D and –S1251N organoids was only effective at 25 μM and higher, while a higher CFTR-activating potency of curcumin was observed in other studies[21,27].

Aside the general similarities in the behavior of the S1251N and G551D gating mutants in the FIS assay and in their response to the potentiators noted above, pronounced differences were found in their basal activity (S1251N > G551D; Fig. 2f,g vs. 3e,f), in their maximal response to genistein (S1251N > G551D; Fig. 2f vs. 3e), and in their sensitivity to curcumin in the presence of VX-770 and genistein (G551D > S1251N; Fig. 3h vs. 2i). At a first glance these differences are rather unexpected because both mutated residues are situated inside the functionally important ATP binding pocket 2 (ABP2) of CFTR, and are predicted to disrupt ATP-induced head-to-tail dimerization of NBD1 and NBD2. However, residue G551 is part of the ABC signature sequence of NBD1, which is involved in ATP hydrolysis rather than ATP binding[47], and the G551D mutation has been shown to abolish ATP hydrolysis and to convert ABP2 from a stimulatory into an inhibitory site[48]. Instead, residue S1251 is located in the Walker A sequence of NBD2 which is crucial for ATP binding[47], suggesting that the S1251N mutation most plausibly impairs ATP binding at site 2 rather than affecting ATP hydrolysis or creating an ATP-inhibitory site. Such functional differences may have a strong impact on the open probability of the mutant CFTR channels and on their differential response to the potentiators. Clearly, additional studies, in particular of the poorly explored S1251N mutant channels, are needed to improve our mechanistic understanding of these differences.

Previous studies indicated that chronic stimulation of potentiators may diminish expression and functionality of VX-809-repaired CFTR-F508del or wild-type CFTR, but not of CFTR-G551D, by yet undefined mechanisms[49,50]. In line with these studies, chronic stimulation with VX-770 did not affect protein expression of CFTR-G551D in organoids (Fig. 3i,j). While single potentiator treatment had only minimal effects on the protein expression of CFTR-G551D or CFTR-S1251N, combinations of potentiators triggered a more pronounced but still modest reduction in the protein levels of these gating mutants, predominantly in conditions containing curcumin

(Fig. 2j,k and 3i,j). Whether a similar reduction in CFTR protein expression occurs upon chronic treatment of F508del organoids is difficult to evaluate, considering the very low intensity of the F508del-CFTR band C in VX-809-pretreated organoids even in the absence of any potentiator (Supplementary Fig. S2c). Moreover, functional studies of CFTR after 48 h of chronic potentiator treatment by the FIS assay are difficult to perform as the chronic presence of a potentiator induces organoid swelling in the absence of forskolin, which by itself suggest increased functional activity (Dekkers *et al*. manuscript submitted). Because it is impossible to exactly mimic chronic potentiator treatment *in vitro* in terms of temporal concentrations reaching CFTR *in vivo*, the clinical implications of small potentiator-dependent reductions in CFTR-S1251N and -G551D levels observed *in vitro* are hard to predict. However, clinical studies with F508del homozygotes indicated that combination treatment with VX-809 and VX-770[15,16] is more effective than VX-809 treatment alone[51], suggesting that positive effects on CFTR gating by potentiator combinations likely outweigh possible CFTR destabilizing effects.

Previous studies[28] (Dekkers *et al.* manuscript submitted) already indicated that maximal FIS rates (~3000 AUC units) can be reached at higher forskolin levels, most likely because the basolateral chloride import, and not the apical CFTR function, becomes rate limiting. Therefore, optimal detection of synergy between the potentiators in organoids carrying the S1251N or G551D mutations required suboptimal forskolin levels (Fig. 2 and 3). In general, the residual and potentiator-induced FIS levels of F508del homozygous organoids (Fig. 4) were greatly reduced compared to organoids generated from compound heterozygotes carrying both F508del and a gating mutation (Fig. 2 and 3), indicating that FIS responses in these organoids mainly reflect the activity of CFTR-S1251N (Fig. 2) or -G551D rather than -F508del (Fig. 3).

Performing the FIS assay on rectal organoids generated from F508del homozygous patients allowed several important conclusions (Fig. 4): (i) even at saturating forskolin concentrations (5 μM) the response to the potentiators genistein and VX-770 could be increased further by the corrector VX-809, suggesting that maximal potentiation is rate limited by low CFTR-F508del protein levels; (ii) the ranking order of the compound potency (VX-770 > genistein > curcumin) was similar as observed for organoids with a gating mutation (Fig. 2c-e and 3a-c); and (iii) genistein, but not curcumin, greatly enhanced FIS of F508del organoids that were treated with VX-770 and VX-809, even at clinically attainable levels (10 μM; Fig. 4f and S2b), while curcumin increased FIS in addition to VX-770 or gensitein only at near-saturating levels (Fig. 4g).

Both genistein and curcumin possess various biological effects including antioxidation, antiproliferation and anticarcinogenic and many clinical trails have been performed to study their clinical efficacy as mono-treatment for various diseases. The low oral bioavailability of both compounds due to poor absorption and rapid metabolism may relate to the ambiguous therapeutic effects and large inter-subject variation observed in these studies[52-54]. Pharmacokinetic studies indicated that plasma levels of active compound can be reached in the nM range for curcumin and μM range for genistein, conditions that induced only limited clinical effects in mono-therapy studies[52,53]. However, the strong synergistic potentiator effects observed here suggest that even low curcumin and genistein plasma levels may be sufficient to functionally repair CFTR gating either by duo-treatment or triple-treatment including VX-770, especially if drugs would further accumulate in the affected tissues.

In conclusion, functional CFTR measurements in rectal CF tissue indicated that (i) organoid measurements can detect potentiator activity more sensitive and robustly compared to ICM, (ii)

VX-770, curcumin and genistein have different mechanisms of CFTR potentiation, (iii) the gating defects in CFTR-S1251N, -G551D and F508del are functionally different from each other, (iv) acute addition of potentiator combinations at suboptimal or near-saturating dosage synergistically repaired gating of CFTR-S1251N and -G551D and to a lesser extent of VX-809-repaired CFTR-F508del, (v) detection of synergy is most optimal at suboptimal CFTR phosphorylation conditions and (vi) expression of CFTR-S1251N and CFTR-G551D are modestly affected by chronic potentiator treatment. These results highlight the potential of combining potentiators for the therapy of CF.

METHODS

Compounds

DMSO stock solutions of VX-770 (20mM; Selleck Chemicals LLC, Houston, USA), genistein (50 mM; Sigma; G6649-25MG) and curcumin (50mM; Fluka; 08511-10MG) were prepared and stored at -80 for a maximum of 6 months. Stock solutions were disposed directly after use and curcumin was protected from light during all procedures.

Human material

Study approval was obtained by the Ethics Committee of the University Medical Centre Utrecht and the Erasmus Medical Centre Rotterdam and informed consent was obtained from all participating subjects. Rectal biopsies were obtained (i) during standard cystic fibrosis care (ii) for diagnostic purposes or (iii) during voluntary participation in studies and used for intestinal current measurements (ICM) and generation of rectal organoids.

Intestinal current measurement (ICM)

Transepithelial, CFTR-dependent anion secretion in human rectal suction or forceps biopsies (in general 4 per subject, for some subjects 1 - 3) was measured using an amendment[36] of the ICM protocol described in detail previously[35]. In short, the biopsies were collected in phosphate-buffered saline on ice and directly mounted in sliders (aperture 0.011 or 0.018 cm^2) adapted to micro-Ussing chambers (P2400; Physiological Instruments, San Diego, U.S.A.). After equilibration and repetitive prewashing of biopsies, the following compounds were added in a standardized order to the mucosal (M) or serosal (S) side of the tissue: amiloride (100 µM, M) to inhibit amiloride sensitive electrogenic Na^+ absorption; forskolin (10 µM; M+S) to activate CFTR-mediated anion secretion; VX-770 (20 µM, but in some F508del / S1251N biopsies 20 – 40 µM; M+S) to potentiate CFTR; genistein (50 µM, but in 1 F508del / S1251N subject 10 and 100 µM; M+S) to further potentiate CFTR; and carbachol (100 µM; S) to initiate the cholinergic Ca^{2+}- and protein kinase C-linked Cl^- secretion. Crude short circuit current values (µA) were converted to µA cm^{-2} on the basis of the surface area of the aperture. The average response of the biopsies per subject to each addition was used to calculate the group averages +/-SD (Fig.1b,c).

Crypt isolation and organoid culture from rectal suction biopsies

Methods for crypt isolation and human organoid culturing were slightly adapted from protocols described previously[35]. In short, rectal biopsies were washed with PBS and incubated with 10 mM

EDTA for 90 - 120 min at 4 °C. Supernatant was harvested and EDTA was washed away. Crypts were isolated by centrifugation and embedded in 50% matrigel (growth factor reduced, phenol-free, BD bioscience) and seeded (~ 10 - 30 crypts in 3 x 10 µl matrigel droplets per well) in 24-well plates. The matrigel was polymerized for 10 - 30 min at 37 °C and immersed in complete culture medium: advanced DMEM / F12 supplemented with penicillin/streptomycin, 10 mM HEPES, Glutamax, N2, B27 (all from Invitrogen), 1 µM *N*-acetylcysteine (Sigma) and growth factors: 50 ng ml^{-1} mEGF, 50% Wnt3a-conditioned medium (WCM) and 10% Noggin-conditioned medium (NCM), 20% Rspo1-conditioned medium (RCM), 10 µM Nicotinamide (Sigma), 500 nM A83-01 (Tocris) and 10 µM SB202190 (Sigma). Growth medium was further supplemented with Primocin (1:500; Invivogen). Vancomycin and gentamycin (both from Sigma) were added during the first week of culture.The medium was refreshed every 2–3 days and organoids were passaged 1:4–1:6 every 7–10 days.

The forskolin-induced swelling assay

Methods to measure forskolin-induced organoid swelling described previously[28] were slightly adapted. In short, rectal CF organoids (passage 1–30) from a 7–10-day old culture were seeded in a flat-bottom 96-well culture plate (Nunc) in 5 µl 50% matrigel commonly containing 20–80 organoids immersed in 100 µl complete culture medium. One day after seeding, organoids were incubated for 30 min with 3 µM calcein-green (Invitrogen) in complete culture medium. After calcein-green staining, forskolin with or without potentiator(s) was added at concentrations as indicated and organoids were directly analyzed by confocal live cell microscopy (LSM710, Zeiss, 5× objective) for 60 min at 37 °C. Two wells were used per condition and experiments were repeated 2–5 times for F508del / S1251N (3 donors) and F508del / F508del (3 donors) organoids and 3–4 times for F508del / G551D organoids (1 donor).

Quantification of forskolin-induced swelling

Forskolin-stimulated organoid swelling was automatically quantified using Volocity imaging software (Improvision). The total organoid area (xy plane) increase relative to t = 0 of forskolin treatment was calculated. In some cases, cell debris and unviable structures were manually excluded based on criteria described in detail in a standard operating procedure (SOP). The area under the curve (AUC; t = 60; baseline = 100%) was calculated using Graphpad Prism.

Western blot analysis

Organoids with S1251N or G551D from a 7 day-old culture were passaged 1:1 in 24-well plates and incubated with DMSO, VX-770, genistein, curcumin or combinations (1 well per condition) in 0.5 ml complete growth medium for 48 hours. The medium with compounds was refreshed after 24 h. Cells were lysed in Laemmli buffer supplemented with complete protease inhibitor tablets (1:50; Roche). Lysates were analyzed by SDS-PAGE and electrophoretically transferred to a polyvinylidene difluoride membrane (Millipore). The membrane was blocked with 5% milk protein in TBST (0.3% Tween, 10 mM Tris pH8 and 150 mM NaCl in H_2O) and probed 3 h at RT with mouse monoclonal E-cadherin-specific (1:10000; DB Biosciences) or CFTR-specific antibodies (450, 570 and 596; 1:5000; Cystic Fibrosis Folding consortium), followed by incubation with HRP-conjugated secondary antibodies (1:3000) and ECL development.

Acknowledgements

We thank S. Heida-Michel, M. Geerdink, M.C.J. Olling-de Kok (Department of Pediatric Pulmonology, Wilhelmina Children's Hospital, University Medical Centre, Utrecht, The Netherlands), E.M. Nieuwhof-Stoppelenburg and E.C. van der Wiel (Department of Pediatric Pulmonology, Erasmus University Medical Centre / Sophia Children's Hospital, Rotterdam, the Netherlands) for providing intestinal biopsies, M.J.C. Bijvelds (Department of Gastroenterology & Hepatology, Erasmus University Medical Centre / Sophia Children's Hospital, Rotterdam, the Netherlands) for performing intestinal current measurements (ICM), and J. Riordan (Department of Biochemistry and Biophysics, University of North Carolina, Chapel Hill, USA) and Cystic Fibrosis Foundation Therapeutics (CFFT) for providing the CFTR monoclonal antibodies. This work was supported by grants of the Dutch Cystic Fibrosis Foundation (NCFS) as part of the HIT-CF program, the Wilhelmina Children's Hospital (WKZ) Foundation, and the Dutch Health Organization ZonMw (# 95104014), the Netherlands

Competing Financial Interest

J.M.B., C.K.E., J.F.D. are inventors on a patent application related to these findings.

REFERENCES

1. Collins, F. S. Cystic fibrosis: molecular biology and therapeutic implications. *Science* **256,** 774–779 (1992).
2. Riordan, J. R. CFTR function and prospects for therapy. *Annu. Rev. Biochem.* **77,** 701–726 (2008).
3. Welsh, M. J. & Smith, A. E. Molecular mechanisms of CFTR chloride channel dysfunction in cystic fibrosis. *Cell* **73,** 1251–1254 (1993).
4. Rogan, M. P., Stoltz, D. A. & Hornick, D. B. Cystic fibrosis transmembrane conductance regulator intracellular processing, trafficking, and opportunities for mutation-specific treatment. *Chest* **139,** 1480–1490 (2011).
5. Bell, S. C., De Boeck, K. & Amaral, M. D. New pharmacological approaches for cystic fibrosis: Promises, progress, pitfalls. *Pharmacol. Ther.* **S0163-7258**: 00122–3 (2014).
6. Liu, X. & Dawson, D. C. Cystic fibrosis transmembrane conductance regulator (CFTR) potentiators protect G551D but not ΔF508 CFTR from thermal instability. *Biochemistry* **53,** 5613–5618 (2014).
7. Van Goor, F. *et al.* Correction of the F508del-CFTR protein processing defect in vitro by the investigational drug VX-809. *Proc. Natl. Acad. Sci. U.S.A.* **108,** 18843–18848 (2011).
8. Van Goor, F. *et al.* Rescue of CF airway epithelial cell function in vitro by a CFTR potentiator, VX-770. *Proc. Natl. Acad. Sci. U.S.A.* **106,** 18825–18830 (2009).
9. Ikpa, P. T., Bijvelds, M. J. C. & de Jonge, H. R. Cystic fibrosis: Toward personalized therapies. *Int. J. Biochem. Cell Biol.* **52**: 192-200 (2014).
10. Rowe, S. M. & Verkman, A. S. Cystic fibrosis transmembrane regulator correctors and potentiators. *Cold Spring Harb Perspect Med* **3,** (2013).
11. Ramsey, B. W. *et al.* A CFTR potentiator in patients with cystic fibrosis and the G551D mutation. *N. Engl. J. Med.* **365,** 1663–1672 (2011).
12. De Boeck, K. *et al.* Efficacy and safety of ivacaftor in patients with cystic fibrosis and a non-G551D gating mutation. *J. Cyst. Fibros.* **13**: 674–80 (2014).
13. Accurso, F. J. *et al.* Effect of VX-770 in persons with cystic fibrosis and the G551D-CFTR mutation. *N. Engl. J. Med.* **363,** 1991–2003 (2010).
14. Davies, J. C. *et al.* Efficacy and safety of ivacaftor in patients aged 6 to 11 years with cystic fibrosis with a G551D mutation. *Am. J. Respir. Crit. Care Med.* **187,** 1219–1225 (2013).
15. Boyle, M. P. *et al.* A CFTR corrector (lumacaftor) and a CFTR potentiator (ivacaftor) for treatment of patients with cystic fibrosis who have a phe508del

CFTR mutation: a phase 2 randomised controlled trial. *Lancet Respir Med.* **2**: 527–38 (2014).

16. Wainwright, C. E. *et al.* Lumacaftor-Ivacaftor in Patients with Cystic Fibrosis Homozygous for Phe508del CFTR. *N. Engl. J. Med.* (2015). doi:10.1056/NEJMoa1409547

17. Char, J. E. *et al.* A little CFTR goes a long way: CFTR-dependent sweat secretion from G551D and R117H-5T cystic fibrosis subjects taking ivacaftor. *PLoS ONE* **9,** e88564 (2014).

18. French, P. J. *et al.* Genistein activates CFTR Cl- channels via a tyrosine kinase- and protein phosphatase-independent mechanism. *Am. J. Physiol.* **273,** C747–53 (1997).

19. Sears, C. L. *et al.* Genistein and tyrphostin 47 stimulate CFTR-mediated Cl- secretion in T84 cell monolayers. *Am. J. Physiol.* **269,** G874–82 (1995).

20. Melin, P. *et al.* The cystic fibrosis mutation G1349D within the signature motif LSHGH of NBD2 abolishes the activation of CFTR chloride channels by genistein. *Biochem. Pharmacol.* **67,** 2187–2196 (2004).

21. Wang, W., Bernard, K., Li, G. & Kirk, K. L. Curcumin opens cystic fibrosis transmembrane conductance regulator channels by a novel mechanism that requires neither ATP binding nor dimerization of the nucleotide-binding domains. *J. Biol. Chem.* **282,** 4533–4544 (2007).

22. Bernard, K., Wang, W., Narlawar, R., Schmidt, B. & Kirk, K. L. Curcumin cross-links cystic fibrosis transmembrane conductance regulator (CFTR) polypeptides and potentiates CFTR channel activity by distinct mechanisms. *J. Biol. Chem.* **284,** 30754–30765 (2009).

23. Eckford, P. D. W., Li, C., Ramjeesingh, M. & Bear, C. E. Cystic fibrosis transmembrane conductance regulator (CFTR) potentiator VX-770 (ivacaftor) opens the defective channel gate of mutant CFTR in a phosphorylation-dependent but ATP-independent manner. *J. Biol. Chem.* **287,** 36639–36649 (2012).

24. Jih, K.-Y. & Hwang, T.-C. Vx-770 potentiates CFTR function by promoting decoupling between the gating cycle and ATP hydrolysis cycle. *Proc. Natl. Acad. Sci. U.S.A.* **110,** 4404–4409 (2013).

25. Moran, O., Galietta, L. J. V. & Zegarra-Moran, O. Binding site of activators of the cystic fibrosis transmembrane conductance regulator in the nucleotide binding domains. *Cell. Mol. Life Sci.* **62,** 446–460 (2005).

26. Sohma, Y., Yu, Y.-C. & Hwang, T.-C. Curcumin and genistein: the combined effects on disease-associated CFTR mutants and their clinical implications. *Curr. Pharm. Des.* **19,** 3521–3528 (2013).

27. Yu, Y.-C. *et al.* Curcumin and genistein additively potentiate G551D-CFTR. *J. Cyst. Fibros.* **10,** 243–252 (2011).

28. Dekkers, J. F. *et al.* A functional CFTR assay using primary cystic fibrosis intestinal organoids. *Nat Med.* **19**: 939–45 (2013).

29. Dekkers, J. F., van der Ent, C. K. & Beekman, J. M. Novel opportunities for CFTR-targeting drug development using organoids. *Rare Dis* **1,** e27112 (2013).

30. Schwank, G. *et al.* Functional repair of CFTR by CRISPR/Cas9 in intestinal stem cell organoids of cystic fibrosis patients. *Cell Stem Cell* **13,** 653–658 (2013).

31. Roth, D. M. *et al.* Modulation of the maladaptive stress response to manage diseases of protein folding. *PLoS Biol.* **12,** e1001998 (2014).

32. Okiyoneda, T. *et al.* Mechanism-based corrector combination restores ΔF508-CFTR folding and function. *Nat. Chem. Biol.* **9,** 444–454 (2013).

33. Eckford, P. D. W. *et al.* VX-809 and related corrector compounds exhibit secondary activity stabilizing active F508del-CFTR after its partial rescue to the cell surface. *Chem. Biol.* **21,** 666–678 (2014).

34. Sato, T. *et al.* Paneth cells constitute the niche for Lgr5 stem cells in intestinal crypts. *Nature* **469,** 415–418 (2011).

35. Sato, T. *et al.* Long-term Expansion of Epithelial Organoids From Human Colon, Adenoma, Adenocarcinoma, and Barrett's Epithelium. *Gastroenterology.* **141**: 1762–72 (2011).

36. Jung, P. *et al.* Isolation and in vitro expansion of human colonic stem cells. *Nat Med* **17**: 1225–7 (2011)

37. Sato, T. & Clevers, H. Growing self-organizing mini-guts from a single intestinal stem cell: mechanism and applications. *Science* **340,** 1190–1194 (2013).

38. Lin, S. *et al.* Identification of synergistic combinations of F508del cystic fibrosis transmembrane conductance regulator (CFTR) modulators. *Assay Drug Dev Technol* **8,** 669–684 (2010).

39. Phuan, P.-W. *et al.* Synergy-based small-molecule screen using a human lung epithelial cell line

yields ΔF508-CFTR correctors that augment VX-809 maximal efficacy. *Mol. Pharmacol.* **86,** 42–51 (2014).

40. Boinot, C., Jollivet Souchet, M., Ferru-Clément, R. & Becq, F. Searching for combinations of small-molecule correctors to restore f508del-cystic fibrosis transmembrane conductance regulator function and processing. *J. Pharmacol. Exp. Ther.* **350,** 624–634 (2014).

41. Roth, E. K. *et al.* The K+ channel opener 1-EBIO potentiates residual function of mutant CFTR in rectal biopsies from cystic fibrosis patients. *PLoS ONE* **6,** e24445 (2011).

42. Clancy, J. P. *et al.* Multicenter intestinal current measurements in rectal biopsies from CF and non-CF subjects to monitor CFTR function. *PLoS ONE* **8,** e73905 (2013).

43. Beekman, J. M. *et al.* CFTR functional measurements in human models for diagnosis, prognosis and personalized therapy: Report on the pre-conference meeting to the 11th ECFS Basic Science Conference, Malta, 26-29 March 2014. *J. Cyst. Fibros.* **13,** 363–372 (2014).

44. Wang, F., Zeltwanger, S., Yang, I. C., Nairn, A. C. & Hwang, T. C. Actions of genistein on cystic fibrosis transmembrane conductance regulator channel gating. Evidence for two binding sites with opposite effects. *J. Gen. Physiol.* **111,** 477–490 (1998).

45. Lansdell, K. A., Cai, Z., Kidd, J. F. & Sheppard, D. N. Two mechanisms of genistein inhibition of cystic fibrosis transmembrane conductance regulator Cl- channels expressed in murine cell line. *J. Physiol. (Lond.)* **524 Pt 2,** 317–330 (2000).

46. Derand, R., Bulteau-Pignoux, L. & Becq, F. The cystic fibrosis mutation G551D alters the non-Michaelis-Menten behavior of the cystic fibrosis transmembrane conductance regulator (CFTR) channel and abolishes the inhibitory Genistein binding site. *J. Biol. Chem.* **277,** 35999–36004 (2002).

47. Ren, X.-Q. *et al.* Function of the ABC signature sequences in the human multidrug resistance protein 1. *Mol. Pharmacol.* **65,** 1536–1542 (2004).

48. Lin, W.-Y., Jih, K.-Y. & Hwang, T.-C. A single amino acid substitution in CFTR converts ATP to an inhibitory ligand. *J. Gen. Physiol.* **144,** 311–320 (2014).

49. Veit, G. *et al.* Some gating potentiators, including VX-770, diminish ΔF508-CFTR functional expression. *Sci Transl Med* **6,** 246ra97 (2014).

50. Cholon, D. M. *et al.* Potentiator ivacaftor abrogates pharmacological correction of ΔF508 CFTR in cystic fibrosis. *Sci Transl Med* **6,** 246ra96 (2014).

51. Clancy, J. P. *et al.* Results of a phase IIa study of VX-809, an investigational CFTR corrector compound, in subjects with cystic fibrosis homozygous for the F508del-CFTR mutation. *Thorax* **67**: 12–8 (2012).

52. Anand, P., Kunnumakkara, A. B., Newman, R. A. & Aggarwal, B. B. Bioavailability of curcumin: problems and promises. *Mol. Pharm.* **4,** 807–818 (2007).

53. Yang, Z., Kulkarni, K., Zhu, W. & Hu, M. Bioavailability and pharmacokinetics of genistein: mechanistic studies on its ADME. *Anticancer Agents Med Chem* **12,** 1264–1280 (2012).

54. Strimpakos, A. S. & Sharma, R. A. Curcumin: preventive and therapeutic properties in laboratory studies and clinical trials. *Antioxid. Redox Signal.* **10,** 511–545 (2008).

55. De Boeck, K. *et al.* New clinical diagnostic procedures for cystic fibrosis in Europe. *J. Cyst. Fibros.* **10 Suppl 2,** S53–66 (2011).

56. de Jonge, H. R. *et al.* Ex vivo CF diagnosis by intestinal current measurements (ICM) in small aperture, circulating Ussing chambers. *J. Cyst. Fibros.* **3 Suppl 2,** 159–163 (2004).

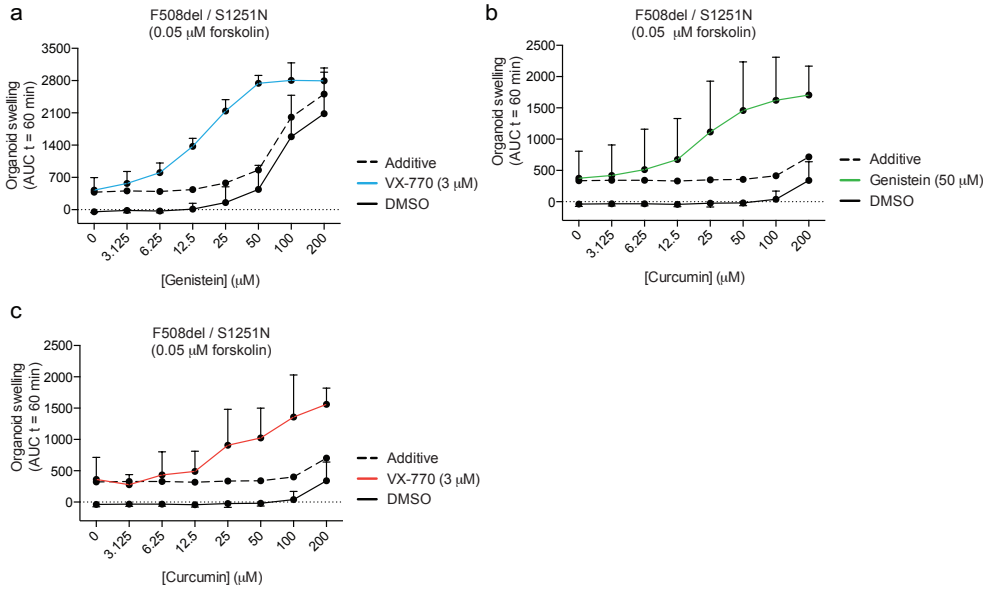

Supplementary figure S1. Dose-dependent potentiator synergy in F508del / S1251N organoids. (a-c) Forskolin-induced swelling of F508del / S1251N organoids stimulated with a dose range of genistein with or without VX-770 treatment (a), or stimulated with a dose range of curcumin with or without genistein (b) or VX-770 (c) at the indicated concentration of forskolin (this concentration was selected using Fig. 2f). The calculated additive responses of the single treatments are indicated as a dashed line. (a-c represent data averaged from 3 F508del / S1251N subjects. Each subject was measured at 2 to 5 independent culture time points in duplicate. Mean ± SD. The SD indicates the inter-subject variation).

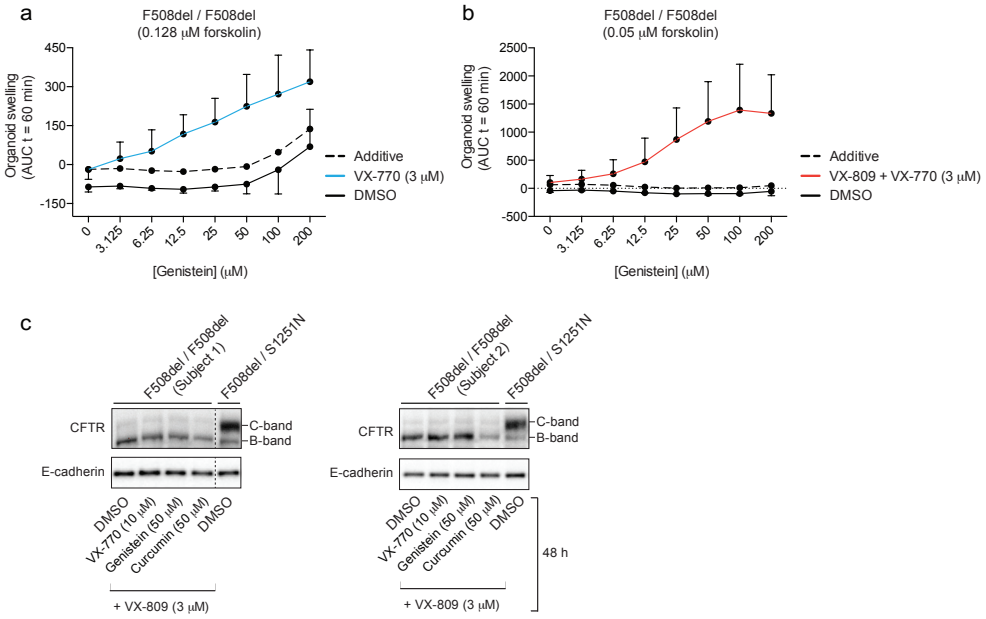

Supplementary figure S2. Dose-dependent potentiator synergy in F508del / F508del organoids. (a,b) Forskolin-induced swelling of F508del homozygous organoids stimulated with a dose range of genistein with or without VX-770 (a) or VX-770 + VX-809 (b) at the indicated concentrations of forskolin. The calculated additive responses of the single treatments are indicated as a dashed line. (a and b represent data averaged from 3 F508del / F508del subjects. Each subject was measured at 2 independent culture time points in duplicate. Mean ± SD. The SD indicates the inter-subject variation). (c) Expression of CFTR and E-cadherin in whole cell lysates of F508del / F508del (2 different donors) and F508del / S1251N organoids detected by Western blot upon treatments as indicated (48 h). Of note, higher compound concentrations were used as compared to Fig. 2j,k and 3i,j. Immature (B-band) and mature (C-band) CFTR is indicated.

Chapter 6

β_2-adrenergic receptor agonists activate CFTR in intestinal organoids and subjects with cystic fibrosis

Lodewijk A.W. Vijftigschild[1,2*], Gitte Berkers[1*], Johanna F. Dekkers[1,2#], Domenique D. Zomer-van Ommen[1,2#], E. Matthes[3], Evelien Kruisselbrink[1,2], Annelotte Vonk[1,2], C.E. Hensen[1], Sabine Heida-Michel[1], Margot Geerdink[1], Hettie M. Janssens[4], Eduard A. van de Graaf[5], Inez Bronsveld[5], Karin de Winter - de Groot[1], Christof J. Majoor[6], Harry G.M. Heijerman[7], John W. Hanrahan[3], Cornelis K. van der Ent[1], Jeffrey M. Beekman[1,2]

[1]Department of Pediatric Pulmonology, University Medical Centre, Utrecht, The Netherlands, [2]Laboratory of Translational Immunology, University Medical Centre, Utrecht, The Netherlands, [3]CF Translational Research Centre, Department of Physiology, McGill University, Montréal, Québec, Canada, [4]Department of Pediatric Pulmonology, Erasmus Medical Center/ Sophia Children's Hospital, Rotterdam, the Netherlands, [5]Department of Pulmonology, University Medical Centre, Utrecht, The Netherlands, [6]Department of Respiratory Medicine, Academic Medical Center, Amsterdam, The Netherlands, [7]Department of Pulmonology & Cystic Fibrosis, Haga Teaching Hospital, The Hague, The Netherlands.

* or #: These authors contributed equally

Submitted

ABSTRACT

Intestinal organoids from subjects with cystic fibrosis (CF) were used to study cystic fibrosis transmembrane conductance regulator (CFTR) function in response to G-protein coupled receptor (GPCR)-targeting drugs. We hypothesized that these drugs can enhance CFTR function in a genotype-specific manner, and that intestinal organoids are a suitable platform for identifying responsiveness to drugs that target GPCRs.

GPCR modulators were screened in primary wild-type and CF intestinal organoids using a recently developed CFTR-dependent rapid swelling assay. β_2-adrenergic receptor (β_2AR) stimulating agonists (β_2-agonists), which are known CFTR activators, were the most potent inducers of CFTR-dependent organoid swelling out of 61 compounds tested. β_2-agonist-induced organoid swelling correlated with the *CFTR* genotype, and could be induced in homozygous CFTR-F508del organoids after rescue of CFTR trafficking by small molecule correctors. The latter observation was confirmed in a CF airway cell line and in highly differentiated primary CF airway epithelial cells. The *in vivo* response to treatment with an oral or inhaled β_2-agonist (salbutamol) in CF patients with residual CFTR function was evaluated in an open label phase 2 pilot study. Ten subjects with at least one R117H or A455E mutation were included, and showed an improvement of the "baseline PD" of the Nasal Potential Difference measurement (+ 6,35mV; $p<0,05$) after treatment with oral salbutamol. Furthermore, plasma that was collected after treatment with oral salbutamol induced CFTR activation in intestinal organoids.

This proof-of-concept study indicates that existing drugs that stimulate CFTR function *in vivo* can be identified using *in vitro* drug screens in intestinal organoids. We found significant but limited CFTR-stimulating activity of salbutamol after oral treatment in subjects with residual CFTR function, which was accompanied with measurement of CFTR activity when plasma was used to stimulate organoids in vitro. Additional clinical trials with more subjects are needed to evaluate the dosage of salbutamol, the level of residual CFTR function and potential long-term effects on pulmonary function.

INTRODUCTION

The *cystic fibrosis transmembrane conductance regulator* (*CFTR*) gene encodes an apical anion channel, and is mutated in subjects with cystic fibrosis (CF)[1]. Subjects with CF have an altered composition of many mucosal surface fluids, leading to dysfunction of the gastro-intestinal and pulmonary systems as well as other organs. The most common mutation is a deletion of phenylalanine at position 508 (F508del) and is present in approximately 90% of subjects with CF, of which ~65% is F508del homozygote (http://www.genet.sickkids.on.ca). CF disease expression is highly variable between subjects due to the complex relations between *CFTR* genotype, modifier genes and environmental factors, which are unique for each individual[2-6].

Approximately 2000 *CFTR* mutations have been described, which are divided into different classes according to their impact on CFTR expression and function[7]. Briefly, class I mutations result in no functional protein (e.g. stop codons and frame shifts), class II mutations severely affect apical trafficking (e.g. F508del), class III mutations disrupt channel regulation or gating (e.g. G551D), class IV mutations reduce channel conductance (e.g. R117H), class V mutations lead to reduced apical expression of normally-functioning CFTR (e.g. A455E), and class VI mutations accelerate CFTR turnover at the plasma membrane. There are clear relations between *CFTR* genotype, residual function and CF disease severity, although at the level of the individual these relations remain not well understood[4].

Novel drugs are being developed to target mutation-specific CFTR defects. The potentiator VX-770 (ivacaftor / KALYDECO™) enhances the activity of apical CFTR and was shown to provide clinical benefit for patients with the G551D gating mutation[8-10]. Recently, this potentiator has been approved by the FDA and EMA for 9 other mutations (G178R, S549N, S549R, G551S, G1244E, S1251N, S1255P, G1349D and R117H; http://investors.vrtx.com/releasedetail.cfm?releaseid=889027). Pharmacological repair of CFTR-F508del has been proven more difficult, however encouraging phase III clinical trial results have been reported for CFTR-F508del homozygous subjects treated with a combination of KALYDECO™ and the corrector lumacaftor (VX-809)[11], which partly restores trafficking of CFTR-F508del to the apical membrane[12]. However, the therapeutic effects are still insufficient to fully restore CF and CFTR-related disease markers, indicating that more effective treatments are still required.

Individual CFTR function depends on endogenous signaling pathways that control its channel function. Various endogenous ligands have been identified which activate CFTR in a cyclic AMP (cAMP)-protein kinase A(PKA)-dependent fashion. Many of these ligands (e.g. vasointestinal peptide, prostaglandins and β-adrenergic stimuli) signal by binding to G-protein coupled receptors (GPCR) that releases cytosolic G-proteins that activate adenylyl cyclase (AC) to generate cAMP[13-15]. While it is known that tissue-specific activity of CFTR is regulated via diverse ligands, the exact composition, temporal regulation, and to what level these ligands control CFTR activity, is not clear.

We hypothesized that cAMP-dependent signaling is a rate-limiting step for CFTR activation *in vivo*, and that CF individuals might benefit from existing drugs that stimulate cAMP. Therefore, we screened a small chemical compound library of GPCR modulators for their ability to stimulate mutant CFTR activity in primary rectal organoids from healthy control and CF subjects. Rectal organoids grow from intestinal stem cells and self-organize into multi-cellular 3-D

structures consisting of a single epithelial layer, with the apical membrane facing a closed central lumen[16-18]. Addition of forskolin, which raises cAMP, stimulates CFTR-dependent fluid secretion into the organoid lumen and induces rapid swelling[19,20]. We here demonstrate that organoid-based measurements can be used to repurpose existing drugs for potential responsive CF subgroups, as well as to support clinical trial design and *in vivo* efficacy.

RESULTS

Screen for GPCR modulators of organoid swelling

To identify compounds that can activate CFTR, we assessed CFTR-dependent swelling of organoids in response to 61 GPCR-modulating compounds (Fig. 1)[20]. Like observed previously, forskolin induced rapid swelling of CFTR-WT organoids, and to a lesser extent of VX-809-treated homozygous CFTR-F508del organoids. As expected, DMSO did not induce swelling (Fig. 1a). Swelling was expressed as area under the curve for each specific condition as shown in Fig. 1a (Fig. 1b). Of the 61 compounds tested, dopamine, epinephrine, ritodrine and salbutamol dose-dependently induced swelling of CFTR-WT organoids, with highest potency for ritodrine and salbutamol and lowest potency for dopamine (Fig. 1c,d). Epinephrine, ritodrine and salbutamol are ligands for β_2AR adrenergic receptors and dopamine for the dopamine receptor. At the highest dose, the response to the 4 compounds was comparable to the forskolin-induced swelling (Fig. 1d). In VX-809-corrected F508del homozygous organoids, swelling was dose-dependently induced by epinephrine, salbutamol and ritodrine, but not by dopamine (Fig. 1c,e). The potency was highest for salbutamol, and lowest for ritodrine. High levels of salbutamol induced swelling to a similar extend as forskolin (Fig. 1d). In conclusion, β_2AR stimulation can potently activate CFTR-WT and drug-corrected CFTR-F508del in organoids.

β_2-adrenergic receptor agonists robustly induce organoid swelling

Next, we assessed β_2AR stimulation by short- and long-acting agonists in organoids with various *CFTR* mutations (Fig. 2). First, salbutamol- and ritodrine-induced swelling was confirmed in organoids derived from three individual F508del homozygous patients. As expected, robust organoid swelling was only observed after treatment with the CFTR-modulators VX-770 or VX-809, and was highest upon VX-770 and VX-809 combination treatment. In line with figure 1, ritodrine was somewhat less potent than salbutamol and forskolin, especially for VX-809 incubated organoids (Fig. 2a). Short-acting (ritodrine, terbutaline and salbutamol) and long-acting (formoterol, salmeterol and isoproterenol) β_2-agonists induced fluid secretion. Inhibition by CFTR-$_{inh}$172 or carvedilol supported CFTR or β-adrenergic receptor specificity, respectively (Fig. 2b). Forskolin and β_2AR-induced swelling differed between organoids with distinct *CFTR* genotypes: we observed no swelling in organoids expressing two *CFTR-null* alleles (*E60X, 4015delATTT*), some swelling in CFTR-A455E or VX-809-corrected homozygous CFTR-F508del organoids, and high swelling in CFTR-R117H expressing organoids (Fig. 2c). Dose-dependencies of β_2-agonist-induced swelling were independent of the *CFTR* genotype or VX-809-rescued F508del, but were highest for long-acting β_2-agonists and lowest for forskolin (Fig. 2d). Representative examples of agonist-induced swelling are indicated in Fig. 2e. Together, these data demonstrate that various β_2-agonists robustly induce CFTR function in a *CFTR* mutation-dependent manner.

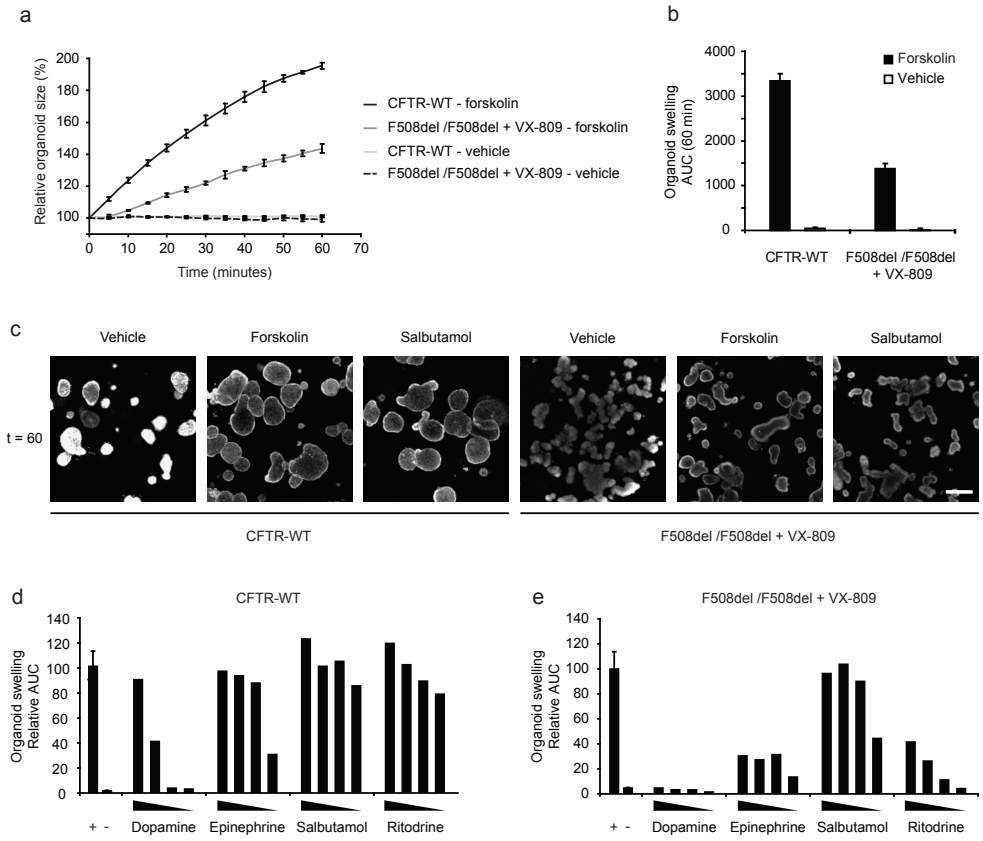

Figure 1. GPCR modulator-induced swelling of healthy control and CFTR-F508del organoids. (a) CFTR wild-type (WT) and F508del homozygous organoids were stimulated with forskolin (5 μM) or DMSO (vehicle, 0.05%) and the relative increase in size was monitored over 60 min. CFTR-F508del homozygous organoids were pre-incubated with VX-809 (3 μM) for 24 h. (b) Quantification of the area under the curve (AUC) of (a), baseline was set at 100%, t = 60 min. (c) Representative images of CFTR-WT and VX-809-corrected CFTR-F508del organoids after 60 minutes of stimulation with DMSO (vehicle), forskolin (5 μM) or salbutamol (10 μM). Scale bar is 200 μm. (d) Positive compounds for induction of fluid secretion using CFTR-WT intestinal organoids after screening a GPCR modulator library (61 compounds). Forskolin (+) and DMSO (-) were used as positive and negative control, respectively. GPCR modulators were tested at the following concentrations: 10 μM, 2 μM, 0.4 μM and 0.08 μM. Data are normalized to the forskolin response. (e) Same compounds as in (c), tested on VX-809 (3 μM)-treated F508del homozygous organoids.

Salbutamol-mediated CFTR activation in bronchial epithelial cells

To confirm that intestinal organoid responses can be relevant for airway epithelial cells, CFTR activation by the β_2-agonist salbutamol was studied in recombinant (CFBE) and primary human bronchial epithelial (HBE) cells. First, we studied CFTR-dependent iodide quenching rates in CFBE41o$^-$ cells that endogenously express CFTR-F508del and were previously transduced with *CFTR-F508del* (CFBE-F508del) or *CFTR-WT* (CFBE-CFTR-WT) cDNA[25]. To measure CFTR-dependent iodide-influx, the cells were stably transduced with a YFP-mKate sensor, as described previously[26]. Quenching of the YFP signal (indicating CFTR activity) was induced by both forskolin and salbutamol in VX-809+VX-770-treated CFTR-F508del and CFTR-WT CFBE cells (Fig. 3a). In addition,

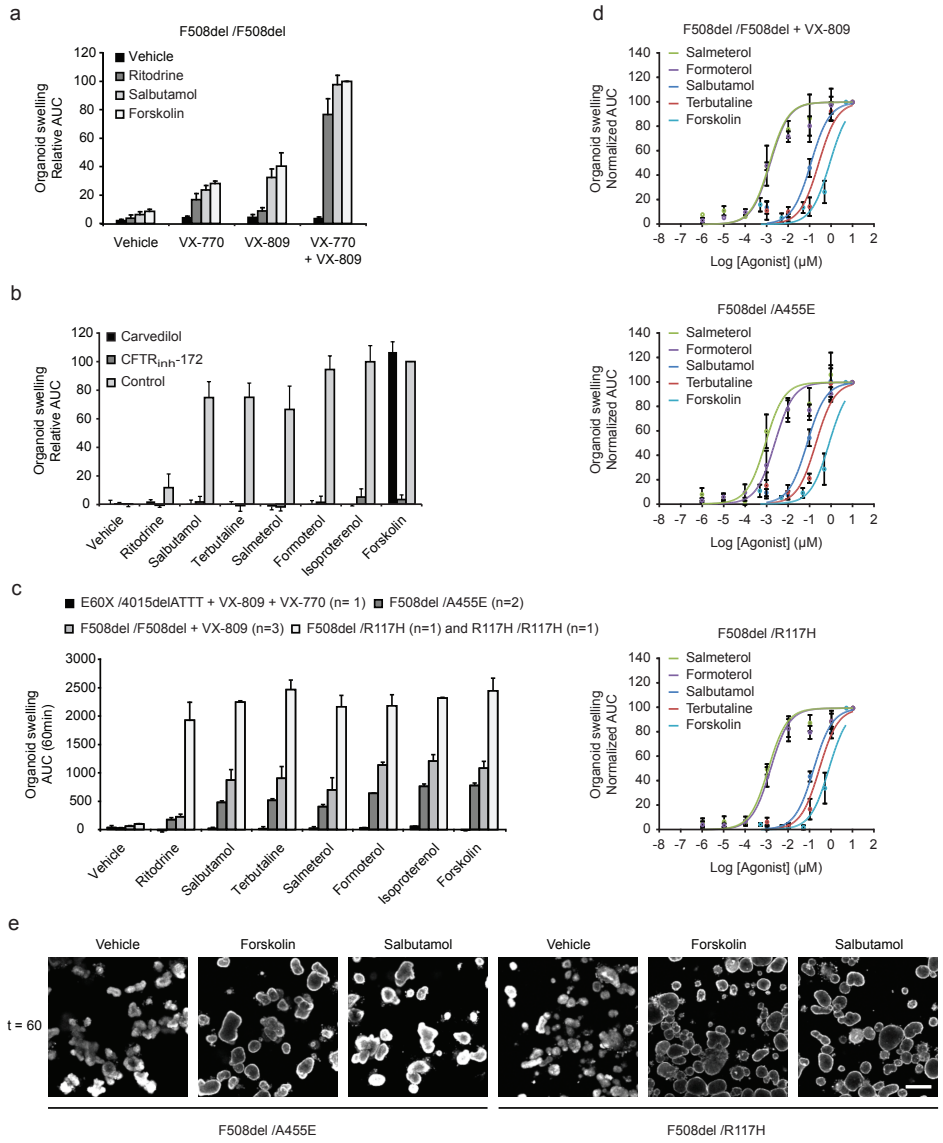

Figure 2. β_2-agonists induce CFTR activity. (a) CFTR-F508del homozygous organoids were stimulated with ritodrine (10 μM), salbutamol (10 μM) or forskolin (5 μM). VX-809 (3 μM) was incubated for 24 h prior to stimulation. VX-770 (1 μM) was added simultaneously with the stimulus. Data were normalized to the combined VX-770 + VX-809 + forskolin response, and organoids from three patients were measured at three independent time points in duplicate, data are presented as mean ± SEM. (b) VX-809 (3 μM) treated CFTR-F508del organoids were incubated with $CFTR_{inh}$-172 or carvedilol before stimulations. β_2-agonists were used at 10 μM and forskolin at 5 μM. All data were normalized to forskolin, and represent three independent measurements in duplicate (mean ± SEM). (c) Organoids derived from patients with different *CFTR* genotypes were stimulated with β_2-agonists (10 μM) or forskolin (5 μM). In parentheses, n = number of patients, measured at three independent time points in duplicate (mean ± SEM). (d) Dose-response curves for different β_2-agonists and forskolin in F508del / F508del, F508del / A455E and F508del / R117H organoids. All data are normalized to highest concentration of stimulus, and represent measurements at three independent time points (mean ± SEM). (e) Representative images of organoids expressing CFTR-F508del and either CFTR-A455E or CFTR-R117H after 60 minutes of stimulation with DMSO (vehicle), forskolin (5 μM) or salbutamol (10 μM). Scale bar is 200 μm.

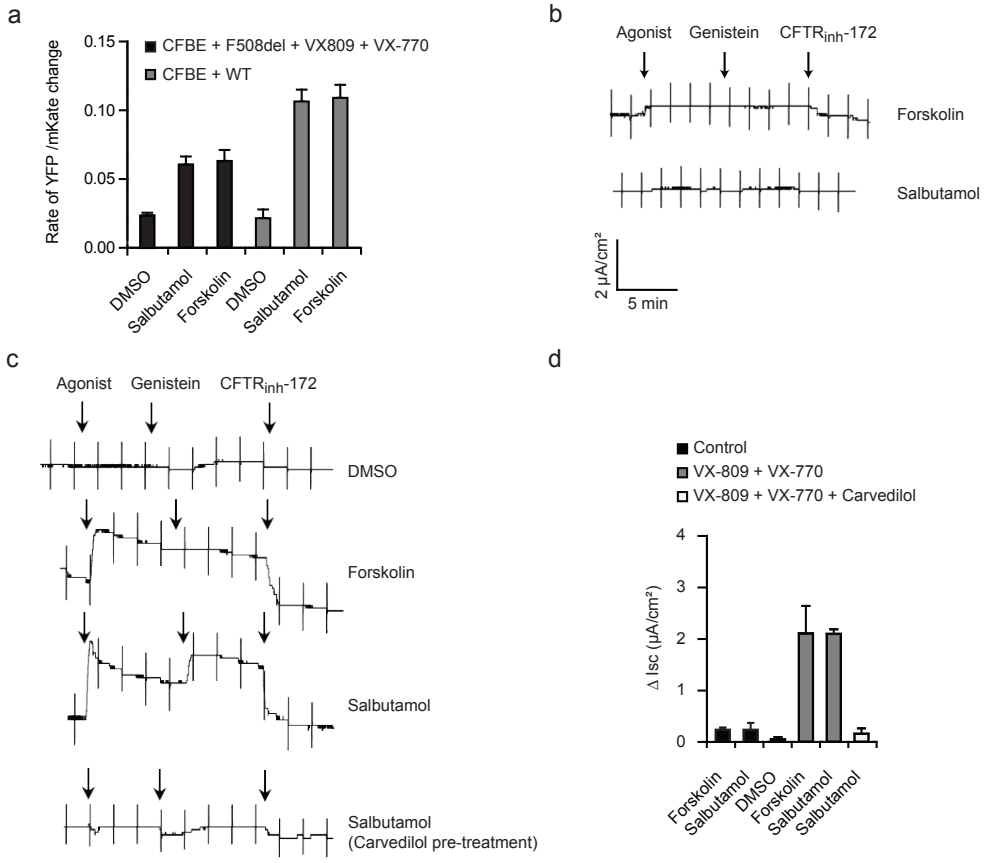

Figure 3. β_2-agonists-induced CFTR activation in bronchial epithelial cells. (a) CFTR activity in CFBE41o$^-$ cells overexpressing CFTR-F508del or CFTR-WT, and stably expressing YFP/mKate, using an YFP quenching assay. CFBE41o$^-$ cells were pre-incubated for 24 h with VX-809 (10 µM), and stimulated with forskolin (25 µM) and VX-770 (10 µM) or salbutamol (10 µM) and VX-770 (10 µM) for 20 min prior to addition of iodide. Data are representative of three independent experiments (mean ± SEM). (b) Highly differentiated primary CFTR-F508del bronchial epithelial cells cultured at the air-liquid interface were analyzed in Ussing chambers experiments. Representative traces of control, forskolin and salbutamol stimulated conditions. Constant current pulses used to monitor trans-epithelial resistance cause the vertical deflections. (c) Representative Ussing chamber tracings for VX-809 (1 µM) and VX-770 (100 nM) treated CF bronchial epithelial cells, stimulated with DMSO, forskolin (10 µM) or salbutamol (10 µM). Scaling is identical to (b). (d) Quantification of (b) and (c), data of three independent experiments is presented (mean ± SEM).

Ussing chamber experiments revealed that salbutamol and forskolin induced a CFTR-dependent Isc in F508del homozygous HBE cells treated with VX-809 and VX-770, but not in cultures without CFTR-repairing treatment (Fig. 3b-d). As expected, the response to forskolin and salbutamol was abolished by CFTR$_{inh}$-172 and the salbutamol-induced response was inhibited by carvedilol (Fig. 3c,d). To conclude, activation of modulator-repaired CFTR-F508del by β_2-agonists was recapitulated in respiratory cell lines and primary cultures.

Open-label phase 2a study with salbutamol in subjects with residual function

To demonstrate that drugs identified by screens in organoids can be used to modulate CFTR function *in vivo*, 10 CF patients were enrolled in a study to compare oral and inhaled salbutamol treatment. One patient was only treated with oral salbutamol due to increased asthma symptoms during the wash-out period. The baseline characteristics of the study population are shown in Table 1. Before and after 3 days of treatment with salbutamol, the sweat chloride concentration (SCC) was determined, nasal potential difference (NPD) measurements were performed and plasma was collected.

To analyze the systemic delivery of salbutamol by inhalation or oral application, we stimulated F508del/R117H organoids with plasma collected before and after either treatment. Plasma collected after oral salbutamol treatment significantly induced F508del/R117H organoid swelling compared to the plasma collected before treatment or after aerosol administration of salbutamol, indicating that plasma concentrations of salbutamol were highest after oral treatment (Fig. 4a). Spiking of pure salbutamol in pooled plasma of subjects before treatment indicated that circulating salbutamol levels were low, approximating 5 nM (Fig. 4b). Consistent with these findings, we observed that only oral treatment improved the median "Baseline PD" of the NPD measurements (+6.35 mV; $p<0.05$; Fig. 4c). There were no significant changes in other parameters (NPD in response to zero-chloride-solution or SCC; data not shown). The adverse events that were reported during treatment with salbutamol are shown in table 2. The data of this phase 2a study suggest that oral, but not inhaled, treatment of β_2-agonists can modestly increase residual CFTR function in nasal epithelium *in vivo*, which was supported by measurements of plasma-induced CFTR function in organoids *in vitro*.

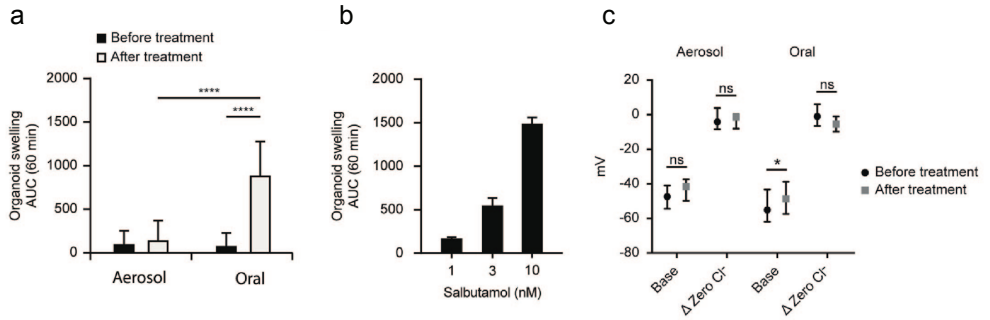

Figure 4. Plasma induced organoid swelling and NPD response to salbutamol. (a) CFTR-R117H/F508del organoids were stimulated with 40% plasma of each subject (n = 10) both before and after treatment via both aerosol and oral administration of salbutamol. Outcomes of subjects were pooled to compare aerosol with oral administration. Data presented as mean ± SD, paired t-tests were performed to determine the significance ($p<0.0001$). (b) To quantify the concentrations of salbutamol in the plasma samples of the subjects, organoids were stimulated with 40% plasma spiked with known concentrations of salbutamol. (c) Changes in NPD measurements, before and after salbutamol treatment. Data presented as median with IQR. The NPD values before and after treatment with salbutamol were compared using a Wilcoxon signed-rank test (* $p<0.05$; ns; not significant).

Characteristic	N(%), median (IQR)
Age in years	38,50 (31,50 – 49,00)
Male	4 (40%)
BMI	22,28 (20,38 – 28,16)
FEV1% predicted	
Median	62,00 (44,75 – 84,75)
Range	31 – 109
CFTR genotype	
F508del/A455E	9 (90%)
F508del/R117H	1 (10%)

Table 1. Baseline characteristics of subjects enrolled in the pilot study.

Adverse Event	During oral therapy (times reported)	During aerosol therapy (times reported)
Agitated feeling	1	
Palpitations	4	
Cough up more sputum	2	
Dry mouth	1	1
Tremor	5	1
Headache	1	1
Painful breathing		1

Table 2. Adverse events reported during treatment with salbutamol.

DISCUSSION

The purpose of this study was to generate proof-of-concept that organoid-based measurements can be used to identify known drugs that may modulate CFTR function *in vivo*. In this study, CFTR function measurements in organoids were applied to (i) identify potential drugs out of multiple candidates, (ii) identify subjects with potential responsive CFTR variants and (iii) to further develop a potential novel bioassay by stimulating organoids with plasma before and after treatment. As a whole, the study indicates that organoid-based measurement can help to design clinical studies for subjects with CF.

We selected β_2-agonists from 61 compounds that can modulate GPCR signalling, which are known activators of CFTR and anion transport. Surprisingly, the potency of β_2-agonists to stimulate CFTR function was equal or even better than forskolin that directly stimulates adenylyl cyclase downstream of GPCR, as observed in both primary intestinal and airway cells (Fig. 2 and 3)[13,29]. The formation of macromolecular complexes between β_2AR and CFTR may enable this efficient coupling of signals from β_2AR to CFTR [30]. The lack of CFTR activation by other compounds in this library most likely reflects the absence of these receptors or their inability to induce sufficient CFTR activating signal.

Measurement of CFTR activity *in vivo* by activators such as β_2-agonists requires a different approach as compared to direct CFTR-protein restoring drugs such as VX-770 and VX-809, and relies on the ability of exogenous β_2-agonists to activate CFTR beyond levels associated with endogenous CFTR activity. As such, NPD provided the most promising readout, as endogenous CFTR activity can be stimulated by exogenous addition of β_2-adrenergic stimuli by approximately 50% in healthy controls[31,32], indicating that CFTR activity in this tissue is rate-limited by endogenous cAMP signaling. Using standard NPD diagnostic measurements, we focussed on changes in baseline PD and reaction to zero chloride perfusion without the application of

additional β_2-adrenergic stimuli (Fig. 4c). Within-subject changes in "baseline PD" showed a significant response upon oral salbutamol treatment towards baseline PD of healthy controls (Fig. 4c). Baseline PD is predominated by ENaC-dependent Na^+ transport which is enhanced in CF, and modulated through direct CFTR-protein targeting drugs[32-34]. We could not demonstrate a significant improvement upon addition of zero chloride solution that measures basal Cl^- transport (Fig. 4c). Average values of subjects with pancreas sufficient and insufficient CF differ more for baseline PD as compared to the zero-chloride response, suggesting that baseline PD may be more sensitive to detect small increases of CFTR activity through effects on ENaC[35]. Alternatively, baseline PD may be modulated independently of CFTR by β_2-adrenergic regulation of Na^+ channels. Additional studies are required to further validate the effect of β_2-agonists therapy in CF, as this proof-of-concept study showed some impact of treatment on a typical CF characteristic of the nasal mucosa, but not a clear detection of Cl^- transport.

We also validated that plasma stimulation of organoids can provide insight into *in vivo* efficacy of treatment. Oral salbutamol treatment was associated with clinical effects in basal PD (Fig. 4c), and detectable CFTR-activating capacity in R117H organoids (Fig. 4a). Inhaled β_2-adrenergic stimuli are known to be associated with lower systemic delivery [36]. In line with these findings, we could not demonstrate CFTR activation of organoids using plasma of subjects treated with inhaled salbutamol (Fig. 4a) or clinical effects on CFTR-related biomarkers (Fig. 4c). For oral treatment, CFTR-activating levels in plasma were low (Fig. 4a), because they corresponded with pure salbutamol concentrations that only begin to stimulate organoids (Fig. 4b). Although plasma levels are not similar to tissue levels, it would suggest that higher dosaging may further improve efficacy of treatment, albeit that systemic side effects of this treatment may prevent such applications. The approach points out that organoid can identify CF drug candidates, and that plasma stimulation of organoids upon treatment can point out whether sufficient circulating levels of drugs can be reached for clinical effects.

As expected, β_2-agonists stimulate swelling of organoids in a *CFTR* mutation-dependent fashion, based on residual function conferred by the *CFTR* genotype or by CFTR-modulating drugs (Fig. 2). Most subjects included in the study were compound heterozygous for F508del/A455E, whose organoids demonstrate residual function between F508del/F508del and F508del/R117H. Because the VX-770+VX-809-corrected CFTR-F508del function in organoids is higher than the level of residual function associated with CFTR-A455E[20], β_2-agonists may have added value for F508del homozygous subjects (or other patients) treated with CFTR-repairing drugs. In this context, co-treatment with β_2-agonists may account for some of the heterogeneity between patients that is observed in the chemical response to CFTR modulator treatment [9, 35]. In addition, further stratification for *CFTR* genotypes with higher residual function may also enhance treatment effects with β_2-agonists.

In conclusion, CFTR function measurements in intestinal organoids were used to screen for CFTR activating drugs, and subjects with CFTR variants that respond to these drugs *in vitro* were selected for *in vivo* treatment. Oral treatment with salbutamol improved some CF characteristics of the nasal mucosa, but treatment efficacy was likely limited due to ineffective dosaging, as apparent from stimulation of organoids with plasma of subjects after treatment. The study supports that intestinal organoids are a valuable tool for selecting drugs, subjects and dosaging regimens for CF clinical trials.

METHODS

Human participants

This study was approved by the Ethics Committee of the University Medical Centre Utrecht and the Erasmus Medical Centre Rotterdam. Informed consent was obtained from all subjects. Organoids from healthy controls and cystic fibrosis subjects were generated from rectal biopsies after intestinal current measurements obtained (i) during standard cystic fibrosis care, (ii) for diagnostic purposes, or (iii) during voluntary participation in studies.

Materials

The GPCR compound library, VX-809 and VX-770 were purchased from SelleckChem (Houston, TX). Carvedilol, forskolin, salbutamol, salmeterol, terbutaline, epinephrine, ritodrine, DMSO (dimethyl sulfoxide), N-acetylcysteine, nicotinamide and S202190 were purchased from Sigma (St. Louis, MO). Formoterol was purchased from Santa Cruz Biotechnologies (Dallas, TX). $CFTR_{inh}$-172 was obtained from the CFF Therapeutics (Chicago, IL). Matrigel was purchased from BD (Franklin lakes, NJ). Calcein AM, supplements N-2 and B-27, Glutamax, advanced DMEM/F12, penicillin-streptomycin, HEPES and mEGF were purchased from Life Technologies (Bleiswijk, Netherlands). A83-01 was purchased from Tocris (Abingdon, UK). TOPflash and FOPflash were purchased from Millipore (Amsterdam, Netherlands).

Human organoid cultures

Rectal crypt isolation and organoid expansion was performed with some adaptations of previously described methods [20, 21]. Briefly, rectal biopsies were thoroughly washed with PBS and incubated in 10 mM EDTA for 90 minutes at 4°C. The crypts were collected by centrifugation and suspended in 50% Matrigel and 50% complete culture medium (advanced DMEM/F12 media supplemented with penicillin, streptomycin, HEPES, GlutaMax, nutrient supplements N-2 and B-27, N-acetylcysteine, nicotinamide, mEGF, A83-01, SB202190, 50% Wnt3a-, 20% Rspo-1- and 10% Noggin-conditioned media) that was allowed to solidify at 37°C for 20 minutes in 3 droplets of 10 µL per well of a 24 wells plate. Hereafter, the droplets were immersed in pre-warmed complete culture medium and cultures were expanded for at least three weeks before assaying CFTR function. Complete culture medium was refreshed three times per week and organoids were passaged weekly. Quality of the conditioned media was assessed by dot blots, ELISA and luciferase reporter constructs (TOPflash and FOPflash) [22, 23].

GPCR compound library

The GPCR small molecule compound library comprises 61 agonists and antagonists that target a wide range of GPCR families including adrenergic, dopamine, opioid, serotonin, histamine and acetylcholine receptors. A complete list of chemicals in the library is given in Supplementary Table 1.

CFTR function measurement in organoids

Organoids were reseeded one day before functional analysis in 96-well plates as described previously[20]. CFTR-F508del organoids were incubated with VX-809 (3 μM) for 24 h, as indicated in text and figure legends. Organoids were stained with Calcein-green AM (2.5 μM) 1 h prior the addition of compound, and each compound was tested at four different concentrations (10 μM, 2 μM, 0.4 μM and 0.08 μM). Forskolin (5 μM) and DMSO were used as positive and negative controls, respectively. Organoid swelling was monitored for 1 h using a ZEISS LSM 710 confocal microscope. The relative increase in surface area was calculated using Volocity (PerkinElmer, version 6.1.1). The area under the curve (AUC) was calculated as described previously [20]. Carvedilol (10 μM) was incubated for 30 min prior to stimulation and organoids were pretreated with $CFTR_{inh}$-172 (150 μM) for 4 h to inhibit CFTR-dependent responses.

Halide sensitive YFP quenching in CFBE41o- cells

$CFBE41o^-$ cell lines overexpressing CFTR-F508del or CFTR-WT were grown in alpha MEM containing 8% heat inactivated fetal calf serum, penicillin and streptomycin at 37°C in a humidified 5% CO_2 incubator as described [24,25]. CFBE41o- cells were transduced with the ratiometric halide-sensitive pHAGFE2-YFP (46L-148Q-152L)-mKATE sensor for measurement of CFTR activity as described previously [26]. Briefly, cells were incubated for 24 h with VX-809 (10 μM). After 20 min stimulation in a chloride-containing buffer, the cells were washed with iodide buffer and the decrease in fluorescence was monitored using a ZEISS LSM 710 microscope for 60 s. The rate of YFP/mKate quenching was calculated using GraphPad 6 (GraphPad Software Inc. La Jolla, CA).

Ussing chamber measurements in primary airway epithelial cells

Primary F508del/F508del human bronchial epithelial cells were cultured at the air-liquid interface for three weeks and pretreated for 24 h with VX-809 (1 μM). Control monolayers from the same patients were handled similarly but exposed to vehicle (0.1% DMSO) during the pretreatment period. For electrophysiological measurements, monolayers were mounted in Ussing chambers (EasyMount, Physiologic Instruments, San Diego, CA) and voltage-clamped using a VCCMC6 multichannel current-voltage clamp (Physiologic Instruments, Inc). The voltage clamp was connected to a PowerLab/8SP interface for data collection (ADInstruments Inc., Colorado Springs, CO) and analysis was performed using a PC as described previously [27]. Solutions were continuously gassed and stirred with 95% O_2/5% CO_2 and were maintained at 37 °C by circulating water bath. Ag/AgCl reference electrodes were used to measure transepithelial voltage and pass current. Pulses (1-mV amplitude, 1-s duration) were delivered every 90 s to monitor resistance. A basolateral-to-apical Cl^- gradient was imposed and amiloride (100 μM) was added on the apical side to inhibit ENaC current. Monolayers were exposed acutely to 10 μM forskolin or salbutamol or to the vehicle 0.1% DMSO. After Isc reached a plateau, a potentiator (either 50 μM genistein or 100 nM VX-770 as indicated) was added, followed by $CFTR_{inh}$-172 to confirm that the current responses were dependent on CFTR. Salbutamol was also assayed after pre-treatment with the antagonist carvedilol (10 μM) for 30 min as a further test of receptor specificity.

Pilot study with inhaled and oral salbutamol

In this open label phase II pilot study, 10 patients were randomly assigned to receive four times daily 200 µg salbutamol per inhalation or four times daily 4 mg salbutamol orally, for three consecutive days (NTR4513). After a wash-out period of at least 4 days, patients received the opposite treatment. We included patients aged ≥18-years-old with a CFTR-A455E or a CFTR-R117H mutation on at least one allele of whom rectal biopsies and organoid cultures showed residual CFTR function in previous studies [20]. Patients were excluded if they had an acute pulmonary exacerbation or an increased risk of side effects of salbutamol. The primary outcome measures were the sweat chloride concentration (SCC) and the "baseline PD" and "reaction to zero-chloride-solution" of the Nasal Potential Difference (NPD) measurement. The NPD-values before and after treatments with salbutamol were compared using a Wilcoxon signed-rank test. The NPD and SCC measurements were performed according to the most recent version of the standard operating procedure (SOP) of the European Cystic Fibrosis Society-Clinical Trials Network (ECFS-CTN). The secondary outcome measure was the CFTR-activating capacity of the patients' plasma in organoids. Therefore, whole blood was collected in sodium-heparin tubes before treatment and after the last dose of salbutamol, when the maximum concentration of salbutamol in the blood was expected (inhaled salbutamol after 30 minutes, oral salbutamol after 2 hours; www.fk.cvz.nl). Plasma was isolated as described previously [28].

Patient plasma-induced organoid swelling

Patient plasma was collected before and after treatment with salbutamol and incubated (40% plasma) with organoids derived from a CF patient with high residual function (R117H/F508del). Organoid swelling was monitored as described above. Reference values were generated by measurement of spiked salbutamol in 40% plasma.

Acknowledgements

We thank M.C.J. Olling-de Kok (Department of Pediatric Pulmonology, Wilhelmina Children's Hospital, University Medical Centre, Utrecht, The Netherlands), E.M. Nieuwhof-Stoppelenburg and E.C. van der Wiel (Department of Pediatric Pulmonology, Erasmus University Medical Centre / Sophia Children's Hospital, Rotterdam, the Netherlands), N. Adriaens (Department of Respiratory Medicine, Academic Medical Centre, Amsterdam, The Netherlands), and M. Smink (Department of Pulmonology & Cystic Fibrosis, Haga Teaching Hospital, The Hague, The Netherlands) for providing intestinal biopsies. This work was supported by grants of the Dutch Cystic Fibrosis Foundation (NCFS) as part of the HIT-CF program, the Wilhelmina Children's Hospital (WKZ) Foundation, and the Dutch health organization ZonMW, The Netherlands

Competing Financial Interest

J.M.B., C.K.E., J.F.D. are inventors on a patent application related to these findings.

REFERENCES

1. Riordan,J.R. CFTR function and prospects for therapy. *Annu. Rev. Biochem.* **77**, 701-726 (2008).
2. Weiler,C.A. & Drumm,M.L. Genetic influences on cystic fibrosis lung disease severity. *Front Pharmacol.* **4**, 40 (2013).
3. Vanscoy,L.L. *et al.* Heritability of lung disease severity in cystic fibrosis. *Am. J. Respir. Crit Care Med.* **175**, 1036-1043 (2007).
4. Sosnay,P.R. *et al.* Defining the disease liability of variants in the cystic fibrosis transmembrane conductance regulator gene. *Nat. Genet.* **45**, 1160-1167 (2013).
5. Kerem,E. *et al.* The relation between genotype and phenotype in cystic fibrosis--analysis of the most common mutation (delta F508). *N. Engl. J. Med.* **323**, 1517-1522 (1990).
6. Castellani,C. *et al.* Consensus on the use and interpretation of cystic fibrosis mutation analysis in clinical practice. *J. Cyst. Fibros.* **7**, 179-196 (2008).
7. Zielenski,J. Genotype and phenotype in cystic fibrosis. *Respiration.* **67**, 117-133 (2000).
8. Van Goor,F. *et al.* Rescue of CF airway epithelial cell function in vitro by a CFTR potentiator, VX-770. *Proc. Natl. Acad. Sci. U. S. A.* **106**, 18825-18830 (2009).
9. Ramsey,B.W. *et al.* A CFTR potentiator in patients with cystic fibrosis and the G551D mutation. *N. Engl. J. Med.* **365**, 1663-1672 (2011).
10. Accurso,F.J. *et al.* Effect of VX-770 in persons with cystic fibrosis and the G551D-CFTR mutation. *N. Engl. J. Med.* **363**, 1991-2003 (2010).
11. Wainwright,C.E. *et al.* Lumacaftor-Ivacaftor in Patients with Cystic Fibrosis Homozygous for Phe508del CFTR. *N. Engl. J. Med.*(2015).
12. Van Goor,F. *et al.* Correction of the F508del-CFTR protein processing defect in vitro by the investigational drug VX-809. *Proc. Natl. Acad. Sci. U. S. A.* **108**, 18843-18848 (2011).
13. Chan,H.C., Fong,S.K., So,S.C., Chung,Y.W., & Wong,P.Y. Stimulation of anion secretion by beta-adrenoceptors in the mouse endometrial epithelium. *J. Physiol* **501 (Pt 3)**, 517-525 (1997).
14. Smith,J.J. & Welsh,M.J. cAMP stimulates bicarbonate secretion across normal, but not cystic fibrosis airway epithelia. *J. Clin. Invest* **89**, 1148-1153 (1992).
15. Waldman,D.B., Gardner,J.D., Zfass,A.M., & Makhlouf,G.M. Effects of vasoactive intestinal peptide, secretin, and related peptides on rat colonic transport and adenylate cyclase activity. *Gastroenterology* **73**, 518-523 (1977).
16. Sato,T. *et al.* Single Lgr5 stem cells build crypt-villus structures in vitro without a mesenchymal niche. *Nature.* **459**, 262-265 (2009).
17. Sato,T. & Clevers,H. Growing self-organizing mini-guts from a single intestinal stem cell: mechanism and applications. *Science* **340**, 1190-1194 (2013).
18. Jung,P. *et al.* Isolation and in vitro expansion of human colonic stem cells. *Nat. Med.* **17**, 1225-1227 (2011).
19. Dekkers,J.F., van der Ent,C.K., & Beekman,J.M. Novel opportunities for CFTR-targeting drug development using organoids. *Rare diseases*1:e27112 (2013).
20. Dekkers,J.F. *et al.* A functional CFTR assay using primary cystic fibrosis intestinal organoids. *Nat. Med.* **19**, 939-945 (2013).
21. Sato,T. *et al.* Long-term expansion of epithelial organoids from human colon, adenoma, adenocarcinoma, and Barrett's epithelium. *Gastroenterology.* **141**, 1762-1772 (2011).
22. de Lau,W. *et al.* Lgr5 homologues associate with Wnt receptors and mediate R-spondin signalling. *Nature* **476**, 293-297 (2011).
23. Korinek,V. *et al.* Constitutive transcriptional activation by a beta-catenin-Tcf complex in APC-/- colon carcinoma. *Science* **275**, 1784-1787 (1997).
24. Swiatecka-Urban,A. *et al.* Pseudomonas aeruginosa inhibits endocytic recycling of CFTR in polarized human airway epithelial cells. *Am. J. Physiol Cell Physiol* **290**, C862-C872 (2006).
25. Bruscia,E. *et al.* Isolation of CF cell lines corrected at DeltaF508-CFTR locus by SFHR-mediated targeting. *Gene Ther.* **9**, 683-685 (2002).
26. Vijftigschild,L.A., van der Ent,C.K., & Beekman,J.M. A novel fluorescent sensor for measurement of CFTR function by flow cytometry. *Cytometry A* **83**, 576-584 (2013).
27. Robert,R. *et al.* Correction of the Delta phe508 cystic fibrosis transmembrane conductance regulator trafficking defect by the bioavailable compound glafenine. *Mol. Pharmacol.* **77**, 922-930 (2010).

28. Dekkers,R. *et al.* A bioassay using intestinal organoids to measure CFTR modulators in human plasma. *J. Cyst. Fibros.* **14**, 178-181 (2015).

29. Walker,L.C. *et al.* Relationship between airway ion transport and a mild pulmonary disease mutation in CFTR. *Am. J. Respir. Crit Care Med.* **155**, 1684-1689 (1997).

30. Naren,A.P. *et al.* A macromolecular complex of beta 2 adrenergic receptor, CFTR, and ezrin/radixin/moesin-binding phosphoprotein 50 is regulated by PKA. *Proc. Natl. Acad. Sci. U. S. A.* **100**, 342-346 (2003).

31. Knowles,M.R., Paradiso,A.M., & Boucher,R.C. In vivo nasal potential difference: techniques and protocols for assessing efficacy of gene transfer in cystic fibrosis. *Hum. Gene Ther.* **6**, 445-455 (1995).

32. Knowles,M.R. *et al.* Abnormal ion permeation through cystic fibrosis respiratory epithelium. *Science.* **221**, 1067-1070 (1983).

33. Knowles,M., Gatzy,J., & Boucher,R. Relative ion permeability of normal and cystic fibrosis nasal epithelium. *J. Clin. Invest.* **71**, 1410-1417 (1983).

34. Rowe,S.M. *et al.* Optimizing nasal potential difference analysis for CFTR modulator development: assessment of ivacaftor in CF subjects with the G551D-CFTR mutation. *PLoS. One.* **8**, e66955 (2013).

35. Wilschanski,M. *et al.* Mutations in the cystic fibrosis transmembrane regulator gene and in vivo transepithelial potentials. *Am. J. Respir. Crit Care Med.* **174**, 787-794 (2006).

36. Halfhide,C., Evans,H.J., & Couriel,J. Inhaled bronchodilators for cystic fibrosis. *Cochrane. Database. Syst. Rev.*CD003428 (2005).

Chapter 7

Predicting the clinical efficacy of CFTR-modulating drugs using rectal cystic fibrosis organoids

Johanna F. Dekkers[1,2], Gitte Berkers[1], Evelien Kruisselbrink[1,2], Annelotte Vonk[1,2], Hugo R. de Jonge[3], Hettie M. Janssens[4], Inez Bronsveld[5], Eduard A. van de Graaf[5], Edward E.S. Nieuwenhuis[6], Roderick H.J. Houwen[6], Frank P. Vleggaar[7], Johanna C. Escher[8], Yolanda B. de Rijke[9], Christof J. Majoor[10], Harry G.M. Heijerman[11], Karin M. de Winter – de Groot[1], Hans Clevers[12], Cornelis K. van der Ent[1], Jeffrey M. Beekman[1,2]

[1]Department of Pediatric Pulmonology, [2]Laboratory of Translational Immunology, Wilhelmina Children's Hospital, University Medical Centre, Utrecht, The Netherlands, [3]Department of Gastroenterology & Hepatology, Erasmus University Medical Centre, Rotterdam, The Netherlands, [4]Department of Pediatric Pulmonology, Erasmus University Medical Centre / Sophia Children's Hospital, Rotterdam, the Netherlands. [5]Department of Pulmonology, University Medical Centre, Utrecht, The Netherlands, [6]Department of Pediatric Gastroenterology, Wilhelmina Children's Hospital, University Medical Centre, Utrecht, The Netherlands, [7]Department of Gastroenterology & Hepatology, University Medical Centre, Utrecht, The Netherlands, [8]Department of Pediatric Gastroenterology, Erasmus University Medical Centre / Sophia Children's Hospital, Rotterdam, the Netherlands, [9]Department of Clinical Chemistry, Erasmus University Medical Centre / Sophia Children's Hospital, Rotterdam, the Netherlands, [10]Department of Respiratory Medicine, Academic Medical Centre, Amsterdam, The Netherlands, [11]Department of Pulmonology & Cystic Fibrosis, Haga Teaching Hospital, The Hague, The Netherlands, [12]Hubrecht Institute for Developmental Biology and Stem Cell Research, and University Medical Centre, Utrecht, The Netherlands

Submitted

ABSTRACT

The identification of subjects with cystic fibrosis (CF) that can benefit from CFTR-modifying drugs is time-consuming and costly, and especially challenging for individuals with rare, non-characterized *CFTR* mutations. Here, we studied individual CFTR function and response to the prototypical CFTR potentiator VX-770 (ivacaftor / KALYDECO™) and corrector VX-809 (lumacaftor) in rectal organoids derived from 70 individuals expressing wild-type *CFTR* or various class I-V *CFTR* mutations. We observed that CFTR residual function and response to therapy are continuous and not categorical variables that depend on both the *CFTR* mutations and the individual's genetic background. Most importantly, *in vitro* drug responses in organoids positively correlated with published outcome data of clinical trials with VX-809 and VX-770, allowing us to preclinically suggest potential *in vivo* responders with rare *CFTR* mutations. We demonstrated proof-of-principle by selecting 2 subjects expressing a non-characterized rare *CFTR* genotype (G1249R / F508del) who demonstrated clear clinical responses upon ivacaftor treatment. These data indicate that *in vitro* CFTR function measurements in rectal organoids can play an important role in identifying subjects that can benefit from CFTR-targeting treatment, independent of the *CFTR* genotype.

INTRODUCTION

Cystic fibrosis (CF) affects approximately 85.000 persons worldwide[1], and is caused by mutations in the *cystic fibrosis transmembrane conductance regulator* (*CFTR*) gene that encodes an epithelial anion channel[2-4]. Nearly 2000 *CFTR* mutations have been identified (www.genet.sickkids.on.ca), which associate with a wide spectrum of phenotypes (www.CFTR2.org), including CF or milder single-organ CFTR-related diseases (CFTR-RD)[5,6]. *CFTR* mutations are classified into six classes according to their effect on CFTR protein expression and function: (I) no synthesis, (II) impaired trafficking, (III) defective channel gating, (IV) altered conductance, (V) reduced levels of normally functioning CFTR, and (VI) impaired cell surface stability[1]. Although the clinical relevance and CFTR-based treatment options have been well characterized for common *CFTR* mutations expressed by large groups of subjects, it remains poorly understood at the level of the individual, as well as for the majority of rare 'orphan' mutations expressed by fewer subjects (www.CFTR2.org)[5].

Pharmacotherapy targeting the mutant CFTR protein has been successfully developed for a limited number of *CFTR* mutations. The CFTR potentiator VX-770 (ivacaftor / KALYDECO™) has been registered for G551D[7,8], S1251N and 7 others *CFTR* gating mutations[9], carried by ~5% of all people with CF. Recent studies indicated that VX-770 combined with the corrector VX-809 (lumacaftor; the combination is termed Okrambi™) has limited but significant effects on lung function in CF subjects homozygous for the most common *CFTR* mutation F508del (approximately 45-50% of subjects)[10,11]. Conventional clinical trials to identify drug-responsive subjects within the approximately 50% of subjects that express other mutations than *CFTR-F508del* are costly and time consuming, and hardly possible for individuals with extremely rare *CFTR* genotypes. Novel cost-effective methods at the level of the individual may help to rapidly extent available CFTR-targeting drugs to subjects with *CFTR* mutations that are currently not registered for treatments.

We here use primary intestinal organoid cultures[12-15] from 70 individuals expressing 27 different *CFTR* genotypes (overview in S1) to study residual and drug-modulated CFTR function, using (i) a recently established forskolin-induced swelling (FIS) assay[16,17] and (ii) a newly developed assay that measures the steady-state lumen area (SLA) of organoids independent of forskolin. Organoids are cultured from rectal biopsies that can be obtained independent of age and with only limited discomfort in most subjects[18,19]. Organoid cultures are genetically and phenotypically stable and can be stored, allowing long-term expansion and biobanking, and large subject-specific data sets (>1000 data points) can be established within several weeks[12]. Here, we correlated *in vitro* responses to VX-809 and VX-770 with published clinical trial data and provide proof-of-principle that subjects with extremely rare *CFTR* mutations can successfully be selected for VX-770 based on organoid measurements.

RESULTS

Residual CFTR function in intestinal organoids

We observed that intestinal organoids of healthy subjects were phenotypically different from organoids of subjects expressing 2 *CFTR* mutations (of which most have been established as CF-causing) during standard culture conditions, in the absence of an additional CFTR stimulus (Fig. 1a). We quantitated this phenotype (termed steady-state lumen area, SLA) by measurement of the

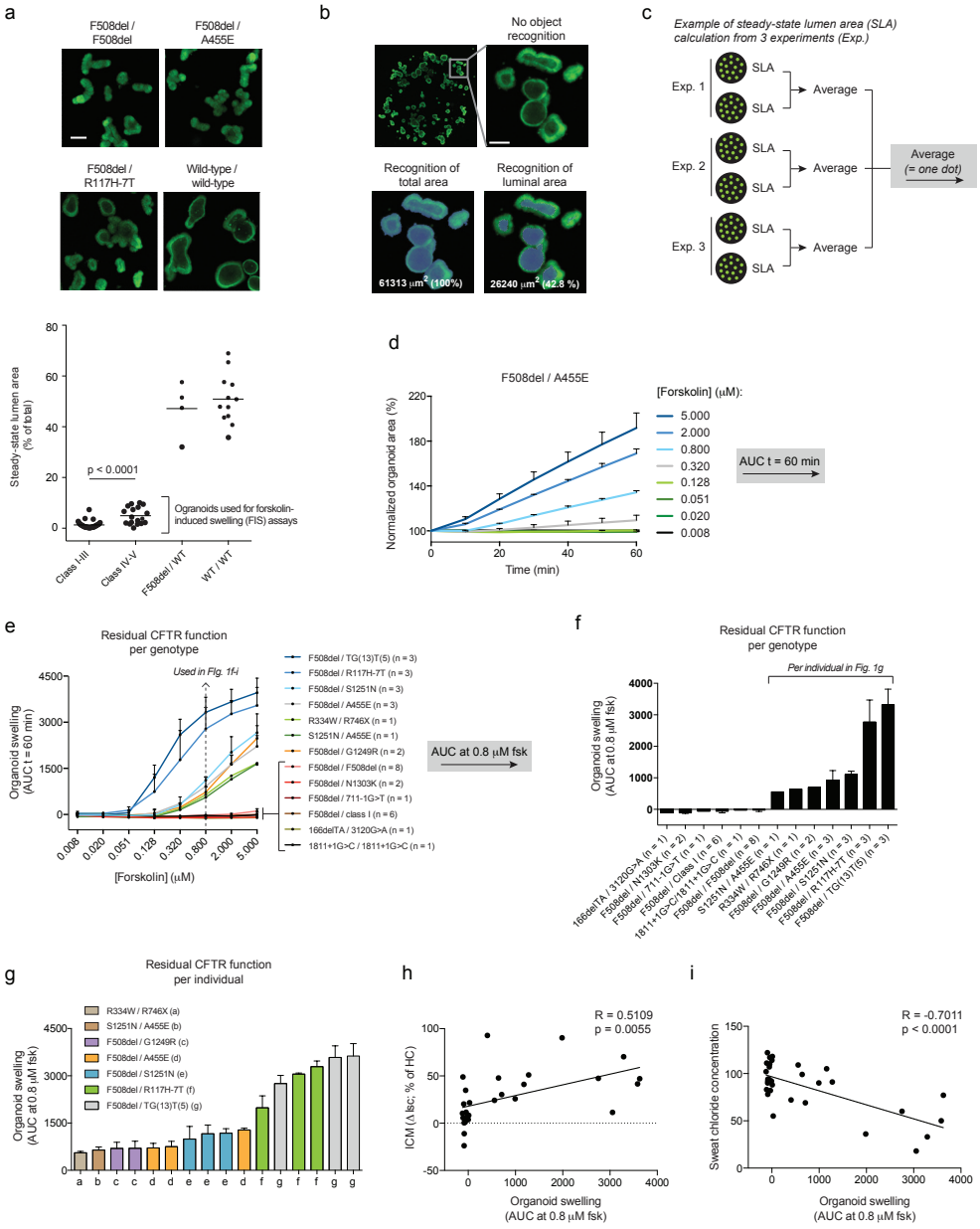

Figure 1. Residual CFTR function in intestinal organoids. (a) Representative confocal images of calcein-green-labeled organoids using standard culture conditions. Scale bar 100 µm. (b) Quantification method of the steady-state lumen area (SLA). Recognition of the total or luminal organoid area (xy plane) by Volocity imaging software is shown. The luminal surface areas (in µm and %) of the total organoid surface area (100%) are indicated in the bottom left corner. Scale bar 80 µm. (c) Quantification of the steady-state lumen area (SLA) of organoids derived from individuals expressing 2 *CFTR* class I-III (n = 35) or class IV-V (n = 18) mutations, or from wild-type (WT) / wild type (n = 12) or F508del / wild-type (n = 4) subjects. See S1 for the classification of different *CFTR* mutations and S2c for the responses per subject. Per subject, 2-5 independent experiments were performed. Data were generated over a period of 2 years. (d) Quantification of the surface area relative to t = 0 (normalized area) of F508del / A455E organoids at different forskolin (fsk) concentrations averaged from two independent wells. Mean ± SD. (e) Forskolin-induced

swelling of organoids with various mutations expressed as the absolute area under the curve (AUC) calculated from tracings comparable to d (baseline = 100%, t = 60 min). The data is similar to the DMSO-treated conditions presented in S5. Mean ± SD. (f,g) Organoid swelling at 0.8 μM forskolin from e per genotype (f; Mean ± SD) or per subject (g; mean ± SEM). (h,i) Pearson correlations of intestinal current measurements (ICM; h) or the sweat chloride concentration (i) versus the organoids swelling at 0.8 μM forskolin. ICM values were normalized to healthy control (HC) responses to correct for the use of two different protocols (see methods). Sweat chloride concentrations were obtained from the Dutch registry database. Each dot represents one individual. (Fig. e-g: data were generated during a period of 1 year, of which ~80% were generated during a period of 4 months using an identical medium batch; All figures: n = number of subjects; each subject was measured at 2-5 independent time points in duplicate; the class I mutations include G542X, R1162X (2x), W1282X, DELE2.3 and E60X)

lumen area as percentage of total organoid area (Fig. 1b and S2a). The SLA clearly discriminated between healthy control (cystic phenotype; SLAs of 35-70%; wild-type / wild-type = 51 ± 10; wild-type / F508del = 47 ± 11; Mean ± SD) and class I-V mutant *CFTR* organoids (non- to mild-cystic; SLA of 0-10%) at the individual level, and between class I-III and class IV-V mutant organoids at group level (class I-III = 1.3 ± 1.4 versus class IV – V = 5.0 ± 3.3; Mean ± SD; $p < 0.0001$) (Fig.1c). Importantly, high SLA (>20%) of organoids is negatively associated with the relative area increase of organoids upon forskolin stimulation (forskolin-induced swelling, FIS)[17], leading to underestimation of wild-type CFTR function (S2b). Organoids from CF subjects were all within an average SLA range that did not impact FIS (Fig. 1c). These data indicate that the SLA is a CFTR-dependent phenotype that discriminates between healthy control and CF, and that FIS rates cannot be directly compared between wild-type and mutant *CFTR* organoids.

We next assessed swelling of organoids derived from 35 individuals expressing various class I-V *CFTR* mutations using 8 different forskolin concentrations (0.008 – 5 μM) to maximize the dynamic range of the assay. As described previously[17], organoid swelling was calculated from 60 min time tracings of the surface area increase relative to t = 0 (Fig. 1d). We observed a forskolin dose-dependent increase in swelling that greatly varied between organoids with different *CFTR* genotypes (Fig. 1e). Swelling at 0.8 μM forskolin was presented to compare different genotypes (Fig. 1f) or individuals with clear detectable residual CFTR function (Fig. 1g), indicating the potential to discriminate between residual CFTR function of organoids expressing different or identical *CFTR* mutations (Fig. 1f,g). At 0.8 μM forskolin, correlations between residual CFTR function of organoids derived from individual donors correlated best with paired *ex vivo* intestinal current measurements[20-22] (Fig. 1h; $R = 0.5109$ and $p = 0.0055$) and the *in vivo* sweat chloride concentration[23,24] (Fig. 1i; $R = -0.7011$ and $p < 0.0001$). Swelling of several cultures expressing severe *CFTR* genotypes (but not of 1811+1G>C / 1811+1G>C and 166delTA / 3120G>A organoids) were most optimally detected at saturating forskolin levels (5 μM; S3) (Fig. 1e,f). The SLA assay less clearly discriminated between individuals with CF-causing mutations (S2c,d), indicating a dynamic range at higher CFTR activity for this assay when compared to FIS.

In conclusion, organoid-based swelling measurements can be used to semi-quantitate individual residual CFTR function over a large dynamic range, and significantly correlate with known *in vivo* and *ex vivo* CFTR-dependent biomarkers.

Pharmacological restoration of CFTR function in intestinal organoids

Next, we studied repair of forskolin-induced swelling by VX-809 and VX-770 in intestinal organoids (See S4 for a detailed analysis description). Organoids devoid of any residual function (1811+1G>C / 1811+1G>C and 166delTA / 3120G>A) did not show drug-induced swelling, indicating expression of non-responsive *CFTR* mutations. All other *CFTR* genotypes responded in a forskolin dose-dependent manner to the treatments, and genotype-specific profiles were observed (examples in Fig. 2a and all genotypes in S5). Single VX-809 treatment modestly increased FIS for most genotypes (most likely via the single *CFTR-F508del* allele), but a greater effect in A455E-expressing organoids suggested a trafficking defect for this mutant (Fig. 2a and S5a). Single VX-770 treatment greatly enhanced FIS of organoids that expressed known class III to V mutations on at least one allele, but only modestly enhanced FIS of organoids expressing class I / class II or class II / class II organoids. VX-809 and VX-770 together synergistically increased FIS of organoids homozygous for F508del or compound heterozygous for F508del and a class I mutation, N1303K, 711-1G>T or A455E, while VX-809 only had minor effect in addition to VX-770 for all other genotypes (Fig. 2a + S5a). These data indicated that the *CFTR* genotype determines the qualitative response to these CFTR-targeting drugs.

To identify an optimal approach for estimating the *in vivo* drug efficacy, we assessed correlations between currently available clinical trial data[9,25,26] (summarized in Fig. 2b) and drug-induced FIS of organoids, quantitated in different ways (per concentration of forskolin, or as AUC of a forskolin dose-range; see S5b for DMSO-corrected responses of the clinically assessed *CFTR* genotypes). We observed the strongest positive correlation between the response to therapy in organoids at 0.128 μM forskolin (Fig. 2c) and the *in vivo* absolute change in % predicted FEV_1 compared to placebo (Fig. 2d; $R = 0.8673$ and $p = 0.0252$).

Based on these data, we constructed a colored reference map to visualize the clinical potential of CFTR-targeting therapy for individuals with *CFTR* genotypes with unknown *in vivo* treatment efficacy (Fig. 2c). This reference map suggested high potential of VX-770 or VX-809 + VX-770 for the subjects expressing G1249R and TG(13)T(5), high potential of VX-809 + VX-770 for the A455E-expressing subjects, and modest potential of VX-809 + VX-770 for the individual compound heterozygous for R334W and R746X. Furthermore, CFTR-N1303K and -711-1G>T are likely non-responsive CFTR mutants, since average responses of F508del / N1303K and F508del / 711-1G>T organoids were not higher than of F508del / class I organoids (Fig. 2c).

Essentially similar data were generated when the forskolin-independent SLA assay was used to measure drug effects after 24 h incubation with VX-770, VX-809 or their combination (S6). This steady-state cumulative functional readout recapitulated relations between the *CFTR* genotype and drug response as observed by the FIS assay (S6a-c + Fig. 2c), but also allowed comparisons with wild-type CFTR function (S6b). However, a significant correlation between drug-induced SLA and clinical trial data was only observed when R117H-7T data was excluded (all genotypes, S6d, $R = 0.7234$ and $p = 0.1042$; no R117H-7T, S6e, $R = 0.968$ and $p=0.0068$), probably because the dynamic range of the SLA assay prevents correction for residual function associated with CFTR-R117H-7T without treatment.

FIS responses to VX-809 and VX-770 per individual were variable between donors with different or identical *CFTR* mutations, indicating that both the *CFTR* mutations and individual's genetic background modifies the response to therapy (Fig. 2e).

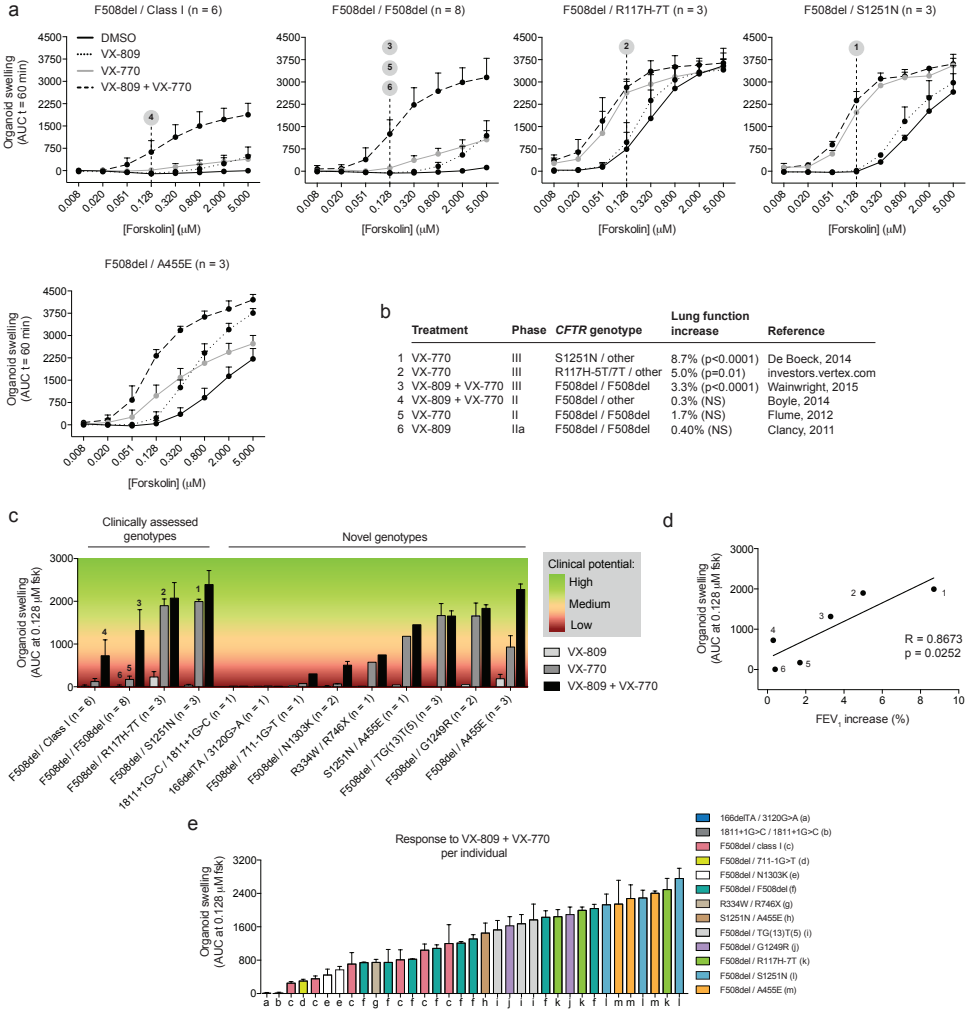

Figure 2. Pharmacological repair of CFTR function in intestinal organoids. (a) Organoids expressing various *CFTR* mutations were treated as indicated (vehicle: DMSO, VX-809 3 μM, VX-770 3 μM) and stimulated with forskolin (fsk). See S4 for detailed analysis. These figures are also presented in S5. The numbers associate with b-d. Mean ± SD. (b) Data overview of clinical trials with CFTR-repairing treatment in subjects expressing different mutated *CFTR* genotypes. The lung function increase represents the treatment difference versus placebo of absolute change in FEV_1 % predicted. Per trial, results of the most optimal treatment strategy are presented. Of the R117H trial, only data from CF subjects aged >18 were used, as subjects aged 6 to 18 had a different mean baseline FEV_1. The numbers associate with a,c,d. (c) The CFTR modulator-repaired swelling at 0.128 μM fsk (AUC t = 60 min) corrected for the DMSO condition presented per genotype. These DMSO-corrected responses were calculated from data presented in a and S5.. The numbers associate with a,b,d. The color profile was based on the clinical effectiveness of studies presented in b. Mean ± SD. (d) Pearson correlation of drug-repaired organoid swelling (results from c) versus the lung function increase (results from b). The numbers associate with a-c. (e) The VX-809 + VX-770-repaired swelling at 0.128 μM fsk (AUC t = 60 min) corrected for the DMSO condition presented per individual. These DMSO-corrected responses were calculated from data presented in a and S5. Mean ± SEM. (All figures: data were generated during a period of 1 year, of which ~80% were generated during a period of 4 months using an identical medium batch; n = number of subjects; each subject was measured at 2-5 independent time points in duplicate; the class I mutations include G542X, R1162X (2x), W1282X, DELE2.3 and E60X).

In conclusion, the FIS assay enables the characterization of drug-repaired CFTR function of organoids derived from individual donors expressing class I-V mutations. Response to therapy in this model at the *CFTR* genotype level associated with published outcome data of clinical trials with CFTR-restoring drugs, supporting the use of this model to select drug-responsive individuals with rare *CFTR* genotypes.

CFTR correction in F508del homozygous organoids

To further demonstrate that inter-subject variability can be consistently measured between donors independent of the CF-causing mutations, swelling of 10 F508del homozygous organoids in response to forskolin or various β_2-agonists was assessed using identical assay and culture conditions to minimize the impact of technical variation (Fig. 3 and S7). β_2-agonists activate CFTR via β_2-adrenergic receptor (β_2AR) stimulation that directly couples to adenylyl cyclase, the pharmacological target of forskolin[27]. We clearly observed subject-specific residual CFTR function and VX-809-induced responses, both upon forskolin and β_2-agonist stimulation (Fig. 3a-c; see S7a-c for responses of the individual experiments; see S7d for β_2-agonists other than salmeterol). Subject-to-subject variation was more prominent for β_2-agonists as compared to forskolin (Fig. 3c + S7d). We furthermore observed a strong correlation between the forskolin-induced non-corrected and VX-809-corrected CFTR function ($R = 0.8449$, $p = 0.0029$; Fig. 3d). Importantly, the subject-specific responses were maintained throughout culture for at least 6 months and after 4 months of liquid nitrogen storage (Fig. 3e-h and S7e-h).

Together, the data indicated that subject-specific residual CFTR function and response to therapy can be detected independent of culture and technical variability in organoids expressing identical CF-causing mutations, demonstrating the impact of the subject-specific genomic background as modulator of residual function and response to therapy.

***In vivo* evidence for organoid-based selection of clinical responders to VX-770**

Two subjects with the extremely rare *CFTR* genotype F508del / G1249R were selected for *in vivo* treatment with ivacaftor based on their high response to VX-770 in organoids (Fig. 4a, 2c and S5a). G1249R was described previously as a mutation in exon 20 of the *CFTR* gene[28], but functional impact has not been described. Upon treatment for 4 weeks with VX-770 (150 mg twice daily), the CFTR-dependent biomarkers nasal potential difference (NPD; Fig. 4b-d) and sweat chloride concentration (SCC; Fig. 4b,e) greatly improved or normalized. Both subjects showed improved pulmonary function as measured by a decrease of airway resistance (Fig. 4f), and an increase of FEV_1 in one subject. No clear response in FEV_1 was observed in the second subject, probably due to marked irreversible fibrosis of the lungs (Fig. 4g). Both patients improved in body weight and the respiratory domain of CF-related quality of life questionnaire (Fig. 4b). After a washout period of 4 weeks, parameters decreased or returned to pre-treatment levels (Fig. 4b,d-g).

In conclusion, these data indicate the potential that *in vitro* organoid assays can identify clinical responders to VX-770, even when they express extremely rare, uncharacterized *CFTR* mutations.

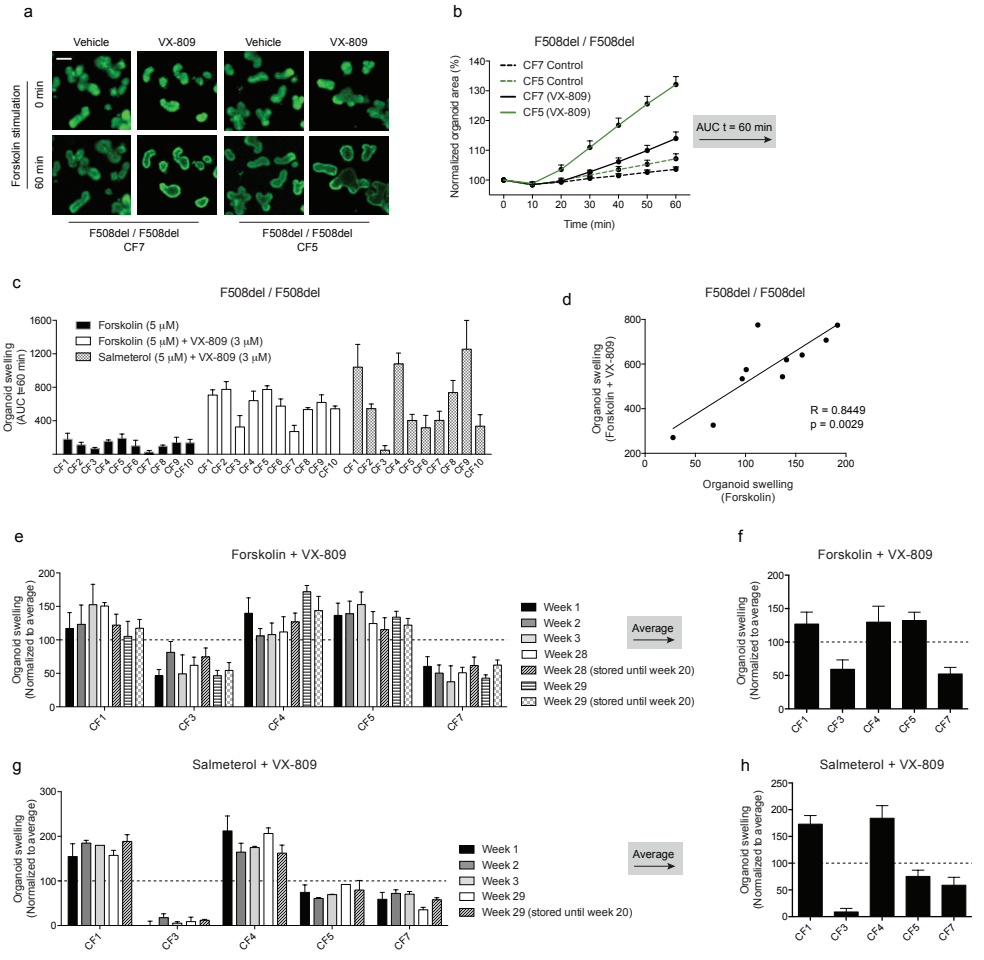

Figure 3. CFTR correction in F508del homozygous organoids. (a,b) Representative confocal images (a) or quantification of the surface area increase relative to t = 0 (averaged from 3 wells; b) of calcein-green-labeled and forskolin-induced organoids derived from two individual F508del homozygous subjects with or without 24 h treatment of VX-809 (3 μM). Scale bar 90 μm. Mean ± SD (c) Swelling of organoids induced by forskolin or pre-incubated for 24 h with VX-809 and induced by forskolin or salmeterol, expressed as the absolute area under the curve (AUC) calculated from time tracings comparable to b (baseline = 100%, t = 60 min). Per experiment, the cultures were assessed simultaneously to limit technical variation. Responses were averaged from 3 independent experiments performed with weekly interval (week 1 - 3; see S7a-c for the results of the independent experiments). (d) Pearson correlation of the non-corrected or VX-809(3 μM)-corrected forskolin-induced swelling from c. (e-h) After the first 3 experiments (week 1-3; similar to data in c), 2 low responding and 3 high forskolin-responding cultures were maintained in culture and measured again at week 28 and 29, or reinitiated after liquid nitrogen storage at week 20 and measured at week 28 and 29. Swelling of VX-809-corrected organoids in response to forskolin (e,f) or salmeterol (g,h) presented per experiment (e,g) or as average (f,h). The responses are normalized to the average response of the 5 cultures per experiment (100%). See S7e-h for the absolute responses. In e and g the SD represents the variation from 3 independent wells; in f and h the SD represents variation between different experiments. Mean ± SD.

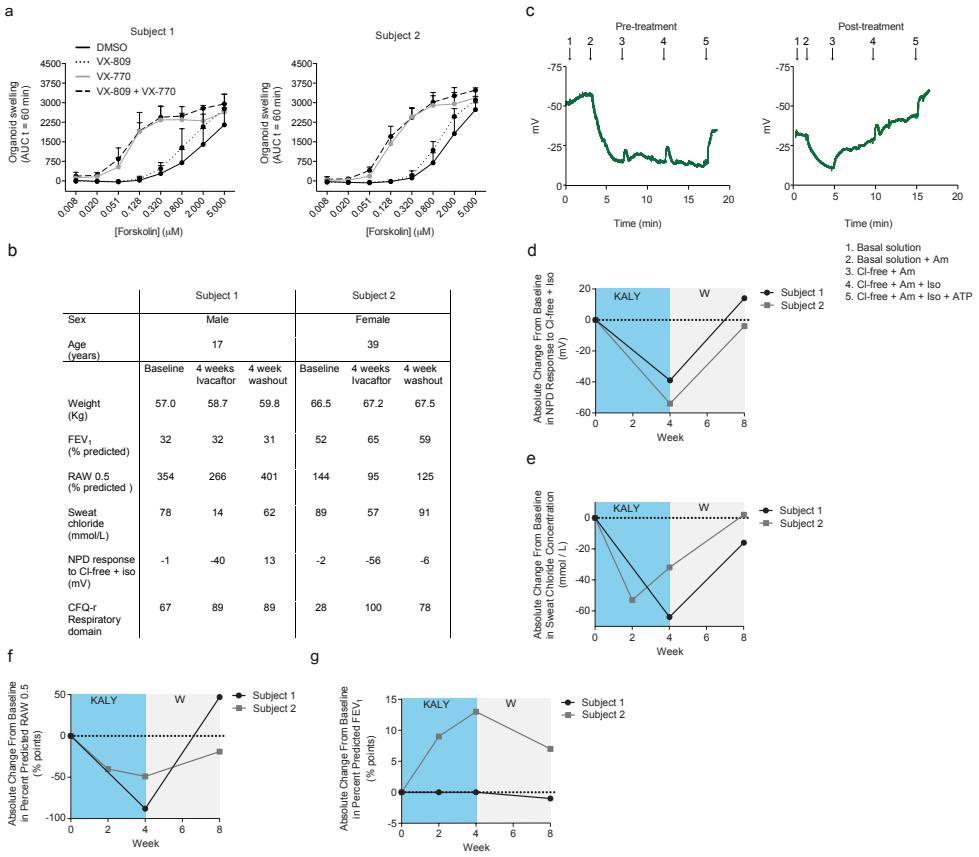

Figure 4. *In vivo* evidence for organoid-based selection of clinical responders to VX-770. (a) F508del / G1249R organoids derived from 2 different donors were treated as indicated (vehicle (DMSO), VX-809 3 µM, VX-770 3 µM) and stimulated with forskolin (fsk). The average response of both subjects is presented in S5s. Subjects were measured at 5 (subject 1) or 4 (subject 2) independent culture time points in duplicate. Mean ± SD. (b) Baseline characteristics and VX-770 (ivacaftor / KALYDECO™) treatment effects of the two CF subjects expressing F508del / G1249R. (c) Tracings of NPD measurements before and after treatment of subject 1, performed according to the standard operating procedure (SOP) of the European cystic fibrosis society clinical trial network (ECFS-CTN). Measurements in the right and left nostril were comparable. (d-g) Effects of 4 weeks of VX-770 (KALY) treatment and a 4-week washout (W) in NPD (d), sweat chloride concentration (e), RAW0.5 (f) and FEV_1 (g). (RAW0.5 = airway resistance at a flow rate of 0.5 liter/sec, FEV_1 = forced expiratory volume in one second, CFQ-r = Cystic Fibrosis Questionnaire-Revised, Cl-free = Chloride-free, Am = Amiloride, Iso = Isoproterenol).

DISCUSSION

This is the most comprehensive study of the subject-specific residual CFTR function and response to the current most promising CFTR-restoring drugs in primary CF cells. The data are most consistent with a model in which residual function and response to therapy are continuous variables (Fig. 1g + 2e), dependent on both the *CFTR* genotype and genetic background. It indicates that the current categorical classification model that associates residual function only to class IV and V mutations is not fully correct. We suggest that a refinement is needed that more accurately types residual

function and pharmacological responses for *CFTR* genotypes, and integrates the subject-specific genetic background to indicate the width of functional variability for a particular *CFTR* genotype.

Relations between the *CFTR* genotype and FIS (Fig. 1e,f) reflect published *CFTR* genotype-phenotype relations obtained from registries (www.CFTR2.org)[29-31]: (i) 1811+1G>C, 3120G>A, 117-1G>T, N1303K and F508del associate with severe CF and low FIS, (ii) A455E, S1251N and R334W associate with milder CF and moderate FIS, and (iii) R117H-7T and TG(13)T(5) associate with CFTR-related diseases and high FIS. Correlations between *in vitro* organoid responses and established CFTR-dependent biomarkers (SCC, ICM) at the individual level (Fig. 1h-i) further support the hypothesis that individual residual function measurements in organoids may have complementary value to current approaches as a diagnostic or prognostic marker for individual disease, but this needs to be established by directly linking clinical disease to FIS levels.

We clearly observed differences between residual function and response to therapy between organoids with identical CF-causing mutations that were stable over over extended culture periods with different media preparations (28 weeks) and independent of biobanking (Figs. 1g + 2e + 3 + S7). These data further extend previous observations demonstrating long-term genomic integrity and epigenetic profiles of organoid cultures[12,15,32,33], and point to the genetic background as modifier of CFTR function and fluid transport (Fig. 1g + 2e + 3). Variability in *CFTR* haplotypes, CFTR transcription, translation, or post-translational processing (folding efficacy, protein stability at the plasma membrane, or signaling efficacy between forskolin and CFTR) may impact swelling in a CFTR-dependent fashion. Non CFTR-dependent mechanisms that control differences in swelling may also play a role, such as aquaporin expression levels, contribution of basolateral ion transport or paracellular fluid transport.

Most importantly, our data suggest that CFTR function analysis in intestinal organoids can be used to select individuals for CFTR modulators (Fig. 2). The relatively high throughput associated with FIS assays allowed us to establish forskolin-dose ranges, and determine the optimal assay conditions for *in vivo* correlations. We found the highest positive correlation with clinical responses at a suboptimal forskolin dose (0.128 μM; Fig. 2d). At this concentration, the dynamic range of the assay upon drug treatment did not yet reach its maximal ceiling for organoids expressing alleles with high residual function (Fig 2a + S5b). Furthermore, average drug responses of F508del / F508del organoids were ~2-fold higher than F508del / Class I organoids (Fig. 2c), suggesting assay readout linearity at this level of CFTR function. While prediction of the VX-809 and VX-770 drug efficacy in intestinal organoids may be optimal at 0.128 μM, other forskolin dosages may be better for establishing correlations with other treatments or clinical parameters.

It is likely that differences between *in vivo* pharmacokinetics of VX-809 and VX-770 single or combination treatment (e.g. can two drugs optimally reach the target tissue as compared to single treatment) are not fully reflected *in vitro*. This may result in discrepancies between *in vitro* results and *in vivo* effects when different treatment modalities are compared. We therefore expect that combination treatment of subjects with A455E *in vivo* will yield better results than combination treatment of F508del homozygous subjects. However, whether comparable clinical effects will be achieved in VX-809/VX-770-treated subjects with A455E and VX-770-treated subjects with S1251N, as suggested by the *in vitro* responses (Fig. 2c), need to be established.

Proof-of-principle for pre-selecting subjects with uncharacterized *CFTR* mutations using organoid-based assays for currently available therapies was provided by successful VX-770 (ivacaftor / KALYDECO™) treatment of two F508del / G1249R subjects (Fig. 4). While both subjects

showed an improved airway resistance (Fig. 4f), the subject with a milder baseline pulmonary phenotype showed a clear improvement in FEV_1 (Fig. 4g). The lack of FEV_1 improvement in the other subject likely results from structural damage associated with severe pulmonary disease and fibrosis that prevents a response to therapy[34]. Clearly, positive treatment effects were achieved for all other parameters and CFTR-dependent biomarkers (Fig. 4b-e), confirming *in vivo* efficacy of VX-770. Further studies to define specificity and sensitivity of this preclinical readout are required, but for now it indicates that a relatively simple preclinical test can be sufficient to identify clinical responders to therapy.

Thus far, we have been able to recapitulate most observations of CFTR modulators such as VX-809 and VX-770 treatment in primary airway cell cultures [35,36]. In contrast with recent data showing that chronic VX-770 treatment diminished VX-809-restored CFTR-F508del expression and function[37,38], we observed that chronic VX-770 and VX-809 co-treatment was clearly better in restoring CFTR-F508del function than single treatments using the SLA assay (S6a-c) (data of 24h and 48h treatment are essentially similar, data not shown). The SLA assay is cumulative steady-state assay readout without a supra-physiological stimulus and cannot directly be compared with chronic VX-770 stimulation followed by an acute CFTR function measurement as described in the airway cells[37,38]. It might very well be that experimental conditions rather than intrinsic tissue differences explain these observations.

In conclusion, we here established relations between the *CFTR* genotype, residual CFTR function and response to therapy using a large collection of intestinal organoids. Importantly, we provide the first proof-of-principle that individual *in vitro* functional measurements can be used to preclinically select *in vivo* responders to CFTR-modulating drugs. Once organoids are established, these stem cell cultures can be biobanked for testing of future (combinations of) therapeutics in a cost-effective manner, without additional patient discomfort. Our data support that organoid-based CFTR function measurements can play an important role to study rare *CFTR* genotypes with unknown disease liability, and may help to identify subject that can benefit from CFTR modulator therapy independent of the *CFTR* genotype.

METHODS

Human material

The Ethics Committee of the University Medical Centre Utrecht and Erasmus Medical Centre Rotterdam approved this study and informed consent was obtained from all participating subjects. Organoids were generated from rectal biopsies after intestinal current measurements (ICM) obtained (i) during standard care, (ii) voluntary participation in studies or (iii) for diagnosis.

Crypt isolation and organoid culture from rectal suction biopsies

Methods were slightly adapted from protocols described previously[12,17]. In short, crypts were isolated, and seeded in 50% matrigel (growth factor reduced, phenol-free, BD bioscience) in 24-well plates (~10–30 crypts in three 10 µl matrigel droplets per well). Growth medium[17] was further supplemented with Primocin (1:500; Invivogen). Vancomycin and gentamycin (both from Sigma) were added during the first week of culture. The medium was refreshed every 2–3 days and organoids were passaged ~1:5 every 7–10 days.

The forskolin-induced swelling (FIS) assay

Methods were slightly adapted from protocols described previously[17]. In short, rectal organoids (passage 1–15) from a 7–10-day old culture were seeded in 96-well culture plates (Nunc) in 5 µl 50% matrigel containing 20–80 organoids, and immersed in 100 µl medium with or without 3 µM VX-809 (Selleck Chemicals LLC). One day after seeding, organoids were incubated for 30 min with 3 µM calcein-green (Invitrogen), stimulated with forskolin with or without 3 µM VX-770 (Selleck Chemicals LLC), and directly analyzed by confocal live cell microscopy (LSM710, Zeiss) (everything performed at 37 °C). The total organoid area (xy plane) increase relative to t = 0 of forskolin treatment was quantified using Volocity imaging software (Improvision). Occasionally, cell debris and unviable structures were manually excluded from image analysis based on criteria described in detail in a standard operating procedure (SOP). The area under the curve (AUC; t = 60 min; baseline = 100%) was calculated using Graphpad Prism.

The steady-state lumen area (SLA) assay

Organoids were seeded as described above, incubated for 24 h with DMSO, 3 µM VX-809, 3 µM VX-770 or their combination, labeled with calcein-green and analyzed by confocal microscopy (all at 37 °C). The total area (xy plane) of all organoids in a well was automatically quantified using Volocity, and the luminal area of all organoids of the same well was marked manually and calculated using Volocity in a blinded fashion. The steady-state lumen area was expressed as the luminal organoid surface area of the total organoid surface area in percentage (Fig. 1b). Occasionally, cell debris and non-viable structures were excluded similarly to the FIS assay.

Intestinal current measurement (ICM)

Initially, transepithelial chloride secretion in human rectal suction or forceps biopsies (four per subject) was measured by a slight adaptation of the procedure described in detail previously[21]. In short, the biopsies were collected in phosphate-buffered saline on ice and directly mounted in sliders (aperture 0.011 or 0.018 cm^2) adapted to micro-Ussing chambers (P2400; Physiological Instruments, San Diego, U.S.A.). After equilibration, the following compounds were added in a standardized order to the mucosal (M) or serosal (S) side of the tissue: amiloride (0.01 mM, M), to inhibit amiloride sensitive electrogenic Na+ absorption; carbachol (0.1 mM, S), to initiate the cholinergic Ca^{2+}- and protein kinase C-linked Cl^- secretion; DIDS (0.2 mM, M), to inhibit DIDS-sensitive, non-CFTR Cl^- channels such as the Ca^{2+}-dependent Cl^- channels; histamine (0.5 mM, S) to reactivate the Ca^{2+}-dependent Cl^- secretion secretory pathway and measure the DIDS-insensitive component of Ca2+-dependent Cl^- secretion; and forskolin/IBMX (0.01/0.1 mM M+S), to fully activate CFTR-mediated anion secretion. Crude short circuit current values (µA) were converted to µA cm^{-2} on the basis of the surface area of the aperture.

More recently, an amendment of this protocol was used (repetitive prewashing, followed by amiloride and forskolin additions prior to the Ca^{2+}-linked secretagogues)[39] which better accentuates forskolin-induced anion current responses by reducing basal cAMP levels. To account for the higher forskolin responses measured in the latter protocol, short circuit responses in CF biopsies were normalized to the average responses observed in healthy controls using identical protocols (32.7 ± 23.2 µA cm^{-2}; N = 9, n = 29, old protocol; 56.0 ± 28.6 µA cm^{-2}; N = 16, n = 60, new protocol) and expressed as % of these healthy control values (Fig. 1h).

Sweat Chloride Concentration (SCC) and Nasal Potential Difference NPD measurements

Both SCC and NPD measurements were performed according to the most recent version of the standard operating procedure (SOP) of the European Cystic Fibrosis Society Clinical Trials Network (ECFS-CTN).

Acknowledgements

We thank S. Heida-Michel, M. Geerdink, M.C.J. Olling-de Kok (Department of Pediatric Pulmonology, Wilhelmina Children's Hospital, University Medical Centre, Utrecht, The Netherlands), E.M. Nieuwhof-Stoppelenburg and E.C. van der Wiel (Department of Pediatric Pulmonology, Erasmus University Medical Centre / Sophia Children's Hospital, Rotterdam, the Netherlands), J. Hulst, F.T.M. Kokke and B.A.E. de Koning (Department Pediatric Gastroenterology, Erasmus University Medical Centre / Sophia Children's Hospital, Rotterdam, the Netherlands), the technicians of the Clinical Chemistry department (Erasmus University Medical Centre / Sophia Children's Hospital, Rotterdam, the Netherlands), N. Adriaens (Department of Respiratory Medicine, Academic Medical Centre, Amsterdam, The Netherlands), and M. Smink (Department of Pulmonology & Cystic Fibrosis, Haga Teaching Hospital, The Hague, The Netherlands) for providing intestinal biopsies and A.G.M Bot, M. Rampersad (Department Clinical Chemistry department, Erasmus University Medical Centre / Sophia Children's Hospital, Rotterdam, the Netherlands) and M.J.C. Bijvelds (Department of Gastroenterology & Hepatology, Erasmus University Medical Centre / Sophia Children's Hospital, Rotterdam, the Netherlands) for performing intestinal current measurements (ICM). This work was supported by grants of the Dutch Cystic Fibrosis Foundation (NCFS) as part of the HIT-CF program, the Wilhelmina Children's Hospital (WKZ) Foundation, and the Dutch Health Organization ZonMw, the Netherlands

Competing Financial Interest

J.M.B., C.K.E., J.F.D. are inventors on a patent application related to these findings. H.C. is an inventor on several patents related to these findings.

REFERENCES

1. Bell, S. C., De Boeck, K. & Amaral, M. D. New pharmacological approaches for cystic fibrosis: Promises, progress, pitfalls. *Pharmacol. Ther.* **S0163-7258**: 00122–3 (2014).
2. Riordan, J. R. *et al.* Identification of the cystic fibrosis gene: cloning and characterization of complementary DNA. *Science* **245,** 1066–1073 (1989).
3. Rommens, J. M. *et al.* Identification of the cystic fibrosis gene: chromosome walking and jumping. *Science* **245,** 1059–1065 (1989).
4. Kerem, B. *et al.* Identification of the cystic fibrosis gene: genetic analysis. *Science* **245,** 1073–1080 (1989).
5. Sosnay, P. R. *et al.* Defining the disease liability of variants in the cystic fibrosis transmembrane conductance regulator gene. *Nat. Genet.* **45,** 1160–1167 (2013).
6. Cutting, G. R. Cystic fibrosis genetics: from molecular understanding to clinical application. *Nat. Rev. Genet.* **16,** 45–56 (2015).
7. Ramsey, B. W. *et al.* A CFTR potentiator in patients with cystic fibrosis and the G551D mutation. *N. Engl. J. Med.* **365,** 1663–1672 (2011).
8. Accurso, F. J. *et al.* Effect of VX-770 in persons with cystic fibrosis and the G551D-CFTR mutation. *N. Engl. J. Med.* **363,** 1991–2003 (2010).

9. De Boeck, K. *et al.* Efficacy and safety of ivacaftor in patients with cystic fibrosis and a non-G551D gating mutation. *J. Cyst. Fibros.* **13**: 674–80 (2014).

10. Boyle, M. P. *et al.* A CFTR corrector (lumacaftor) and a CFTR potentiator (ivacaftor) for treatment of patients with cystic fibrosis who have a phe508del CFTR mutation: a phase 2 randomised controlled trial. *Lancet Respir Med* **2**, 527-38 (2014).

11. Wainwright, C. E. *et al.* Lumacaftor-Ivacaftor in Patients with Cystic Fibrosis Homozygous for Phe508del CFTR. *N. Engl. J. Med.* (2015). doi:10.1056/NEJMoa1409547

12. Sato, T. *et al.* Long-term Expansion of Epithelial Organoids From Human Colon, Adenoma, Adenocarcinoma, and Barrett's Epithelium. *Gastroenterology* **141**: 1762–72 (2011).

13. Sato, T. & Clevers, H. Growing self-organizing mini-guts from a single intestinal stem cell: mechanism and applications. *Science* **340,** 1190–1194 (2013).

14. Jung, P. *et al.* Isolation and in vitro expansion of human colonic stem cells. *Nat Med* **17**: 1225–7 (2011).

15. Sato, T. *et al.* Single Lgr5 stem cells build crypt-villus structures in vitro without a mesenchymal niche. *Nature* **459,** 262–265 (2009).

16. Dekkers, J. F., van der Ent, C. K. & Beekman, J. M. Novel opportunities for CFTR-targeting drug development using organoids. *Rare Dis* **1,** e27112 (2013).

17. Dekkers, J. F. *et al.* A functional CFTR assay using primary cystic fibrosis intestinal organoids. *Nat Med* **19**: 939–45 (2013).

18. Derichs, N. *et al.* Intestinal current measurement for diagnostic classification of patients with questionable cystic fibrosis: validation and reference data. *Thorax* **65,** 594–599 (2010).

19. Sousa, M. *et al.* Measurements of CFTR-mediated Cl- secretion in human rectal biopsies constitute a robust biomarker for Cystic Fibrosis diagnosis and prognosis. *PLoS ONE* **7,** e47708 (2012).

20. Mall, M., Hirtz, S., Gonska, T. & Kunzelmann, K. Assessment of CFTR function in rectal biopsies for the diagnosis of cystic fibrosis. *J. Cyst. Fibros.* **3 Suppl 2,** 165–169 (2004).

21. de Jonge, H. R. *et al.* Ex vivo CF diagnosis by intestinal current measurements (ICM) in small aperture, circulating Ussing chambers. *J. Cyst. Fibros.* **3 Suppl 2,** 159–163 (2004).

22. Li, H., Sheppard, D. N. & Hug, M. J. Transepithelial electrical measurements with the Ussing chamber. *J. Cyst. Fibros.* **3 Suppl 2,** 123–126 (2004).

23. GIBSON, L. E. & COOKE, R. E. A test for concentration of electrolytes in sweat in cystic fibrosis of the pancreas utilizing pilocarpine by iontophoresis. *Pediatrics* **23,** 545–549 (1959).

24. Quinton, P. M. Chloride impermeability in cystic fibrosis. *Nature* **301,** 421–422 (1983).

25. Flume, P. A. *et al.* Ivacaftor in subjects with cystic fibrosis who are homozygous for the F508del-CFTR mutation. *Chest* **142,** 718–724 (2012).

26. Clancy, J. P. *et al.* Results of a phase IIa study of VX-809, an investigational CFTR corrector compound, in subjects with cystic fibrosis homozygous for the F508del-CFTR mutation. *Thorax* **67**, 12-8 (2011).

27. Uezono, Y. *et al.* Receptors that couple to 2 classes of G proteins increase cAMP and activate CFTR expressed in Xenopus oocytes. *Recept. Channels* **1,** 233–241 (1993).

28. Dijkstra, D. J., Scheffer, H. & Buys, C. H. A novel mutation (G1249R) in exon 20 of the CFTR gene. *Hum. Mutat.* **4,** 161–162 (1994).

29. Gan, K. H. *et al.* A cystic fibrosis mutation associated with mild lung disease. *N. Engl. J. Med.* **333,** 95–99 (1995).

30. McKone, E. F., Emerson, S. S., Edwards, K. L. & Aitken, M. L. Effect of genotype on phenotype and mortality in cystic fibrosis: a retrospective cohort study. *Lancet* **361,** 1671–1676 (2003).

31. Antiñolo, G. *et al.* Genotype-phenotype relationship in 12 patients carrying cystic fibrosis mutation R334W. *J. Med. Genet.* **34,** 89–91 (1997).

32. Middendorp, S. *et al.* Adult stem cells in the small intestine are intrinsically programmed with their location-specific function. *Stem Cells* **32,** 1083–1091 (2014).

33. Huch, M. *et al.* Long-term culture of genome-stable bipotent stem cells from adult human liver. *Cell* **160,** 299–312 (2015).

34. Wood, M. E. *et al.* Ivacaftor in severe cystic fibrosis lung disease and a G551D mutation. *Respirol Case Rep* **1,** 52–54 (2013).

35. Van Goor, F., Yu, H., Burton, B. & Hoffman, B. J. Effect of ivacaftor on CFTR forms with missense mutations associated with defects in protein processing or function. *J. Cyst. Fibros.* **13,** 29–36 (2014).

36. Yu, H. *et al.* Ivacaftor potentiation of multiple CFTR channels with gating mutations. *J. Cyst. Fibros.* **11,** 237–245 (2012).

37. Cholon, D. M. *et al.* Potentiator ivacaftor abrogates pharmacological correction of ΔF508 CFTR in cystic fibrosis. *Sci Transl Med* **6,** 246ra96 (2014).

38. Veit, G. *et al.* Some gating potentiators, including VX-770, diminish ΔF508-CFTR functional expression. *Sci Transl Med* **6,** 246ra97 (2014).

39. De Boeck, K. *et al.* New clinical diagnostic procedures for cystic fibrosis in Europe. *J. Cyst. Fibros.* **10 Suppl 2,** S53–66 (2011).

SUPPLEMENTARY FIGURES

CFTR genotype	Mutation class[a]
E60X / 4015delATTT	I / I
166delTA / 3120G>A	I / I[b]
1811+1G>C / 1811+1G>C	I / I
F508del / DELE2.3	II / I
F508del / W1282X	II / I
F508del / E60X	II / I
F508del / G542X	II / I
F508del / R1162X (2x)	II / I
F508del / 3500-2A>G	II / I[b]
F508del / 2183-AA>G	II / I
F508del / N1303K (2x)	II / I[b]
F508del / 711-1G>T	II / I
F508del / L927P	II / IV
F508del / F508del (15x)	II / II
R334W / R746X	IV / I
F508del / S1251N (3x)	II / III
F508del / G1249R (2x)	II / III[b] or IV[b]
F508del / R117H-7T (6x)	II / IV
R117H-7T / R553X	IV / I
R117H-7T / R1162X	IV / I
R117H-7T / R117H-7T	IV / IV
F508del / A455E (3x)	II / V and II[b]
S1251N / A455E	III / V and II[b]
R117H-7T / A455E	IV / V and II[b]
F508del / TG(13)T(5) (4x)	II / V
F508del / wild-type (4x)	II / -
Wild-type / wild-type (12x)	- / -

Supplementary figure S1. Overview of all *CFTR* genotypes and their corresponding mutation classes.

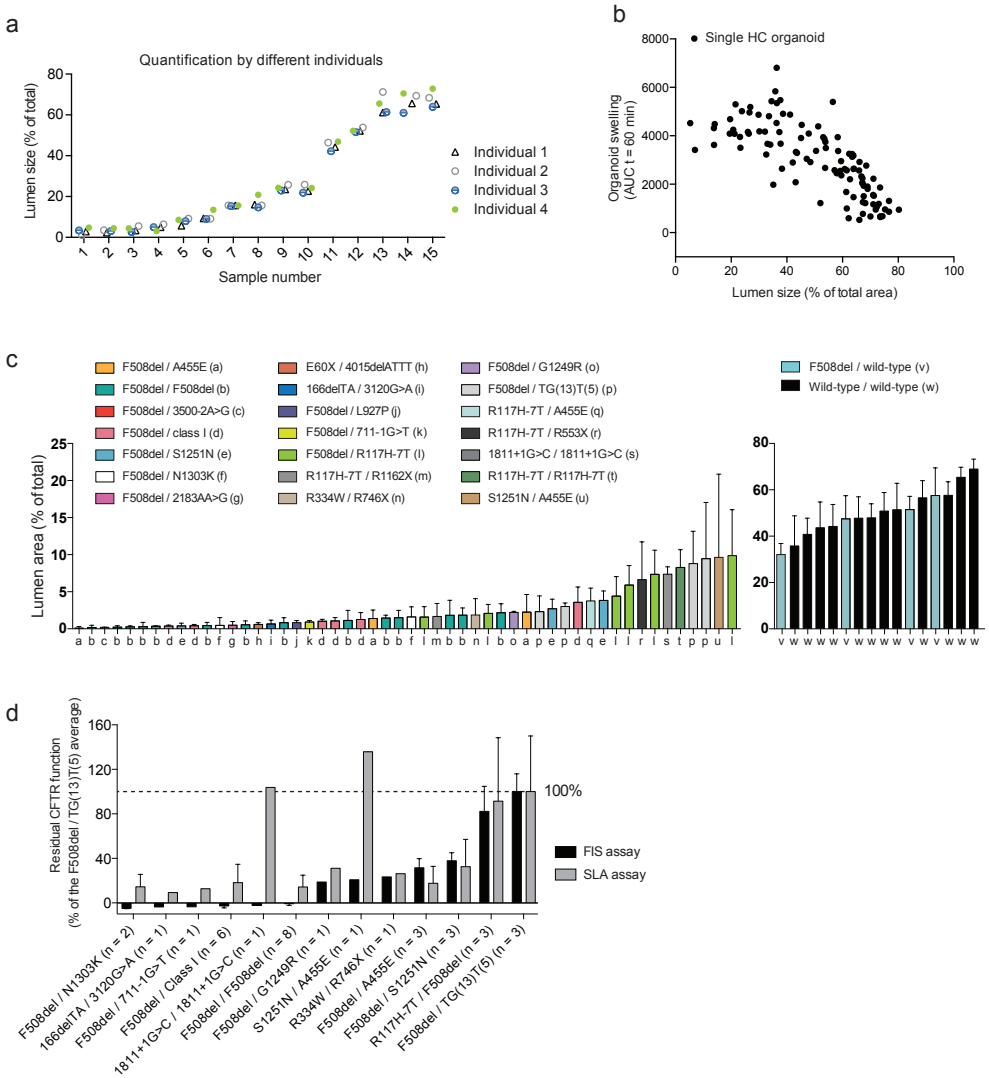

Supplementary figure S2. Characteristics of the steady-state lumen area assay in organoids. (a) Limited observer variability when steady-state organoid lumen area of different samples by 4 independent individuals was quantitated in a blinded fashion. (b) Paired analysis of the forskolin-induced swelling and steady-state lumen area per single healthy control (HC) organoid. The data were derived from three independent wells of the same experiment (c) quantification of the steady-state lumen area of organoids derived from individual donors (similar to Fig. 1c) expressing *CFTR* mutations as indicated. For each subject, 2-5 independent experiments were performed. Mean ± SD. (d) Analysis of residual CFTR function in various mutant *CFTR* organoids measured by forskolin-induced swelling (FIS; similar to Fig. 1c) or the steady-state lumen area (SLA). Responses are normalized to the average response of F508del / TG(13)T(5) organoids (100%). Mean ± SD. (The class I mutations include G542X, R1162X (2x), W1282X, DELE2.3 and E60X).

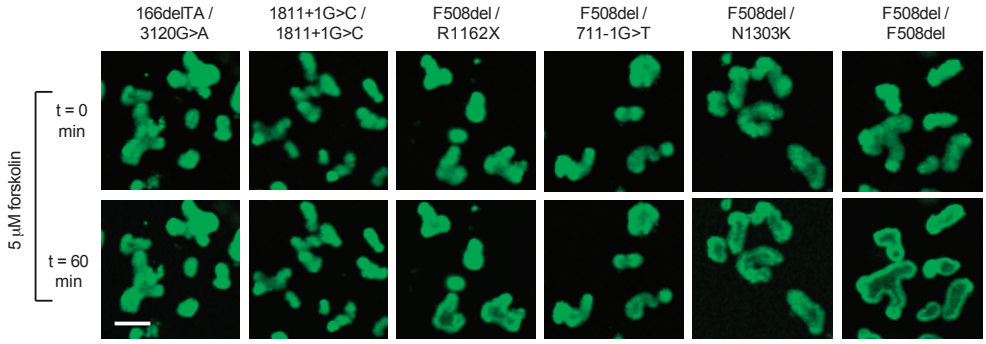

Supplementary figure S3. Detectable residual CFTR function in several forskolin-stimulated organoids expressing severe *CFTR* mutations. Representative confocal images of calcein-green-labeled organoids at the indicated timepoints of forskolin stimulation. Scale bar 80 μM.

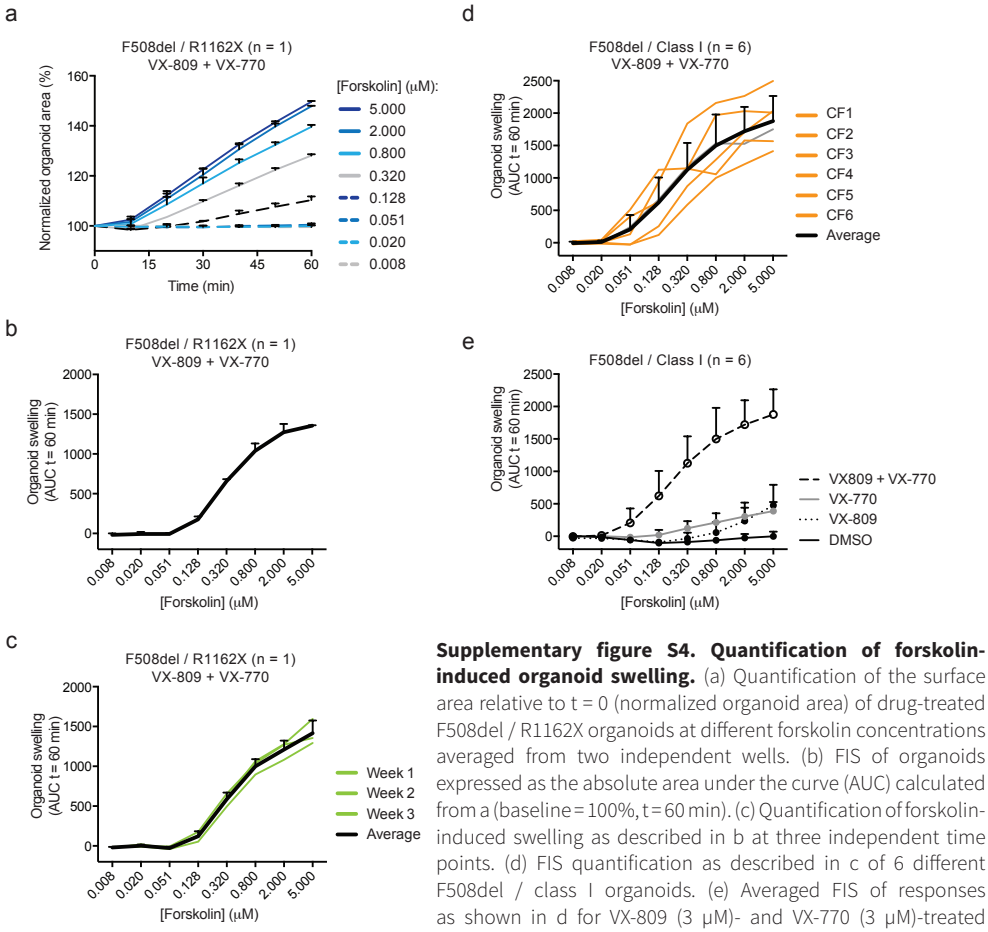

Supplementary figure S4. Quantification of forskolin-induced organoid swelling. (a) Quantification of the surface area relative to t = 0 (normalized organoid area) of drug-treated F508del / R1162X organoids at different forskolin concentrations averaged from two independent wells. (b) FIS of organoids expressed as the absolute area under the curve (AUC) calculated from a (baseline = 100%, t = 60 min). (c) Quantification of forskolin-induced swelling as described in b at three independent time points. (d) FIS quantification as described in c of 6 different F508del / class I organoids. (e) Averaged FIS of responses as shown in d for VX-809 (3 μM)- and VX-770 (3 μM)-treated organoids. In addition, responses to DMSO, VX-809 or VX-770 are shown. Each data point represents responses of F508del / Class I organoids derived from six different individuals, measured at 2 - 3 independent culture time points in duplicate (Mean ± SD).

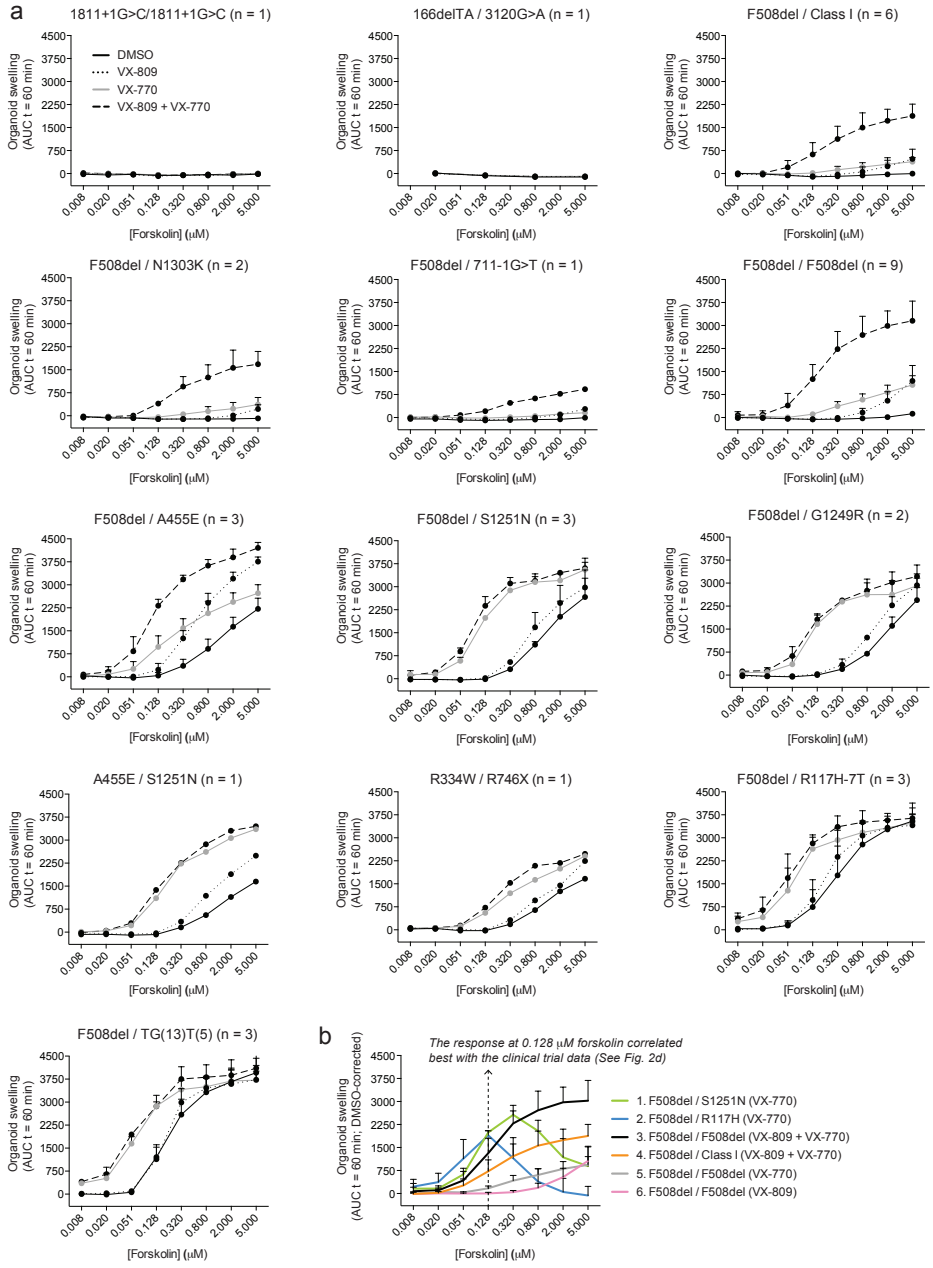

Supplementary figure S5. Genotype-specific profiles of residual and drug-corrected CFTR function in forskolin-stimulated mutant *CFTR* organoids. (a) Forskolin-induced swelling of various mutant *CFTR* organoids, which are untreated or treated with VX-809 (3 μM), VX-770 (3 μM) or both at the indicated forskolin concentrations. Swelling is presented as absolute area under the curve (AUC) calculated form time tracings as shown in Fig. 1a and S3a (Baseline = 100%; t = 60 min.) (Mean ± SD; data were generated during a period of 1 year, of which ~80% were generated during a period of 4 months using an identical medium batch to limit technical variation; n = number of subjects; each subject was measured at 2-5 independent time points in duplicate; the class I mutations include G542X, R1162X (2x), W1282X, DELE2.3 and E60X). (b) Responses of clinically assessed genotypes and treatments (see Fig. 2b) derived from a, corrected for the DMSO-treated condition.

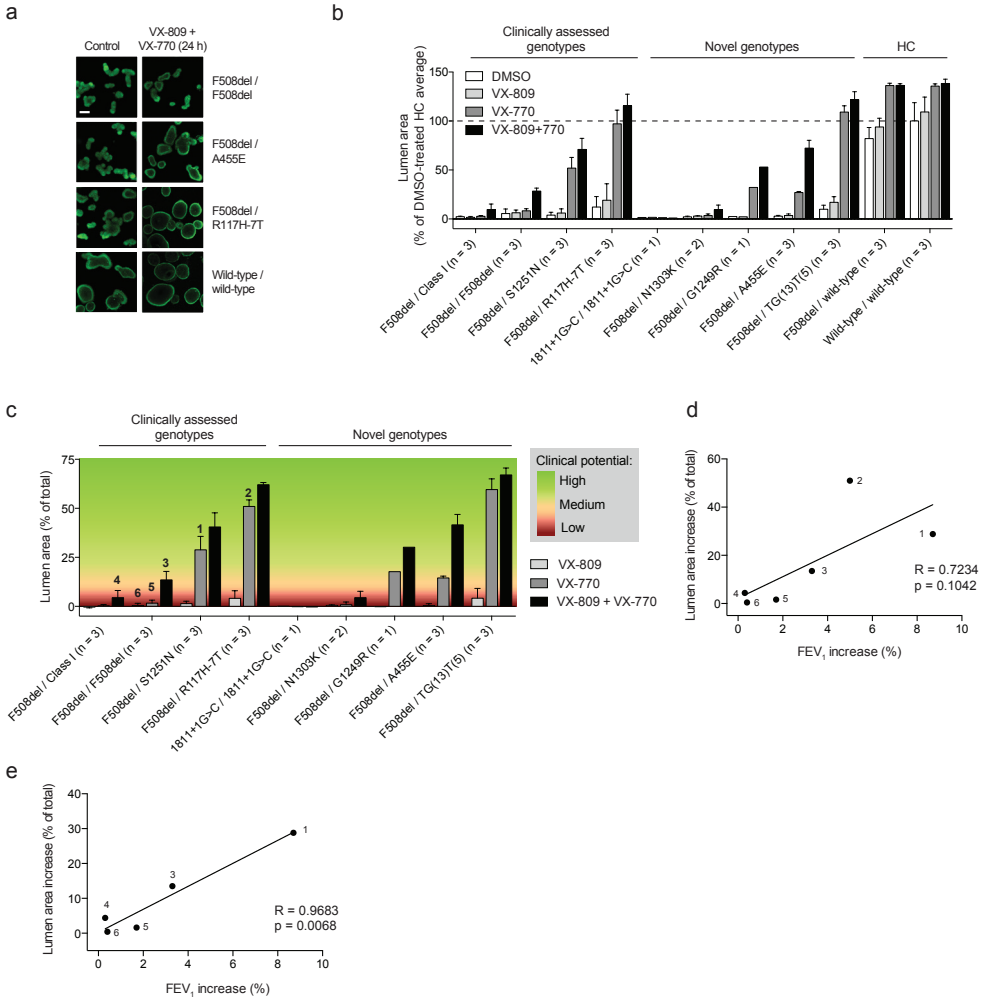

Supplementary figure S6. The steady-state organoid lumen area quantitates residual and drug-corrected CFTR function. (a) Representative confocal images of calcein-green-labeled organoids with or without 24h VX-809 + VX-770 treatment (VX-809 3 μM, VX-770 3 μM). Scale bar 100 μm. (b,c) Quantification of the steady-state lumen area of various organoids incubated for 24 h with treatments as indicated and normalized to the average of the DMSO-treated wild-type / wild-type organoids per experiment (100%; b) or presented as absolute steady-state lumen area corrected for DMSO (c). The numbers refer to Fig. 2b. Data were generated in a time frame of 5 weeks with a single medium batch. Mean ± SD; n = number of subjects; each subject was measured at 2-5 independent time points in duplicate; the class I mutations include G542X, R1162X and W1282X. (d,e) Pearson correlation of the drug-induced steady-state lumen area increase (the numbers refer to the results in c) versus the lung function increase in clinical trials using all genotypes from Fig. 2b (d) or without R117H (e).

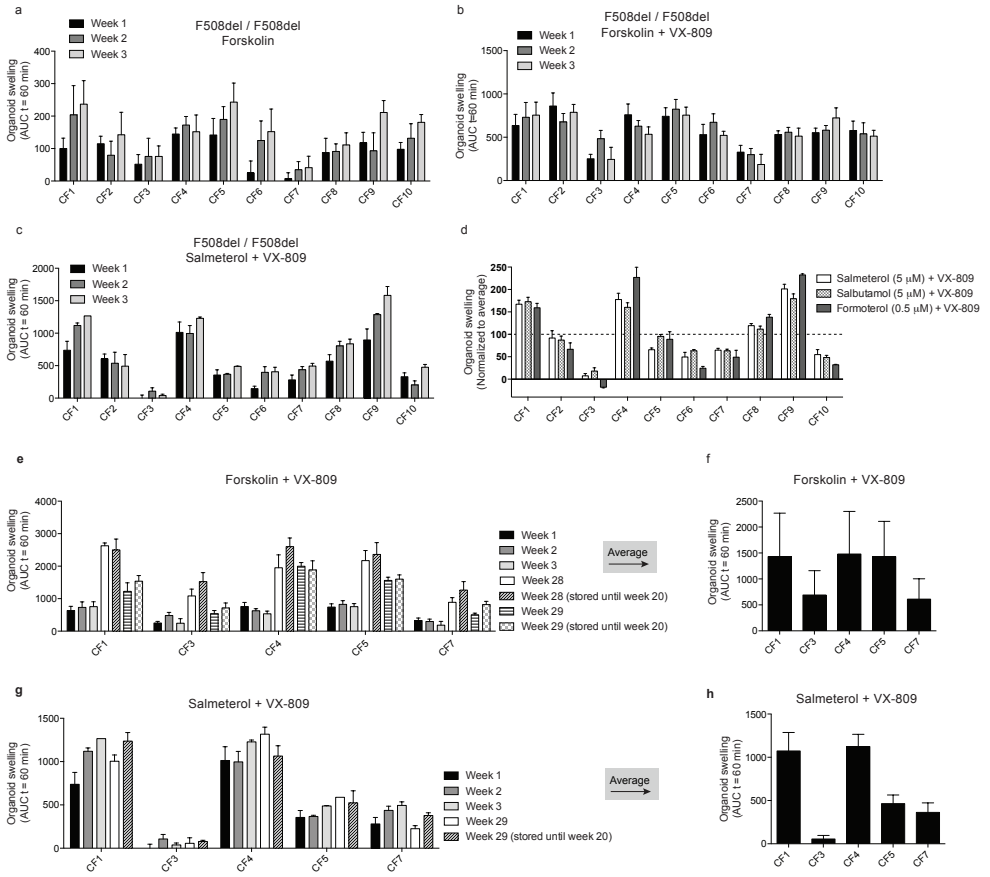

Supplementary figure S7. CFTR correction in F508del homozygous organoids. (a-c) Swelling of organoids induced by forskolin (a) or pre-incubated for 24 h with VX-809 and induced by forskolin (b) or salmeterol (c), expressed as the absolute area under the curve (AUC) calculated from time tracings comparable to Fig. 3b (baseline = 100%, t = 60 min). Responses were averaged from 3 independent wells. Mean ± SD. (see Fig. 3c for the averaged data) (d) Swelling of the F508del homozygous organoid panel in response to salmeterol, salbutamol and formoterol, normalized to the average response of the 10 cultures. (e-h) After the first 3 experiments (week 1-3; similar to data in b and c), 2 low responding and 3 high forskolin-responding cultures were maintained in culture and measured again at week 28 and 29, or reinitiated after liquid nitrogen storage at week 20 and measured at week 28 and 29. Swelling of VX-809-corrected organoids in response to forskolin (e,f) or salmeterol (g,h) presented per experiment (e,g) or as average (f,h). See Fig. 3e-h for the normalized responses. In e and g the SD indicates the variation from 3 independent wells; in f and h the SD indicates variation between different experiments. Mean ± SD.

Chapter 8

Functional repair of CFTR by CRISPR/Cas9 in intestinal stem cell organoids of cystic fibrosis patients

Gerald Schwank[1*], Bon-Kyoung Koo[1,3*], Valentina Sasselli[1], Johanna F Dekkers[4,5], Inha Heo[1], Turan Demircan[1], Nobuo Sasaki[1], Sander Boymans[1], Edwin Cuppen[1,7], Cornelis K van der Ent[4], Edward E S Nieuwenhuis[6], Jeffrey M Beekman[4,5], Hans Clevers[1,2*]

[1]Hubrecht Institute/KNAW and [2]University Medical Center Utrecht, Uppsalalaan 8, Utrecht 3584 CT, The Netherlands, [3]Current address: Wellcome Trust - Medical Research Council Stem Cell Institute, University of Cambridge, Cambridge CB2 1QR, UK, [4]Department of Pediatric Pulmonology, [5]Department of Immunology, Wilhelmina Children's Hospital, University Medical Center, Lundlaan 6, Utrecht 3584 EA, The Netherlands, [6]Department of Pediatric Gastroenterology, Wilhelmina Children's Hospital, University Medical Center, Lundlaan 6, Utrecht 3584 EA, The Netherlands, [7]Department of Medical Genetics, UMC Utrecht, Universiteitsweg 100, Utrecht 3584 GG, The Netherlands

*These authors contributed equally

Cell Stem Cell 2013;13:653-8

ABSTRACT

Single murine and human intestinal stem cells can be expanded in culture over long time periods as genetically and phenotypically stable epithelial organoids. Increased cAMP levels induce rapid swelling of such organoids by opening the cystic fibrosis transmembrane conductor receptor (CFTR). This response is lost in organoids derived from cystic fibrosis (CF) patients. Here we use the CRISPR/Cas9 genome editing system to correct the CFTR locus by homologous recombination in cultured intestinal stem cells of CF patients. The corrected allele is expressed and fully functional as measured in clonally expanded organoids. This study provides proof-of-concept for gene correction by homologous recombination in primary adult stem cells derived from patients with a single-gene hereditary defect.

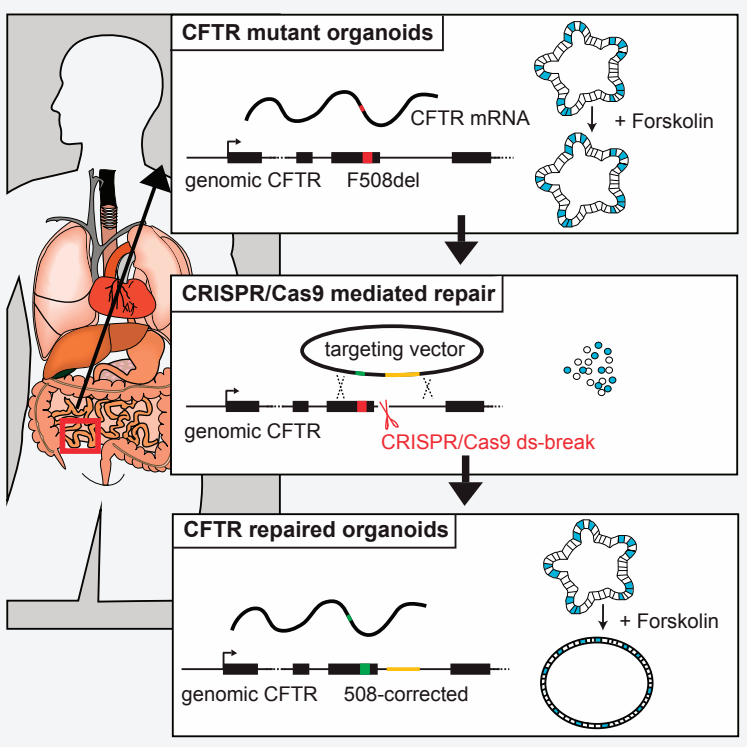

MAIN TEXT

We have previously described a culture system that allows apparently indefinite *in vitro* expansion (for >1 year) of single murine Lgr5$^+$ intestinal stem cells into a 3D small intestinal epithelium [1]. A crucial ingredient is the Wnt-agonistic R-spondin1, a ligand of Lgr5 [2,3]. Intestinal organoids or 'miniguts' comprise nearly intact physiology; self-renewing Lgr5$^+$ stem cells and the niche-supporting Paneth cells are located in a domain that resembles the crypt, and enterocytes as well as goblet - and enteroendocrine cells move upwards to build a villus-like domain that lines the central lumen. Minor adaptation of this culture condition allowed us to develop similar types of organoid cultures for colon, stomach, liver and pancreas using mouse and human tissues [4-8]. Successful transplantation of clonal organoids derived from single Lgr5$^+$ stem cells into damaged tissue has been demonstrated for mouse colon and liver, making the organoid system a promising tool for adult stem cell/gene therapy [9,10]. Recently, several groups have demonstrated the use of the CRISPR/Cas9 system for genome engineering in various species [11-24]. The system utilizes the type II prokaryotic CRISPR/Cas9 adaptive immune system, and targets the Cas9 nuclease by a 20-nt guide sequence cloned upstream of a 5'-NGG 'protospacer adjacent motif' (PAM) [25]. The induced site-specific double strand breaks are repaired either by non-homologous end-joining (NHEJ) to yield indels [26], or by homologous recombination (HR) if homologous donor templates are available [27], thereby enhancing the efficiency of HR-based gene targeting [28-31]. The high efficiency and simple design principle of the CRISPR/Cas9 system prompted us to evaluate its use for gene manipulation of adult stem cells in Lgr5/Rspondin-based organoid cultures.

We first optimized the CRISPR/Cas9 system by targeting the murine *APC* locus in adult intestinal stem cells. The optimized protocol involves culturing intestinal organoids in Wnt-conditioned media, trypsinization to obtain a single cell suspension, and Lipofectamine-mediated transfection with plasmids expressing Cas9 and sgRNAs targeting *APC* (Fig. S1A and B) [32]. Of note, only Lgr5$^+$ stem cells -and none of the other epithelial cell types- will grow out in a clonal fashion into secondary organoids in culture [1,8]. As APC is a negative regulator of the Wnt pathway, stem cells in which both *APC* alleles are inactivated will grow out in the absence of the normally essential Wnt agonist R-spondin1. Two weeks after seeding transfected single cells, multiple organoids grew out from the pool of cells co-transfected with each of five different sgRNAs. In contrast to budding wild type organoids, selected *APC* mutant organoids showed a cystic morphology (Fig. 1A and 1A'), and sequencing of isolated clones confirmed mutations in the targeted *APC* locus (Fig. 1B, Fig. S1C). No organoids grew in control transfections without the specific sgRNAs. Double-targeting of the two negative Wnt regulators RNF43 and its homolog Znrf3 [33,34] also resulted in surviving organoids with frameshifts in both targeted loci (Fig. S1D), demonstrating the possibility to efficiently generate four allele-knock-out organoids in a single transfection. We then tested the CRISPR/Cas9 system on human adult intestinal stem cells, by targeting the *APC* locus. As human intestinal stem cells in culture require additional Wnt for self-renewal and expansion [7,8], transfected stem cells were seeded in medium lacking both Wnt and R-spondin. Organoids only grew out from the pool of cells co-transfected with the specific sgRNA, and selected clones showed a cystic morphology (Fig. 1C'). Sequencing confirmed mutations in the targeted region (Fig 1D), demonstrating the

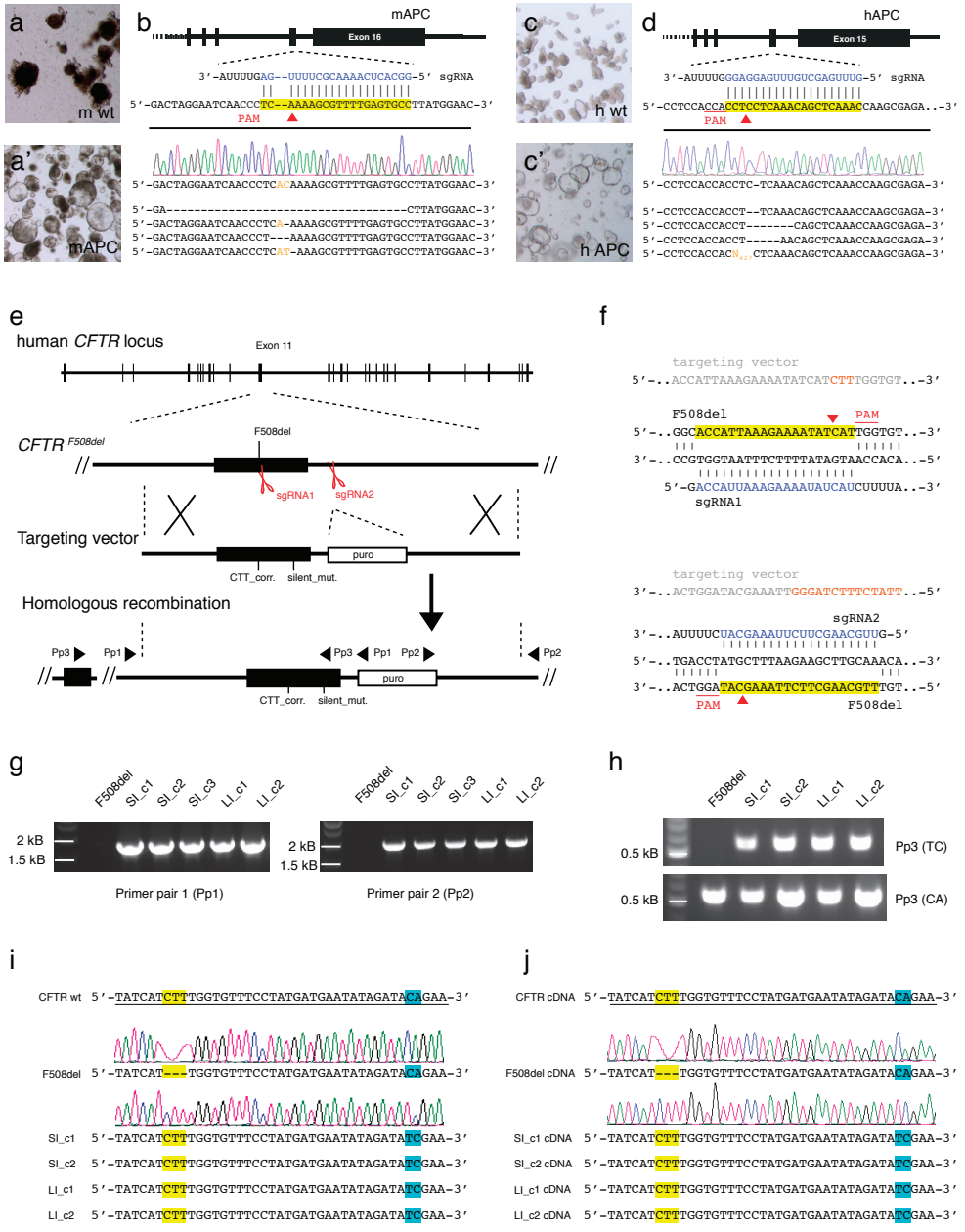

Figure 1. CRISPR/Cas9 mediated genome editing in adult stem cells. (a – d) Generation of Indels in the mouse and human *APC* locus. (e – j) Correction of the human *CFTR F508del* allele by induced homologous recombination. (a) Wild type mouse intestinal organoids in complete growth medium, and (a') *APC* mutant mouse intestinal organoids generated with the CRISP/Cas9 system and selected in medium without R-spondin. Note that organoids change their morphology from budding structures (wild type) to cystic structures (APC). (b) Schematic of the targeted region of the mouse *APC* locus, and sequences of 5 mutant alleles from selected clones. Regions of the sgRNA complementary to the protospacer (yellow) are shown in blue, red arrowheads indicate cleavage sites. (c) Wild type human intestinal organoids in complete growth medium, and (C') *APC* mutant human intestinal organoids selected in medium without Wnt and R-spondin. (d) Schematic of the targeted region of the human *APC* locus, and

sequences of 5 mutant alleles from selected clones. (e) Strategy of the genome modification using CRISPR/Cas9 to induce double-strand breaks in the *CFTR* locus, and a template for homology directed repair. Top line, structure of the *CFTR* gene. Black boxes illustrate exons, thin strokes introns. Red scissors show cleavage sites of sgRNA1 and sgRNA2, white box in the targeting vector indicates the puromycin selection cassette. A 2-bp silent mutation is introduced downstream of the CTT F508del correction, and allows allele specific PCR testing. Pp1, Pp2, Pp3 illustrate PCR primer pairs. (f) Schematic representation of base pairing of the targeting locus with sgRNA1 (upper panel) and sgRNA2 (lower panel), respectively. Top lines illustrate the corresponding sequences in the targeting vector. Non-matching bases are shown in orange, and are based on the F508del correction (CTT addition) and insertion of the selection cassette, respectively. (g) PCR analysis showing insertion of the targeting vector by homologous recombination. Positions of Pp1 and Pp2 primers-pairs are illustrated in (E). SI_c1: clone derived from SI organoids of patient 1 corrected by cleavage with sgRNA1. SI_c2: clone derived from SI organoids of patient 1 corrected by cleavage with sgRNA2. SI_c3: same as SI_c2, but integration of the selection cassette did not result in F508del correction. LI_c1: clone derived from LI organoids of patient 2, corrected by cleavage with sgRNA1. LI_c2: clone derived from LI organoids of patient 2, corrected by cleavage with sgRNA2. (h) RT-PCR analysis of the CFTR cDNA with primers specific for the corrected allele Pp3(TC) and the uncorrected allele Pp3(CA), respectively. Pp3 forward primer is located in exon 10. (I,j) PCR amplification products of the corrected alleles (from G and H) were sequenced. This revealed correction of the F508del mutation in the genomic locus (i) and cDNA (j). Note that the clones shown here are heterozygous for the corrected allele and retained one copy of the mutant allele (data not shown). See also Figure S1, Table S1, and Table S2.

potential of the CRISPR/Cas9 system for genome editing of adult human stem cells in primary intestinal organoids.

To investigate the possibility of gene correction in adult stem cells using CRISPR/Cas9, we focused on the cystic fibrosis transmembrane conductor receptor (CFTR) in primary cultured small intestinal (SI) and large intestinal (LI) stem cells. *CFTR* encodes an anion channel essential for fluid and electrolyte homeostasis of epithelia. Mutations in this receptor cause CF [35-37], a disease which leads to the accumulation of viscous mucus in the pulmonary and gastrointestinal tract and to a current median life expectancy of approximately 40 years [38]. We established SI and LI organoids from two different pediatric CF patients, respectively. Both patients were homozygous for the most common *CFTR* mutation, a deletion of phenylalanine at position 508 (CFTR F508del) in exon11, which causes misfolding, endoplasmic reticulum retention and early degradation of the CFTR protein [39]. To first demonstrate the loss of the CFTR function, we performed the previously established forskolin-induced swelling assay. Forskolin activates CFTR by raising the amount of intracellular cyclic AMP, leading to fluid secretion into the lumen and swelling of organoids [40]. Unlike wild type organoids, the CFTR F508del patient organoids did not expand their surface area upon forskolin treatment (Fig. 2A, C and D), confirming loss of function of CFTR as published previously.

We then transfected the patient organoids independently with two different sgRNAs targeting either *CFTR* exon11 or intron11, together with a donor plasmid encoding wild type CFTR sequences (Fig. 1E). Downstream of the corrected F508del mutation, we introduced a silent mutation into the donor sequence enabling allele-specific PCR testing. Within the intronic sequence, we incorporated a puromycin resistance cassette (Fig. 1E). The sgRNAs were designed to cut the genomic CFTR sequence, but not the homologous sequence within the targeting vector (Fig. 1F). After transfection single cells were plated, and organoids derived from puromycin-resistant individual stem cells were selected and tested for site-specific integration of the donor plasmid

by PCR with primers outside of the 5' and 3' homology arms and within the puromycin selection cassette (Fig. 1E). For both patients, we retrieved several organoid clones with each of the two sgRNAs (Table S1 - selected clones are shown in Fig. 1G). We confirmed site-specific knock-in events and correction of the F508del allele by sequencing the recombined allele (Fig 1I). Note that sequencing the second allele revealed heterozygous CFTR repair in the majority of clones (Table S1). Transfection with sgRNA2, which induces a double strand break 203 base pairs downstream of the F508del mutation also generated a clone with an anecdotal knock-in event where the recombination appeared downstream of the mutation, and repair was not achieved (Fig 1G (SI-c3)). To validate expression of the corrected allele, we performed RT-PCR using a forward primer in exon 10, and an allele specific reverse primer that binds exclusively to the introduced silent mutations in exon 11. Expression of the repaired allele was absent in uncorrected control organoids, and detected in all transgenic clones (Fig. 1H and J). RT-PCR with a reverse primer specific for the uncorrected allele confirms heterozygousity of the knock-in events.

It has been reported that sgRNAs can potentially tolerate mismatches in the 20bp protospacer target sequence, which can lead to the generation of undesirable 'off-target' indels [19,41,42]. To assess off-target effects of the CRISPR/Cas9 system in our adult primary stem cell system, we computationally identified possible off-target sites for each of the two sgRNAs (sequences with 1-3 mismatches to the protospacer followed by the NGG-PAM motive). We identified 29 potential off-target sites for sgRNA1, of which 25 were sequenced and analyzed in an individual clone. Only 1 site contained a 4bp insertion in the protospacer sequence (Table S2). Notably, the mutation was heterozygous and located within an intron, making phenotypic consequences highly unlikely. For the sgRNA2, we identified and sequenced 17 off-target sites in one clone, and no mutations were found (Table S2). Also, when protospacer-homology regions with 4 mismatches (10 sites for sgRNA1, 8 sites for sgRNA2) were analyzed we did not find any indels (Table S2), confirming previous studies that suggest off-target effects to be limited to sites with only 1-3 mismatches [19]. Our results therefore demonstrated high specificity of the CRISPR/Cas9 system in adult stem cells.

To assess whether the CFTR function in corrected organoids was restored, we performed the forskolin assay with transgenic lines. By live-cell microscopy, we observed rapid expansion of the organoid surface area in the corrected organoids, whereas swelling was absent in untransfected control organoids (Fig. 2A, Movie S1). Quantification of swelling by automated image analysis demonstrated a relative increase of the total organoid surface area to 177% (+/- 1.4 SEM) and 167% (+/- 3.8 SEM) for two corrected SI organoid clones (Fig. 2C and E), and to 187% (+/- 3 SEM) and 180% (+/- 1.5 SEM) for two corrected LI organoid clones (Fig. 2D and F). These numbers are comparable to forskolin-induced surface area increase of wild type organoids, and exceed CFTR rescue capacities obtained with chemical correctors [40]. Untransfected F508del organoids increased only marginally in surface area (Fig. 2C-F), which is consistent with very limited residual CFTR function of the F508del allele [40]. We next tested whether the forskolin-induced swelling of the corrected organoids was sensitive to chemical inhibition of CFTR by CFTRinh-172 [43]. Indeed, forskolin-induced swelling was fully abolished in presence of the inhibitor (Fig. 2C-F, Movie S1). Together, these data demonstrated that the corrected F508del allele was fully functional, and was able to rescue the CFTR phenotype in organoids.

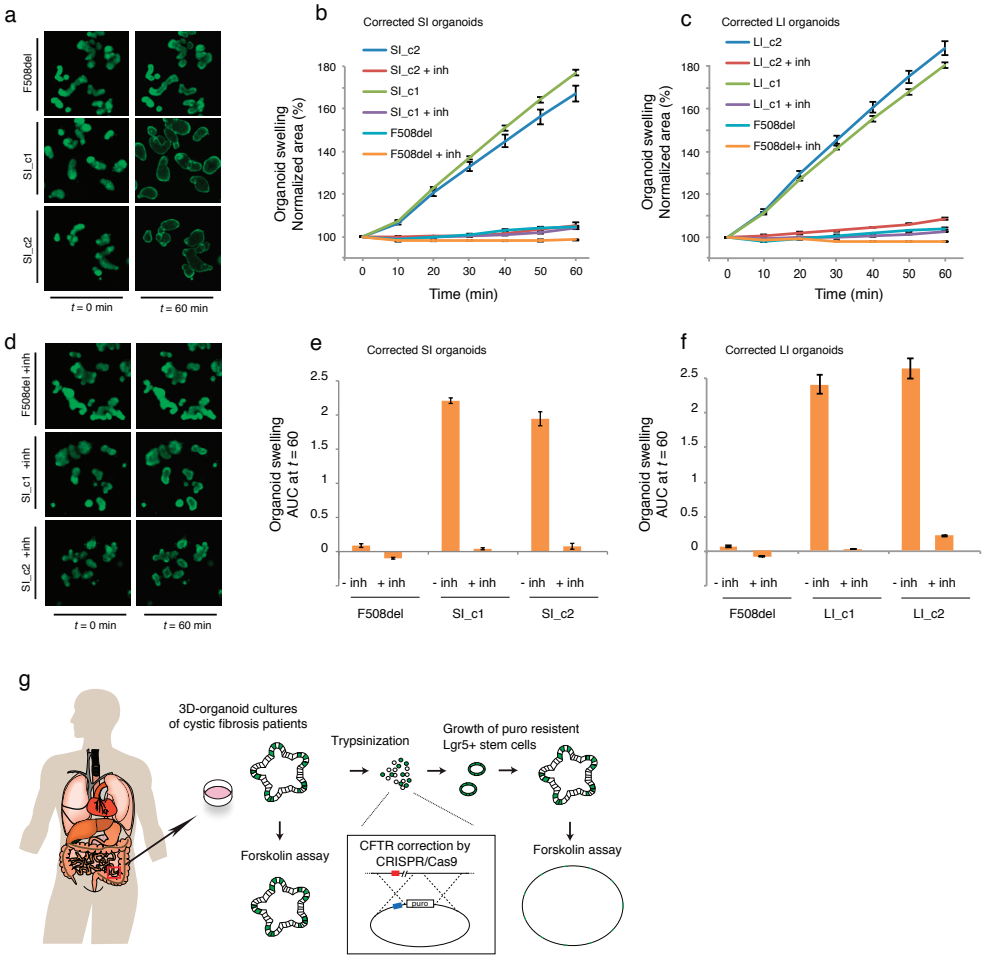

Figure 2. Functional analysis of the restored CFTR function in corrected organoids. (a) Confocal images of calcein-green labeled and forskolin stimulated SI organoids without, and (b) in the presence of a chemical CFTR inhibitor. SI_c1, SI_c2: clones derived from SI organoids corrected by cleavage with sgRNA1and sgRNA2, respectively. F508del: uncorrected control organoids of the corresponding patient. t=0 min, t=60 min indicate timepoints after forskolin induction. (c,d) Quantification of organoid swelling of corrected SI organoid clones (c) and LI organoid clones (d). The total organoid surface area is normalized to t_0 min and measured in three independent wells. Error bars indicate the standard error of the mean (SEM). inh, chemical CFTR inhibitor. (e,f) Forskolin induced swelling expressed as the absolute area under the curve calculated from the c and d, respectively (baseline = 100%, t=60 min). Error bars indicate SEM. (g) Schematic illustration of the gene correction protocol. Stem cells are labeled in green. Note that after transfection only stem cells that integrated the selection cassette can grow out and form new organoids. See also Movie S1.

In summary, we have isolated and expanded adult intestinal stem cells from two CF patients, corrected the mutant F508del allele using the CRISP/Cas9 mediated homologous recombination, and demonstrated functionality of the corrected allele in the organoid system (Fig. 2G). Together with previous studies, in which *in vitro* expanded organoids were successfully transplanted into colons of mice [10], this work provides a potential strategy for future gene therapy in patients.

Although given its multi-organ involvement CF does not appear to be a prime candidate for clinical application of adult stem cell gene therapy, this approach may present a safe complement to induced pluripotent stem cell-based approaches, and in the future could be applied to different single-gene hereditary defects. The advantage of combining HR-based gene correction strategies with organoid culture technology rests in the possibility of clonal expansion of single adult patient stem cells and selection of recombinant clonal organoid cultures harboring the desired, exact genetic change.

METHODS

Human material for organoid cultures

Approval for this study was obtained by the ethics committees of the University Medical Centre Utrecht, the Erasmus MC Rotterdam, and the RWTH Aachen University Hospital. Written informed consent was obtained. Material of one F508del-CFTR homozygous individual (patient 1) was derived from proximal ileum rest-sections upon surgery due to meconium ileus, and material of a second F508del-CFTR homozygous individual (patient 2) was generated from rectal suction biopsies after ICMs.

Mouse material for organoid cultures

Experimental setup was approved by the animal welfare committee (DEC) of the Royal Dutch academy of sciences (KNAW). Rosa-CreERT2 mice were used to generate mouse small intestinal organoids.

Organoid culture

Crypts were isolated from mouse and human intestinal tissues by incubating for 1 hour with 2mM EDTA in PBS at 4 °C, and plated in drops of matrigel[1,8]. After polymerization previously described growth medium was added[44]. Mouse intestinal growth medium contains advanced DMEM/F12 medium (Invitrogen) including B27 (Invitrogen), N2 (Invitrogen), N-Acetylcysteine (Sigma-Aldrich), noggin (Peprotech), Rspo1[45], and epidermal growth factor (Peprotech). Human intestinal growth medium additionally contains Wnt conditioned media (50%, produced using stably transfected L cells), TGF-β type I Receptor inhibitor A83-01 (Tocris), Nicotinamide (Sigma-Aldrich) and P38 inhibitor SB202190 (Sigma-Aldrich). Confluent organoids were mechanically dissociated by pipetting. Fragmented organoids were centrifuged and resuspended in cold matrigel.

Organoid Transfection

The organoid lipofection protocol is described in detail in[32]. In short: Mouse organoids were cultured in medium plus Nicotinamide and Wnt-conditioned medium to enrich for stem cells. Before transfection mouse organoids were trypsinized for 5 min at 37 °C to obtain single cells. Human organoids were grown in expansion media, and trypsinized for 10 min at 37 °C. After trypsinization cells were resuspended in 450µl growth medium (mouse cells in growth medium plus Nicotinamide, Wnt, and the Rho kinase inhibitor Y-27632; human cells in human expansion media plus Y-27632), and plated in 48 well plates at high density (80-90% confluent). Nucleic

acid-Lipofectamine® 2000 complexes were prepared according to the standard Lipofectamine® 2000 protocol. 4µl of Lipofectamine® 2000 reagent in 50µl Opti-MEM® medium, and 0.7µg of the sgRNA plasmid plus 0.7µg of the Cas9 plasmid in 50µl Opti-MEM® medium were mixed together, incubated for 5 minutes, and added to the cells (50µl per well). The plate was centrifuged at 600*g* at 32 °C for 1 hour, and incubated for 4 hours at 37°C before single cells were re-plated in matrigel. Growth medium plus Y-27632 was exchanged with selection medium 3 days after transfection. At this stage single cells were already grown into small organoids consisting of approximately 16 cells. CFTR corrected organoids were selected in medium containing Y-27632 and 500ng/ml puromycine. Note that on average less than 1 organoid per well is puromycine resistant. For clonal expansion single organoids were picked.

Vector construction

The human codon-optimized Cas9 expression plasmid was obtained from Addgene (41815). sgRNA plasmids: The sgRNA-GFP plasmid was obtained from Addgene (41819) and used as a template for generating target specific sgRNAs (described in fig S1). The GFP targeting sequence was exchanged by inverse PCR followed by DpnI digestion and T4 ligation. Specifically, a common forward primer 5'-phospho-GTTTTAGAGCTAGAAATAGCAAGTTAAAATAAGG-3' was used in combination with target specific reverse primers (i.e. reverse complement target sequences without the PAM for sgRNA1, 5'-ATGATATTTTCTTTAATGGT-3' and sgRNA2, 5'-ATGCTTTAAGAAGCTTGCAA-3' were fused to the 5' end of a common reverse oligo 5'-CGGTGTTTCGTCCTTTCCACAAGAT-3') to generate pU6-sgRNA1 and pU6-sgRNA2 by using the high-fidelity Phusion polymerase (NEB) on the pU6-gGFP plasmid. CFTR targeting vector: The human BAC clone *RP11-30E5* was used to PCR amplify the CFTR homology arms using high-fidelity Phusion DNA polymerase (New England BioLabs). The 5' homology arm spans the region chr7:117198376-117199878, and the 3' homology arm spans the region chr7:117199875-117201568 (GRCh37/hg19 alignment). The 3229-bp AAT-PB:PGKpuroΔtk selection cassette was PCR amplified from the pMCS- AAT-PB:PGKpuroΔtk plasmid[46]. The PCR products were cloned into pJET1.2 (CloneJET, ThermoScientific) by In-Fusion Advanced PCR cloning (Clontech). The silent mutations that mark the homologous wild type template were introduced following standard PCR-mutagenesis protocols. All construct sequences were confirmed by Sanger sequencing on a 3730xl DNA Analyzer (BioRad).

CFTR locus and off-target sequence analysis

Genomic DNA from organoids was isolated using standard buffers and phenol:chloroform extraction. Total RNA was extracted using the RNeasy Kit (Qiagen, Hilden, Germany) and treated with RNase-Free DNase (Quiagen). The cDNA library was generated using GoScript Reverse Transcriptase (Promega) and oligo (dT)15 primers (Promega). Primers for the PCR analysis were designed using SeqBuilder and Primer3 software. Allele specific CFTR primers were designed to bind to the region with the inserted silent mutations with their 3' end. The 5'GCATGCTTTGATGACGCTTCGA3' primer is specific to the corrected allele, and the 5'GCATGCTTTGATGACGCTTCTG3' primer is specific to the wildtype allele. To analyse off-target regions a custom made algorithm was used to blast the target sequences of sgRNA1 and sgRNA2 against the human reference genome GRCh37/hg19, and to identify sequences with 1 to 4 base miss-matches within the first 20 nucleotides upstream of the NGG protospacer. Off-target sequences for sgRNA1 and sgRNA2 where PCR amplified from

DNA of corrected organoids (SI_c1 and SI_c2, respectively) by using the high-fidelity Phusion DNA polymerase (New England BioLabs) and Primer3-designed sequence specific primer pairs. PCR amplicons were sequenced either directly or upon cloning into pJET1.2 (CloneJET, ThermoScientific). Sanger sequencing was performed in house on a 3730xl DNA Analyzer (BioRad) or outsourced to Macrogen Inc. Sequence analysis and alignments were performed by using DNASTAR Lasergene 9 Core suite package.

Forskolin-induced organoid swelling assay

Organoids from a 7-day old culture were seeded in a flat-bottom 96-well culture plate (Nunc) in 5 µl matrigel containing 20–80 organoids and 100 µl culture medium. One day after plating, organoids were incubated for 30 min with 100 µl standard culture medium containing 2 µM calcein-green (Invitrogen). After the calcein-green incubation, 5 µM forskolin was added and organoids were directly analyzed by confocal live cell microscopy (LSM710, Zeiss, 5× objective). 3-8 wells were used per condition. For CFTR inhibition, organoids were pre-incubated for 3 hours with 75 µM CFTRinh-172 (B7; Cystic Fibrosis Foundation Therapeutics, Inc).

Quantification of organoid surface area

Forskolin-stimulated organoid swelling was automatically quantified using Volocity imaging software (Improvision). The total organoid area (XY plane) increase relative to t = 0 of forskolin treatment was calculated and averaged from 3-8 individual wells per condition. The area under the curve (AUC) was calculated using Graphpad Prism.

Acknowledgements

We thank K. Tenbrock (Department of Pediatrics, the RWTH Aachen University, Germany) for providing intestinal rest-material, and A. Smith (Wellcome Trust Centre for Stem Cell Research, University of Cambridge) for providing Rosa-CreERT2 mice. This work was funded by grants from the European Research Council (EU/232814-StemCeLLMark), the KNAW/3V-fund, the SNF fellowship for advanced researchers PA00P3 139732 (G.S.), the Human Frontiers in Science Program long-term fellowship LT000422/2012 (G.S.), the Wellcome Trust (097922/C/11/Z) (B.-K.K.), the EU Marie Curie Fellowship EU/330571-FP7-IIF (I.H.), the Astellas Foundation (N.S.), and JSPS (N.S.).

REFERENCES

1. Sato, T., *et al.* Single Lgr5 stem cells build crypt-villus structures in vitro without a mesenchymal niche. *Nature* **459**, 262-265 (2009).
2. Carmon, K.S., Gong, X., Lin, Q., Thomas, A. & Liu, Q. R-spondins function as ligands of the orphan receptors LGR4 and LGR5 to regulate Wnt/beta-catenin signaling. *Proc Natl Acad Sci U S A* **108**, 11452-11457 (2011).
3. de Lau, W., *et al.* Lgr5 homologues associate with Wnt receptors and mediate R-spondin signalling. *Nature* **476**, 293-297 (2011).
4. Barker, N., *et al.* Lgr5(+ve) stem cells drive self-renewal in the stomach and build long-lived gastric units in vitro. *Cell stem cell* **6**, 25-36 (2010).
5. Huch, M., *et al.* Unlimited in vitro expansion of adult bi-potent pancreas progenitors through the Lgr5/R-spondin axis. *The EMBO journal* **32**, 2708-2721 (2013).

6. Huch, M., *et al.* In vitro expansion of single Lgr5+ liver stem cells induced by Wnt-driven regeneration. *Nature* **494**, 247-250 (2013).

7. Jung, P., *et al.* Isolation and in vitro expansion of human colonic stem cells. *Nat Med* **17**, 1225-1227 (2011).

8. Sato, T., *et al.* Long-term expansion of epithelial organoids from human colon, adenoma, adenocarcinoma, and Barrett's epithelium. *Gastroenterology* **141**, 1762-1772 (2011).

9. Huch, M., Boj, S.F. & Clevers, H. Lgr5(+) liver stem cells, hepatic organoids and regenerative medicine. *Regenerative medicine* **8**, 385-387 (2013).

10. Yui, S., *et al.* Functional engraftment of colon epithelium expanded in vitro from a single adult Lgr5(+) stem cell. *Nat Med* **18**, 618-623 (2012).

11. Chang, N., *et al.* Genome editing with RNA-guided Cas9 nuclease in zebrafish embryos. *Cell Res* **23**, 465-472 (2013).

12. Cho, S.W., Kim, S., Kim, J.M. & Kim, J.S. Targeted genome engineering in human cells with the Cas9 RNA-guided endonuclease. *Nature biotechnology* **31**, 230-232 (2013).

13. Cong, L., *et al.* Multiplex genome engineering using CRISPR/Cas systems. *Science* **339**, 819-823 (2013).

14. Friedland, A.E., *et al.* Heritable genome editing in C. elegans via a CRISPR-Cas9 system. *Nature methods* **10**, 741-743 (2013).

15. Hou, Z., *et al.* Efficient genome engineering in human pluripotent stem cells using Cas9 from Neisseria meningitidis. *Proc Natl Acad Sci U S A* (2013).

16. Hwang, W.Y., *et al.* Efficient genome editing in zebrafish using a CRISPR-Cas system. *Nature biotechnology* **31**, 227-229 (2013).

17. Jinek, M., *et al.* RNA-programmed genome editing in human cells. *Elife* **2**, e00471 (2013).

18. Li, J.F., *et al.* Multiplex and homologous recombination-mediated genome editing in Arabidopsis and Nicotiana benthamiana using guide RNA and Cas9. *Nature biotechnology* **31**, 688-691 (2013).

19. Mali, P., *et al.* CAS9 transcriptional activators for target specificity screening and paired nickases for cooperative genome engineering. *Nature biotechnology* (2013).

20. Nekrasov, V., Staskawicz, B., Weigel, D., Jones, J.D. & Kamoun, S. Targeted mutagenesis in the model plant Nicotiana benthamiana using Cas9 RNA-guided endonuclease. *Nature biotechnology* **31**, 691-693 (2013).

21. Shen, B., *et al.* Generation of gene-modified mice via Cas9/RNA-mediated gene targeting. *Cell Res* **23**, 720-723 (2013).

22. Wang, H., *et al.* One-step generation of mice carrying mutations in multiple genes by CRISPR/Cas-mediated genome engineering. *Cell* **153**, 910-918 (2013).

23. Xiao, A., *et al.* Chromosomal deletions and inversions mediated by TALENs and CRISPR/Cas in zebrafish. *Nucleic Acids Res* **41**, e141 (2013).

24. Yu, Z., *et al.* Highly Efficient Genome Modifications Mediated by CRISPR/Cas9 in Drosophila. *Genetics* (2013).

25. Jinek, M., *et al.* A programmable dual-RNA-guided DNA endonuclease in adaptive bacterial immunity. *Science* **337**, 816-821 (2013).

26. Barnes, D.E. Non-homologous end joining as a mechanism of DNA repair. *Curr Biol* **11**, R455-457 (2001).

27. van den Bosch, M., Lohman, P.H. & Pastink, A. DNA double-strand break repair by homologous recombination. *Biol Chem* **383**, 873-892 (2002).

28. Bibikova, M., Beumer, K., Trautman, J.K. & Carroll, D. Enhancing gene targeting with designed zinc finger nucleases. *Science* **300**, 764 (2003).

29. Porteus, M.H. & Carroll, D. Gene targeting using zinc finger nucleases. *Nature biotechnology* **23**, 967-973 (2005).

30. Thomas, K.R. & Capecchi, M.R. Site-directed mutagenesis by gene targeting in mouse embryo-derived stem cells. *Cell* **51**, 503-512 (1987).

31. Urnov, F.D., *et al.* Highly efficient endogenous human gene correction using designed zinc-finger nucleases. *Nature* **435**, 646-651 (2005).

32. Schwank, G., Andersson-Rolf, A., Koo, B.K., Sasaki, N. & Clevers, H. Generation of BAC transgenic epithelial organoids. *PLoS ONE* **8**, e76871 (2013).

33. Hao, H.X., *et al.* ZNRF3 promotes Wnt receptor turnover in an R-spondin-sensitive manner. *Nature* **485**, 195-200 (2012).

34. Koo, B.K., *et al.* Tumour suppressor RNF43 is a stem-cell E3 ligase that induces endocytosis of Wnt receptors. *Nature* **488**, 665-669 (2012).

35. Kerem, B., *et al.* Identification of the cystic fibrosis gene: genetic analysis. *Science* **245**, 1073-1080 (1989).

36. Riordan, J.R., *et al.* Identification of the cystic fibrosis gene: cloning and characterization of complementary DNA. *Science* **245**, 1066-1073 (1989).

37. Rommens, J.M., *et al.* Identification of the cystic fibrosis gene: chromosome walking and jumping. *Science* **245**, 1059-1065 (1989).

38. Ratjen, F. & Doring, G. Cystic fibrosis. *Lancet* **361**, 681-689 (2003).

39. Cheng, S.H., *et al.* Defective intracellular transport and processing of CFTR is the molecular basis of most cystic fibrosis. *Cell* **63**, 827-834 (1990).

40. Dekkers, J.F., *et al.* A functional CFTR assay using primary cystic fibrosis intestinal organoids. *Nat Med* **19**, 939-945 (2013).

41. Hsu, P.D., *et al.* DNA targeting specificity of RNA-guided Cas9 nucleases. *Nature biotechnology* (2013).

42. Pattanayak, V., *et al.* High-throughput profiling of off-target DNA cleavage reveals RNA-programmed Cas9 nuclease specificity. *Nature biotechnology* (2013).

43. Thiagarajah, J.R., Song, Y., Haggie, P.M. & Verkman, A.S. A small molecule CFTR inhibitor produces cystic fibrosis-like submucosal gland fluid secretions in normal airways. *Faseb J* **18**, 875-877 (2004).

44. Sato, T. & Clevers, H. Primary mouse small intestinal epithelial cell cultures. *Methods Mol. Biol.* **945,** 319–328 (2013).

45. Kim, K.-A. *et al.* Mitogenic influence of human R-spondin1 on the intestinal epithelium. *Science* **309,** 1256–1259 (2005).

46. Yusa, K. *et al.* Targeted gene correction of α1-antitrypsin deficiency in induced pluripotent stem cells. *Nature* **478,** 391–394 (2011).

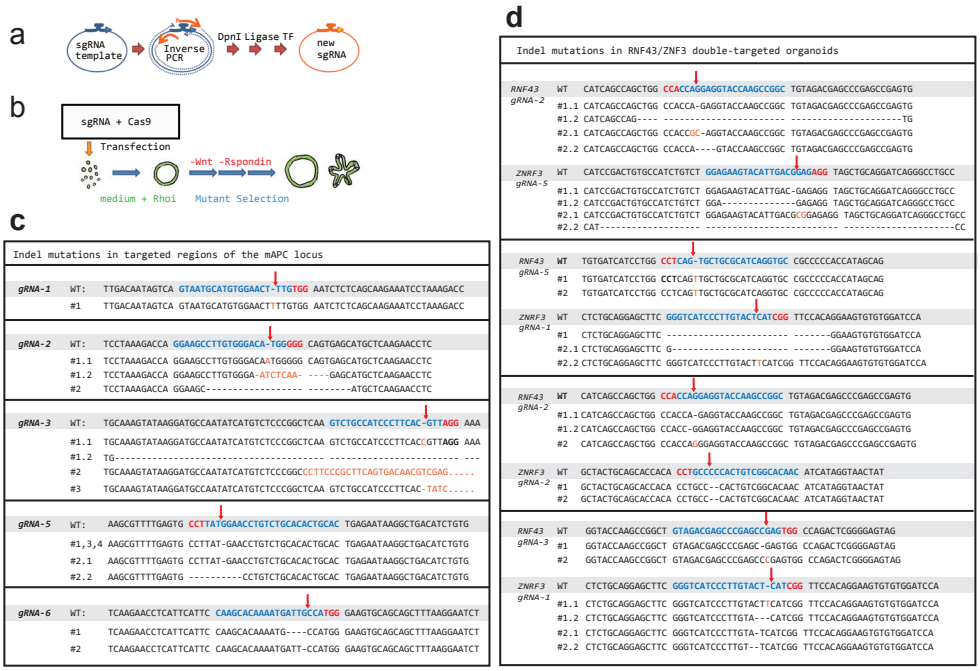

	Transfection		Selection		HR - confirmation	
	Number of organoids trypsinized		Number of puro resistent clones		Number of correctly targeted clones	
	sgRNA1	sgRNA2	sgRNA1	sgRNA2	sgRNA1	sgRNA2
LI organoids	≈1400	≈1400	31	11	3	3
SI organoids	≈1400	≈1400	23	24	5	6

Table S1. Summary of the CFTR corrected organoid clones (related to Figure 1). Note that a single organoid consists of up to 1000 cells. HR was confirmed by PCR with primers outside of the homology arms and inside the puromycin cassette (see Fig. 1G). 16 clones were heterozy-gous for the corrected allele. The uncorrected allele was detected with forward primers upstream of the homology arm and reverse primers downstream of the puro cassette. One clone was homozygous or hemizygous for the corrected allele (cells with one targeted allele and a deletion of the other allele are undistinguishable from homozygous clones).

genomic location	locus details	sequence	#mm	Ins del
sgRNA1	**exon CFTR**	ACCATTAAAGAAAATATCATTGG		
chr7:144939809-144939831	Intron *EEPD1*	ACCATTAGAGAAAATATAATGGG	2	no
chr1:187009331-187009351	intergenic	AACATTAAAGAAAAAAACATTGG	3	no
chr1:62494550-62494572	intron *SMYD3*	ACCATTAAAGAAAATATGTCTGG	3	no
chr4: 144939809-144939831	Intron *GYPB*	TCCATTAAAATAAATATCATAGG	3	yes
chr4:245944979-245945000	intron LPHN3	AGCATTAAAGAAAATAAAATTGG	3	no
chr4:112377853-112377875	intergenic	AGCATTAAAGAAAATCTCTTCGG	3	no
chr4:140456280-140456302	intron *SETD7*	ACAATTAAAAAAAAAATCATTGG	3	no
chr4:46745000-46745022	intron *COX7B2*	ATGATTAAAGAAAATATTTATGGG	3	no
chr6:36987926-36987948	intron *FGD2*	AACATTAAAGAAAATAACCTTGG	3	no
chr7:103412387-103412409	intron *RELN*	ACAATTAAAGAAAATCTTAATGGG	3	no
chr7:8597257-8597279	intron *NHPX1*	ACCATTAAAGGAAATAACAATGG	3	no
chr8:96758290-96758312	non coding RNA	AAGATTAAATAAAATATCATGGG	3	no
chr9:9648956-9648978	intron *PTPRD*	ACCAAGGAAGAAAATATCATAGG	3	no
chr9:87375273-87375295	intron *NTRK2*	ATTATTAAAGAAAATATTATAGG	3	no
chr10:90191635-90191657	intron *RNLS*	ACCATTATAGACAATATCCTGGG	3	no
chr12:10035709-100357113	intron *ANKS1B*	ACAATGAAAGAAACTATCATCGG	3	no
chr13:105263327-105263349	intergenic	AACATTAAAGAACATAGCATGGG	3	no
chr14:93962942-93962964	intron *UNC79*	ACCATTAAAGAAAGAATTATAGG	3	no
chr14:89626574-89626596	3' UTR *FOXN3*	GCCATTAAAGAAAATTTCTTAGG	3	no
chr14:53804624-53804646	intergenic	ACCTTTAAGGAAAATATCAAAGG	3	no
chr14:52731749-52731771	intergenic	ACCTTTAATGAAAATATCTTAGG	3	no
chr16:72045145-72045167	intron *DHODH*	ACCATTTCAGAAAATCTCATCGG	3	no
chr16:54221345-54221367	intergenic	ACAATGAAAGAAAATGTCATTGG	3	no
chr18:68490314-68490336	intergenic	AGTATTAAATAAAATATCATTGG	3	no
chr18:10200114-10200136	intergenic	ATCATTCAAGAAATTATCATTGG	3	no
chr22:32366364-32366386	intergenic	ACAAATAAAGCAAATATCATCGG	3	no
chr22:43396760-43396782	intron *PACSIN2*	AGCATTAAAGAAAATAACAAAGG	3	no
chr22:35364325-35364347	intergenic	ACCATTCAAGAAAATAATATTGG	3	no
chrX:77339695-77339717	intergenic	ATCATTAAAGAAAAAATATTGG	3	no
chrX:62518406-62518428	centrosome	ACCTTTAAAAAAAATGTCATTGG	3	no
chr1:105948788-105948810	intergenic	GCATTTAAAGAAAATGTCATGGG	4	no
chr3:139560789-139560811	intergenic	GCCATTAAAGAAGTTATAATGGG	4	no
chr4:8958983-8959005	intergenic	GCAATTAGAGACAATATCATTGG	4	no
chr5:102131691-102131713	intergenic	GCCTTTAAACAAAATATCACAGG	4	no
chr6:121848124-121848146	intergenic	GCCATTAAAAACAATATTATAGG	4	no
chr6:22164608-22164630	intron *LINC00340*	GCCATTAAGGAAAACATTATGGG	4	no
chr8:130386171-130386193	intergenic	GCCACAAAAGAAAATATCCTTGG	4	no
chr11:58004832-58004854	intergenic	GCCATTAGAGAAAATAACTTGGG	4	no
chr12:95649771-95649793	intron *VEZT*	GCCATTAAAGCACATGTCATGGG	4	no
chrX:123167313-123167335	intron *STAG2*	GCTATTAAAGAAACTAACATAGG	4	no
sgRNA2	**Intron CFTR**	TTGCAAGCTTCTTAAAGCATAGG		
chr17:58056091-58056113	non-coding RNA	TTGGAAGCTACTTAAAGCATGGG	2	no
chr6:25779595-25779617	3' UTR *SLC17A4*	CTGCAAGCTACTAAAAGCATAGG	3	no
chr1:58657028-58657050	intron *DAB1*	TTGCAAACTTTTTAAAGCAGTGG	3	no
chr7:51634668-51634690	intergenic	TTGCAGGCTTGTTCAAGCATGGG	3	no
chr9:115601652-115601674	intron *SNX30*	TTGAAAGCTTTTTAAAGCAGAGG	3	no
chr9:17681101-17681123	intron *SH3GL2*	TTGAAAGCTTCTAGAAGCATGGG	3	no
chr11:30802944-30802966	intergenic	TAGTTAGCTTCTTAAAGCATAGG	3	no
chr12:70467917-70467939	intergenic	TTGCAACCAACTTAAAGCATTGG	3	no
chr12:30385557-30385579	intergenic	TTGCAAGTTCCTTAAGGCATGGG	3	no
chr12:13969458-13969480	intergenic	TTCCATGCTTCTTATAGCATGGG	3	no
chr13:79247211-79247233	intergenic	TTGAAAGTTTCTTAAAGTATAGG	3	no
chr13:32162691-32162711	intergenic	TTGCAGGCTGCGTAAAGCATGGG	3	no
chr15:59126563-59126583	intron *FAM63B*	TTAAAAGCTTCTTAAAGCATGGG	3	no
chr19:7302275-7302295	intergenic	TTGCAGGCTTCAAAAAGCATGGG	3	no
chr21:23012696-23012716	intergenic	TAAGAAGCTTCTTAAAGCATAGG	3	no
chrX:80130295-80130315	intergenic	TTGCAAGCTACTTGAAGCCTGGG	3	no
chrX:128332989-128333009	intergenic	TTGCAAGCTTTTTAAATCCTTGG	3	no
chr1:69424091-69424113	intergenic	GTGAAAACTTCTTAAAGGATGGG	4	no
chr2:27852632-27852654	intron *GPN1*	GTGCAATATTCTTAAGGCATGGG	4	no
chr2:99368471-99368493	intergenic	GTGGCAGCTTCTCAAAGCATTGG	4	no
chr6:58655505-58655527	intergenic	GTGCATGCTACTTAAAGTATAGG	4	no
chr7:78196869-78196891	intron *MAGI2*	GTGCAAGCTAATTAAAGGATTGG	4	no
chr9:36328950-36328972	intergenic	GTACAAGCTTCTTAATGCACAGG	4	no
chr15:81904154-81904176	intergenic	GTGCAAGGTTCATAAAGCAGGGG	4	no
chr18:36562574-36562596	intergenic	GAGCAAGCTTATTAAAGCAGAGG	4	no

Table S2. Sequence analysis of predicted off-target loci of sgRNA1 and sgRNA2 corrected organoids (related to Figure 1). The clones SI_c1 and SI_c2 were analyzed. Genomic DNA sequences with 1-3 mismatches to the sgRNAs were computationally identified in the human reference genome (GRCh37/hg19), and analyzed by Sanger sequencing. In addition also a few less likely off-target loci with 4 mismatches to the sgRNA were analyzed. PAM sequence is shown in blue, mismatches in the protospacer sequence are highlighted in red. Only 1 heterozygous insertion was found in a sgRNA1 off-target site.

Chapter 9

General discussion

Since June 2015, approximately 35 Dutch CF subjects expressing specific gating mutations are receiving KALYDECO™ (VX-770 / ivacaftor), 'the most important new drug of 2012' according to Forbes magazine. The success of this life changing treatment, approved for ~5% of all CF subjects, has prompted a huge worldwide effort to ensure that the majority of CF patients, if not all, can receive 'curative' treatments in the future. What crucial steps are needed to ensure that 100% of CF subjects can receive effective treatments, and what role can intestinal organoids play? This chapter discusses (i) the characteristics of organoid-based CFTR measurements in relation to other functional CFTR readouts, and how organoids can contribute to (ii) the development of novel CF therapies, (iii) facilitate the development of personalized / precision medicine and (iv) may impact drug development and therapy of diseases other than CF.

HOW DO ORGANOIDS RELATE TO EXISTING *IN VITRO* CELL MODELS?

A variety of assays is available to study CFTR function *in vitro*, *ex vivo* and *in vivo*. Their value is largely dependent on the context of a study, i.e. the strengths and weaknesses of each assay determine for what purpose it can be used best (**Table 1**). For CF, assays gain value when they recapitulate the human *in vivo* pulmonary CFTR function as accurate and simple as possible, with as limited impact on subjects as possible.

Cell lines

The CF community has classically relied on a variety of cell line models that have been successfully used for drug identification and development[1,2], defining the disease liability of a large variety of the most relevant *CFTR* mutations[3], and stratify patient subgroups for mutation-specific CFTR therapies[4-9]. Their strength is simplicity in terms of culturing, costs and CFTR function analysis. However, cell lines are prone to artifacts inherent to heterologous CFTR (over) expression[10]. Efficacy of compounds can be variable between different cell lines, and many CFTR-function restoring compounds identified in cell lines are not active in primary cells. The recent extension study for KALYDECO™ to non-G551D gating mutations also showed that 1 out of 9 selected mutations (G970R) based on cell line studies did not respond[7,9], further indicating that CFTR expression systems in cell lines do not always faithfully recapitulate mutant CFTR function.

Primary pulmonary models

Primary epithelial cell models express endogenous CFTR and further provide an individuals' cellular context, including polymorphisms in the *CFTR* gene and CF modifier genes. Classical human bronchial epithelial (HBE) cells are generated from lung explants or biopsies, but loose their capacity to self-renew and differentiate upon passaging[11,12]. Availability and compliance substantially limit acquisition of primary bronchial cultures from individuals with rare *CFTR* genotypes, but cultures from nasal cells can compensate for this. Recently developed protocols indicate that basal cells can retain stemness by 'conditionally reprogramming' cells using a layer of fibroblast feeder cells and Rho kinase inhibitor (ROCK). These cultures are karyotype-stable, nontumorigenic and are claimed to provide an infinite cell source[13-15]. Progress has also been reported in differentiating induced pluripotent stem cells (iPSCs) into airway cells[16]. This approach generates a limitless supply of patient-specific cells, but technical advances are needed

Model	Functional CFTR assay	Throughput	Applications	Specific pro's	Specific con's
Cell lines	Fluorescence-based assays Ussing chamber TCM	High, unlimited culturing	High-throughput screening Hit-to-lead drug development Define the consequence of CFTR variants Selection of drug-responsive CFTR variants	Inexpensive Simple culturing Widely available No burden to subjects	Prone to artifacts Difficult to study complex alleles No subject specificity
HBE cells	Ussing chamber TCM	Medium, limited by amount of ussing chambers and proliferation capacity	Hit-to-lead drug development Personalized drug development Biobanking	Respiratory origin Patient-Specific	Short-lived Availability & Compliance Complex culture medium & protocols Complex functional readout
CRCs	Ussing chamber TCM	Medium, limited by amount of ussing chambers	Personalized drug development Biobanking (sustainable)	Respiratory origin Patient-Specific Long-lived Possible from nasal cells	Complex culture medium & protocols Complex functional readout Long-term stability not defined
iPSCs	Ussing chamber TCM	Medium, limited by amount of Ussing chambers	No current application	Possible from many cell types Patient-specific Unlimited cuturing	Genetic instability Unoptimized culture protocols Complex functional readout
Rectal organoids	Forskolin-induced swelling (FIS) Steady-state lumen area (SLA)	High, unlimited culturing	CF diagnosis Hit-to-lead drug development (Personalized) drug development Possibly high-throughput screening Biobanking (sustainable)	Patient specific Highly sensitive (FIS) Simple & robust readout Unlimited cuturing Genetic & phenotypic stability Low patient burden	May not fully reflect the lung Difficult to access apical site Complex culture medium Available in few centers
Rectal biopsies	Ussing chamber ICM	In 4-8 data points	CF diagnostics *Ex vivo* drug efficacy studies	Sensitive Easy application in young children Measures both Cl^- and HCO_3^- transport Study of CFTR modulation in native tissue	Short viability of biopsies Requires experienced staff Some adults are reluctant
Nasal epithelium	Nasal potential difference	1-2 data point(s)	Diagnostic biomarker Measure for *in vivo* drug efficacy	Reflects the respiratory tract Responses to *in vivo* treatment	Requires experience staff Large intra-subject variability Difficult to perform in young children
Sweat duct	Sweat chloride test	1-2 data point(s)	Diagnostic biomarker Measure for *in vivo* drug efficacy	Widely available Cheaper than ICM and NPD Not influenced by infections	Biomarker for systemic treatments only Large intra-subject variability
Sweat duct	β-adrenergic sweat secretion	Limited data points	Diagnostic biomarker Measure for *in vivo* drug efficacy	Assay is linear at high CFTR function	Biomarker for systemic treatments only Available in few centers

Table 1. Overview of models to measure CFTR function. (HBE = human bronchial epithelial; CRC = 'conditionally reprogrammed' cells; iPSC = induced pluripotent stem cell; TCM = trans-epithelial current measurement; FIS = forskolin-induced swelling; SLA = steady state lumen area)

to ensure their genomic integrity and optimal airway differentiation protocols[17]. The functional CFTR readout in these cultures is complex: proper generation of polarized, differentiated airway epithelium requires transfer of basal cells to filters that are exposed to air for several weeks after which transepithelial current measurements in Ussing chambers are performed. This methodology is time consuming, technically challenging, costly and has limited throughput.

Intestinal organoids

The forskolin-induced swell assay in organoids is completely dependent of CFTR, robust and requires only a simple experimental setup. The unlimited culture capacity allows for the generation of large data sets from individual subjects within several weeks after isolation, and cells auto-differentiate into polarized, multicellular epithelial structures that recapitulate the *in vivo* tissue hierarchy. In addition to previous studies indicating that organoids are genetically stable[18-21], we extent these observations by showing that patient-specific drug responses are stable over 6 months of culturing and independent of biobanking (**Chapter 7**). Within a few years, we established over 200 primary rectal organoid cultures at a success rate of approximately 95%. The biobanking of these cells will provide a sustainable source of primary cells for CF studies. However, various challenges are also associated with the organoid methodology:

1. *Intestine versus airway:* Responses of intestinal cells may not fully represent responses of airway cells, which may be especially relevant for drugs that target the CFTR proteostasis network. Up until now, organoid cultures resemble functional responses of airway cultures in terms of dose-dependencies to VX-809 and VX-770 (**Chapter 2**[22] **and 5**)[23,24], and hierarchy of CFTR modulator efficacies (**Chapter 2**[22]**, 4 and 5**)[22,25]. Responses furthermore reflect the hierarchy of *CFTR* mutations regarding residual CFTR function or response to VX-809 and VX-770 observed in cell lines (**Chapter 2**[22]**, 4, 5 and 7**)[8,9]. Whereas primary HBEs remain the gold standard in the field, the validation of CFTR function measurements in organoids as predictive model for *in vivo* disease severity and therapy is now actually stronger: we demonstrated the largest genotype-phenotype relation in primary cells thus far and indicated a positive correlation between responses in organoids and response *in vivo* (both for residual function and therapy), and only this model has been successfully used to prospectively select individuals for therapy (**Chapter 7**). In addition, we do not see the drastic downregulation of VX-809-corrected F508del-CFTR by chronic VX-770 treatment (**Chapter 7**), which was recently reported in HBE[26,27] and is not consistent with *in vivo* efficacy of treatment[28,29]

2. *3D versus 2D:* It is difficult to access the apical region and perform direct CFTR ion transport studies. Using protocols described recently[30] and in collaboration with Prof. Edward E.S. Nieuwenhuis and Dr. Sabine Middendorp (University Medical Centre, Utrecht), we are establishing 2-D monolayers grown on filters from intestinal CF and wild-type organoids, which facilitate transepithelial current measurements in Ussing chambers. This would open new opportunities for the study of CFTR modulation, but also the easier study of apical secretions and host-pathogen interactions.

3. *Standardization of culture reagents.* Due to the lack of fully synthetic, commercially available culture reagents, our studies have used three types of conditioned media to generate organoid culture medium. Although we used quality control criteria for the conditioned media, full standardization over long time periods remains difficult. It is relatively easy to produce medium batches that generate viable cultures, but standardization of culture conditions so that a functional assay performs stable in time adds another layer of complexity. Fully synthetic components may allow further optimization of the assay.

4. *Increasing assay throughput.* The set up of the forskolin-induced swell assay allows one person already to generate hundreds of data points (one data point = 96-well with 20-100 organoids) per week (~750 max). The assay can be upgraded to higher throughput as we have demonstrated that automated dispension of organoids and compounds in 384-wells format is feasible. The generation of sufficient cell numbers is technically feasible, but costly compared to cell lines. Nevertheless, a 384-wells setup is expected to further increase the quality and throughput of the assays.

HOW DO ORGANOID ASSAYS RELATE TO HUMAN BIOASSAYS?

The sweat chloride concentration (SCC), nasal potential difference (NPD) measurement and intestinal current measurement (ICM) are current diagnostic markers. They have demonstrated that CFTR residual function levels associate with the *CFTR* genotype and disease severity at group level[3,31-40] (**Chapter 1**). Complementation of different human biomarkers (**Table 1**) is useful for the optimal definition of an individual's diagnosis, prognosis and response to therapy.

Organoid assays as diagnostic biomarker

The sweat chloride test has a wide dynamic window that discriminates between different phenotypes at group level (severe CF, mild CF, CFTR related diseases, carriers and healthy control; **Fig. 1**). However, its diagnostic limitation results from great overlap in SCC between individuals from different groups. NPD and ICM have different dynamic windows (**Fig. 1**), and are especially useful to diagnose subjects with an intermediate or borderline sweat test (30<SCC<60)[3,31-35,37,39-41]. Still, diagnosis can be difficult in some cases[42]. The recently introduced β-adrenergic sweat secretory test exclusively discriminates CF patients from healthy controls and is the first biomarker that measures half-maximal function in heterozygotes carrying one *CFTR* mutation[41], providing the opportunity to define the amount of CFTR function needed to cure CF. We can type the steady-state lumen area assay as having a dynamic window at high CFTR function and being discriminative between CF and non-CF at the individual level, and between class I-III and class IV-V mutant organoids at group level (**Fig. 1; Chapter 7**). Compared to the classical biomarkers, both the β-adrenergic sweat secretory test and steady-state lumen area assay seem to have better capacity to discriminate CF from healthy controls, but application is limited to a few specialized centers and these assays need further validation. An advantage of organoids is that rectal biopsies can be relatively easily isolated and shipped to specialized centers for standardized analysis. For now, the main diagnostic opportunity of organoid-based measurements is to complement the classical diagnostic tests in uncertain cases.

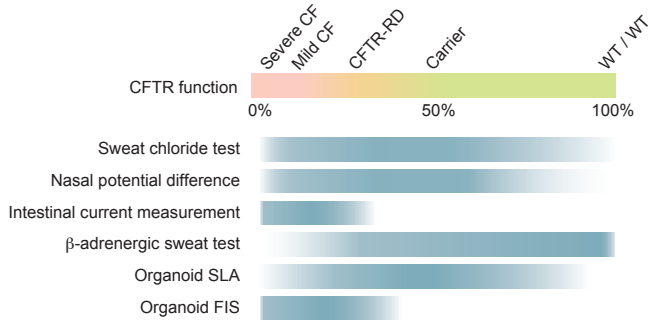

Figure 1. Difference in dynamic window of subject-specific functional CFTR readouts. (CFTR-RD = CFTR-related disease; WT = wild-type; SLA = steady state lumen area; FIS = forskolin-induced swelling)

Organoid assays as prognostic biomarker

The classical CFTR-dependent biomarkers depend on single or several data points per individual and associate with considerable technical and biological variability. Repeated measurements to accurately type residual CFTR function are costly and time-consuming. For this reason, the value of these methods has mainly been demonstrated for diagnosis[43,44]. By contrast, organoid-based measurements allow for the generation of large data sets to control for intra- and inter-experimental variation and accurate definition of the individual's residual CFTR function. The FIS assay, which has a dynamic window at low CFTR function (**Fig. 1**), has been used to discriminate between residual CFTR function in organoids with different or identical *CFTR* mutations (**Chapter 2**[22] **and 7**). Both cross-sectional and longitudinal correlation studies are required to assess whether CFTR function in organoids is predictive for the progression of (lung) disease.

Organoid assays as therapeutic biomarker

Since the arrival of novel CFTR-targeting drugs, the field is exploring the use of CFTR-dependent *in vivo* readouts to monitor treatment effects, mostly at the group level. The SCC, NPD and β-adrenergic sweat test have been successfully used to measure effects of CFTR-repairing treatment in clinical trials[43,44] (**Chapter 7**), illustrating their potential as therapeutic biomarkers. No studies have used ICM as endpoint so far, but the potential to investigate CFTR modulators in native rectal tissue has been provided[45] (**Chapter 5**). However, our studies also indicate that this tissue is likely not well penetrated by CFTR potentiators(**Chapter 5**), which hampers the use of *ex vivo* rectal biopsies for assessment of individual potentiator efficacy. Individual relations between FEV_1 and direct *in vivo* CFTR biomarkers have not been identified[46,47], suggesting no relation between these markers, or that the impact of variation of these measures is too big.

Organoids are not suited to directly measure the *in vivo* drug efficacy, because treatment effects are washed out upon culture. However, they provide a cost-effective platform for preclinical drug efficacy testing for the individual. Organoid responses may correlate better with clinical endpoints than the classical biomarkers due to the highly accurate measurements. In addition, in clinical settings they can be used to model the individual pharmacokinetics by stimulating organoids with patient plasma in the FIS assay[48] (**Chapter 6**). Recent data indicated that we can detect high KALYDECO™ activity in plasma of the 2 subjects with G1249R (**Chapter 7**), and that both samples associated with a different VX-770 activity (Group JM Beekman, unpublished). Although further

validation is required, for the first time we have the opportunity to monitor and possibly predict the efficacy of treatment per individual based on *in vitro* modeling of pharmacodynamic and pharmacokinetic properties.

THE DEVELOPMENT OF NOVEL CF THERAPIES

We have provided evidence that organoids can be used to study therapeutic interventions for all mutational classes of CFTR, using a variety of genetic and pharmacological approaches (**Fig. 2**). This indicates that intestinal organoid studies can play a prominent role in drug development for the majority of patients. Below, I discuss some of the essential lessons that we have learned from different approaches to repair CFTR in intestinal organoids, and the potential impact for patients.

One-size-fits-all: *CFTR* gene repair

The limited success of previous *CFTR* gene therapy trials supports the need to further improve *CFTR* gene delivery. Ideally, lung stem cells are targeted to provide long-term benefits, but up until now their exact nature remains unclear. The definition of viral components that achieve high transduction efficiency of airway cells needs further attention. In addition, we still do not know how many cells in the lungs need to be transduced to normalize the mucosal secretions: i.e. can 10% of cells with normal levels of wild-type CFTR function act as an epithelial portal for ions to compensate for the lack of ion transport in the other 90% of cells?

Together with the group of Prof. Eric Alton (Imperial College Londen, UK) and Prof. Zeger Debyser (KU Leuven, Belgium) we have provided proof-of-concept that rAAV2/5- or Sendai/Lenti-based vectors can successfully deliver functional CFTR in adult intestinal stem cells (unpublished). We also found that despite considerable amounts of wild-type *CFTR* were transduced (high level of CFTR C-band levels), the overall activity was lower than expected when compared to VX-809-corrected C-band levels. This may indicate that low but homogenously distributed CFTR

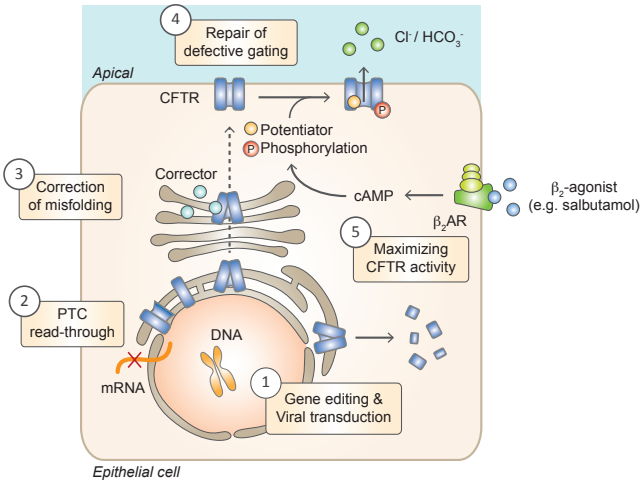

Figure 2. Overview of approaches used to repair CFTR in organoids. Therapies that target defects in CFTR biosynthesis at various levels to restore ion transport across the apical membrane provide opportunities for curative CF treatment. Functional CFTR measurements in organoids have facilitated the development, validation and mechanistic understanding of strategies to (1) correct *CFTR* at the DNA level, (2) induce read-through of premature termination codons, (3) correct CFTR folding and trafficking and (4 & 5) enhance CFTR activity at the plasma membrane.

function is more favorable than a high function in fewer cells, or that cDNA-CFTR is less effectively translated into functional protein. From these studies, it is clear that intestinal organoids have potential to assist in the development of viral vectors. Pulmonary organoids will be more suited to select appropriate vectors that can transduce airway cells.

Intestinal CF organoids were also used to generate proof-of-concept of *CFTR-F508del* gene correction by CRISPR/Cas9-mediated homologous recombination (HR) in primary adult stem cells (**Chapter 8**[49]). This study opens the opportunity to regenerate CF organs *in vivo* with autologous gene-corrected stem cells. Studies in mice already demonstrated that organoids can successfully integrate in the intestine or liver[50,51]. The success of this technique to treat lung disease in CF subjects will depend on (i) the development of protocols to robustly expand pulmonary stem cells, (ii) generation and selection of stem cells that harbor the exact genetic change without off-target effects, (iii) efficient engraftment of stem cells into the lungs, and (iv) long-term safety of integrated cells. Recently established culture conditions for long-term expansion of pulmonary organoids (Prof. Hans Clevers *et al*, Hubrecht laboratory, Utrecht, unpublished data) can enable the study of these critical steps in relevant CF animal models.

In addition, organoids have been generated from other severely affected tissues in CF[19,51,52], providing opportunities for regenerative medicine of pancreatic and liver-associated CF disease. However, alternative therapeutic approaches, such as *in vivo* gene therapy and systemic pharmacotherapy, may limit the incentive for development of these experimental procedures that hold a promise to 'cure' organ-specific manifestations of CF.

MUTATION-SPECIFIC TREATMENTS BY SMALL MOLECULES

Correcting CFTR trafficking

Together with Prof. Gergely Lukacs (McGill University, Montréal, Canada), we demonstrated in organoids that compounds targeting distinct sites within CFTR-F508del synergize with VX-809 to correct the folding defect (**Chapter 3**)[25]. Based on this work and other studies, 'second-generation' screens have been performed to search for compounds that target specific folding defects in CFTR-F508del or that synergize with VX-809 to overcome the 'efficacy ceiling' of corrector mono-therapy[53]. Indeed, the first corrector combinations will soon be clinically tested in a Vertex-sponsored trial with two correctors and KALYDECO™ in F508del homozygotes. As expected from *in vitro* data, corrector combination treatment together with a potentiator may drastically exceed the efficacy of the current small molecule approaches for CFTR-F508del and push mutant CFTR function into a range associated with limited or no disease.

How to correct other folding defects, i.e. is VX-809 the most optimal corrector for each folding mutation, or only for F508del? In **Chapter 4**, we demonstrated that distinct folding mutants require different correctors for optimal functional repair and identified bithiazoles as the most promising compounds to correct CFTR-A455E. We used these data to search for existing drugs with similarities to these bithiazoles together with Dr. Andre Falcao (University of Lisbon, Portugal) who develops *in silico* models to quantitate chemical space relations between compounds[54,55]. Using

this algorithm, we have screened >300.000 compounds and identified experimental compounds (using Chembl database) and approved drugs (using DrugBank) that have similar properties in terms of chemical space to the four bithiazoles, which are now being evaluated for efficacy of CFTR-A455E repair. This approach could be a cost-effective method to repurpose existing drugs for rare *CFTR* mutations.

In addition, we found with Prof. William Balch (The Scripps Research Institute, la Jolla, CA), that CFTR-F508del misfolding induces an adaptive stress response that further exacerbates the disease state. Restoration of the adaptive stress response restores the cellular protein folding and improves the disease phenotype, supporting the use of proteostasis modulators to treat CF[56]. Thus, normalizing and perhaps even lowering the fidelity of the protein folding quality control system appears a valid strategy to increase the function of mutated CFTR, especially in the context of correctors, such as VX-809.

CFTR potentiators: potentiate the potentiator

Because current potentiator treatment in subjects with a gating mutation does not normalize CFTR-dependent biomarkers[4-7,57], more effective potentiator strategies are needed. In a collaborative project with Dr. Hugo de Jonge (Erasmus University Medical Center, Rotterdam), we have shown that combining potentiators may provide a novel approach to target defective CFTR gating (**Chapter 5**), which is in line with corrector combinations to efficiently repair CFTR trafficking (**Chapter 3**). Based on these findings, the combination of VX-770 and the natural food component genistein is currently being clinically assessed in Dutch patients with the S1251N mutation. Results of the trial may not only support potentiator combination therapy for CF, which becomes especially relevant when multiple potentiators are commercially available, but also highlight the potential of inexpensive food supplements to modulate CFTR, as was suggested by others[58].

CFTR activators

A limited but significant *in vivo* effect of oral salbutamol treatment in subjects with residual CFTR function was accompanied by a modest induction of CFTR activity when plasma was used to stimulate organoids *in vitro* (**Chapter 6**). These data suggest that CFTR can be activated by existing drugs beyond levels associated with endogenous CFTR activity, and that higher dosing of β_2-agonists may further improve efficacy of treatment. However, systemic side effects may prevent such applications. The efficacy and safety profile of follow-up studies will further define the clinical potential of chronic β_2-agonist treatment to maximize residual CFTR function or efficacy of direct CFTR-repairing drugs. As part of a project of Dr. Hugo R. de Jonge (Erasmus University Medical Centre, Rotterdam), we are furthermore exploring the role of CFTR activation via cyclic guanosine monophosphate(cGMP)-dependent signalling in organoids (unpublished).

PTC read-through in organoids with nonsense mutations

Organoids have also been used to modulate *CFTR* mRNA translation by premature termination codon (PTC) read-through agents (van Ommen & Vijftigschild *et al*, manuscript submitted). In line with previous studies[59-63], the aminoglycoside G418 induced low but detectable read-through

of *CFTR* nonsense mutations in organoids, while no functional read-through was induced by PTC124. However, lack of functional PTC124 in organoids is conflicting with subject-specific PTC124 activity reported in open-label phase 2 trials[64-66], and with retrospective analysis of the phase III trial data that suggest mild clinical efficacy in tobramycin-free subjects[59]. Mechanisms for these discrepancies are unclear, but may depend on model specificity. When G418-induced CFTR function in organoids was further stimulated with VX-809 and VX-770, the level of function only reached that of untreated F508del homozygous organoids. Together, data suggest that compounds need to be developed that have drastically improved efficacy, and these may still only work in combination with CFTR-protein-targeting drugs.

THE DEVELOPMENT OF PERSONALIZED/PRECISION MEDICINE FOR CF USING ORGANOIDS

Stratification of CF subjects is important to maximize the cost-effective use of CFTR-repairing drugs, while reducing side effects that may result from life-long treatments starting at a young age. Inclusion of specific subgroups for clinical trials with CFTR modulators depends on defining drug-responsive CFTR variants *in vitro*, in combination with specific inclusion and exclusion criteria based on individual clinical disease parameters. This model has been successfully used to provide (i) licensing of KALYDECO™ for subjects with G551D[4-6], and eight other gating mutations[7], (ii) FDA-approval of KALYDECO™ for patients with R117H and (iii) FDA-approval of Okrambi™ (VX-809 + VX-770) for F508del homozygotes[29]. Similarly, based on efficacy data in organoids (**Chapter 7**), we are currently preparing a Vertex-sponsored clinical trial for Okrambi™ treatment of Dutch subjects with A455E. Although this model of clinical trial design has been proven to be effective, it is also costly and time-consuming, as took three years to extent KALYDECO™ to 9 non-G551D mutations.

Because conventional, adequately powered randomized controlled trials cannot be applied to individuals or small patient subgroups, alternative drug development pathways are required for drug licensing and coverage for CF patients with rare *CFTR* mutations. The 'adaptive pathways approach' is part of the European medicines agency's (EMA) efforts to improve timely access for patients to new medicines. It involves early discussion between a wide range of stakeholders to explore ways for optimizing drug development and reimbursement[67,68]. For example, Ataluren (PTC124) has recently been conditionally approved for Duchenne muscular dystrophy patients, which have a serious unmet medical need. Either full approval or withdrawal of the product depends on the complete safety and efficacy profile of an ongoing phase III clinical trial.

In this context, Dutch regulatory agencies, insurance companies, Vertex, the non-profit organization Hubrecht Organoid Technology (the HUB), CF clinicians and the Dutch CF patient foundation are discussing the conditional approval of KALYDECO™ for subjects expressing rare *CFTR* mutations based on organoid measurements. Proof-of-concept that organoids can be used to successfully select KALYDECO™ responders was provided in **Chapter 7**. The approach may be designed as follows (**Fig. 3**): (i) conditional approval is provided for subjects identified as KALYDECO™-responders in organoids (criteria for *in vitro* responders and non-responders should be defined), (ii) efficacy of treatment is assessed in a 'n-of-1' trial by intensive monitoring

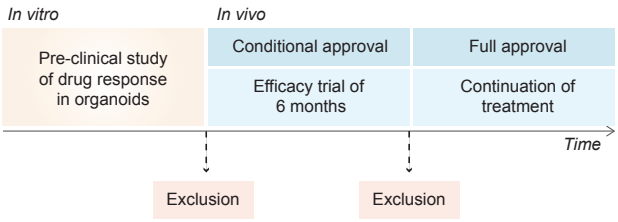

Figure 3. Alternative pathway to extend KALYDECO™ treatment to patients with rare *CFTR* mutations.

(e.g. spirometry, SCC, NPD, ICM, drug activity in plasma) in cycles where drug and placebo are double-blindly administered and assessed, and (iii) decisions for full approval are based on the individual's safety and efficacy profile (criteria for *in vivo* responders and non-responders should be defined).

The approval of Okrambi™ for ~50% of the CF population and the indication of KALYDECO™ for an increasing number of *CFTR* mutations also raises concerns: how can we maintain a sustainable, economically viable healthcare system when potential life-saving treatments are priced at 150.000-200.000 euros per person per year? Because the clinical efficacy of Okrambi™ was limited, and highly variable between F508del homozygous individuals[28,29], stratification within this population may be important to increase cost-effectiveness of treatment. Organoid-based measurement can define high and low Okrambi™ responders (**Chapter 2**[22] **and 7**), but the clinical relevance of these differences needs to be further defined. Recruitment of Dutch F508del homozygotes for the Phase III VX-661 and VX-770 combination trial will allow us to generate prospective associations. In addition to optimizing stratification methods, economic competition or drug extension to patients with non-CF conditions may reduce the high costs associated with these potential life-saving CF treatments.

For now, the main opportunity of organoids is to stratify subjects with rare *CFTR* mutations for KALYDECO™ treatment and shorten the time to reimbursement. The inclusion of CF subjects for Dutch clinical trials (described above), together with the recent introduction of KALYDECO™ for 35 Dutch CF subjects, will allow us to further establish *in vitro-in vivo* relations and define the model's predictive therapeutic capacity. Organoid-based measurements may even gain more value in the future when multiple CFTR modulators are available: the patient-specific profile of the response to single drugs as well as combinations can be defined, without additional burden to the subject.

SWELLING BEYOND CYSTIC FIBROSIS

Agonist-induced volume changes in organoids may have impact for non-CF conditions as well. Recently, cigarette smoking and chronic obstructive pulmonary disease was found associated with reduced CFTR function, suggesting that potentiators may be beneficial for this disease that is currently the 3rd leading cause of deaths in the US[69,70]. Given the central role of CFTR in pulmonary mucus biology and innate defense, other diseases associated with aberrant mucus production and infections may also benefit from CF therapeutics, such as CFTR potentiators or activators that aim to increase CFTR function.

At the other end of the spectrum, CFTR gain-of-function diseases include secretory diarrhea that results from pathogens that activate CFTR function (such as V. cholera), and cause ~4% of all deaths worldwide. Currently, oral rehydration solution-based therapy can be used to replenish the loss of salts and water, but these interventions do not reduce the CFTR hyperactivity[71]. As we found that cholera toxin induces rapid organoid swelling (**Chapter 2**[22]), we have used organoids to confirm that cheap sugar-based structures can inhibit cholera toxin-induced CFTR function (in collaboration with Prof. Roland Pieters, Utrecht University, unpublished). Others have adapted assay conditions to measure osmotic- or cholera toxin-dependent volume changes of murine jejunal organoids trapped in a "pinball machine-like" array during continuous superfusion, without fluorescent labeling or presence of matrigel[72]. This method allows measuring the same organoid upon addition of successive stimuli that directly reach the organoid. However, compared to the initial assay[22], the throughput is highly decreased and organoid viability in these conditions limits prolonged incubations with compounds. Prof. Mark Donowitz and coworkers (Johns Hopkins hospital, Baltimore, USA) recently showed that human intestinal organoids recapitulate both chloride secretion via CFTR as well as sodium absorption via the Na^+/H^+ exchanger NHE3[73], two important processes for the pathophysiology of diarrhea. They are now establishing assay conditions to measure function of NHE3.

Protocols have also been developed to grow human epithelial organoids from the gut, liver, pancreas, prostate and stomach[19,51,52,74-76]. Collaborators found agonist-induced swelling for several of these organoids, indicating a simple swell readout can form the basis for other ion channel assays and drug discovery efforts. The generation of knockdowns by the CRISPR/Cas9 methodology (**Chapter 8**[49]) can assist to pinpoint dependency of volume changes to specific channels, and develop novel organoid-based assays to select modulators of various ion channels that couple to fluid secretion.

The precision or personalized medicine approach that we pioneer for CF may be used for other diseases. The monogenetic origin of CF and the existence of non-biased CFTR dependent readouts *in vivo*, such as SCC and NPD, are excellent conditions to setup and validate the use of organoids as tool for personalized medicine in CF, especially for CFTR targeting drugs. Understanding the relations between the *CFTR* genotype, protein function and response to therapy in CF will be important to develop similar approaches for complex genetic diseases such as cancer, in which the treatment window and genetic diversity are far more challenging as compared to CF[77].

CONCLUDING REMARKS

It started with a remarkable observation: forskolin induces rapid swelling of wild-type organoids. Only four years later, work at the bench has generated impact at the bedside: two Dutch subjects have been successfully selected for the first CFTR-targeting treatment based on organoids. This thesis describes the first steps in the development of a laboratory model that can accurately define an individual's residual CFTR function and response to therapy. The potential of the model has been provided, validation of its predictive capacity is next. These studies in organoids helped us to better understand relations between the *CFTR* genotype, residual CFTR function, and response

to therapy, and have facilitated the development of CFTR-targeting therapies and precision/personalized medicine. They will undoubtedly play an important role in the development of future therapeutic options that aim to bring curative treatments to all CF subjects.

REFERENCES

1. Rowe, S. M. & Verkman, A. S. Cystic fibrosis transmembrane regulator correctors and potentiators. *Cold Spring Harb Perspect Med* **3,** (2013).
2. Verkman, A. S. & Galietta, L. J. V. Chloride channels as drug targets. *Nat Rev Drug Discov* **8,** 153–171 (2009).
3. Sosnay, P. R. *et al.* Defining the disease liability of variants in the cystic fibrosis transmembrane conductance regulator gene. *Nat. Genet.* **45,** 1160–1167 (2013).
4. Accurso, F. J. *et al.* Effect of VX-770 in persons with cystic fibrosis and the G551D-CFTR mutation. *N. Engl. J. Med.* **363,** 1991–2003 (2010).
5. Ramsey, B. W. *et al.* A CFTR potentiator in patients with cystic fibrosis and the G551D mutation. *N. Engl. J. Med.* **365,** 1663–1672 (2011).
6. Davies, J. C. *et al.* Efficacy and safety of ivacaftor in patients aged 6 to 11 years with cystic fibrosis with a G551D mutation. *Am. J. Respir. Crit. Care Med.* **187,** 1219–1225 (2013).
7. De Boeck, K. *et al.* Efficacy and safety of ivacaftor in patients with cystic fibrosis and a non-G551D gating mutation. *J. Cyst. Fibros.* **13**: 674–80 (2014).
8. Van Goor, F., Yu, H., Burton, B. & Hoffman, B. J. Effect of ivacaftor on CFTR forms with missense mutations associated with defects in protein processing or function. *J. Cyst. Fibros.* **13,** 29–36 (2014).
9. Yu, H. *et al.* Ivacaftor potentiation of multiple CFTR channels with gating mutations. *J. Cyst. Fibros.* **11,** 237–245 (2012).
10. Ikpa, P. T., Bijvelds, M. J. C. & de Jonge, H. R. Cystic fibrosis: Toward personalized therapies. *Int. J. Biochem. Cell Biol.* **52**, 192-200 (2014).
11. Karp, P. H. *et al.* An in vitro model of differentiated human airway epithelia. Methods for establishing primary cultures. *Methods Mol. Biol.* **188,** 115–137 (2002).
12. Neuberger, T., Burton, B., Clark, H. & Van Goor, F. Use of primary cultures of human bronchial epithelial cells isolated from cystic fibrosis patients for the pre-clinical testing of CFTR modulators. *Methods Mol. Biol.* **741,** 39–54 (2011).
13. Suprynowicz, F. A. *et al.* Conditionally reprogrammed cells represent a stem-like state of adult epithelial cells. *Proc. Natl. Acad. Sci. U.S.A.* **109,** 20035–20040 (2012).
14. Palechor-Ceron, N. *et al.* Radiation induces diffusible feeder cell factor(s) that cooperate with ROCK inhibitor to conditionally reprogram and immortalize epithelial cells. *Am. J. Pathol.* **183,** 1862–1870 (2013).
15. Liu, X. *et al.* ROCK inhibitor and feeder cells induce the conditional reprogramming of epithelial cells. *Am. J. Pathol.* **180,** 599–607 (2012).
16. Wong, A. P. *et al.* Directed differentiation of human pluripotent stem cells into mature airway epithelia expressing functional CFTRTR protein. *Nat. Biotechnol.* **30,** 876–882 (2012).
17. Liang, G. & Zhang, Y. Genetic and epigenetic variations in iPSCs: potential causes and implications for application. *Cell Stem Cell* **13,** 149–159 (2013).
18. Middendorp, S. *et al.* Adult stem cells in the small intestine are intrinsically programmed with their location-specific function. *Stem Cells* **32,** 1083–1091 (2014).
19. Huch, M. *et al.* Long-term culture of genome-stable bipotent stem cells from adult human liver. *Cell* **160,** 299–312 (2015).
20. Sato, T. *et al.* Single Lgr5 stem cells build crypt-villus structures in vitro without a mesenchymal niche. *Nature* **459,** 262–265 (2009).
21. Sato, T. *et al.* Long-term Expansion of Epithelial Organoids From Human Colon, Adenoma, Adenocarcinoma, and Barrett's Epithelium. *Gastroenterology* **141**: 1762–72 (2011).
22. Dekkers, J. F. *et al.* A functional CFTR assay using primary cystic fibrosis intestinal organoids. *Nat Med* **19**: 939–45 (2013).
23. Van Goor, F. *et al.* Correction of the F508del-CFTR protein processing defect in vitro by the

investigational drug VX-809. *Proc. Natl. Acad. Sci. U.S.A.* **108,** 18843–18848 (2011).

24. Van Goor, F. *et al.* Rescue of CF airway epithelial cell function in vitro by a CFTR potentiator, VX-770. *Proc. Natl. Acad. Sci. U.S.A.* **106,** 18825–18830 (2009).

25. Okiyoneda, T. *et al.* Mechanism-based corrector combination restores ΔF508-CFTR folding and function. *Nat. Chem. Biol.* **9,** 444–454 (2013).

26. Veit, G. *et al.* Some gating potentiators, including VX-770, diminish ΔF508-CFTR functional expression. *Sci Transl Med* **6,** 246ra97 (2014).

27. Cholon, D. M. *et al.* Potentiator ivacaftor abrogates pharmacological correction of ΔF508 CFTR in cystic fibrosis. *Sci Transl Med* **6,** 246ra96 (2014).

28. Boyle, M. P. *et al.* A CFTR corrector (lumacaftor) and a CFTR potentiator (ivacaftor) for treatment of patients with cystic fibrosis who have a phe508del CFTR mutation: a phase 2 randomised controlled trial. *Lancet Respir Med* (2014). doi:10.1016/S2213-2600(14)70132-8

29. Wainwright, C. E. *et al.* Lumacaftor-Ivacaftor in Patients with Cystic Fibrosis Homozygous for Phe508del CFTR. *N. Engl. J. Med.* (2015). doi:10.1056/NEJMoa1409547

30. Moon, C., VanDussen, K. L., Miyoshi, H. & Stappenbeck, T. S. Development of a primary mouse intestinal epithelial cell monolayer culture system to evaluate factors that modulate IgA transcytosis. *Mucosal Immunol* **7,** 818–828 (2014).

31. Knowles, M. R., Paradiso, A. M. & Boucher, R. C. In vivo nasal potential difference: techniques and protocols for assessing efficacy of gene transfer in cystic fibrosis. *Hum. Gene Ther.* **6,** 445–455 (1995).

32. de Jonge, H. R. *et al.* Ex vivo CF diagnosis by intestinal current measurements (ICM) in small aperture, circulating Ussing chambers. *J. Cyst. Fibros.* **3 Suppl 2,** 159–163 (2004).

33. Wilschanski, M. *et al.* Mutations in the cystic fibrosis transmembrane regulator gene and in vivo transepithelial potentials. *Am. J. Respir. Crit. Care Med.* **174,** 787–794 (2006).

34. Bronsveld, I. *et al.* Residual chloride secretion in intestinal tissue of deltaF508 homozygous twins and siblings with cystic fibrosis. The European CF Twin and Sibling Study Consortium. *Gastroenterology* **119,** 32–40 (2000).

35. Sousa, M. *et al.* Measurements of CFTR-mediated Cl- secretion in human rectal biopsies constitute a robust biomarker for Cystic Fibrosis diagnosis and prognosis. *PLoS ONE* **7,** e47708 (2012).

36. Knowles, M. R. *et al.* Abnormal ion permeation through cystic fibrosis respiratory epithelium. *Science* **221,** 1067–1070 (1983).

37. Veeze, H. J. *et al.* Determinants of mild clinical symptoms in cystic fibrosis patients. Residual chloride secretion measured in rectal biopsies in relation to the genotype. *J. Clin. Invest.* **93,** 461–466 (1994).

38. GIBSON, L. E. & COOKE, R. E. A test for concentration of electrolytes in sweat in cystic fibrosis of the pancreas utilizing pilocarpine by iontophoresis. *Pediatrics* **23,** 545–549 (1959).

39. Quinton, P. M. Chloride impermeability in cystic fibrosis. *Nature* **301,** 421–422 (1983).

40. Derichs, N. *et al.* Intestinal current measurement for diagnostic classification of patients with questionable cystic fibrosis: validation and reference data. *Thorax* **65,** 594–599 (2010).

41. Quinton, P. *et al.* β-adrenergic sweat secretion as a diagnostic test for cystic fibrosis. *Am. J. Respir. Crit. Care Med.* **186,** 732–739 (2012).

42. Caldrer, S. *et al.* Challenging the diagnosis of cystic fibrosis in a patient carrying the 186-8T/C allelic variant in the CF transmembrane conductance regulator gene. *BMC Pulm Med* **14,** 44 (2014).

43. Beekman, J. M. *et al.* CFTR functional measurements in human models for diagnosis, prognosis and personalized therapy: Report on the pre-conference meeting to the 11th ECFS Basic Science Conference, Malta, 26-29 March 2014. *J. Cyst. Fibros.* **13,** 363–372 (2014).

44. De Boeck, K. *et al.* CFTR biomarkers: time for promotion to surrogate end-point. *Eur. Respir. J.* **41,** 203–216 (2013).

45. Roth, E. K. *et al.* The K+ channel opener 1-EBIO potentiates residual function of mutant CFTR in rectal biopsies from cystic fibrosis patients. *PLoS ONE* **6,** e24445 (2011).

46. Rowe, S. M. *et al.* Optimizing nasal potential difference analysis for CFTR modulator development: assessment of ivacaftor in CF subjects with the G551D-CFTR mutation. *PLoS ONE* **8,** e66955 (2013).

47. Seliger, V. I., Rodman, D., Van Goor, F., Schmelz, A. & Mueller, P. The predictive potential of the sweat chloride test in cystic fibrosis patients with the G551D mutation. *J. Cyst. Fibros.* **12,** 706–713 (2013).

48. Dekkers, R. *et al.* A bioassay using intestinal organoids to measure CFTR modulators in human plasma. *J. Cyst. Fibros.* **14**, 178-81 (2014).

49. Schwank, G. *et al.* Functional repair of CFTR by CRISPR/Cas9 in intestinal stem cell organoids of cystic fibrosis patients. *Cell Stem Cell* **13,** 653–658 (2013).

50. Yui, S. *et al.* Functional engraftment of colon epithelium expanded in vitro from a single adult Lgr5^{+} stem cell. *Nat Med* **18,** 618–623 (2012).

51. Huch, M. *et al.* In vitro expansion of single Lgr5+ liver stem cells induced by Wnt-driven regeneration. *Nature* **494,** 247–250 (2013).

52. Boj, S. F. *et al.* Organoid models of human and mouse ductal pancreatic cancer. *Cell* **160,** 324–338 (2015).

53. Boinot, C., Jollivet Souchet, M., Ferru-Clément, R. & Becq, F. Searching for combinations of small-molecule correctors to restore f508del-cystic fibrosis transmembrane conductance regulator function and processing. *J. Pharmacol. Exp. Ther.* **350,** 624–634 (2014).

54. Teixeira, A. L. & Falcao, A. O. Noncontiguous atom matching structural similarity function. *J Chem Inf Model* **53,** 2511–2524 (2013).

55. Teixeira, A. L. & Falcao, A. O. Structural similarity based kriging for quantitative structure activity and property relationship modeling. *J Chem Inf Model* **54,** 1833–1849 (2014).

56. Roth, D. M. *et al.* Modulation of the maladaptive stress response to manage diseases of protein folding. *PLoS Biol.* **12,** e1001998 (2014).

57. Char, J. E. *et al.* A little CFTR goes a long way: CFTR-dependent sweat secretion from G551D and R117H-5T cystic fibrosis subjects taking ivacaftor. *PLoS ONE* **9,** e88564 (2014).

58. De Stefano, D. *et al.* Restoration of CFTR function in patients with cystic fibrosis carrying the F508del-CFTR mutation. *Autophagy* **10,** 2053–2074 (2014).

59. Kerem, E. *et al.* Ataluren for the treatment of nonsense-mutation cystic fibrosis: a randomised, double-blind, placebo-controlled phase 3 trial. *Lancet Respir Med* **2,** 539–547 (2014).

60. Finkel, R. S. *et al.* Phase 2a study of ataluren-mediated dystrophin production in patients with nonsense mutation Duchenne muscular dystrophy. *PLoS ONE* **8,** e81302 (2013).

61. Hoffman, E. P. & Connor, E. M. Orphan drug development in muscular dystrophy: update on two large clinical trials of dystrophin rescue therapies. *Discov Med* **16,** 233–239 (2013).

62. McElroy, S. P. *et al.* A lack of premature termination codon read-through efficacy of PTC124 (Ataluren) in a diverse array of reporter assays. *PLoS Biol.* **11,** e1001593 (2013).

63. Howard, M., Frizzell, R. A. & Bedwell, D. M. Aminoglycoside antibiotics restore CFTR function by overcoming premature stop mutations. *Nat Med* **2,** 467–469 (1996).

64. Sermet-Gaudelus, I. *et al.* Ataluren (PTC124) induces cystic fibrosis transmembrane conductance regulator protein expression and activity in children with nonsense mutation cystic fibrosis. *Am. J. Respir. Crit. Care Med.* **182,** 1262–1272 (2010).

65. Kerem, E. *et al.* Effectiveness of PTC124 treatment of cystic fibrosis caused by nonsense mutations: a prospective phase II trial. *Lancet* **372,** 719–727 (2008).

66. Wilschanski, M. *et al.* Chronic ataluren (PTC124) treatment of nonsense mutation cystic fibrosis. *Eur. Respir. J.* **38,** 59–69 (2011).

67. Eichler, H.-G. *et al.* Adaptive licensing: taking the next step in the evolution of drug approval. *Clin. Pharmacol. Ther.* **91,** 426–437 (2012).

68. Eichler, H.-G. *et al.* From adaptive licensing to adaptive pathways: delivering a flexible life-span approach to bring new drugs to patients. *Clin. Pharmacol. Ther.* **97,** 234–246 (2015).

69. Dransfield, M. T. *et al.* Acquired cystic fibrosis transmembrane conductance regulator dysfunction in the lower airways in COPD. *Chest* **144,** 498–506 (2013).

70. Sloane, P. A. *et al.* A pharmacologic approach to acquired cystic fibrosis transmembrane conductance regulator dysfunction in smoking related lung disease. *PLoS ONE* **7,** e39809 (2012).

71. Donowitz, M. *et al.* Translational approaches for pharmacotherapy development for acute diarrhea. in *Gastroenterology* **142,** e1–9 (2012).

72. Jin, B.-J. *et al.* Microfluidics platform for measurement of volume changes in immobilized intestinal enteroids. *Biomicrofluidics* **8,** 024106 (2014).

73. Kovbasnjuk, O. *et al.* Human enteroids: preclinical models of non-inflammatory diarrhea. *Stem Cell Res Ther* **4 Suppl 1,** S3 (2013).

74. Karthaus, W. R. *et al.* Identification of multipotent luminal progenitor cells in human prostate organoid cultures. *Cell* **159,** 163–175 (2014).

75. Huch, M., Boj, S. F. & Clevers, H. Lgr5(+) liver stem cells, hepatic organoids and regenerative medicine. *Regen Med* **8,** 385–387 (2013).

76. Bartfeld, S. *et al.* In vitro expansion of human gastric epithelial stem cells and their responses to bacterial infection. *Gastroenterology* **148,** 126–136.e6 (2015).

77. van de Wetering, M. *et al.* Prospective derivation of a living organoid biobank of colorectal cancer patients. *Cell* **161,** 933–945 (2015).

9

Chapter 10

Nederlandse samenvatting
Dankwoord
List of publications

Nederlandse Samenvatting

HOOFDSTUK 1: INTRODUCTIE

Ieder persoon zit anders in elkaar. Hierdoor komen ziektes verschillend tot uiting en reageert iedereen op zijn eigen manier op medicatie. De ontwikkeling van op maat gemaakte therapie voor de individuele patiënt is een belangrijke focus van de hedendaagse gezondheidszorg, zo ook voor mensen met taaislijmziekte of cystic fibrosis (CF). CF is de meest voorkomende levensverkortende erfelijke ziekte in de westerse wereld. Wereldwijd lijden er ongeveer 85.000 mensen aan. CF-patiënten hebben problemen in verschillende organen, waaronder de longen, darmen en alvleesklier. De gemiddelde levensverwachting voor pasgeborenen met deze aandoening is ~37 jaar.

CF wordt veroorzaakt door mutaties in het zogeheten CFTR-gen (stukje erfelijk materiaal), waarvan ongeveer 2000 verschillende variaties zijn beschreven. De type mutatie bepaalt op welke manier het CFTR-eiwit (het gen-product) niet goed functioneert. Dit eiwit fungeert in de cel als kanaal voor zouten, zoals chloride en bicarbonaat, en is essentieel voor de vloeistof huishouding van verschillende organen. Als CFTR niet goed functioneert leidt dit in de long tot productie van een taaie slijmlaag en chronische infecties. Een individu krijgt CF als hij zowel van zijn moeder als vader een CFTR-mutatie erft. De combinatie van CFTR-mutaties (het CFTR-genotype), de rest van het erfelijk materiaal en omgevingsfactoren bepalen samen de ernst van de ziekte en reactie op medicatie van een CF-patiënt. Over het algemeen leiden de zogeheten ‘zware’ mutaties tot een ernstig ziektebeeld, terwijl de ‘milde’ mutaties zich uiten in een minder ernstig ziektebeeld. Toch verschilt het ziektebeeld ook aanzienlijk tussen patiënten met dezelfde mutaties om redenen die we nog niet goed begrijpen.

Op het gebied van CF-medicatie is er een belangrijk tijdperk aangebroken. Terwijl de conventionele behandeling voornamelijk gericht is op het onderdrukken van symptomen die gepaard gaan met de ziekte, zijn er gedurende de laatste 10 jaar middelen ontwikkeld die aangrijpen op het onderliggende defect in CF: het gemuteerde CFTR-eiwit. Deze CFTR-reparerende middelen zouden mogelijk in de toekomst de ziekte kunnen genezen.

Sinds kort zijn er twee van dit soort medicijnen op de markt (lees hierover meer in hoofdstuk 7), en dit is een enorme doorbraak. Helaas is deze medicatie nog lang niet voor alle patiënten beschikbaar en werkt het bij veel patiënten nog niet zo goed. Bovendien is de reactie van patiënten die deze medicatie krijgen heel verschillend. Het is dus van belang dat er effectievere

CFTR-reparerende medicatie wordt ontwikkeld en dat we juist die patiënten kunnen behandelen die ook daadwerkelijk op de medicatie reageren.

Hiervoor is het van groot belang dat we in het lab modellen ontwikkelen die het individu zo goed mogelijk nabootsen en waarin we de functie van het CFTR-eiwit zo nauwkeurig mogelijk kunnen bepalen. Met persoonsgebonden modellen in het lab kunnen we (i) verschillen tussen patiënten beter leren begrijpen, (ii) effectievere medicatie ontwikkelen en (iii) toewerken naar een optimale behandeling voor de individuele patiënt. Dit proefschrift beschrijft de ontwikkeling van een nieuw model om iedere unieke patiënt in het laboratorium te kunnen bestuderen.

HOOFDSTUK 2: DE CF-PATIËNT NABOOTSEN MET MINI-DARMEN

Door recente technologische ontwikkelingen is het mogelijk om darmstamcellen van een persoon 'oneindig' te vermenigvuldigen in het laboratorium in de vorm van 'mini-darmen' of organoïden. Zulke intestinale organoiden maken wij van kleine hapjes weefsel (biopten) uit het rectum van CF-patiënten of gezonde personen. Ongeveer vier jaar geleden ontdekten wij iets interessants: als we CFTR in organoiden van gezonde personen activeren, zwellen de structuren in korte tijd flink op. Dit komt omdat er in organoiden een holte aanwezig is die wordt gevuld met zouten en vocht zodra het CFTR-kanaal na activatie open gaat, alsof er een ballon wordt opgeblazen. Omdat CFTR in patiënten met taaislijmziekte afwezig is of niet goed werkt is deze zwelling in organoiden van mensen met CF afwezig of verminderd (Fig. 1a). Door middel van fluorescentie microscopie en speciale software kunnen we de zwelling van een heleboel organoiden tegelijk heel nauwkeurig meten. Zo hebben we gezien dat de ernst van de CFTR-mutaties samenhangt met de hoeveelheid zwelling (zware mutatie = weinig zwelling; milde mutatie = meer zwelling). Ook zien we dat CFTR-reparerende middelen in CF-organoiden de zwelling weer kunnen herstellen (Fig. 1a,b). Kortom, de mate van zwelling van mini-darmen is dus een uitleesmaat voor de activiteit van CFTR en kan worden gebruikt om per patiënt de functie van CFTR en reactie op CFTR-herstellende medicijnen te bepalen.

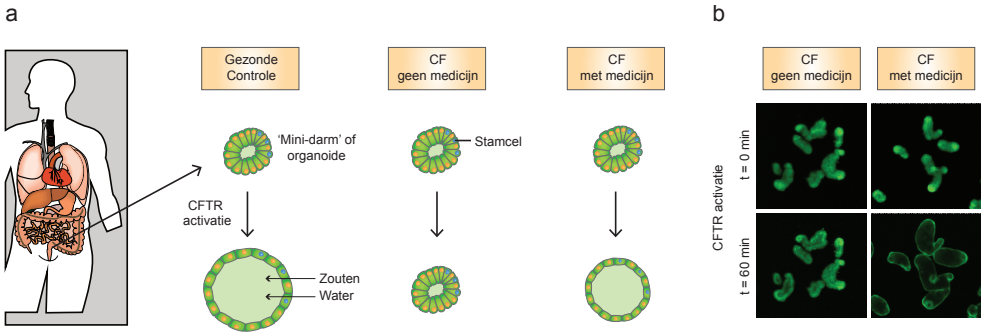

Figuur 1. Een nieuwe methode om CFTR-functie te meten in mini-darmen of organoiden. (a) Een illustratie van zwelling van organoiden na CFTR activatie. Organoiden bestaan uit een verzameling van cellen, waaronder stamcellen. (b) Microscopie afbeeldingen van CF-organoiden met of zonder medicijnbehandeling en voor of na activatie van CFTR. We kleuren de cellen fluorescerend groen om ze zichtbaar te maken onder de microscoop.

HOOFDSTUK 3: EFFICIËNT 'REPAREREN' DOOR TE COMBINEREN

F508del is de meest voorkomende mutatie die wordt gedragen door ~90% van alle patiënten met CF. Om deze reden wordt er voornamelijk onderzocht hoe wij het chloridekanaal met specifiek deze mutatie (CFTR-F508del) kunnen repareren. Om goed te kunnen functioneren moet CFTR in een cel op de juiste manier worden 'gevouwen' en getransporteerd. Je kunt je CFTR voorstellen als een groot papier, pas als het papier goed gevouwen wordt kan het een vliegtuig worden en op de juiste bestemming aankomen. Bij CFTR-F508del is vouwing en transport verstoord en wordt het eiwit door de cel opgeruimd. Dit is te vergelijken is met een misgevouwen vliegtuig wat je als een propje weggooit.

Speciale medicijnen genaamd 'correctoren' kunnen aan het CFTR-F508del-eiwit binden en de vouwing verbeteren. Als het ware gebruik je een plakbandje om een verkeerd gevouwen vliegtuig qua vorm bij elkaar te houden. In samenwerking met de onderzoeksgroep van G. Lukacs uit Canada hebben we in organoiden onderzocht hoe we zo efficient mogelijk met deze correctoren de vouwing van het CFTR-F508del kunnen herstellen. We vonden dat verschillende correctoren op een andere plaatsen in het CFTR-F508del aangrijpen en elkaars werking sterk verbeteren. Je hebt als het ware je papieren vliegtuigje op meerdere plekken met verschillende plakbandjes verstevigd, en de combinatie van deze plakbandjes werkt veel beter dan de losse plakbandjes bij elkaar opgeteld. De tweede generatie corrector therapie die nu wordt ontwikkeld voor CFTR-F508del bestaat uit dit soort elkaar versterkende medicijnen en kan de effectiviteit van behandeling sterk verbeteren.

HOOFDSTUK 4: VERSCHIL MOET ER ZIJN

Naast CFTR-F508del bestaan er ook andere mutaties die leiden tot een verstoring van eiwitvouwing en transport. Zijn correctors voor verschillende CFTR-mutanten even effectief? Dit hebben we onderzocht in organoiden van CF-patiënten met de F508del-, N1303K- of A455E-mutatie. De resultaten hebben aangetoond dat CFTR-N1303K door geen enkele corrector kan worden gerepareerd. Of anders gezegd, geen enkele plakmethode kan het papieren vliegtuig beter laten vliegen. Voor patiënten met deze mutatie moeten dus andere medicijnen ontwikkeld worden. VX-809 is momenteel de enige CFTR-corrector die recentelijk als medicijn is goedgekeurd en werkt het meest optimaal voor patiënten met F508del. Onze studie liet zien dat andere correctors dan VX-809 veel beter werken voor CFTR-A455E. Oftewel, het ene type papieren vliegtuig kun je beter repareren met lijm, terwijl je het andere type vliegtuig beter kan repareren met plakband. A445E is de op één na meest voorkomende mutatie bij Nederlandse CF-patiënten. We zijn op dit moment op zoek naar een al bestaand medicijn wat specifiek voor deze patiënten als efficiënte corrector kan werken.

HOOFDSTUK 5: 'SUPER FOOD' VOOR CF-PATIËNTEN?

Bij sommige CF-patiënten is de vouwing en transport van CFTR normaal, maar is juist het proces van openen (gating) verstoord. Stoffen die het CFTR-kanaal kunnen 'potentiëren' en hiermee

gating kunnen herstellen noemen we 'potentiatoren'. VX-770 is momenteel de enige potentiator die als medicijnen beschikbaar is CF-patiënten met een gating mutatie (~5% van alle patiënten). Omdat dit medicijn het ziektebeeld wel kan verbeteren maar niet kan genezen wordt er nog steeds hard gezocht naar betere therapieën.

Sommige natuurlijke stoffen kunnen het CFTR-kanaal ook potentiëren, zoals een extract uit de geelwortel (curcumine) en het hoofdbestanddeel van soja (genisteïne). In organoiden van patiënten met gating-mutaties hebben we aangetoond dat alle drie de stoffen elkaars werking versterken. Deze data wijzen erop dat zowel VX-770, curcumine als genisteïne een ander werkingsmechanisme hebben en ondersteunen het gebruik van potentiator combinaties als therapie voor CF. In Nederland worden er nu ongeveer 35 patiënten behandeld met VX-770. Voor een aantal van deze patiënten wordt momenteel in een klinische studie onderzocht of het extra toedienen van het voedingssupplement genisteïne positieve effecten heeft op hun gezondheid.

HOOFDSTUK 6: ASTMAMEDICATIE HERGEBRUIKEN VOOR CF?

Het CFTR chloride kanaal staat vooral dicht en het openen wordt door hormonen of andere lichaamseigen stoffen geactiveerd. Medicijnen die standaard worden gebruikt ter behandeling van astma, zoals salbutamol, kunnen ook het CFTR openen door de lichaamseigen stoffen na te bootsen. We hebben in organoiden laten zien dat zulke astma medicijnen CFTR inderdaad kunnen activeren, maar alleen voor CFTR varianten die geassocieerd zijn met een relatief mild ziektebeeld, zoals CFTR-R117H en CFTR-A455E. In een klinische studie hebben we de toediening van salbutamol bij CF-patiënten met deze mutaties bestudeert. Met behulp van organoiden konden wij een geringe activiteit van het medicijn in het bloed van patiënten terugvinden, wat gepaard ging met een zeer milde maar toch significante klinische verbetering. Deze studie geeft aan dat organoiden nuttig kunnen zijn om reeds bestaande medicatie te hergebruiken voor patiënten met CF. De lange termijn effectiviteit en veiligheid van salbutamol bij patiënten met CF moet in vervolgstudies verder worden onderzocht.

HOOFDSTUK 7: DE EFFECTIVITEIT VAN MEDICIJNEN VOORSPELLEN IN HET LAB

Er zijn momenteel twee CFTR-reparerende of 'genezende' medicijnen ontwikkeld. De potentiator VX-770 is geregistreerd voor negen verschillende CF-mutaties (~5% van alle patiënten) en VX-809 in combinatie met VX-770 is goedgekeurd voor patiënten homozygoot voor F508del (~45-50% van alle patiënten). We streven ernaar om deze medicijnen zo snel mogelijk beschikbaar te stellen voor patiënten met andere mutaties die ook baat hebben bij deze medicatie. Helaas zijn de conventionele klinische studies duur en tijdrovend en niet mogelijk voor kleine groepen patiënten of individuen met zeldzame CFTR-mutaties. Kunnen we organoiden gebruiken om de reactie van patiënten met zeldzame mutaties op bestaande therapieën te voorspellen? In dit hoofdstuk hebben we de reactie op VX-770, VX-809 of de combinatie bestudeerd in organoiden van patiënten met allerlei verschillende CFTR-mutaties. Terwijl voor sommige organoiden geen enkele behandeling effectief was, reageerde anderen sterk op VX-770 (G1249R) of de combinatiebehandeling (A455E). De organoiden hadden goed voorspeld: twee patiënten met de zeer zeldzame G1249R-mutatie

reageerden beiden erg goed op VX-770 en kunnen nu deze behandeling blijven krijgen. Deze aanpak is uniek in de wereld, en vormt mogelijk een kosteneffectieve methode om deze dure medicijnen zo snel mogelijk bij de juiste patiënten te krijgen. Er lopen momenteel een vijftal klinische studies om de voorspellende waarde van het model verder te valideren.

HOOFDSTUK 8: KNUTSELEN AAN GENETISCH MATERIAAL

In hoofdstuk 8 schakelen we over naar de ontwikkeling van een nieuwe vorm van gentherapie, een methode die voor genezing van alle CF-patienten kan zorgen. Het doel: in stamcellen het defecte gen vervangen door een gezond gen. Een mogelijke strategie is als volgt: (i) in het laboratorium wordt het gemuteerde gen in stamcellen van de patiënt gerepareerd, (ii) stamcellen met de juiste genetische correctie worden in het laboratorium vermenigvuldigd en (iii) de gerepareerde stamcellen worden in de long de patiënt terug getransplanteerd. Hoewel we dit stadium nog lang niet hebben bereikt is de eerste belangrijke stap gezet. In samenwerking met het lab van Prof. H. Clevers (Hubrecht Instituut, Utrecht) hebben we namelijk aangetoond dat we het gemuteerde CFTR-gen in de stamcellen van intestinale CF-organoiden op een hele specifieke manier kunnen repareren. Een belangrijke volgende stap is om dit te vertalen naar de long. De toekomst zal uitwijzen of in het laboratorium gerepareerde stamcellen op een efficiënte en veilige manier kunnen worden gebruikt voor de behandeling van CF.

Conclusie

Dit boekje beschrijft een nieuwe meetmethode in intestinale organoiden om de functie van CFTR voor elk individu op een hele nauwkeurige manier te kunnen bepalen. Dit model leert ons taaislijmziekte beter te begrijpen en speelt een belangrijke rol in de ontwikkeling van 'genezende' CF-therapieën en op maat gemaakte medicatie voor de individuele patiënt. Zo hopen we voor iedere patiënt met organoiden te kunnen gaan voorspellen welke medicatie het beste past (Fig. 2). In hoeverre organoiden de reactie op medicatie kunnen voorspellen gaan we in grote studies verder onderzoeken. Het belangrijkste doel op korte termijn is om door middel van organoiden de bestaande CFTR modulerende stoffen (VX-770 en VX-809) beschikbaar te stellen voor zoveel mogelijk patiënten met zeldzame mutaties die baat hebben bij deze middelen. Ongetwijfeld zal dit model bijdragen aan de ontwikkeling van 'genezende' medicatie voor uiteindelijk 100% van alle patiënten met CF.

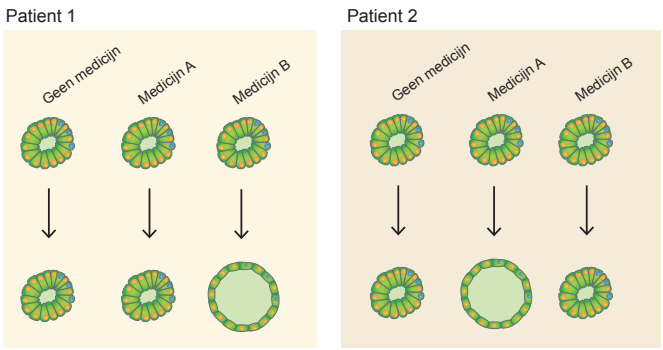

Figuur 2. Op maat gemaakte medicatie door middel van organoiden. Met behulp van intestinale organoiden kunnen we per patiënt de reactie op verschillende medicijnen bepalen. In dit voorbeeld zou patiënt 1 geholpen zijn met medicijn B, terwijl patiënt 2 geholpen is met medicijn A. We gaan nog verder uitzoeken hoe goed deze metingen de reactie bij de patiënt zelf kunnen voorspellen.

Dankwoord

Het is niet vaak voorgekomen dat ik van een bagagedrager gevallen ben… maar wel bij mijn promotor! **Kors**, wat ben ik blij dat ik in jouw team heb mogen werken. De samenwerking tussen lab en kliniek was ontzettend motiverend en liet me steeds weer beseffen waarvoor wij onderzoek doen: de patiënt. Ik bewonder de rust die je uitstraalt en jouw vermogen om zaken voor elkaar te krijgen. Je hebt me geleerd om altijd in mogelijkheden te denken. Ik zal met heel veel plezier terugkijken op onze wetenschappelijke samenwerking en al het leuke wat daarbij kwam, zoals de tripjes naar het buitenland, het lunchen in the basket, de familiedag en het jaarlijkse kerstontbijt.

'Gewoon doen!' **Jeff**, mijn copromotor, ik kan niet anders zeggen dan dat de afgelopen jaren met jou als baas een geweldig avontuur zijn geweest. Ik weet nog goed dat ik met zwetende handjes kwam vertellen dat ik wel wilde promoveren. Wie had ooit gedacht dat het project zo goed zou uitpakken? Professor worden voor je 40e? Ik hoop echt dat het je gaat lukken! Ik heb ontzettend veel van je geleerd (Fedex maakt geen vliegtuigen) en ben heel blij met de vrijheid die je mij tijdens het traject hebt gegeven. Ik bewonder (en verwonder me over) jouw gedrevenheid, enthousiasme, kennis, kwaliteit, creativiteit, doorzettingsvermogen, zelfvertrouwen en optimisme (zelfs als die reviewers het weer eens niet begrepen hadden). Wat ik nog meer bewonder: je Darth Vader pop, lichtgevende zwaard en fluorescerend gele Nike Air Max (met een luchtlaag van voor tot achter). Een andere baan als postdoc, het zal even wennen worden. Maar wie weet, misschien kunnen we ooit nog eens samen een paper 'dumpen in the Lancet'!

Team Beekman, wat zal ik jullie missen! De geordendheid van **Evelien**, (onze enige echte lab manager), de woordgrapjes van **Annelot** ('How CFTR you?' houden we er in!), de vrolijkheid van **Do** ('hihi'), de behulpzaamheid van **Lodewijk** (de 'LAW') en de droge opmerkingen van **Gitte** ('Tot zover de anonimiteit van patiënt CF73'). Het brood beleggen uit de lunchbox, de 'CFTR nights', het bedenken van een 1 april grap voor **Jeff**, de blunders ('Waarom plakt er een biopt tegen het raam?') en nog veel meer. De harde kern van team Beekman, **Evelien** en **Annelot**, ik had me geen fijnere analisten kunnen voorstellen om mee te mogen werken, jullie zijn gewoon echt ontzettend goed! Ik ben heel dankbaar voor al het werk dat jullie mij uit handen hebben genomen ('het zijn echt nog maar een paar lumens…'), de gezelligheid en jullie grote rol in bijna alle hoofdstukken van dit proefschrift, iets om heel trots op te zijn. **Annelot**, mijn fiets-, bikram-, submit- en wijn-maatje, ik ben blij dat jij mijn paranimf bent! **Nienke, Arianne, Adrian, Peter** en **Rosa**, allemaal hele leuke en goede studenten, ik heb veel van jullie geleerd. **Marit, Pauline en Jennifer**, met jullie als oud collega's heb ik een hele leuke tijd gehad. En **Marne en Gimano**, heel veel succes met jullie Postdoc!

Afdeling kinderlongziekten/allergologie, wat een leuke groep mensen. **Gitte**, slim, efficiënt, grappig, gezellig en een ster in het bedenken van acroniemen. Als superman vloog je door de gangen tussen lab en kliniek ('Labiek'). Bedankt voor jouw hulp met hoofdstuk zeven! **Karin**, **Bert** en **Suzan**, heel leuk en motiverend om te zien hoe jullie als artsen zo hebben meegeleefd en meegedacht met het onderzoek, en natuurlijk onmisbaar zijn geweest in het aanleveren van patiëntmateriaal. **Sabine** en **Margot**, super behulpzame, fijne en gezellige collega's, dank voor het includeren van patiënten en het structureren van administratieve rompslomp. **Myriam**, staat altijd voor iedereen klaar, lief en behulpzaam, door jou voelt een bezoekje aan de afdeling echt een beetje als thuiskomen. Ook dank aan alle arts onderzoekers (**Pauline**, **Francine**, **Kim**, **Jacobien**, **Anne en co**) en alle anderen van de afdeling voor de leuke tijd!

Te herkennen aan het gele tonnetje: **Hugo de Jonge**, ook wel bekend als 'de wandelende encyclopedie'. Met in dat tonnetje steeds weer een nieuwe compound om op de organoids te testen. Hugo, ik blijf me verwonderen over jouw passie voor onderzoek. Jouw 'mini-colleges' waren erg leerzaam ('in de zweetklier werkt CFTR andersom, anders zouden we allemaal kikkers zijn') en jouw advies voor bijna elk project was ontzettend waardevol. Ik ben blij dat we samen aan het mooie curcumin/genistein project hebben kunnen werken.

Het enorme succes van deze wetenschapper blijft me verbazen. **Hans Clevers**, de samenwerking met jou en jouw lab zijn essentieel geweest voor het tot stand komen van dit proefschrift. Ontzettend bedankt voor de leerzame samenwerking en jouw hulp bij het verkrijgen van mijn droombaan in Melbourne. **Gerald** and **Bon Kyoung**, it was a pleasure to work with you on the CRISPR/Cas9 project. Furthermore many thanks to all the members of the Clevers Lab, especially **Stieneke**, who helped me with organoid culturing, lent me organoid goodies or answered my questions. The HUB (**Rob, Sylvia, Tulay** and all the others), I am grateful for your role in establishing the CF organoid biobank and efforts to further characterize the potential of the model.

CF Nederland. Ook dank ik alle betrokken onderzoekers (**Hugo, Ineke, Bertrand, Bob**), **longartsen, kinderlongartsen, gastro-enterologen, onderzoeksverpleegkundigen, analisten en secretaresses** uit alle verschillende CF Centra in Nederland voor het aanleveren van patiëntmateriaal, de input tijdens de 4-maandelijkse CF-Nederland bijeenkomsten en de gezelligheid en discussies bij congressen. In het bijzonder dank ik **Hettie** voor de coördinatie van patiënt inclusie vanuit Rotterdam, en **Inez** voor de patiënt inclusie vanuit de volwassen zorg in Utrecht. **Vincent** en **Jacqueline**, als leden van de Nederlandse Cystic Fibrosis Stichting dank ik jullie hartelijk voor het vertrouwen, de financiële ondersteuning, de plezierige samenwerking en jullie inzet voor een betere toekomst voor CF patiënten.

Onze 'organoid-maatjes' van het WKZ, groep **Edward Nieuwenhuis** / **Sabine Middendorp**, mede door jullie is het CF organoid project zo snel van de grond gekomen. **Caroline, Kerstin, Anke** en alle anderen, fijn dat wij samen hebben kunnen overleggen, brainstormen, en dat wij onze frustraties hebben kunnen delen als de kweekjes het moeilijk hadden ('het zal de WNT wel weer zijn!').

Waar het allemaal begon: in de groep van **Paul Coffer**. Eerst als master student, toen nog even als OIO. Door het altijd gemotiveerde team en de interactieve sfeer heb ik hele goede herinneringen aan mijn tijd bij jullie. **Paul, Jorg, Ruben, Daisy, Marthe, Stephin, Veerle, Ana Rita en alle andere Coffers**, bedankt voor de leuke tijd!

Wat was ons onderzoek zonder menselijke cellen? Ik ben alle **CF patiënten, ouders en gezonde vrijwilligers** dan ook erg dankbaar voor de medewerking en hoop van harte dat ons onderzoek iets voor de patiënten kan betekenen.

Gergely Lukacs and colleagues, it has been great to work with you on the beautiful corrector combination study. To all other **collaborators around the world**, thanks for your support, discussions and fun on the CF conferences.

AIO Room number 1! Back in the old days (**Zsolt, Lotte, Shamir, Annelies, Saskia, Julia, Liset, Justin and Viola**) or in its current composition (**Luuk, Pieter, Caroline, Sandra, Chiara, Nadia, Elena en Lotte**), it has been great to drink coffee with you, discuss about research and enjoy lunch or dinners. Dingetje…eh **Zsolt**! Grappig, slim en bijdehand, maar wel een beetje mainstream. Het was fijn theezakjes met jou te mogen delen. Ik ben blij dat jij nog steeds mijn maatje bent om wetenschap te bespreken, vakantie verhalen te delen en heerlijke wijn te drinken! **Lotte**, mijn gezellige, enthousiaste en vrolijke kamergenoot, we waren een goed team om **Zsolt** in bedwang te houden! Mijn grote dank gaat uit naar nog veel meer mensen van de **LTI** voor alle gezelligheid, discussies en input: **Michiel, Linde, Leo, Nienke, Kiki, Jurgen, Trudy, Jeanette, Dan, Wouter, Berent, Thijs, Theo, Ewoud, Willemijn, Marianne, Jenny, Sigrid, Lieneke, Rianne, Mark, Maarten, Kristof, Robert, Maud, Gerdien, Emmerik, Alsya, Yvonne, Saskia, Kirsten** en iedereen die ik ben vergeten!

En af en toe even helemaal niet aan werk hoeven denken… daar heb je vrienden voor! **Chris, Sab, Sjo, Ballon, en het is die Schneijder**, de ontspannen avondjes, weekendjes en geniale vakantie in Maleisië waren heeeeeerlijk! Helaas zijn jullie suggesties voor proefschrift titels net niet door de selectie gekomen… Lieve **Sab**, paranimf, wat ben ik blij dat jij in hetzelfde schuitje zat en we zoveel samen hebben kunnen werken, sporten, klagen en lachen. **Nien, Badr, Clotjes, Irene, Mark, Tum, Lau, Tjallema, Lies, Johan, Eva, MC, Emiel, Jos en Steef**, ik heb genoten van de zeilweekendjes, puempjes, Berlijn, Lowlands, andere festivals, klaverjasavonden en de VriMiBo's! En natuurlijk **Knut, Li, San, Jol, Joos, Ien, Gaab, Iet, Son, Auk,** alle avondjes vrouwengeklets, festivals en onze bijzondere vakantie in Sri Lanka had ik niet willen missen!

Lieve familie, **mam, pap, Breier, Frans, Jan Willem, Vincent, Julia, Caro, Jeroen, Maxim, Jasmijn, Eef, Theun, Thijs, Viggo, Feline, Piek, Robbert, Fiene, Daan en Kiki**, bedankt voor jullie liefde, de heerlijke weekendjes in Goes, de gezellige verjaardagsfeestjes, de anti-RSI tips, onophoudelijke medeleven en interesse en begrip in drukke tijden. Mam en pap, jullie trouwdag 3 november zal vanaf nu een extra bijzondere dag zijn. Lieve **René** en **Eleine** (en de rest van de schoonfamilie), dank voor jullie interesse, medeleven en gezelligheid!

Lieve **Chris**, je kunt de woorden vast niet meer horen: promoveren, beurzen en RSI. Het laatste half jaar stond bij jou in het teken om letterlijk en figuurlijk de pijn voor mij te verlichten en daar ben ik je eeuwig dankbaar voor. En fijner teamgenootje had in me niet kunnen wensen! Ik kan niet wachten op ons avontuur in Australië.

List of publications

Ommen DD*, Vijftigschild LAW*, Kruisselbrink E, Vonk AM, Dekkers JF, Janssens HM, de Winter-de Groot KM, van der Ent CK, Beekman JM. Limited premature termination codon suppression by read-through agents in cystic fibrosis intestinal organoids. **Journal of Cystic Fibrosis,** accepted

Roth DM, Hutt DM, Tong J, Bouchecareilh M, Wang N, Seeley T, Dekkers JF, Beekman JM, Garza D, Drew L, Masliah E, Morimoto RI, Balch WE. Modulation of the maladaptive stress response to manage diseases of protein folding. **PLoS Biol.** 2014 Nov 18;12(11):e1001998

Eckford PD*, Ramjeesingh M*, Molinski S, Pasyk S, Dekkers JF, Li C, Ahmadi S, Ip W, Chung TE, Du K, Yeger H, Beekman J, Gonska T, Bear CE. VX-809 and related corrector compounds exhibit secondary activity stabilizing active F508del-CFTR after its partial rescue to the cell surface**. Chem Biol.** 2014 May 22;21(5):666-78

Schwank G*, Koo BK*, Sasselli V, Dekkers JF, Heo I, Demircan T, Sasaki N, Boymans S, Cuppen E, van der Ent CK, Nieuwenhuis EES, Beekman JM, Clevers H. Functional repair of CFTR by CRISPR/Cas9 in intestinal stem cell organoids of cystic fibrosis patients. **Cell stem cell.** 2013 dec 5;13(6):653-8**s**

Dekkers JF, van der Ent CK, Beekman JM. Novel opportunities for CFTR-targeting drug development using organoids. **Rare diseases**, 2013 Nov 11;1:e27112

Dekkers JF, Wiegerinck CL, de Jonge HR, Bronsveld I, Janssens HM, de Winter-de Groot KM, Brandsma AM, de Jong NW, Bijvelds MJ, Scholte BJ, Nieuwenhuis EE, van den Brink S, Clevers H, van der Ent CK, Middendorp S, Beekman JM. A functional CFTR assay using primary cystic fibrosis intestinal organoids. **Nat Med.** 2013 Jul;19(7):939-45

Okiyoneda T, Veit G, Dekkers JF, Bagdany M, Soya N, Xu H, Roldan A, Verkman AS, Kurth M, Simon A, Hegedus T, Beekman JM, Lukacs GL. Mechanism-based corrector combination restores ΔF508-CFTR folding and function. **Nat Chem Biol**. 2013 Jul;9(7):444-54

van Meegen MA, Terheggen SW, Koymans KJ, Vijftigschild LA, Dekkers JF, van der Ent CK, Beekman JM. CFTR-mutation specific applications of CFTR-directed monoclonal antibodies. **J Cyst Fibros.** 2013 Sep;12(5):487-96

Berends ET, Dekkers JF, Nijland R, Kuipers A, Soppe JA, van Strijp JA, Rooijakkers SH. Distinct localization of the complement C5b-9 complex on Gram-positive bacteria. **Cell Microbiol.** 2013 Dec;15(12):1955-68

Dekkers JF, van der Ent CK, Kalkhoven E, Beekman JM. PPARg as therapeutic target in cystic fibrosis. **Trends Mol Med.** 2012 May;18(5):283-91

Beekman JM, Vervoort SJ, Dekkers JF, van Vessem ME, Vendelbosch S, Brugulat-Panès A, van Loosdregt J, Braat AK, Coffer PJ, Syntenin-mediated regulation of Sox4 proteasomal degradation modulates transcriptional output, **Oncogene**. 2012 May 24;31(21):2668-79

Submitted manuscripts

Dekkers JF, van Mourik P, Vonk AM, Kruisselbrink E, Berkers G, de Winter – de Groot KM, Janssens HM, Bronsveld I, van der Ent CK, de Jonge HR*, Beekman JM*. Potentiator combinations synergistically repair CFTR gating in rectal cystic fibrosis organoids.

Dekkers JF, Gogorza RA, Kruisselbrink E, Vonk AM, Janssens HM, de Winter - de Groot KM, van der Ent CK, Beekman JM. Optimal correction of distinct CFTR folding mutants in rectal cystic fibrosis organoids.

Dekkers JF, Berkers G, Kruisselbrink E, Vonk AM, de Jonge HR, Janssens HM, Bronsveld I, van de Graaf EA, Nieuwenhuis EES, Houwen RHJ, Vleggaar FP, Escher JC, de Rijke YB, Majoor CJ, Heijerman HGM, de Winter – de Groot KM, Clevers H, van der Ent CK, Beekman JM. Predicting the clinical efficacy of CFTR-modulating drugs using rectal cystic fibrosis organoids.

Vijftigschild LAW*, Berkers G*, Dekkers JF#, Zomer – van Ommen DD#, Matthes E, Kruisselbrink E, Vonk AM, Hensen CE, Heida – Michel S, Geerdink M, Janssens HM, van de Graaf EA, Bronsveld I, de Winter – de Groot KM, Majoor CJ, Heijerman HGM, Hanrahan JW, van der Ent CK, Beekman JM. β_2-adrenergic receptor agonists activate CFTR in intestinal organoids and subjects with cystic fibrosis.

Vidović D*, Carlon* MS, Dekkers JF†, da Cunha MF†, Hollenhorst MI, Bijvelds MJC, Ramalho AS, Van den Haute C, Baekelandt V, Janssens HM, de Boeck K, Sermet-Gaudelus I, de Jonge HR, Gijsbers R‡, Beekman JM‡, Edelman A‡ and Zeger Debyser Z. rAAV-mediated gene transfer of a truncated CFTR rescues the cystic fibrosis phenotype in human intestinal organoids and a CF mouse model.

Yin Y, Bijvelds MJC, Dang W, van der Eijk AA, Knipping K, Tuysuz N, Dekkers JF, Wang Y, de Jonge J, Sprengers D, van der Laan LJW, Beekman JM, ten Berge D, Metselaar HJ, de Jonge H, Koopmans MPG, Peppelenbosch MP and Pan Q. Personalized modeling rotavirus infection and therapy using primary intestinal organoids.

* or #: These authors contributed equally